THREE-DIMENSIONAL MODELING OF PROGRESSIVE SEISMIC ACTIVITY APPLYING BLOCK MODELING TECHNIQUES

by

Eduardo A. Córdova

A thesis submitted to the faculty of
The University of Utah
in partial fulfillment of the requirements for the degree of

Doctor of Philosophy

Department of Mining Engineering

The University of Utah

December 2013

The University of Utah Graduate School

STATEMENT OF DISSERTATION APPROVAL

The dissertation of **Eduardo A. Córdova**

has been approved by the following supervisory committee members:

Michael G. Nelson	, Chair	**May 29, 2013** Date Approved
Michael K. McCarter	, Member	**May 29, 2013** Date Approved
Felipe Calizaya	, Member	**May 29, 2103** Date Approved
John McLennan	, Member	**May 31, 2013** Date Approved
Erich U. Petersen	, Member	**May 31, 2013** Date Approved

and by **Michael G. Nelson**, Chair/Dean of

the Department/College/School of **Mining Engineering**

and by David B. Kieda, Dean of The Graduate School.

ABSTRACT

A new approach has been developed to use, store, and display seismic information as a time-dependent variable in block models.

The research illustrates a new technique to model seismic events and combine them into block models, providing the user with the ability to analyze these data as a function of time in a four-dimensional (4-D) model, with the possibility of combining different analysis criteria to display the data, create sections of the information in any direction needed, and cut the data at any elevation to see what has happened through the life and development of the mine.

Seismic data, comprising points in three dimensions placed spatially by their location coordinates (x: east, y: north, and z: elevation), are interpolated into a block model to develop solids in three dimensions (3-D) at various energy or magnitude cut-offs. These data are then accumulated in a (4-D) array which can be used to display the evolution of seismicity over a period of time. The data in the blocks can be filtered using the associated location errors, and the number of seismic stations triggered by the seismic events.

A model was developed with seismic data collected between the years 1992 and 2012 from a large underground mine, using panel caving techniques. The data comprised approximately 2.1 million seismic events. The seismicity was interpolated using inverse-

distance interpolations to a block model that consisted of 1,875,000 blocks of 20×20×20 m, with block model extents of 2.5, 3, and 2 km in the east, north, and elevation directions, respectively. The model was developed for the entire mine, using yearly and monthly resolutions for the accumulated parameters.

The results from the accumulated energy model were used to analyze the pre-mining seismic conditions of a project that started in 2010 and that it is located between two other projects, one to the north that started in the year 1990 and the other to the south that started in 1998.

The seismic history of the mine can be displayed and analyzed using the developed technique, defining areas of progressive deterioration associated to the energy levels released by the seismic events.

Dedicated to

Marcela

TABLE OF CONTENTS

LIST OF FIGURES

LIST OF TABLES

ACKNOWLEDGEMENTS

I am grateful to have been able to pursue my graduate studies at the University of Utah. I would like to thank my advisor, Dr. Michael G. Nelson, for his unconditional friendship and help during my graduate work as an M.S and Ph.D. student, and also for performing burdensome proof-readings of all the things I wrote. I want to acknowledge the members of my committee, Dr. Felipe Calizaya, Dr. Michael K. McCarter, Dr. Erich U. Petersen, and Dr. John McLennan, for all the guidance and advice provided for my work.

I am also grateful for the financial support of the William C. Browning Graduate Scholarship, and the University of Utah´s Mining Engineering Department.

I extend sincere thanks to Pam Hofmann, secretary of the Mining Department, for all her help and assistance during the time I was a student.

Finally, I would like to thank my wife Marcela and my family for all their patience and unconditional support over the time that this work took to complete.

1. INTRODUCTION

Induced seismicity in mining is usually studied using seismic software packages that show the seismic events as point clouds, with associated locations, and these data are related to the mine activity (undercutting, cave advance, blasting, etc.) being done at the time the events happen.

The idea of three-dimensional (3-D) modeling is to display something that is complex to imagine because it may consist of many elements, or because these elements have different variables that cannot be envisioned easily just by looking at tables and graphs.

The purpose of the modeling technique described here is to use block models to visualize seismic activity over time in 3-D and four dimensions (4-D), to better understand how mining-induced seismicity has been developed in the mine.

A simple and robust modeling technique should be easy to explain and implement in a logical manner, allowing the use of the same technique and modeling process in different platforms.

If the information can be analyzed and displayed by using a technique that accumulates the energy associated with the seismic events in a block model, it will be possible to represent the of the induced seismicity with respect to the mining activities in a simpler manner, making analysis and study easier.

A set of data with coordinates can be represented in a 2-D (two-dimensional) space as a graph that is defined by the x and y coordinates. In mining and surveying applications, the easting (X) and northing (Y) coordinates are used, providing the ability to display the data in a defined system where it can be referenced and located with respect to known areas or places.

The human brain can easily locate and understand the data in a 2-D environment, but when the data are presented in a 3-D format, by adding an elevation attribute to it, the amount of data and its display become more and more complex as the model grows, increasing the difficulty of relating to and understanding the combinations of different variables.

The commonly-used seismic packages (JDI by ISS, Norsar3D) are based on working on a 3-D environment but using 2-D data, giving the ability to display maps or sections on a 2-D surface on a 3-D space. Using this approach, the data can be better viewed and understood for later interpretation or display.

A three-dimensional (3-D) package allows the display of large, three-dimensional data sets, and also facilitates the interpretation of these data by providing drafting and drawing tools that can be used in different sections and on a 3-D or 4-D setting, providing an important impact in the mine business (Brown 2004).

The approach used here follows the idea of using the seismic information in correlation with a block model of the area, so seismic attributes, such as energy, magnitude, associated location error, and number of stations that recognized each event, can be interpolated and combined within the block model for their analysis.

Adding the seismic attributes of the events, including the date and time for each, to the block model makes it possible to analyze the evolution of the weekly, monthly, or yearly seismicity. The time attribute can be correlated to the stages in mining at different milestones of the mine life.

A seismic time model can show how the seismicity has evolved and moved through the rock mass, providing insights and guidelines on the condition of areas that have yet to be mined.

The study was conducted using actual seismic data from a database comprising almost 2.1 million events that occurred over a period of 21 years at a large underground copper mine. The mine initially used the block caving method, but transitioned to panel caving during the study period.

2. BACKGROUND

Seismic data are collected from an array of geophones and accelerometers placed at various locations inside of the mine. The locations are chosen to achieve the optimal sensitivity for the variables being recorded.

The output data from each seismic station come as a series of events differentiated by the time or occurrence and the attributes for each event such as location, location error, moment, energy, and triggers or stations activated by the event.

These data, which may include a few or millions of events, can be interpolated into a block model to study the behavior of the events through the rock mass, and spatially place them in 3-D to allow correlation them with mining activity.

2.1 Block Models

The main idea of a block model is to partition the ore body or area of interest into units small enough to give interesting pictures of reality (Stanley 1979), with each block containing the desired information, such as lithology, structure, seismic activity, ore grades, etc., associated with a given block.

Block models were initially conceived as a way to store estimated values from existing data sets, and to use these values to determine which blocks represent a portion of the ore body that can be extracted economically.

Block models can be used in many ways, but it must be considered that a single model that satisfies all curiosities and forms of expertise is difficult to construct (Stanley 1979).

A block model can be thought of as a box that contains the area of interest that needs to be studied. The box contains many smaller boxes or blocks, each of which can store a number of variables associated with its volume.

The main parameters needed to define a block model are:

- Origin: The origin is usually the lowest point of the box, which translates to the lowest east, north, and elevation coordinates of the block model.
- Rotation: This attribute is only used if the block model needs to be rotated in the model axes to optimize the number of blocks used in the block model.
- Extents: The extents define how far in each direction the block model extends. Thus, a model with an origin of (100, 50, 200) and the extents on each coordinate of (100, 200, 100) will extend from the 100 to 200 on the east, from 50 to 250 on the north, and from 200 to 300 on the elevation.
- Block Size: The block size defines the size of the smaller blocks that compose the block model. For a regular block size of 10 m on each side, the previous example will be composed of 10 blocks in the east direction, 20 blocks in the north direction, and 10 blocks in the elevation orientation. The number of blocks can be calculated by multiplying the previous values. The model, which is 10×20×10 blocks, will have a total of 2,000 blocks.

- Variables: The variables are used to store data inside each block; a block can have as many variables as the software or file size restrictions of the operating system installed on the computer will allow. A variable can be of any of four types:
    - Alphanumeric: Strings of letters or numbers combined.
    - Byte: This is a variable that uses a single bit of memory, usually with integer numbers in a range from 0-255.
    - Short: A short integer number using two bytes of memory in the range of values from -32,768 up to 32,768.
    - Integer: Integer numbers taking up to 4 bytes of memory in the range from -2,000,000,000 to 2,000,000,000.
    - Float: A real number taking up to 4 bytes and used with values that have up to seven significant figures.
    - Double: A real number with greater precision, taking up to 8 bytes and used with values that have up to fourteen significant figures.

  It can be easily seen that as the number of variables increases, so does the size of the block model in use, and also the size of the block model file.

2.2 Composites Files

A composites file is a set of points usually derived from drill-hole data where the length of the hole is divided into intervals, and a set of 3-D coordinates is defined for the top, middle, and bottom section of each interval.

The coordinates of each sample point on a drill-hole are used to estimate the distance from the known data point to the center of the block or the point being

estimated. This distance in turn is used to determine which samples should be included in a given estimation, based on the respective distances of the samples from the point of interest (POI) being estimated, and also to calculate the weights that are used in the estimation of each block.

2.3 Inverse-distance Interpolations

Distance weighting methods became more popular when computer assistance became available because of the large number of repetitive calculations required (Hughes and Davey 1979).

The inverse-distance interpolation is a technique used to estimate an unknown value at a point or area of interest, for example, the center of a block, from known data around the point of interest.

The technique relies on the distance of the samples to the POI where a value needs to be estimated, and assigns weights to the samples depending on how close they are to the POI.

The known values are assigned weights that represent the respective influences of the surrounding samples upon the block being evaluated (Barnes 1979), and they are used to calculate a weighted average at POI.

The inverse-distance method can incorporate a power parameter. For example, inverse-distance-squared (ID2) places much more importance on samples that are closer to the POI than ID1, and ID3 (inverse-distance-cubed) gives even more importance to samples closer to the POI than ID2.

The weight assigned to the known points increases as the distance from the POI decreases, with greater values of "p" assigning more importance or weight to values closer to the point being estimated.

Inverse-distance estimation techniques are based on the idea that things that are close to one another are more likely to be alike than points that are more widely spaced.

The regular formula for inverse-distance estimation is presented in Eq. 1.

$$u(x) = \sum_{i=0}^{N} \frac{w_i(x)u_i}{\sum_{j=0}^{N} w_j(x)} \qquad \text{(Eq 1)}$$

$$w_i(x) = \frac{1}{d(x,x_i)^p} \qquad \text{(Eq 2)}$$

where,

x: interpolated arbitrary point

x_i: interpolating known point

d: given distance from point x_i to x

N: total number of known points used in the interpolation

p: positive real number called the power parameter

Many natural phenomena in nature exhibit an inverse distance effect, including gravity, magnetism, and the attenuation of light and sound, to mention a few (Hughes and Davey 1979).

2.4 Seismic Information

A seismic system consists of hardware (a network of sensors) and the software that is used to collect the seismic data from the sensors (Essrich 2005).

The collected information is interpreted and used as one of the tools that help understand various phenomena occurring in underground mines, such as caving, stability of major infrastructure, activity in production areas, and the effects of mining on geological features (Hudyma et al. 2010).

The analysis of seismic events is usually carried out by studying them in an isolated manner, without taking into consideration the previous evolution of seismicity over different areas of the mine. Seismic history has never been added to a block model as a time-dependent, numerical input that can be further analyzed and studied with relation to the other properties of the blocks and the back-analysis of these blocks with respect to newer relevant seismic events.

2.4.1 Seismic Monitoring System

The specific objectives of seismic monitoring in a block caving environment are to monitor seismic events related to induced stress concentrations, to monitor seismic events related to cave propagation, and to monitor seismic events related to preconditioning of the rock mass (White 2004).

A seismic monitoring system is composed of seismometer stations distributed optimally within the observation area where the data need to be recorded. In general, the area of interest should be surrounded by the recording devices in all three dimensions to

optimize the accuracy of the location of the events in all three directions, east, north, and elevation.

The density of stations within the system will determine the accuracy of the location of a seismic event, allowing the effective determination of the locations of different seismic events over time. The recording devices (geophones and accelerometers) transmit the signals from the seismometer stations to the recording center where the signal is processed for data storage and immediate or further interpretation.

Depending on the system capacity, the data can be continuously recorded or recorded only when relevant events occur, based on criteria such as magnitude, energy, or stations activated by the event. When the predefined conditions are met, the data within a time window before and after the event are stored in the recording center (K-UTEC 2003). The system continuously collects data in a memory loop for a given interval, and the data are recorded once the triggering conditions are met.

2.4.2 Seismic Sensing Devices

The two very common instruments used to record of seismic events are geophones and accelerometers.

The geophone is an electro-mechanical system that transforms the movement of the rock mass to an electrical signal proportional to the particle velocity in the medium, as shown in Figure 2.1. Most seismic transducers operate on the principle of measuring the ground motion relative to an inertial mass (Mendecki 1997). The instrument uses a magnetic coil suspended by springs within a steel case. When the material to which the instrument is attached begins to vibrate, the case moves while the coil remains stationary.

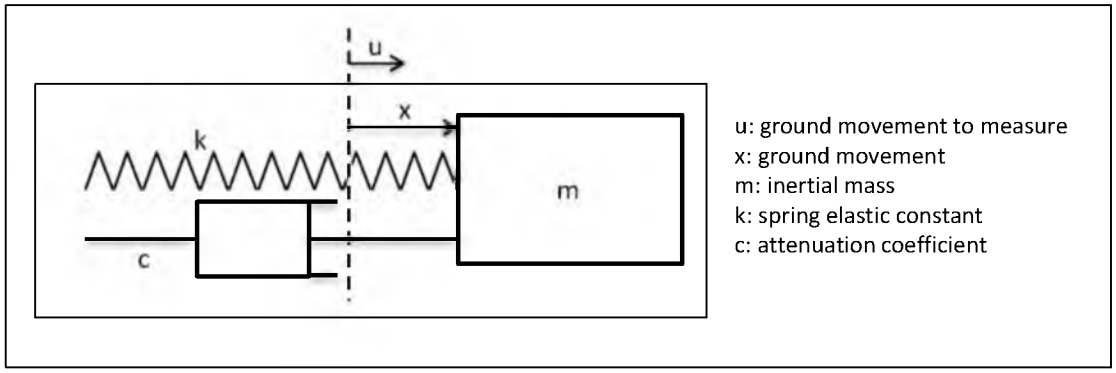

FIGURE 2.1 Inertial sensor schematic

The movement of the case in relation to the coil generates an electrical voltage proportional to the velocity of the coil with respect to the case. The variation in the electrical current through the coil is used to estimate the intensity of the vibration.

Geophones in mining applications usually work at frequencies of 4.5 Hz; these geophones have a usable frequency bandwidth between 3 Hz and 2,000 Hz. The geophones provide a low-cost tool with large bandwidth and excellent readability.

Accelerometers are sensors based on a piezo-electric effect generated by small crystals that are accelerated by the movement of the substrate to which the instrument is attached. That movement compresses the crystal and produces a signal that is electronically adjusted to make it proportional to the acceleration of the particles.

Accelerometers have higher sensitivity at higher frequencies than geophones. For very small seismic events that have high frequency content, such as those that result from caving, accelerometers are required to obtain accurate measurements (White 2004).

2.4.3 Seismic Network Characterization

A seismic network can be defined by three main aspects related to the quality and resolution of the movements that can be recorded by the system (Codelco, 2001).

- Sensibility: The sensibility is related to the minimum magnitude that can be registered by the seismic network. The magnitude describes the network sensitivity and it corresponds to the magnitude over which the events are registered. This parameter depends mainly on the installed sensors and the spacings between them.
- Recording Capacity: Recording capacity is based on the rate at which the information is recorded by the system.
- Network Errors: Network errors are related to the quality of the system and how accurately it can define the locations of events and the reliability of the parameters recorded by the network.

The minimum magnitude recognized by the system can be estimated by the Gutenberg-Richter curve (Gutenberg and Richter 1954).

The curve is constructed using the logarithmic values of the quantity of events over a defined magnitude at different ranges.

The magnitude at which this curve adopts a decreasing lineal tendency defines the minimum magnitude recordable by the system.

A sample Gutenberg-Richter plot where the minimum magnitude achieved by the system is around –0.4 is shown in Figure 2.2.

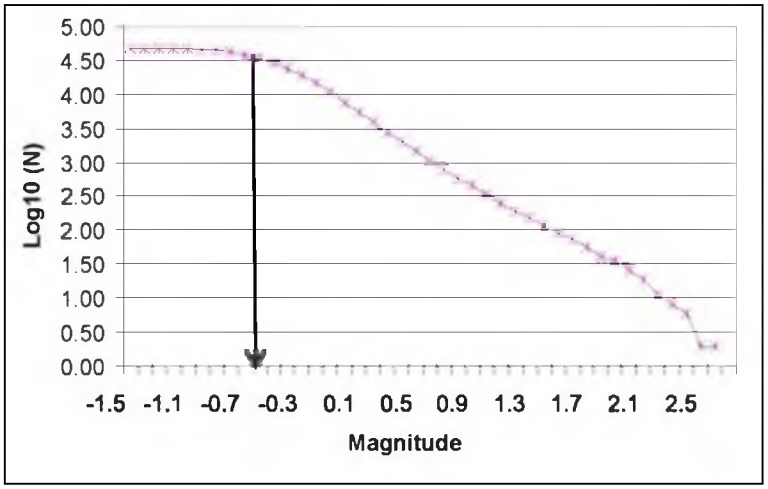

FIGURE 2.2 Sample Gutenberg-Richter curve

2.5 Induced Seismicity

Seismicity in mines is often referred to as induced seismicity because it is induced by the mining activities related to the extraction of the ore.

Seismicity occurs when rock is strained to its breaking point by mining-induced and/or tectonic stresses. The perturbation of the stress field may trigger a slip on faults that are in unstable equilibrium or rupture previously intact rock, releasing large amounts of energy (Durrheim 2005).

An increase in the stresses does not always result in rock breakage. For example, when an open-pit mine interacts with an underground caving project, the caving of the pit can concentrate stresses on the rock mass between the two projects, aiding the cave propagation by causing existing fractures to extend and create new fractures. The creation of new fractures can even affect primary fragmentation and reduce secondary breaking requirements (Moss 2006).

Mines can exhibit different kinds of induced seismicity. For example, small-scale, localized events, with a high frequencies in high-stress areas, can be produced by the undercutting of an area, while large-scale events related to shear in intact rocks may represent the evolution of the cave upwards (Turner 2000).

Seismicity recorded in mines usually shows bimodal patterns. The first mode typically has magnitudes ranging from 0.0 to 0.5, and is associated with rock mass fracturing immediately ahead of the undercut and the propagating cave back, while the second mode has magnitudes up to 2.1, and results from events located at geological discontinuities at a greater distance from mining activity. The second mode events are usually connected with stress redistribution ahead of the undercut abutment and around the cave (Glazer, 2004).

The distribution of mining-induced seismicity is a good indicator of structural stress conditions; seismicity usually results from a geologic structure being stressed to its limits. The redistribution of stresses can create concentrations of stored elastic energy that might drive seismic rock failure, and as mine excavations approach these concentrations, the mining-induced disturbance of stress levels can accelerate the loading of the intact rock, pillars, and faults to the point of failure (Whyatt 1996).

In a study conducted to understand the characteristics of mining-induced seismicity and rock bursts in deep hard rock mines (Swanson, 1991), seismic events were studied over a 20-month period at a metal mine in Idaho. Each seismic event was analyzed for its Richter magnitude, time of the occurrence, location, and relation to rock bursting.

One important result was that the accumulated seismic energy for the area was a result of only 5% or eight of the events, while half of these eight events did not produce any damage. The results were interpreted to show that the accumulation of energy in seismic areas where bursting or similar problems arise results mainly from sudden accumulations of energy and not from many events with low energy releases.

Other research has shown that the radiated seismic energy from an event provides a measure of the stress release at the source (White 2004).

3 CONCEPTUAL APPROACH

The approach developed in this work is based on studying the energy of each event and associating this energy with the blocks in the block model. The concept is based on the idea that the energy involved in a seismic event affects the rock associated in the place where the event takes place. The rock is subjected to forces and deformations resulting from the mining activities, and the energy is slowly accumulated until the internal strength of the rock mass is exceeded, generating a seismic event. The stored energy is released as elastic waves in the seismic event, damaging the rock to a greater or lesser extent.

As the number of events progresses and more events are located within the block boundaries, the energy releases continue to affect the blocks, leaving a deteriorative effect in each.

The releases of energy from mining-induced seismicity, as represented by recorded seismic events, can be used in combination with a block model to provide a new way of visualizing the historic seismic activity of an area at the mine. By interpolating to estimate the amounts of energy that have passed through a block, it is possible to define and delineate areas of the mine where significant deterioration may have occurred, as represented by the associated seismic activity.

In general, the interpolation techniques used here are based on estimating an average of the samples inside or around the block model, but by understanding the way

the system works, the process can be modified to actually estimate the sum of all the events that take place inside a block.

As described above, the simple inverse-distance (ID) interpolation method creates an average of the values around a block by using the distance from the center of the block to the samples to assign a weight to each sample to use on the estimation of the block. To assign greater weights to values that are closer to the center of the block, the distance in the ID method can be raised to a power, x, as shown by the general expression for the inverse-distance method in Eq. 3. Similarly, if a simple average is desired, a power of zero can be used for 'x' in Eq. 3.

$$ID = \sum_{i=1}^{n} \frac{\frac{1}{(d_i)^x} * w_1 + \cdots + \frac{1}{(d_n)^x} * w_n}{\frac{1}{(d_i)^x} + \cdots + \frac{1}{(d_n)^x}} \qquad \text{(Eq. 3)}$$

where,

d: distance from the sample to the center of the block

w: sample value to interpolate

x: inverse distance power

n: total number of samples

With x = 0, the interpolation estimates the average of all the energy values inside a block. To calculate the sum of all the energy events inside each block, the average is multiplied by the number of samples used in the interpolation. Interpolation routines in standard mine-planning software (Vulcan, Gemcom, Datamine, or Minesight) can store the number of samples used in the estimation of each block, so by multiplying the

number of samples and the estimated average of the energy, the sum of the energy inside of the block can be easily calculated.

When the true associated energy for each block has been estimated, it is possible to study how the energy is accumulated each year, by storing the progressive accumulation of energy in the correspondent variables for each year or month. For example, the accumulated energy of a block up to year 2001 will consist of the sum of accumulated energy values up to the year 2000 plus the real energy values for the year 2001.

The blocks with the interpolated information can then be sorted by desired parameters, such as average number of triggers activated, average location error associated with the samples, or a combination of both, to search for areas where high releases of energy over time could produce problems or indicate increased deterioration due to a history of seismic activity.

4 MODELING APPROACH

The recorded seismic events are obtained from the seismic network system, which provides location coordinates, magnitude, energy, moment, location error, and the number of triggered stations for each event.

4.1 Input Data

The data for the model were delivered in a CSV (comma-separated values) format, separated by spaces. The file was divided into events that could be located in three dimensions using the provided coordinates, and these events were converted to a composites file suitable for use with an inverse-distance estimation technique. In the composites file, a header line provides the information for each column within the file. For ease of use and to minimize the use of nonrequired data, the files can be manipulated in MS Excel if they contain fewer than 1 million events, or by using MS Access if they have more.

It is of course desirable to model only the variables of interest, and the file can be easily filtered using MS Excel, MS Access, or any other type of database manager.

Once the data are manipulated in the database package, they can be exported to a new CSV file with the new attributes (variables that are going to be interpolated) and definitions (numerical configurations of the variables), according to the input file format accepted by the modeling package selected.

The main column number, fields, units, and format for each variable are presented in Table 4.1.

The data are processed and manipulated in a database to create an input file that is suitable for import into a mine-modeling program such as Vulcan, Datamine, Gemcom, or Minesight. Vulcan was used in the work described here.

4.2 Postprocessed Data

The new input file is a CSV file. It has the inputs needed from the EVP files, but also includes the new columns that are required to reconfigure the data as a composites file.

TABLE 4.1: Column definitions in the seismic events file (EVP)

Column	Field	Units	Format
1	Date	-	yyyymmdd
2	Time	-	hhmmss
3	Location Error	m	integer
4	Location (X)	m	float
5	Location (Y)	m	float
6	Location (Z)	m	float
7	Moment	Nm	float
8	Energy	J	float
9	Moment P	Nm	float
10	Energy P	J	float
11	Moment S	Nm	float
12	Energy S	J	float
13	Number of triggers	-	Integer
14	Corner frequency	Hz	float
15	Static Stress Drop	Pa	float
16	Dynamic Stress Drop	Pa	float
17	Moment deviation	Nm	float
18	Energy Deviation	J	float
19	Corner frequency S	Hz	float

The use of a composites file makes it possible for the software to interpolate and extrapolate values from the seismic data into the blocks of the block model.

Each event of the EVP file is assigned coordinates as if it were a composite from the composites file. The format of the postprocessed data is presented in Table 4.2.

To show the manipulation used with each file, each field will be explained:

- compid: This field is the name of the composited group, since the same file can contain different composites groups.

TABLE 4.2: Postprocessed EVP as composite file

Column	Field	Units	Format
1	compid	-	Alphanumeric
2	dhid	-	Alphanumeric
3	MIDX	m	float
4	MIDY	m	float
5	MIDZ	m	float
6	TOPX	m	float
7	TOPY	m	float
8	TOPZ	m	float
9	BOTX	m	float
10	BOTY	m	float
11	BOTZ	m	float
12	Length	m	float
13	From	m	float
14	To	m	float
15	Geocod	-	float
16	Bound	-	float
17	Energy	J	float
18	Location Error	m	integer
19	Num.Triggers	-	integer
20	Ore	-	float

- dhid: This field stores the year and date combined using a concatenating function to obtain a format yyyymmdd_hhmmss, and can be used to restrict which samples or events are used in the estimations.
- MIDX, MIDY, MIDZ: These are the x, y, and z coordinates of the event. This field is later used to estimate the distance from the events to the center of the blocks, and weight their importance.
- TOPX, TOPY, TOPZ: These values are the same as the MIDX, MIDY, and MIDZ fields, and are only added to conform to the required composites file structure.
- BOTX, BOTY, BOTZ: These values are also the same as the MIDX, MIDY, and MIDZ fields, and are again added only to conform to the composites file structure needed.
- Length: This is a constant field with a value of one for the spatial length of each event.
- From: This is a constant field with a value of zero indicating the start of the event or sample.
- To: This is a constant field with a value of one indicating the end of the spatial length of the event.
- Geocod: This is a field used for insertion or addition of geological codes as needed to restrict the interpolations by lithology.
- Bound: This is a boundary code which allows the events need to be selected by a set of triangulations.
- Energy: This is the energy field from the EVP database, with the energy in joules.

- Location Error: This field represents the error in the location of the event, and can be used to restrict the number of events to use to a certain error range.
- Num.Triggers: This variable shows the number of seismic stations or triggers that were activated by the event
- Ore: This is a constant field with a value of zero, and is not used in the interpolation.

4.3 Block Model

To interpolate the data from the composites file, a block model large enough to cover the area of interest was created. The block model must also have the variables that are going to be used to store each one of the interpolations.

The block model used has an origin at the coordinates x=–500 m, y=–1,000 m, and z=1000 m. The extents of the model are 2,500 m in the east direction, 3,000 m in the north direction, and 2,000 m in the vertical direction.

The seismicity is analyzed by years, so a variable was created for each year in the block model from the year 1992 up to 2012.

The interpolated value of the average energy for each block is stored in a variable with the form yXXXX, where 'y' is the energy and XXXX is the year, ranging from 1992 to 2012. A second set of variables was also created to store the number of samples used for the estimation of each block, with the form nXXXX, where 'n' is the number of samples, and a third set of variables was created to show the real interpolated value of the sum of the energy in each block, rXXXX, where 'r' is the real value. Finally, the accumulated interpolated values for each year have the form aXXXX, where 'a' is the

accumulated value. Each of the variables created is of the data type "double," and has an assigned default value of zero.

The basic configuration of the model in the software is presented in Figures 4.1 to 4.6.

The model comprises a total of 84 different variables that can be assigned to blocks in the block model, when an anslysis is designed on a yearly basis.

4.4 Interpolation

To calculate the sum of the energy from seismic events for each block of the block model, three variables are used: one variable to estimate an average of the energy values, a second variable to store the number of samples used in the estimation for each block, and a third variable which is the product of the first two, and represents the total energy released by all the events inside of the block.

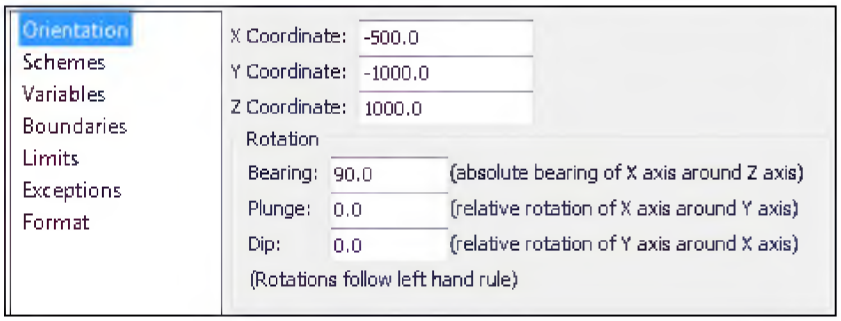

FIGURE 4.1 Block model orientation parameters

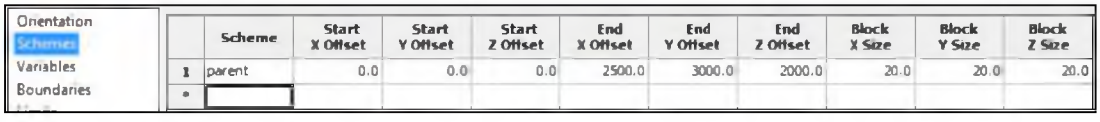

FIGURE 4.2 Extent and size of the blocks in the block model

Orientation
Schemes
Variables
Boundaries
Limits
Exceptions
Format

	Variable	Data Type	Default Value
1	y1992	Double (Real * 8)	0
2	y1993	Double (Real * 8)	0
3	y1994	Double (Real * 8)	0
4	y1995	Double (Real * 8)	0
5	y1996	Double (Real * 8)	0
6	y1997	Double (Real * 8)	0
7	y1998	Double (Real * 8)	0
8	y1999	Double (Real * 8)	0
9	y2000	Double (Real * 8)	0
10	y2001	Double (Real * 8)	0
11	y2002	Double (Real * 8)	0
12	y2003	Double (Real * 8)	0
13	y2004	Double (Real * 8)	0
14	y2005	Double (Real * 8)	0
15	y2006	Double (Real * 8)	0
16	y2007	Double (Real * 8)	0
17	y2008	Double (Real * 8)	0
18	y2009	Double (Real * 8)	0
19	y2010	Double (Real * 8)	0
20	y2011	Double (Real * 8)	0
21	y2012	Double (Real * 8)	0

FIGURE 4.3 Variables for each year in the block model

Orientation
Schemes
Variables
Boundaries
Limits
Exceptions
Format

	Variable	Data Type	Default Value
22	n1992	Double (Real * 8)	0
23	n1993	Double (Real * 8)	0
24	n1994	Double (Real * 8)	0
25	n1995	Double (Real * 8)	0
26	n1996	Double (Real * 8)	0
27	n1997	Double (Real * 8)	0
28	n1998	Double (Real * 8)	0
29	n1999	Double (Real * 8)	0
30	n2000	Double (Real * 8)	0
31	n2001	Double (Real * 8)	0
32	n2002	Double (Real * 8)	0
33	n2003	Double (Real * 8)	0
34	n2004	Double (Real * 8)	0
35	n2005	Double (Real * 8)	0
36	n2006	Double (Real * 8)	0
37	n2007	Double (Real * 8)	0
38	n2008	Double (Real * 8)	0
39	n2009	Double (Real * 8)	0
40	n2010	Double (Real * 8)	0
41	n2011	Double (Real * 8)	0
42	n2012	Double (Real * 8)	0

FIGURE 4.4 Variables for the number of samples estimated on each block

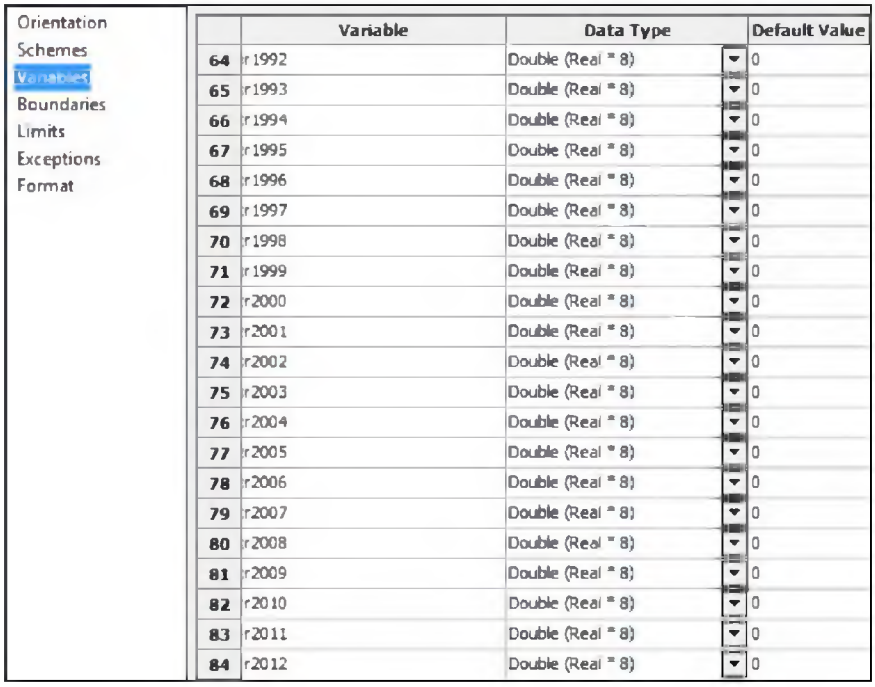

	Variable	Data Type	Default Value
64	r1992	Double (Real * 8)	0
65	r1993	Double (Real * 8)	0
66	r1994	Double (Real * 8)	0
67	r1995	Double (Real * 8)	0
68	r1996	Double (Real * 8)	0
69	r1997	Double (Real * 8)	0
70	r1998	Double (Real * 8)	0
71	r1999	Double (Real * 8)	0
72	r2000	Double (Real * 8)	0
73	r2001	Double (Real * 8)	0
74	r2002	Double (Real * 8)	0
75	r2003	Double (Real * 8)	0
76	r2004	Double (Real * 8)	0
77	r2005	Double (Real * 8)	0
78	r2006	Double (Real * 8)	0
79	r2007	Double (Real * 8)	0
80	r2008	Double (Real * 8)	0
81	r2009	Double (Real * 8)	0
82	r2010	Double (Real * 8)	0
83	r2011	Double (Real * 8)	0
84	r2012	Double (Real * 8)	0

FIGURE 4.5 Variables for the final yearly estimated values

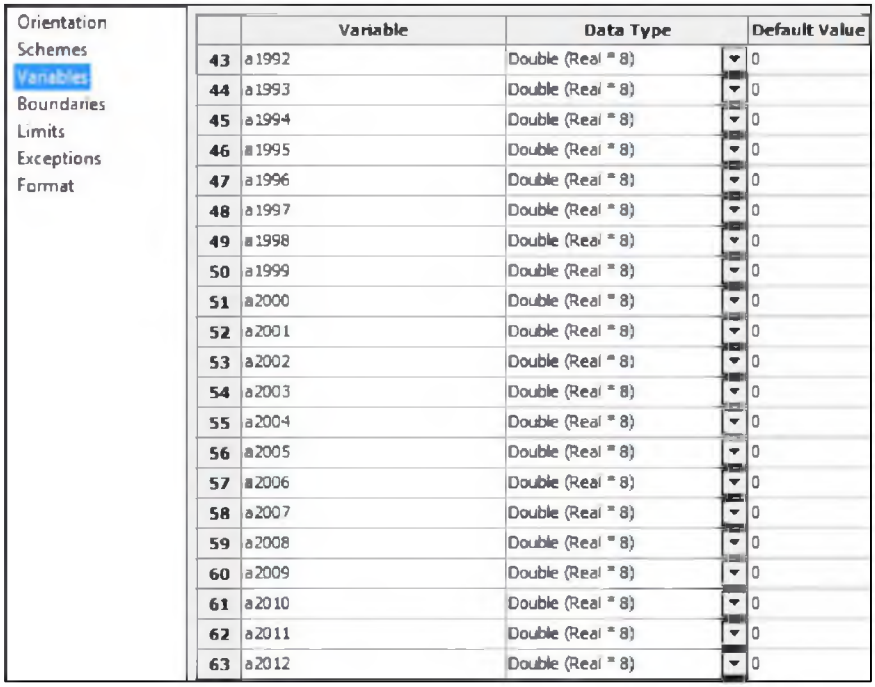

	Variable	Data Type	Default Value
43	a1992	Double (Real * 8)	0
44	a1993	Double (Real * 8)	0
45	a1994	Double (Real * 8)	0
46	a1995	Double (Real * 8)	0
47	a1996	Double (Real * 8)	0
48	a1997	Double (Real * 8)	0
49	a1998	Double (Real * 8)	0
50	a1999	Double (Real * 8)	0
51	a2000	Double (Real * 8)	0
52	a2001	Double (Real * 8)	0
53	a2002	Double (Real * 8)	0
54	a2003	Double (Real * 8)	0
55	a2004	Double (Real * 8)	0
56	a2005	Double (Real * 8)	0
57	a2006	Double (Real * 8)	0
58	a2007	Double (Real * 8)	0
59	a2008	Double (Real * 8)	0
60	a2009	Double (Real * 8)	0
61	a2010	Double (Real * 8)	0
62	a2011	Double (Real * 8)	0
63	a2012	Double (Real * 8)	0

FIGURE 4.6 Variables for studying the accumulated interpolated values each year

To establish the averages of the values involved in the interpolations, with variables such as location error and the numbers of triggers, an inverse-distance approach was applied.

Figures 4.7–4.10 show an example of the energy interpolation for the year 1992, with copies of the relevant screens from Vulcan. The interpolated value is stored in y1992 and the number of samples used in the interpolation is stored in n1992 (Figure 4.7).

The search region defined is dependent on the block size in the block model. For cubic blocks of 20 m on each side, the search area used is 10 m in each direction from the center of the block, thus including a total of 800 cubic meters in the search for the total number of samples that fall inside of the block volume (Figure 4.8).

The inverse-distance power used in the interpolation is zero, so that the interpolation calculates a weighted average of the values inside of the block (where each value has the same weight). The interpolated value is then used in conjunction with the variable that stores the number of samples to estimate the sum of the energy that was accumulated inside each block (Figure 4.9). Using a value of one in the inverse-distance interpolation would provide a weighted average where the values closer to the center of the block have a greater weight in the estimation of the block average.

The medium composite coordinates are used to position the samples in space and to establish the values that fall inside of the boundaries of each block. The energy or magnitude values of these composites are used in the interpolation for each of the blocks (Figure 4.10).

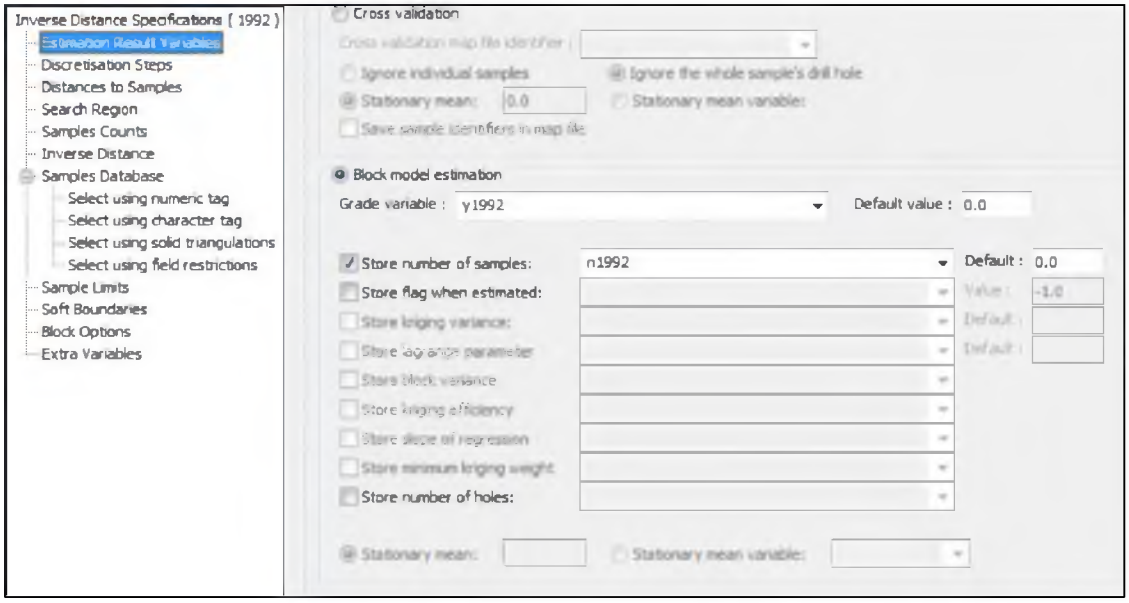

FIGURE 4.7 Estimation and storage variables used for year 1992

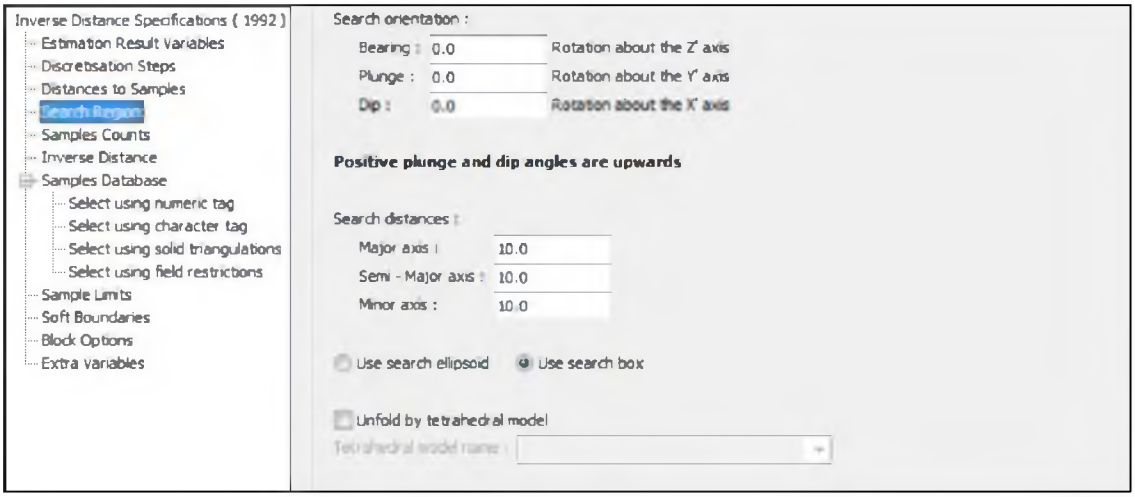

FIGURE 4.8 Search region restrictions used for 20m cubic blocks

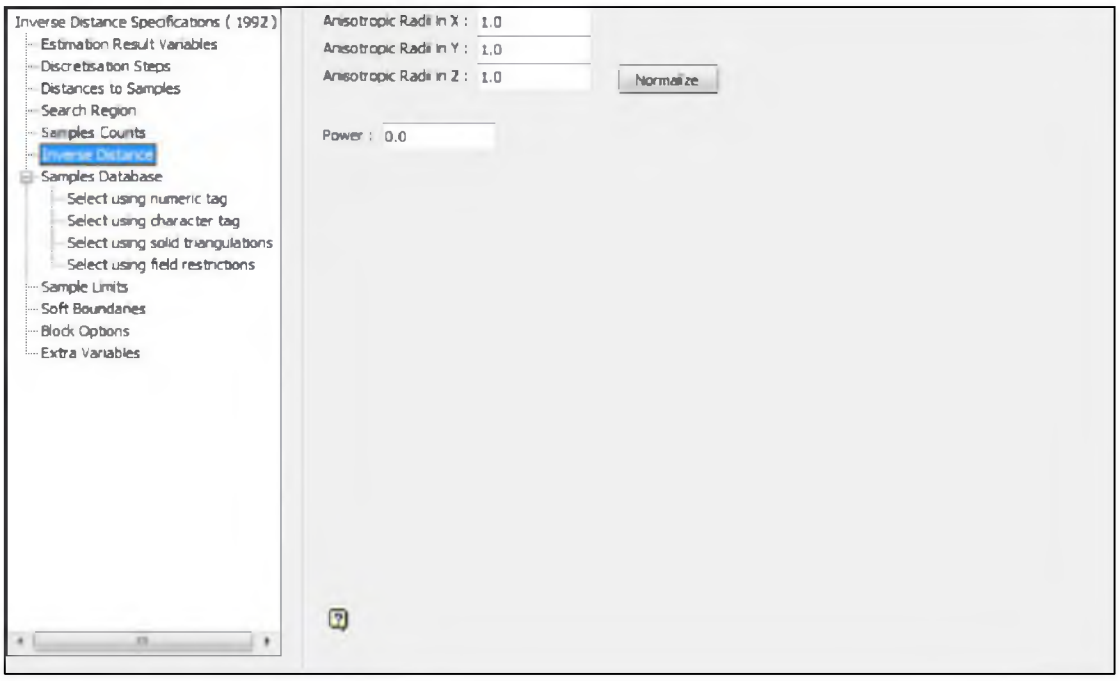

FIGURE 4.9 Inverse distance power to zero used in the interpolation

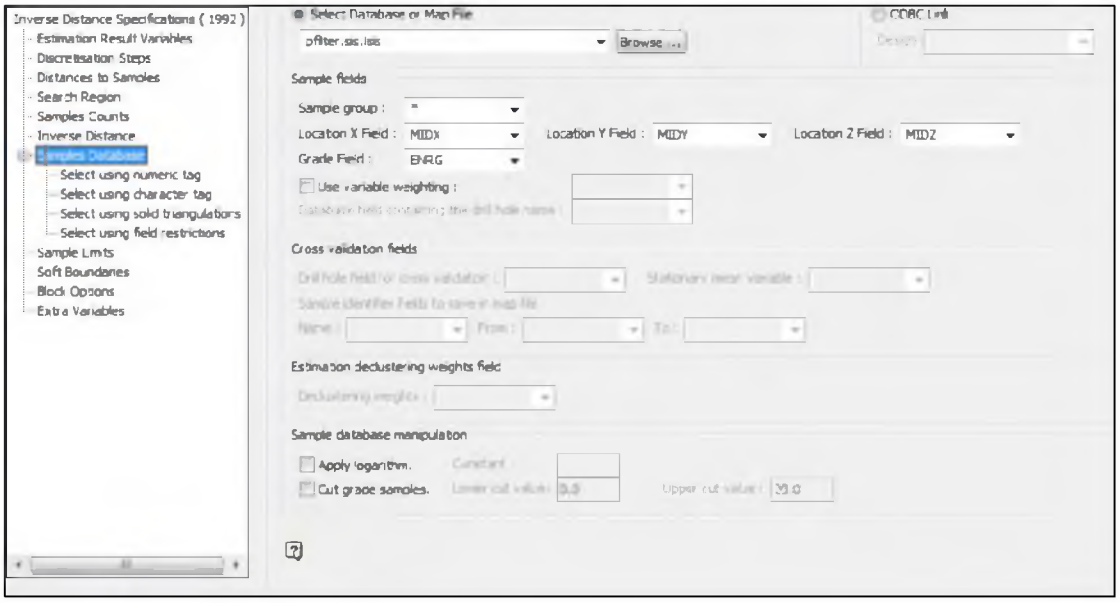

FIGURE 4.10 Location fields used in the interpolation

4.5 Data Display

The advantage of interpolating data into blocks is that the estimated values can be displayed in 3-D, as sections and volumes. The sections can be displayed as pure blocks or if needed, sets of sections can be created for any selected direction, to display text data stored within the blocks, as shown in Figures 4.11 to 4.13.

The advanced loading options in Vulcan and other programs allow the user to restrict the display of one variable based on selected combinations of restrictions. For example, the user may select blocks in which the energy or magnitude is above a defined cutoff value (hiding the values that are not required in the visualization), and also to restrict the blocks with an average location error less than 20 m or an average number of seismic stations that recorded the events in each block to more than six.

The use of such options and combinations allows the analysis of areas where high concentrations of energy are located, while also minimizing the location errors of the events by using location and trigger restrictions.

When all the relevant information from the seismic database is assigned to blocks, it is possible to quantify and analyze the interpolated values at various ranges, and to associate them with existent mining conditions at certain periods.

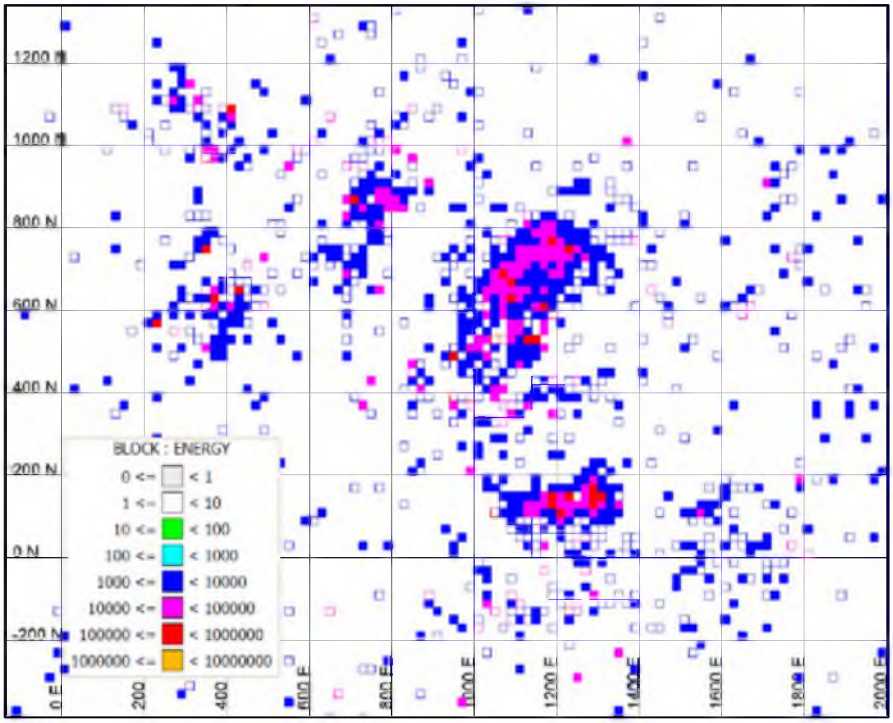

FIGURE 4.11 Level 2220 plan view of blocks with energy cut-off set at 10,000 J

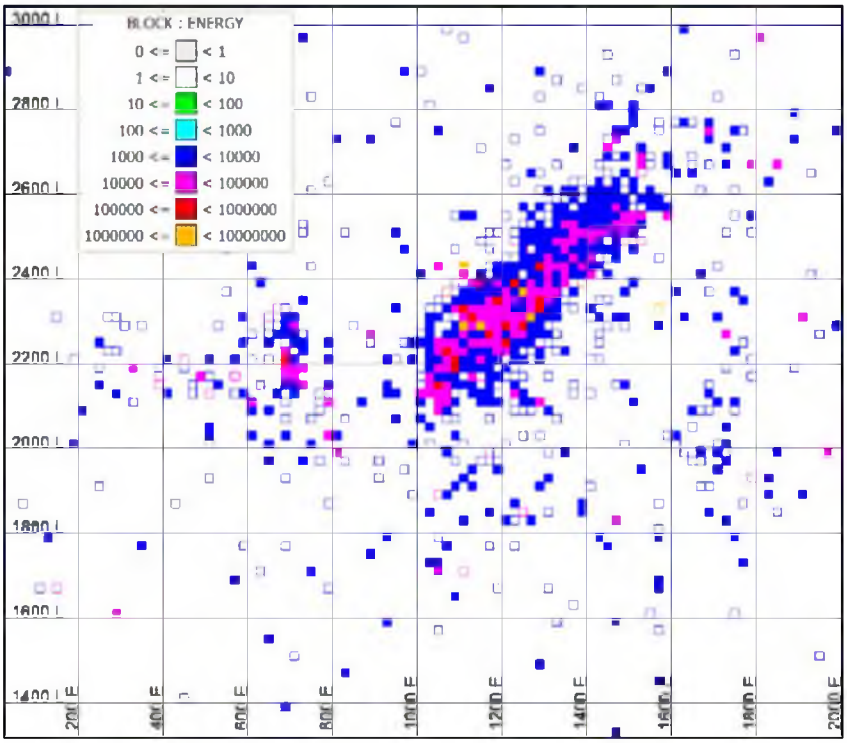

FIGURE 4.12 WE section 700N of blocks with energy cut-off set at 10,000 J

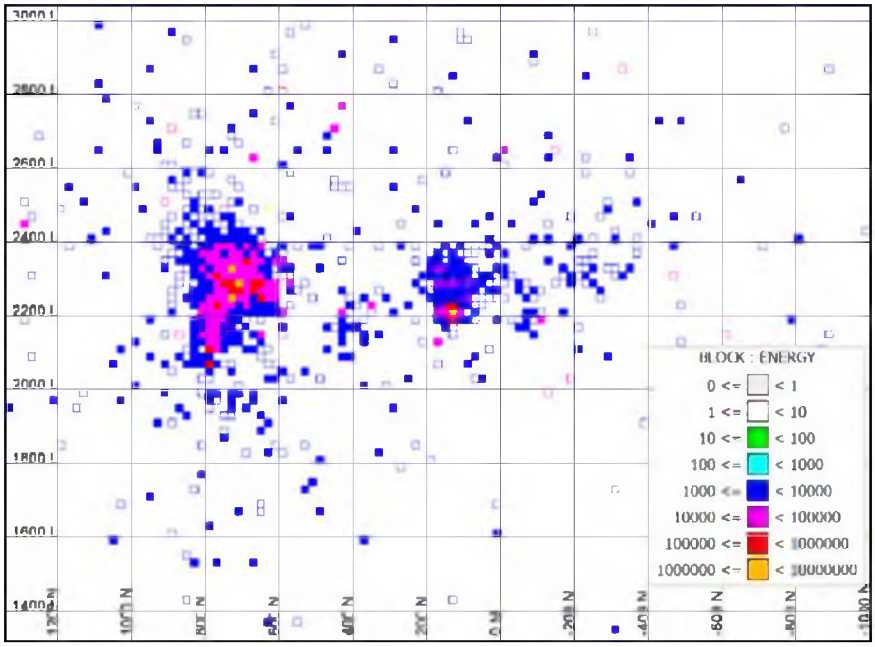

FIGURE 4.13 NS section 1200E of blocks with energy cut-off set at 10,000 J

5 THREE-DIMENSIONAL MODELING OF PROGRESSIVE SEISMIC ACTIVITY USING BLOCK MODELING TECHNIQUES

5.1 Scope of the Study

In this study, the modeling of the seismic events was developed using data from a large underground copper mine that is mined using panel caving techniques. The mine is composed of several smaller production areas, also referred to as mines, that work as independent units.

The development is carried in a top-down manner, with older projects that are caved and depleted on the upper levels of the mine, and the new producing projects being developed below the older areas.

The caving history of the mine has created a subsidence cave that extends to the surface, and as new projects are developed, they continue to connect to the existing cave from the previous projects in the upper levels.

The study was conducted using actual seismic data from the underground mine. The area under study covers a total of 7.5 km^2 (2.5 km on the east, 3 km on the north, and 2 km in elevation).

The seismic data at the mine have been collected since 1992 and thus represent the evolution of the seismic events for a period of 21 years, with more than two million events recorded.

The modeling was first developed at a yearly resolution, to check the results and the consistency of the modeling process. When the yearly models were seen to be satisfactory, a monthly model was also developed to obtain a better time resolution.

5.2 Elements of the Model

The modeling process can be divided in a series of steps (Figure 5.1). In the first step, the output data from the seismic network are organized into the required format, with the date, time, location error, triggered stations, energy, and magnitude for each event. In the second step, the information is preprocessed in a database manager package to create a file readable by the interpolation package in Vulcan. In the third step, the parameters for the block model are defined—origin, extents, size of blocks, and interpolation parameters. In the fourth step, the data are interpolated into the blocks, and the interpolated variables are manipulated as required. Finally, in the fifth step, the desired models are created and analyzed.

5.2.1 Input Data File

The model is based on the information collected from the seismic network for the events associated with the different mining-related activities taking place from 1992 to 2012. The data were provided as a comma-separated-values (CSV) file, comprising information on date, time, location error, location coordinates, moment, energy, and triggers for each of the associated seismic events.

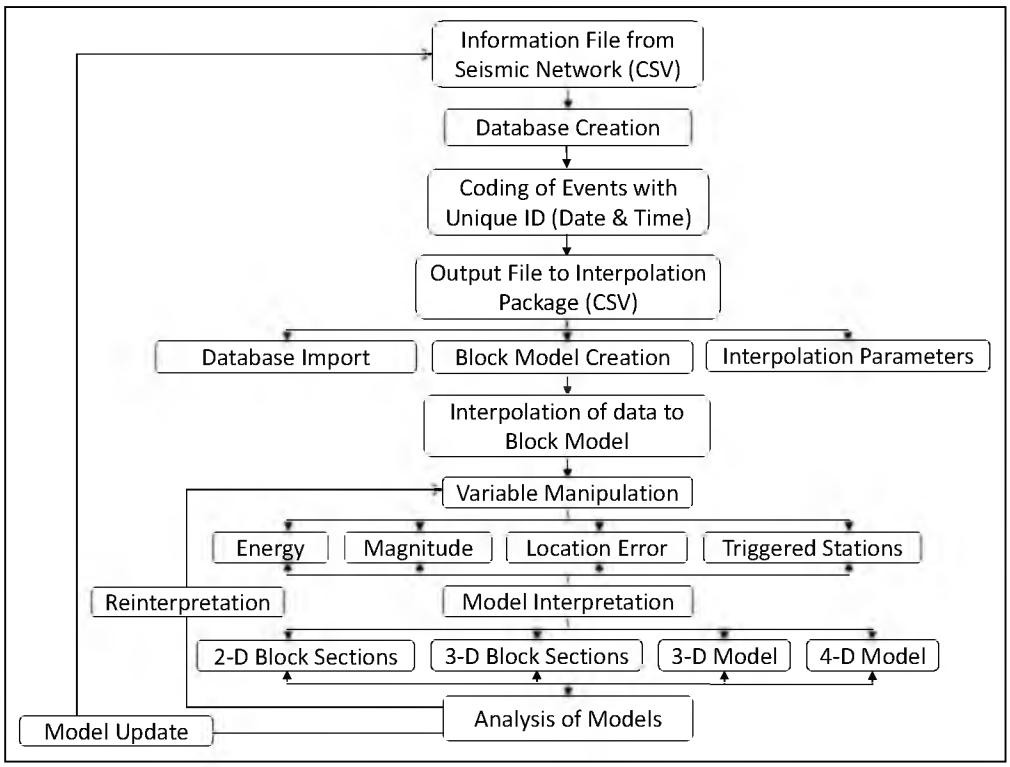

FIGURE 5.1 Activities for modeling the progressive seismic activity

5.2.2 Data Preprocessing

The input data are loaded into MS Access to build a database that can be accessed by the interpolation software, where each event is associated with its specific location using the input data file coordinates. The events are uniquely marked by combining the date and time of the event. The variables from the input data file that must be considered are also selected and associated with the events. The resulting data file can be used to interpolate the seismic event values in the file from the selected variables into the blocks of the block model. The generated file resembles the original seismic event file, but with the variables ordered in a different manner and with added variables that are used in the interpolation process.

5.2.3 Block Model

A block model covering the area of interest is defined by the origin coordinates (the minima in the east and north and the lowest point in the elevation of a box that covers the area of interest) and the extension of the model from that origin point. The used origin coordinates were East: 500 m, North: –1,000 m, and Elevation 1,000 m, with elevation in meters above sea level. The extents from the origin point are 2,500 m to the east, 3,000 m to the north, and 2,000 m in elevation. The resulting model covers a volume of 15,000,000 m^3. The block size used was the same as that used in the mine operations model, 20×20×20 m. Thus, the model has a total of 1,875,000 blocks.

5.2.4 Data Interpolation

The data were loaded into Vulcan to combine it with the block model using the modified inverse-distance interpolation technique previously described. That technique locates the events located inside each block and interpolates the data as monthly or weekly variables.

The data interpolated into each block are associated by the block identification variable for the date. For example, the variable for May 2010 is y201005, and the events within the block for May 2010 have the unique id of 201005xxx, where xxx represents the rest of the string containing the day and time of the event.

The interpolated data (magnitude, energy, triggered stations, and location error) come from the seismic file, and are interpolated into the blocks of the block model.

5.2.5 Interpolation Verification

Once the interpolations are performed, the data interpolated into the block model are checked against the seismic events from the database. An example is shown in Figure 5.2. In the upper left of the block in white, the value 2.27 is the rounded average of the energy (in joules) inside the block. That average comes from four values, as shown with the number four at the center of the block. The lower right corner of the block shows the value for the sum of the energy of the events within the block dimensions, 9.06 J.

The 9.06 J value comes from multiplying the average energy, 2.27 J, and the number of samples (four). The colors of the blocks in Figure 5.2 represent the changes in the energy for each block shown.

To check that the values were correct, the seismic events inside of the block dimensions were isolated in the MS Access database, as shown at the bottom of Figure 5.2. Here the four values correspond to values from the year 2010, the first on April 10 at 7:15 A.M., the second on July 12 at 8:14 A.M., the third on September 26 at 8:27 A.M., and the last on October 9 at 3:39 AM. The database image also shows that there were four events located inside the block for the 2010 period.

When the first yearly models were working correctly, the next step was to take the analysis to a finer level of detail, using monthly data 1992 to 2012. Monthly modeling provides a better analysis resolution when analyzing the correlation of relevant seismic events and the previous releases of energy at the mine. Obviously, the size of the model increased markedly when it was expanded to include monthly data.

The use of many variables in the block models depends solely on the accepted file size for the system and the number of parameters allowed by the interpolation software.

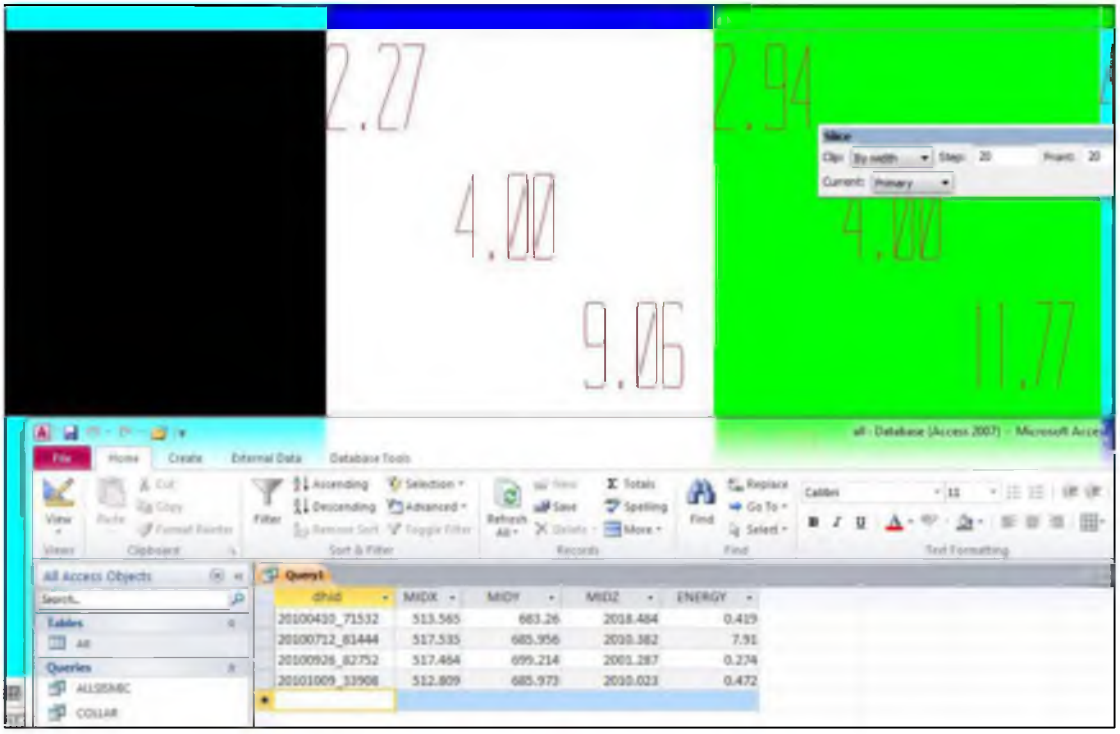

FIGURE 5.2 Energy average, number of samples, and multiplication result with values from the MS Access Database

The monthly model requires at least 980 variables for each block in the block model: 252 variables for each monthly interpolation, and the same number for the number of samples, location error, and triggered stations, respectively. These variables are required to store just averages, number of samples, real values, and accumulated values on a monthly basis. Thus, the block model becomes quite large, and an appropriately sized computer is required to expedite manipulation and analysis.

5.2.6 Modeling the Interpolated Data

The interpolated data for the blocks are analyzed and grouped into volumes to display any of the block model variables in space.

Triangulations are created as shells of the information extracted from the block model. A triangulation is a closed solid shell defined by triangles. This creation of triangulations for different types of data restrictions allows the convenient visualization of the seismic data from a variety of perspectives. A few of the base models created are:

- Energy and magnitude for a specific year or month, filtered by trigger number, location error, or both.
- Energy or magnitude for a specific accumulation of years, which can also be filtered by triggers, location error, or both.
- Energy or magnitude located inside a specific area in the mine, such as an area to cave, a mine level, or a future project footprint.

The interpolated data are used to create 3-D, solid shapes that represent accumulations of seismic energy, as restricted by the number of triggered stations, location error, or any other variable in the interpolated data.

5.2.7 Sectioning the Data Solids

The interpolated data from the block model were used to create sections of the blocks and of the triangulation solids to display the seismic variables with restrictions like those mentioned in Section 5.1.5.

5.2.8 Model Results

The resulting values from the interpolation were used to create 3-D solids representing the associated released energy by year at the mine (Figure 5.3).

A similar model was developed to show in 3-D solids the accumulated seismic energy at the mine every year 1992 to 2012. Figure 5.4 shows an example of the radiated seismic energy for year 2011 and its comparison to the radiated seismic energy from 1992 up to 2011.

The same procedure can be used to study the compare the accumulated seismic energy for other years of the model, for example, between 2005 and 2010.

The initial results of the models with a yearly resolution, from 1992 to 2012, are presented in Appendix A. The solids shown represent the energy radiated from the events at a cut-off level of 90,000 J for each year.

The second model developed accumulates the events on a yearly basis, modeling how the seismic radiated energy is accumulated year after year for the whole mine, starting in 1992. The results for the second base model are presented in Appendix B.

5.3 Detailed Yearly Modeling

The effect of the seismic activity can be studied in more detail by focusing on specific criteria. For example, one could isolate specific areas at a certain elevation or between certain coordinates, or look at the energy ranges in the sections under study.

Figures 5.5 to 5.16, are west-east, north-south, and plan sections, all at an elevation of 2,194 m. They show how the radiated energy in joules can be sequentially studied, at increasingly fine detail, by filtering the blocks by location error and number of triggers.

The ranges used to color the data are representative of the wide spectrum of values in the blocks.

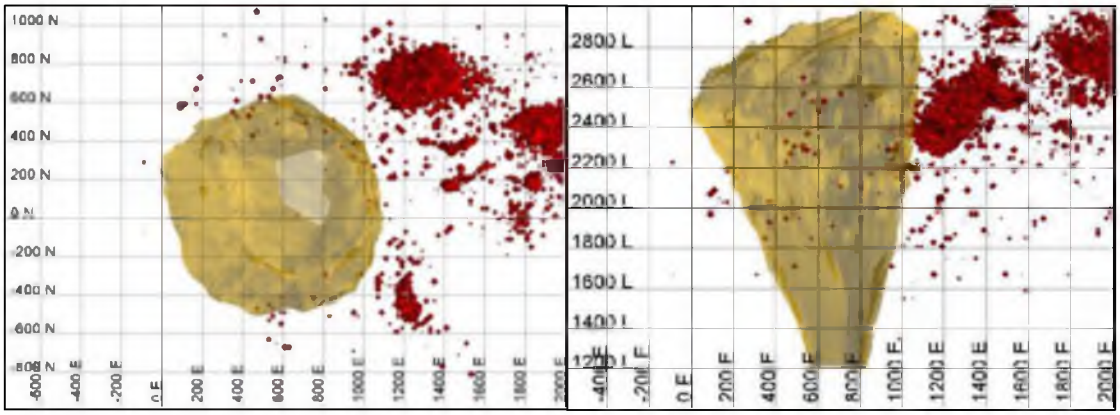

FIGURE 5.3 Plan (left) and WE view (right) of the 3-D generated solids for the radiated energy during the year 1995

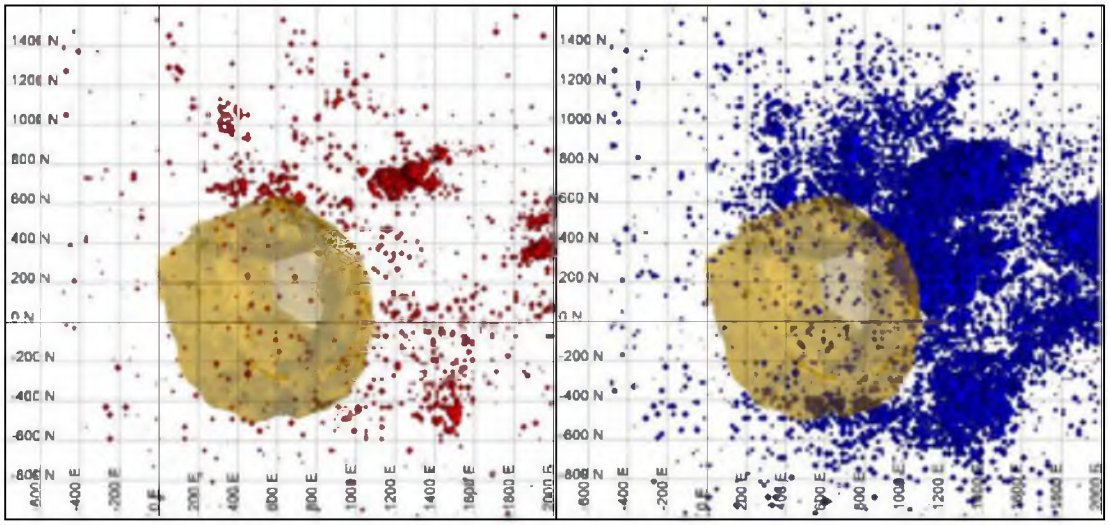

Figure 5.4 Plan view of the radiated seismic energy during year 2011 (left) and the accumulated seismic energy up to year 2011 (right)

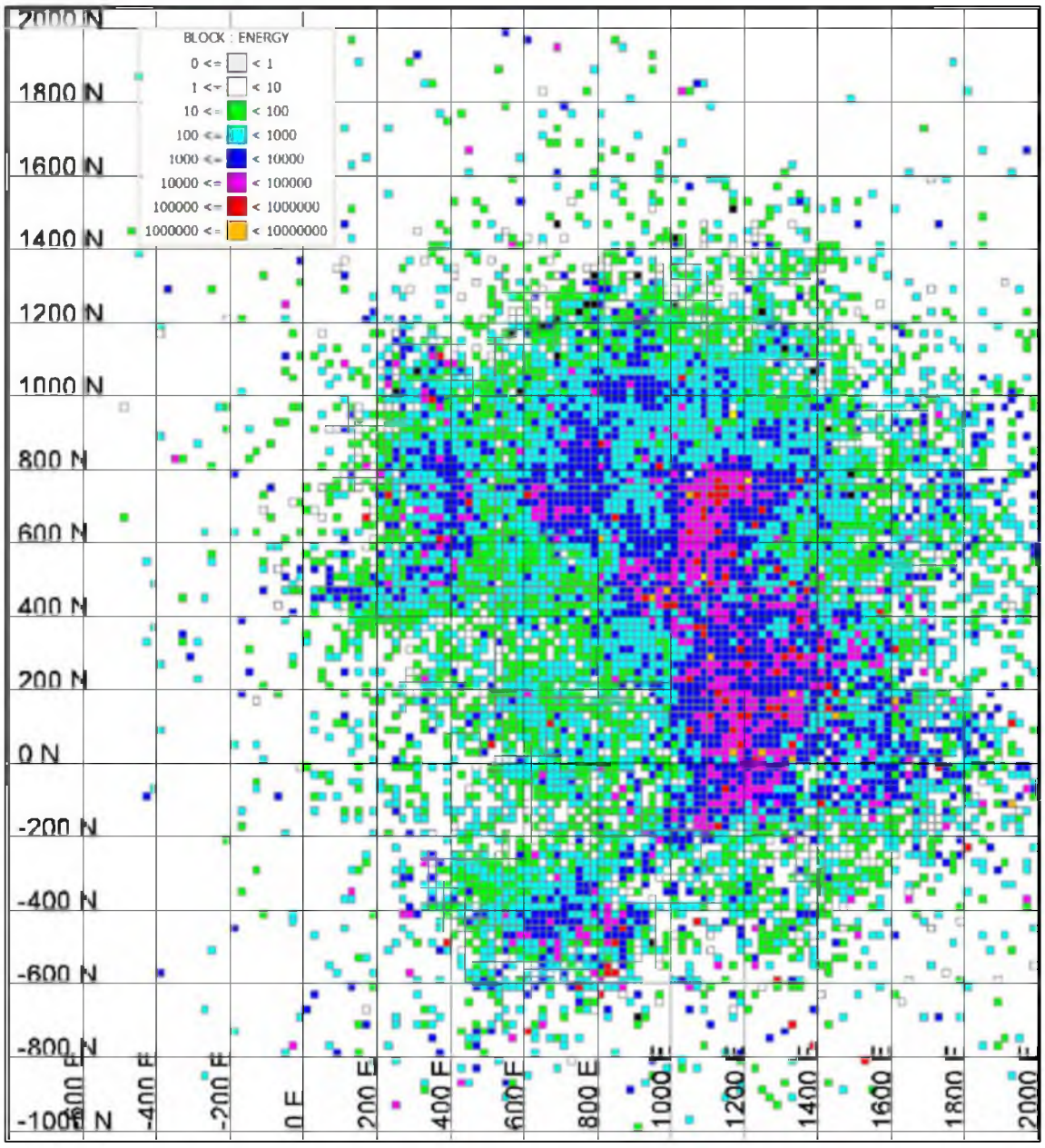

FIGURE 5.5 Plan view level 2,194 - Accumulated energy in blocks up to year 2012

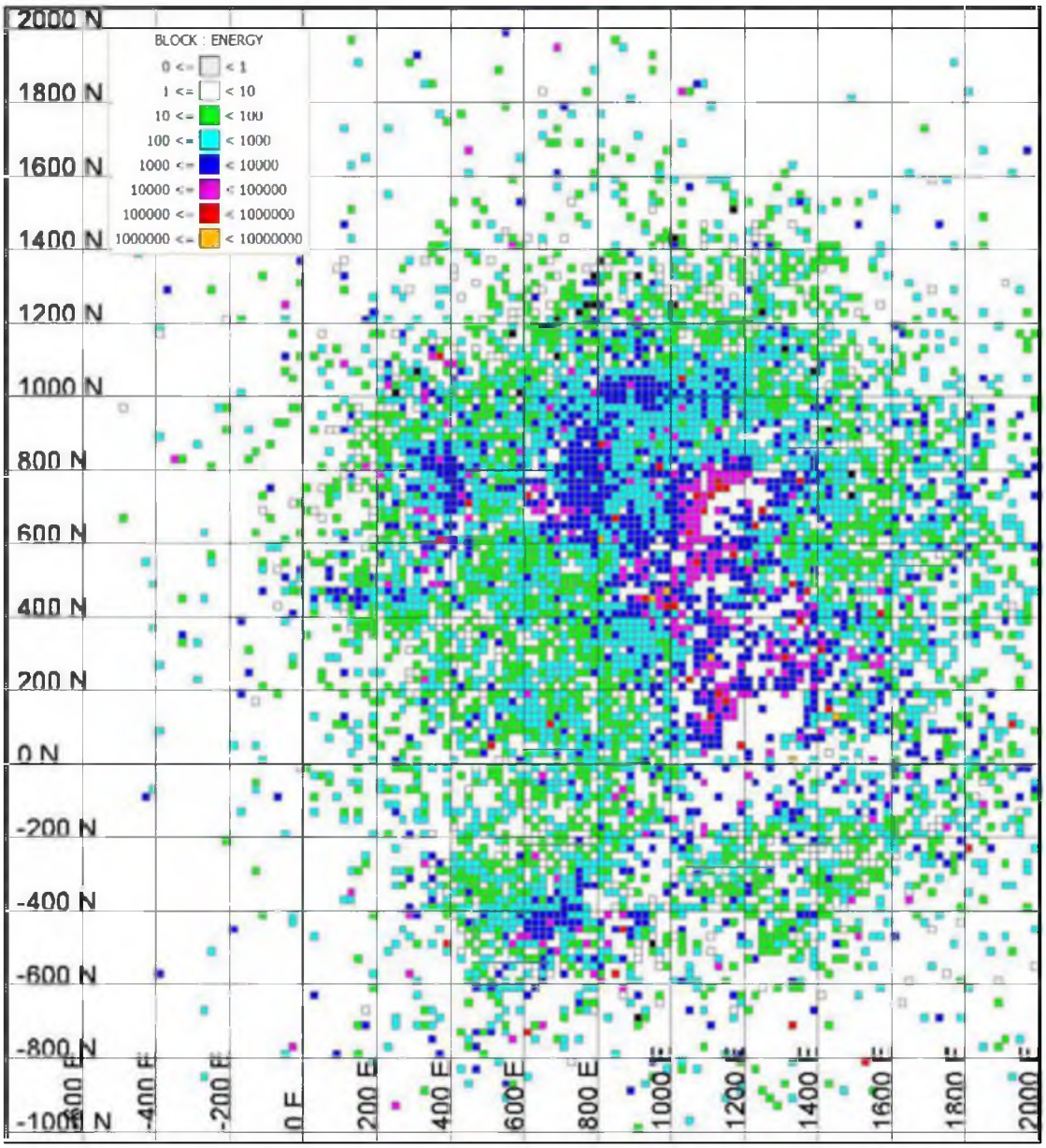

FIGURE 5.6 Plan view level 2,194 - Accumulated energy in blocks up to year 2012 with average of triggered stations greater than or equal to 5

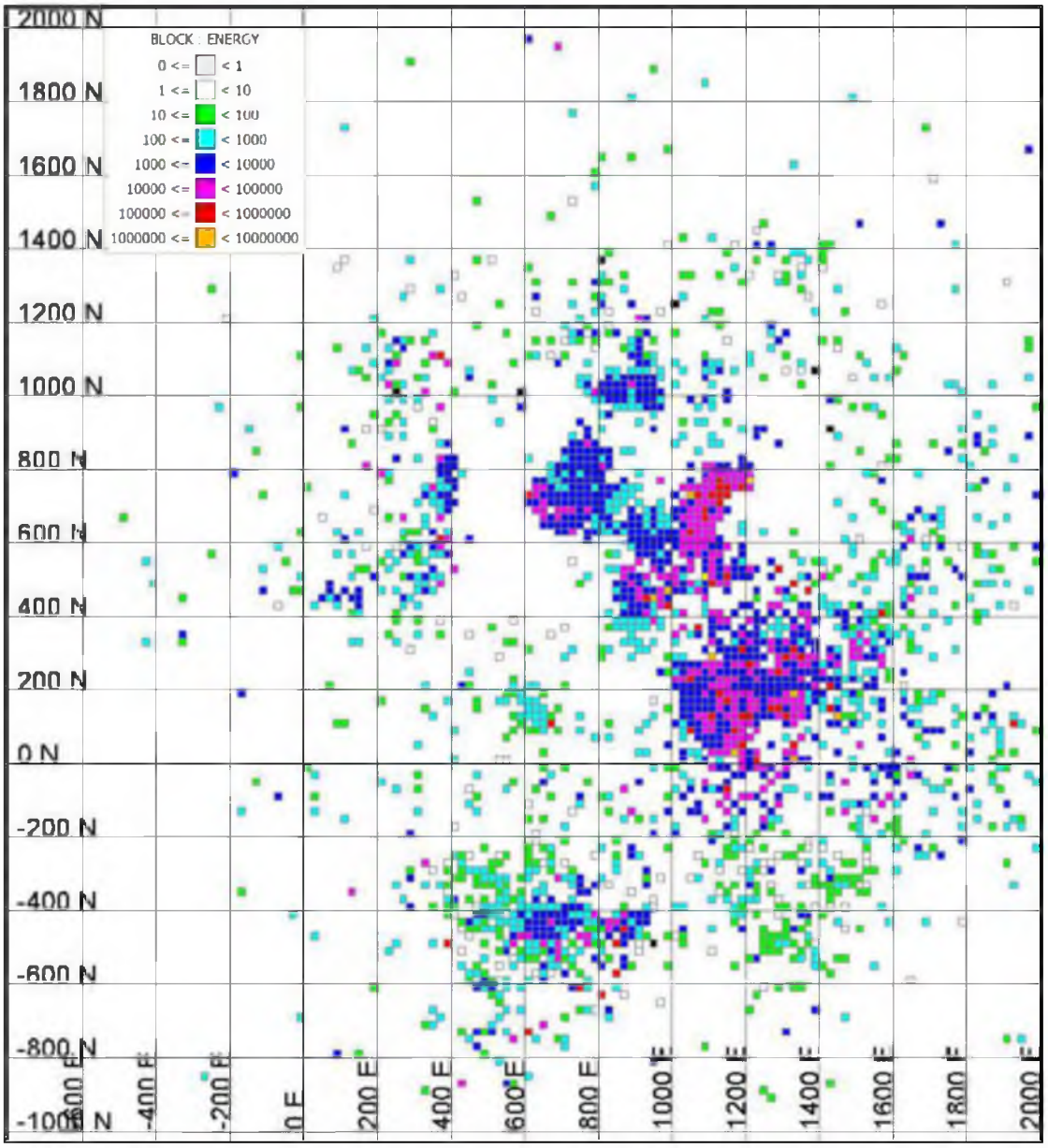

FIGURE 5.7 Plan view level 2,194 - Accumulated energy in blocks up to year 2012 with an average location error in blocks of less than 20 m

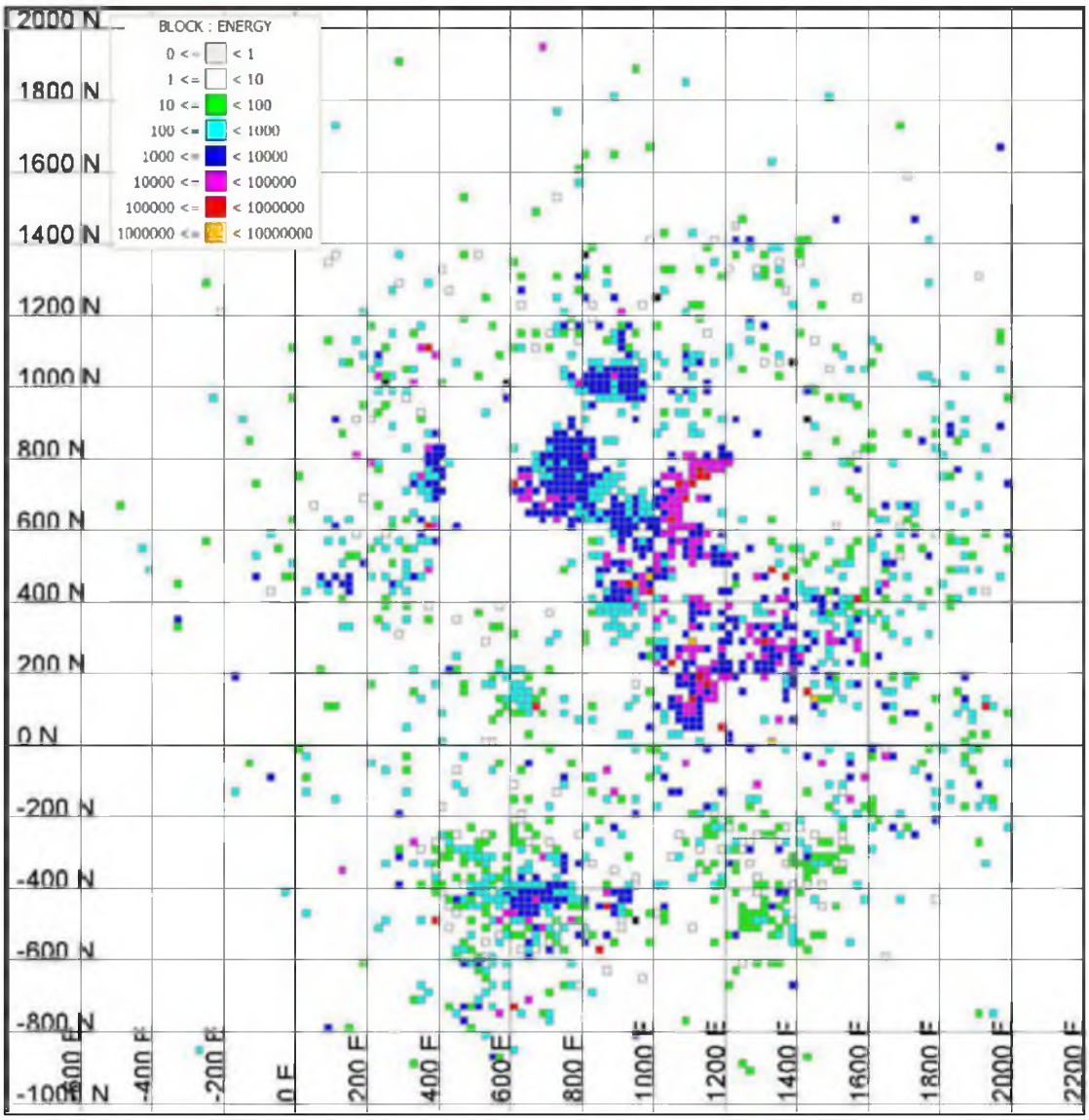

FIGURE 5.8 Plan view level 2,194 - Accumulated energy in blocks up to year 2012 with an average location error in blocks less than or equal to 20m and an average of 5 or more stations triggered by the events within the block

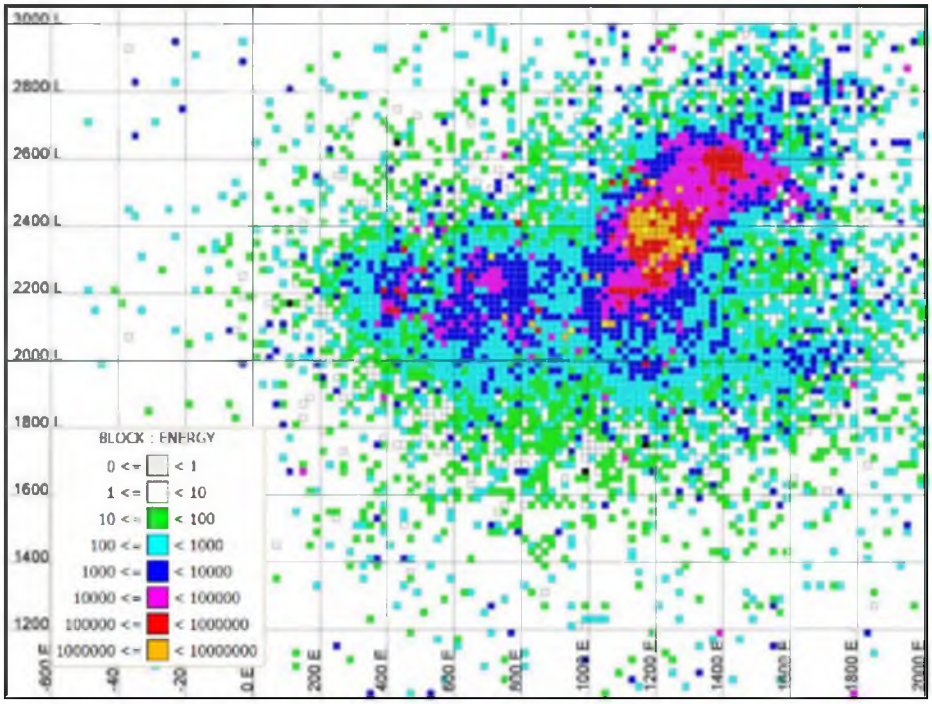

FIGURE 5.9 Section 700N - Accumulated energy in blocks up to year 2012

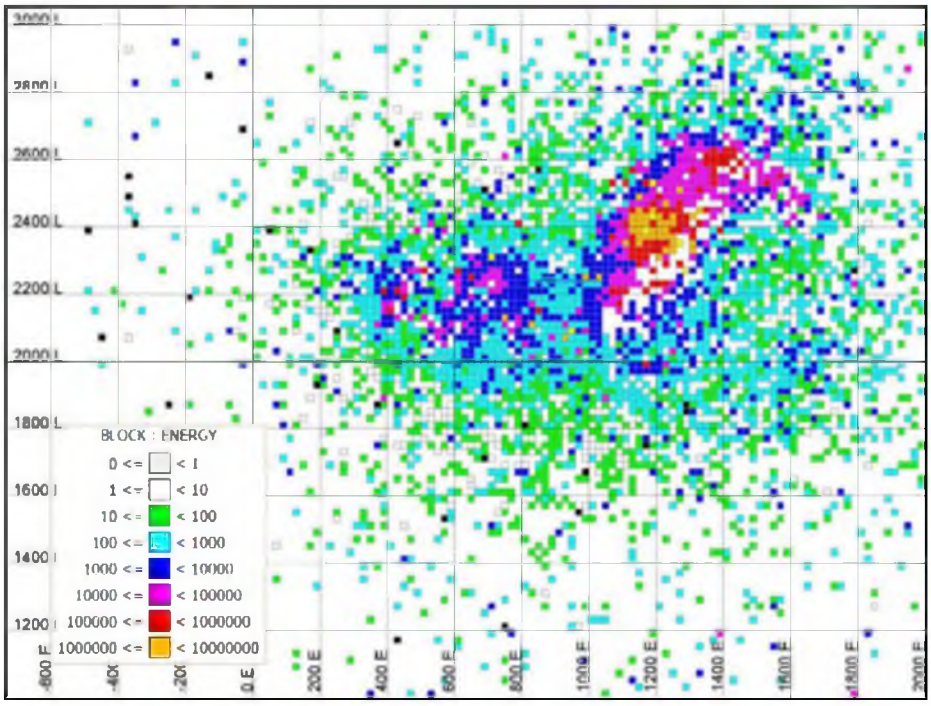

FIGURE 5.10 Section 700N - Accumulated energy in blocks up to year 2012 with average of triggered stations greater than or equal to 5

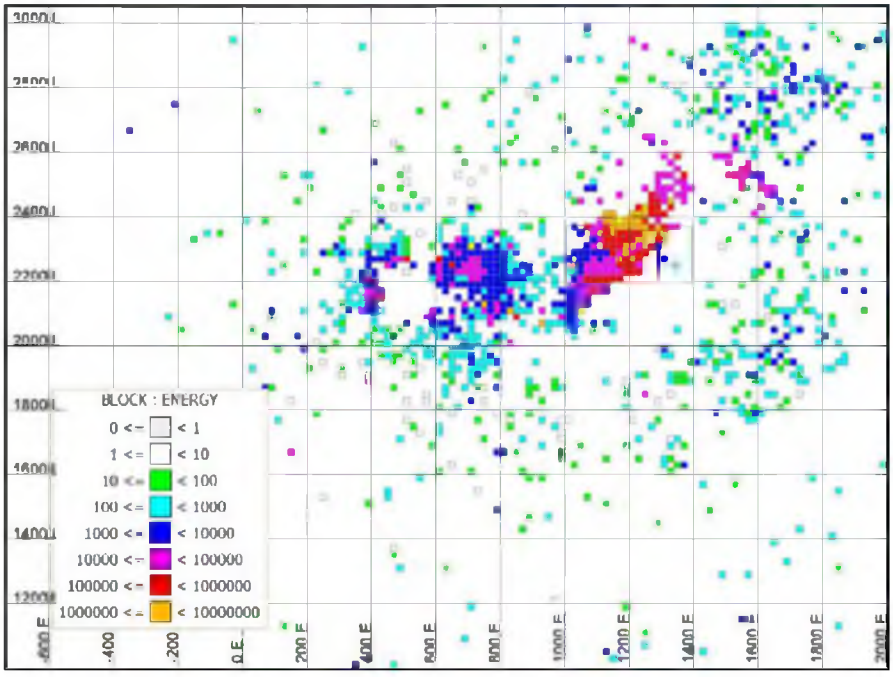

FIGURE 5.11 Section 700N - Accumulated energy in blocks up to year 2012 with an average location error in blocks of less than 20 m

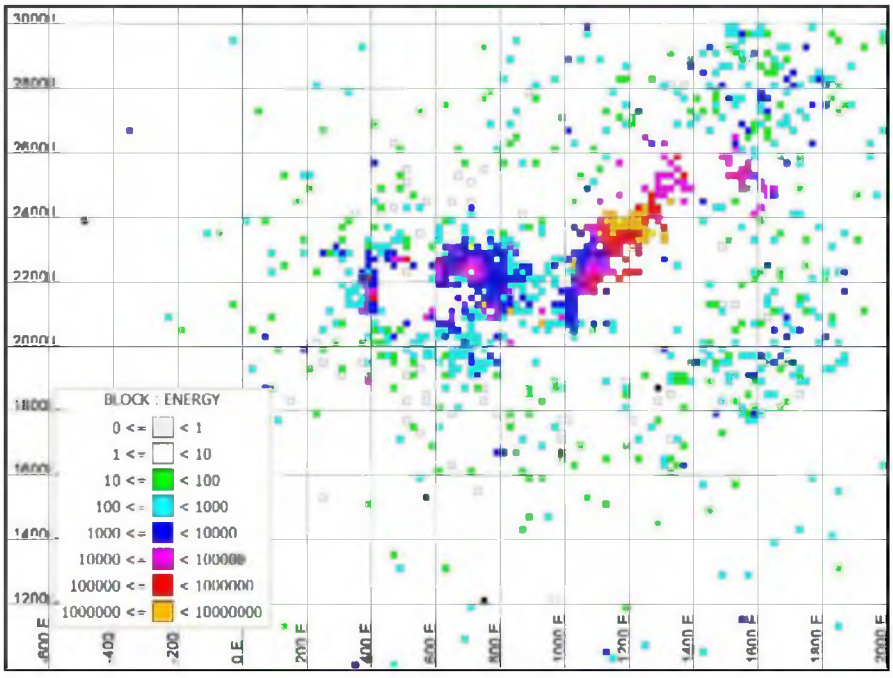

FIGURE 5.12 Section 700N - Accumulated energy in blocks up to year 2012 with an average location error in blocks less than or equal to 20m and an average of 5 or more stations triggered by the events within the block

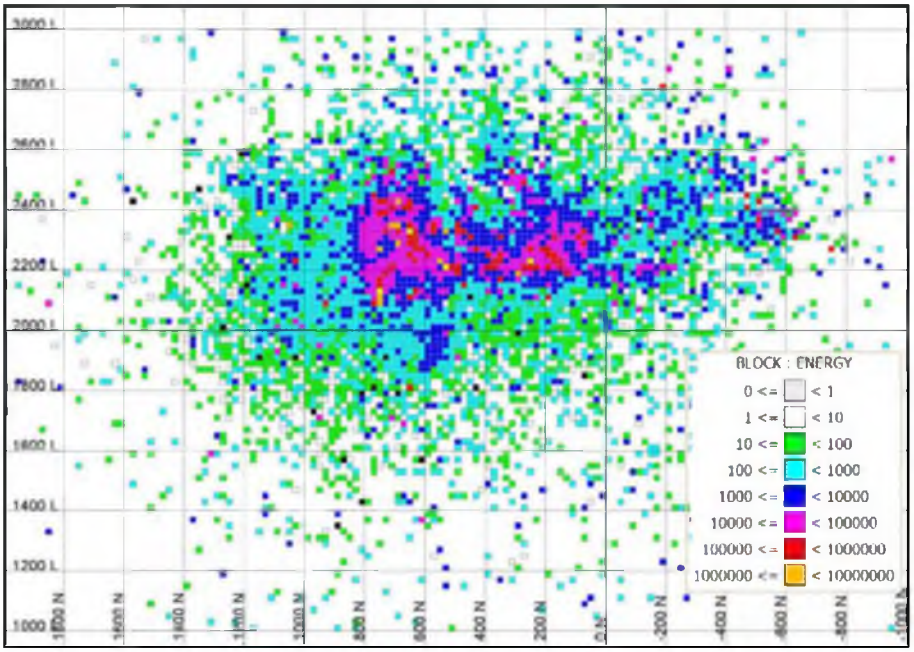

FIGURE 5.13 Section 1,100E - Accumulated energy in blocks up to year 2012

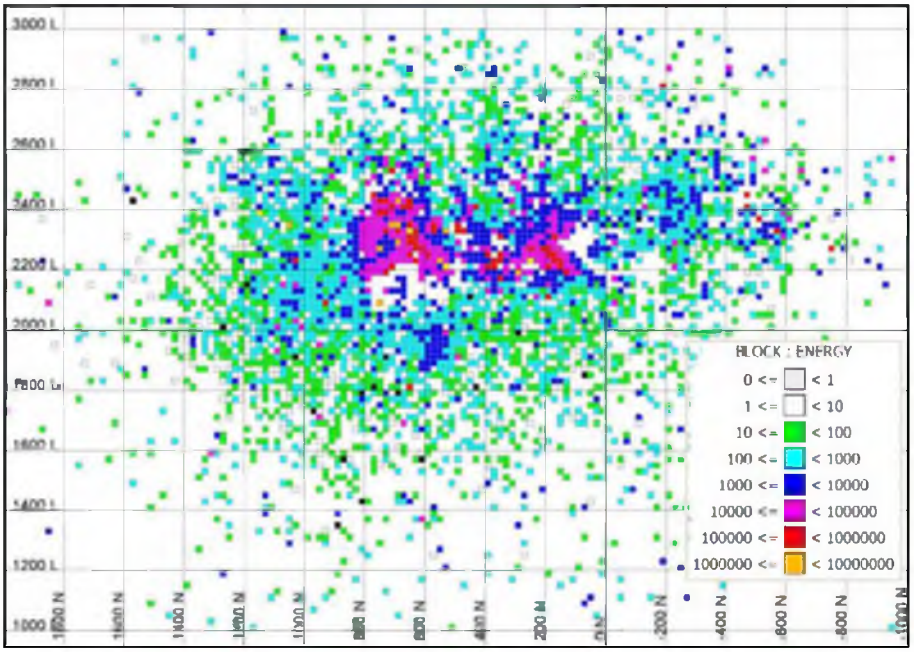

FIGURE 5.14 Section 1,100E - Accumulated energy in blocks up to year 2012 with average of triggered stations greater than or equal to 5

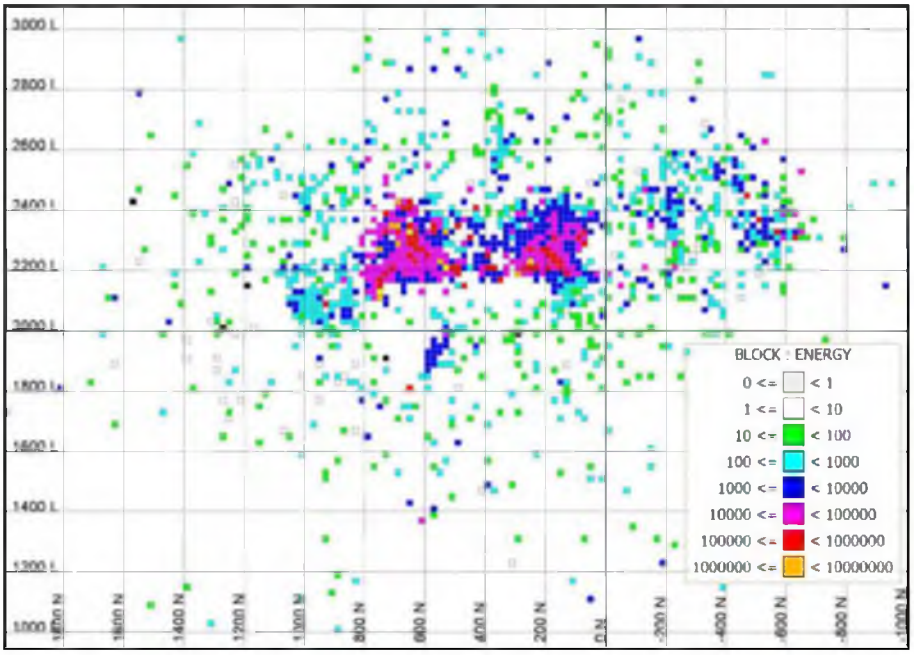

FIGURE 5.15 Section 1,100E - Accumulated energy in blocks up to year 2012 with an average location error in blocks of less than 20 m

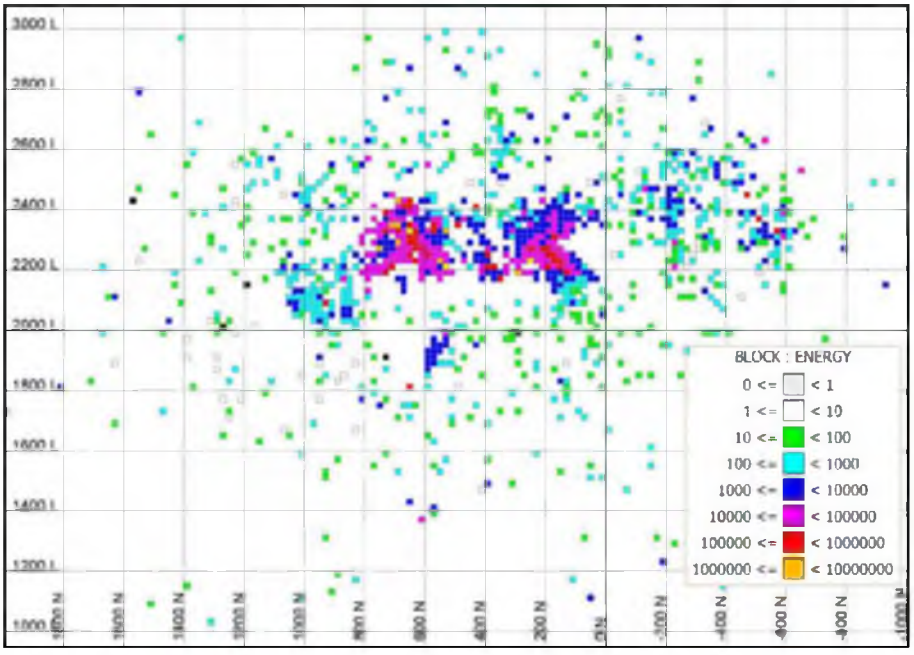

FIGURE 5.16 Section 1,100E - Accumulated energy in blocks up to year 2012 with an average location error in blocks less than or equal to 20 m and an average of five or more stations triggered by the events within the block

A value of 90,000 j or higher could be considered a high accumulation of energy. By comparing different cut-off values for energy display values to known rock conditions in the mine, the cut-off value used to define areas with high energy accumulation could increase or decrease. As the cut-off value used increases, fewer blocks will be selected and used in the generation of the 3-D solids, resulting in a smaller representative volume. Using a lower cut-off value will have the opposite effect.

The effect of restricting the data lowers the number of blocks from the original interpolation selected for display, by displaying or loading only the blocks that comply with the established restrictions imposed on location error lower and number of triggers.

5.4 Three-dimensional Sections

Intersecting sections of blocks can be used to present a 3-D sectional view of the data, showing areas of interest and their possible intersections with volumes of interest where there may be a concentration of a certain type of data, such as accumulated seismic energy.

The advantage of creating sections is that they can be viewed in multiple directions, facilitating understanding of how the seismic events are located with relation to various activities infrastructure in the mine.

The 2-D data are loaded in a 3-D space to show how the data are related to other 3-D developments of the mine.

The Figures 5.17 to 5.20 show how the filtering restrictions (location error and number of triggered stations) can be used to select and represent blocks in which the values for seismic energy have a higher confidence.

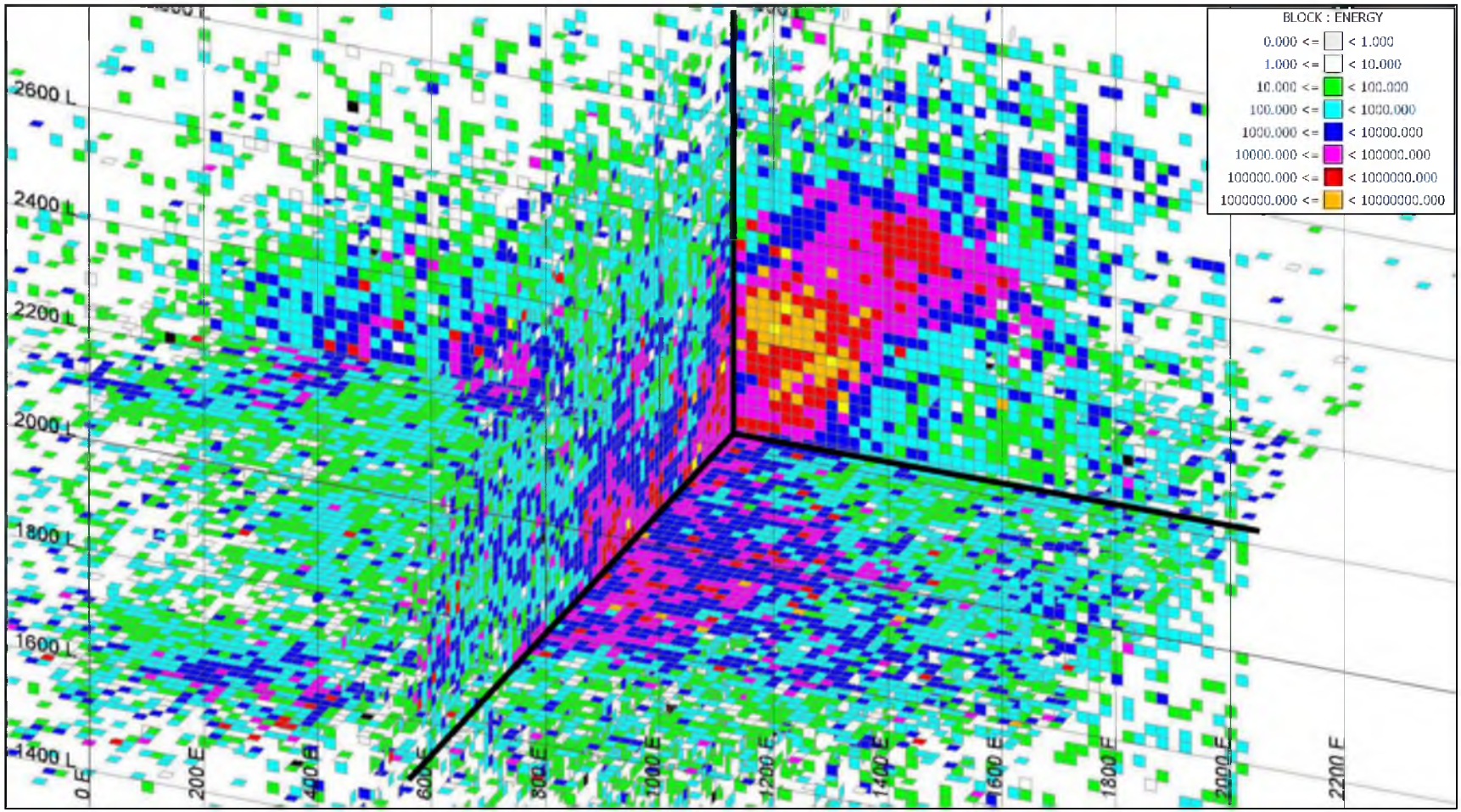

FIGURE 5.17 Side view looking NE - Accumulated energy in blocks up to year 2012

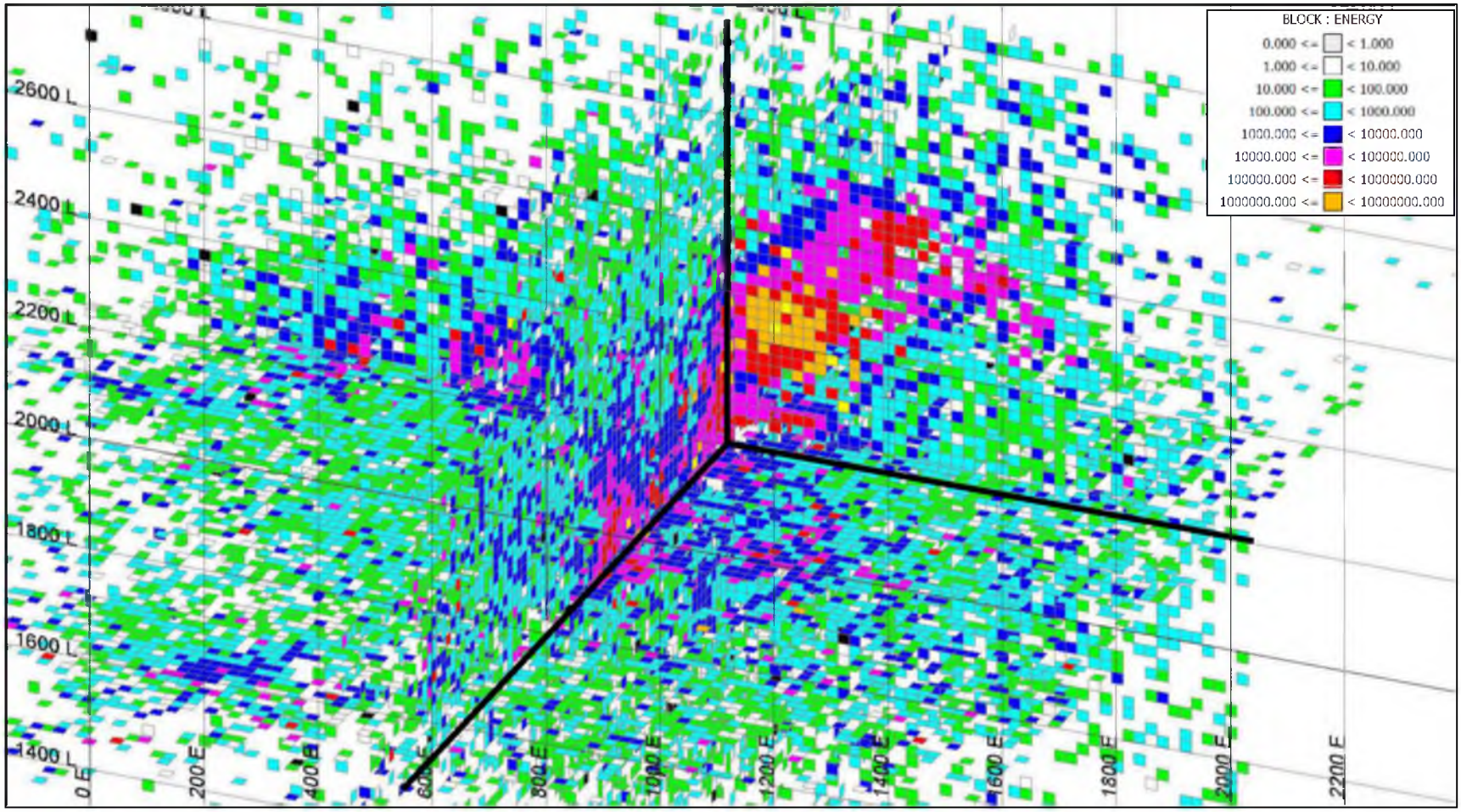

FIGURE 5.18 Side view looking NE - Accumulated energy in blocks up to year 2012 with average of triggered stations greater than or equal to five

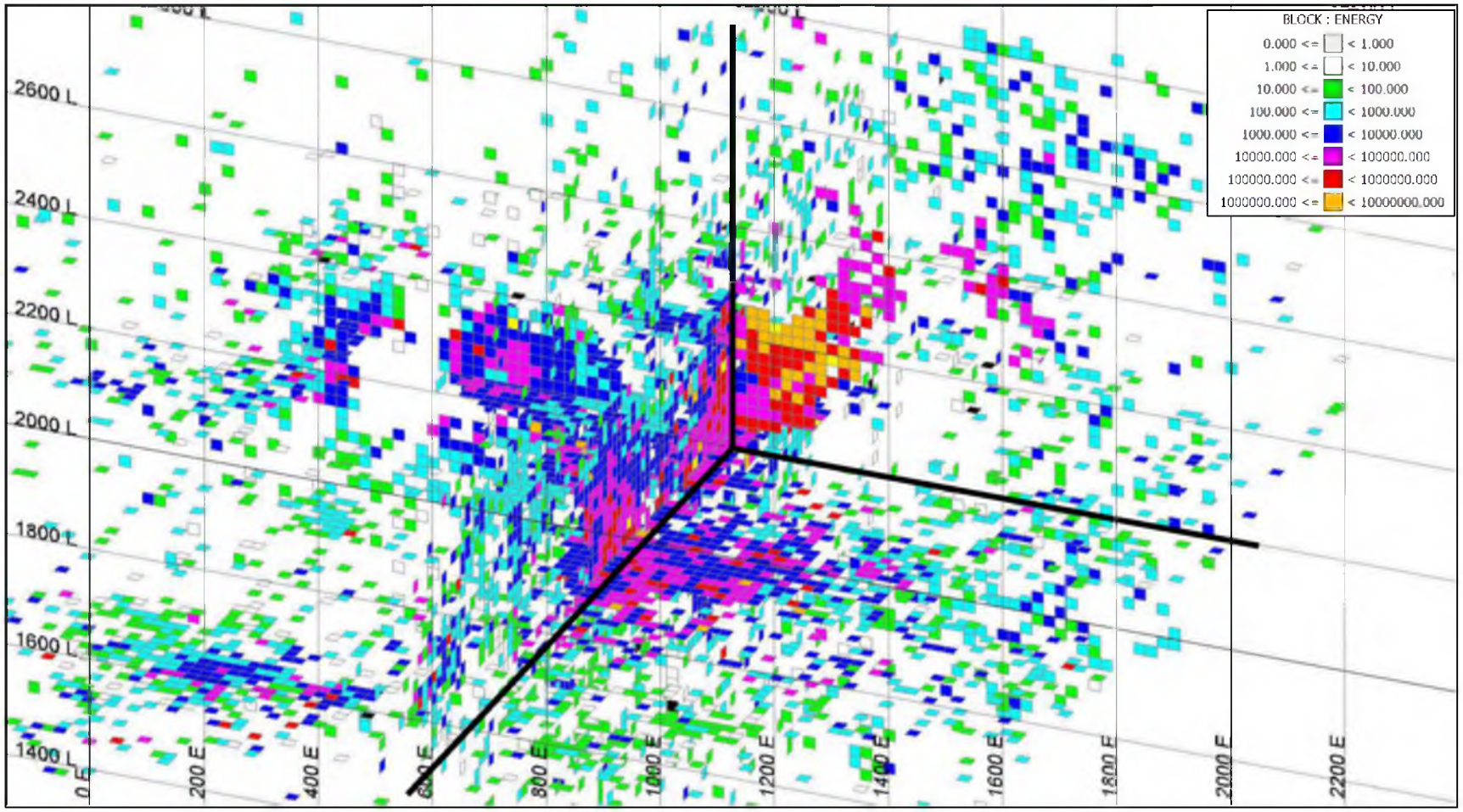

FIGURE 5.19 Side view looking NE - Accumulated energy in blocks up to year 2012 with an average location error in blocks of less than 20 m

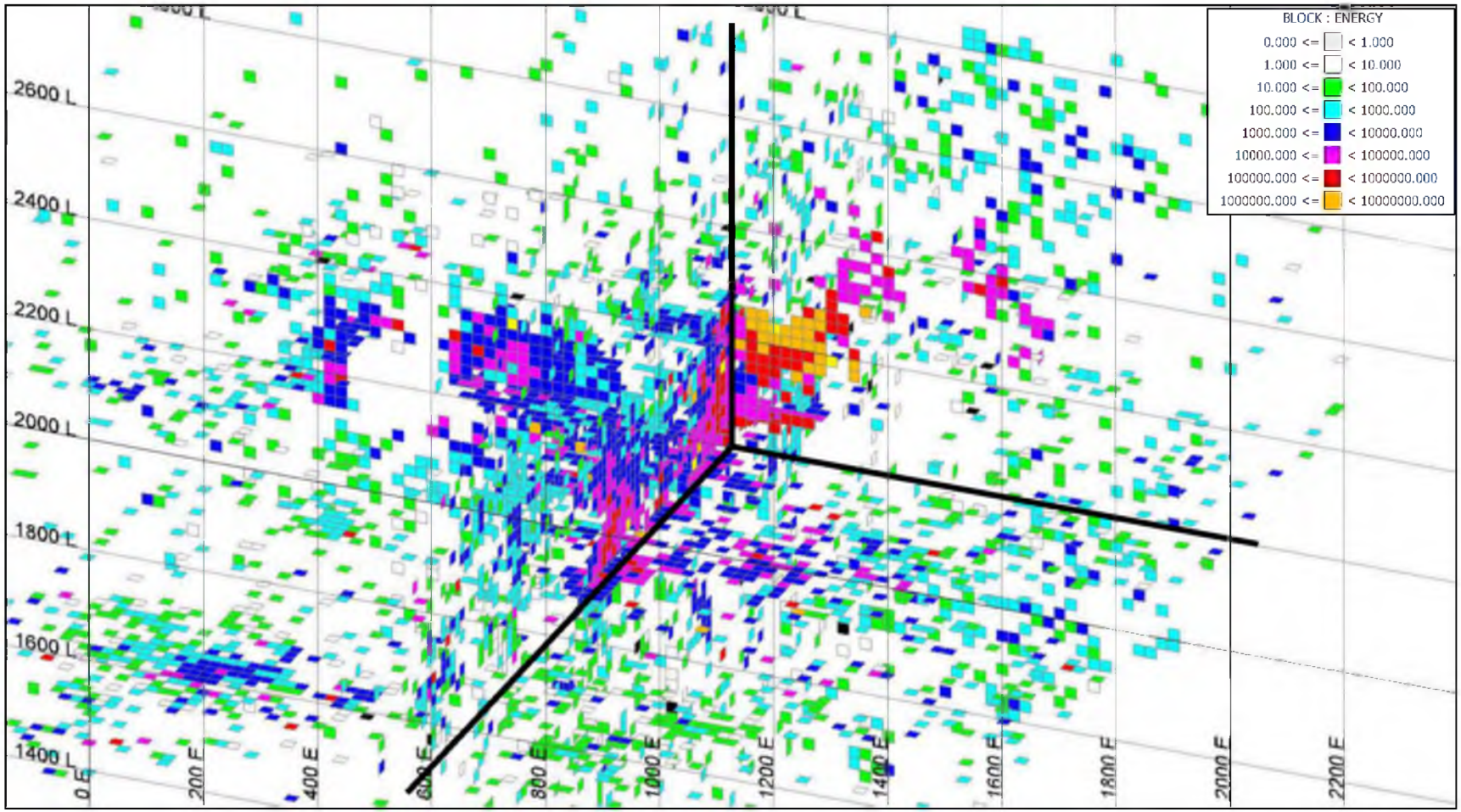

FIGURE 5.20 Side view looking NE - Accumulated energy in blocks up to year 2012 with an average location error in blocks less than or equal to 20 m and an average of five or more stations triggered by the events within the block

The blocks with greater confidence come in this case by selecting blocks that have a lower location error and an average of at least 5 stations triggered by the seismic events. When such filtering restrictions are applied to the generation of 3-D solids, smaller volumes result, because fewer blocks are selected for the generation of the solid triangulations.

5.5 Discussion of the Results

It has been shown that the interpolation of seismic variables such as energy, location error, and number of triggers activated into a block model can facilitate the effective and useful representation of seismic data. In many ways, this method is more effective than using points placed in 3-D and studying them as semistatic, isolated events.

The addition of a time stamp to the events used for such interpolations allows the differentiation of localized events in time and their use in separate interpolations to study selected periods of time such as years, months, or weeks.

The use of block models allows the detailed study of individual variables for any defined time period, and of the accumulation of seismic effects over such time periods.

The block models can be used to create sets of iso-triangulations over a specific range of values and times, to provide a better 3-D visualization of the data, and to load these triangulations with other geometries of the mine under study.

The advantage of using different variables in the same analysis opens the possibility of loading the data in 3-D but also differentiating the data by restricting their display with such criteria as average number of seismic monitoring stations activated by the events and the average location error associated for each block.

The interpolated data can also be used to differentiate and represent triangulations that show how selected constraints affect the display of the interpolated seismic attributes in the blocks.

6 APPLICATIONS

The ability to visualize and analyze the seismic history of a mine using a block model can aid in establishing the seismic fingerprint or embedded history at any area of the mine that might have been affected by previous developments and surrounding projects. Some examples will be given.

6.1 Seismic Energy Conditions on a Planned Project

At a large underground mine, where panel caving is the main mining method, a new project is planned in an area between two older projects. The location of the new project provides an uncommon setting since the new block that will be caved sits between the two areas that have already been in production for a few years (Figure 6.1).

The undercut level (UCL) of the project placed to the north is at the same level as that of the new project, and the UCL of the project to the south is 100 m higher (Figure 6.2). The new block that will be caved extends upward 220 m to the previous caved area on the west side, and its size increases as it goes to the east, with an estimated maximum height of up to 600 to 700 m as it gets closer to the mountainside.

The new block to cave is a mineralized pillar that sits between the two previously mined areas and its surrounding caved areas of influence associated with them (Figure 6.3).

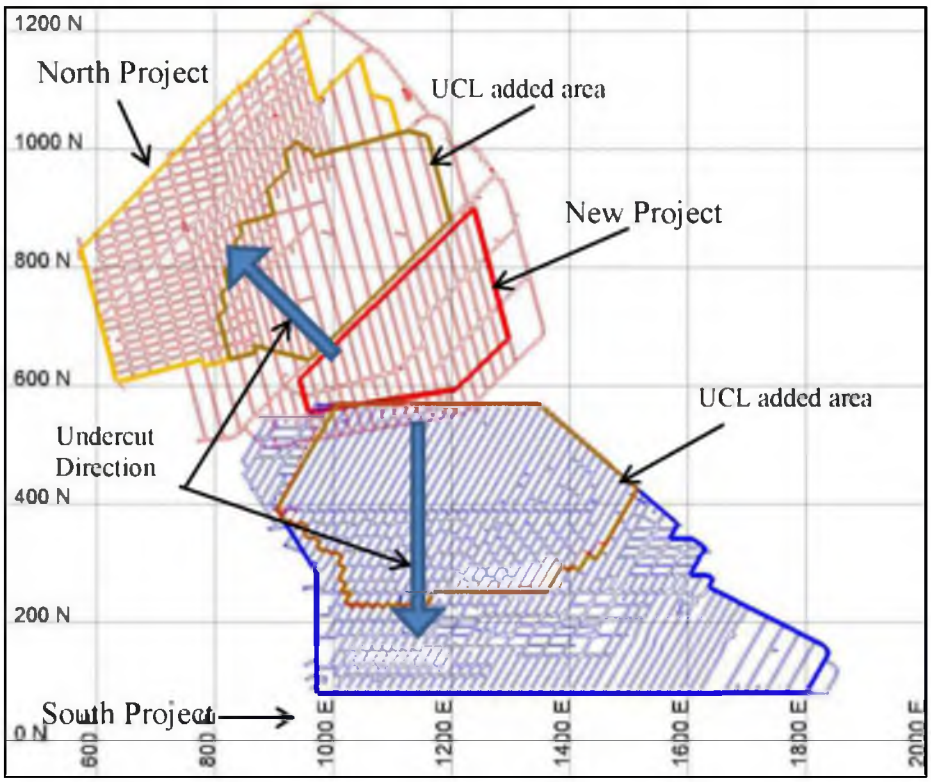

FIGURE 6.1 Plan view of active areas and new project at the center

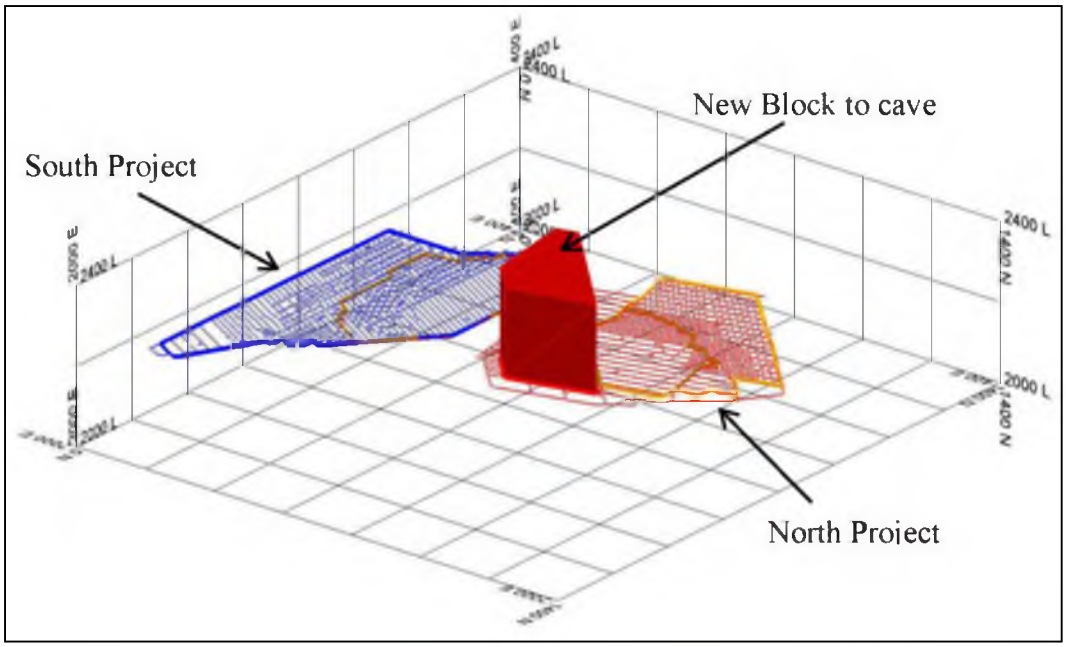

FIGURE 6.2 View looking SE of the projects and block to cave

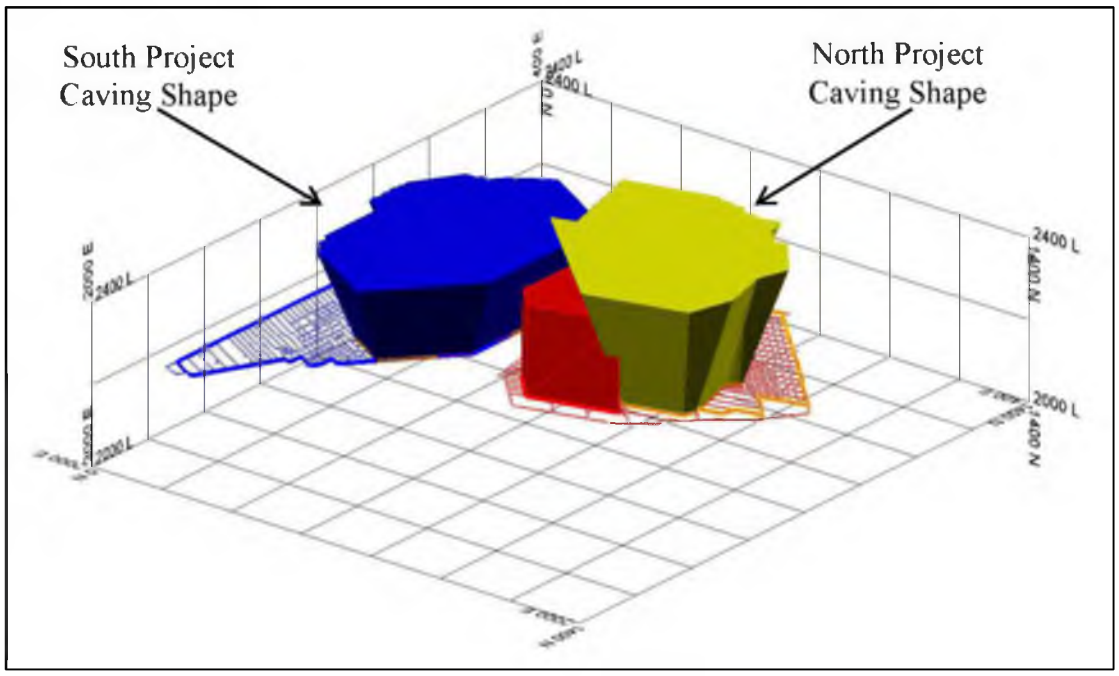

FIGURE 6.3 Modeled caving shapes from active North and South Projects

6.1.1 Progressive Evolution of Seismic Energy

The seismic activity was analyzed to follow the conditions in the areas adjacent to the new project before the new project is developed, and to understand how the seismic activity progressed inside of the block that will be caved in the new project, during the mining of the two adjacent areas.

The effect of the previous mining activity around the new project showed that there was an associated seismic influence from that activity over the area of the new project. Since all the blocks from the block model include the time and accumulated seismic effect, the analysis was restricted to blocks that lie inside of the volume the new project will cave.

In a first step it was seen that the seismicity movement inside of the block to be caved, shown in green in Figure 6.4, was consistent with the mining activities that first

took place on the north side of the block, with an increase of the seismicity in that area. The seismic activity from mining to the south can also be seen.

The volume to be caved, shown in red, was extended vertically upwards so it would intersect the two adjacent caves from the previously mined North and South Projects. The study also showed the effects of the caving activity from the North and South Projects in the sides of the volume representing the new project. The green color, which represents seismic activity in the red volume, shifted to first the right from the caving of the North Project (Figure 6.4), and then to the left from the caving of the South Project (Figure 6.5).

It was seen that the seismic activity progressed between 1992 and 2009, and was concentrated in the central area of the red volume (central project) and to the west side. The evolution of the seismic activity as blocks is shown in Figure 6.6. This information is shown as solid shapes in Figure 6.7. This provides another view of how the seismic activity has moved inside of the area between the two projects.

Figure 6.6 and Figure 6.7 both show that there has not been a significant history of seismicity on the east side of the new project.

The evolution of the seismicity was tracked with the model. In 1992 the North Project was in production where the caving of that project was taking place. In 1999, the South Project started, and Figure 6.5 shows how the seismic activity shifted to the south side of the new project area.

The evolution of the seismic activity is displayed for each year from 1992 to 2012 in Figures 6.8 to 6.28.

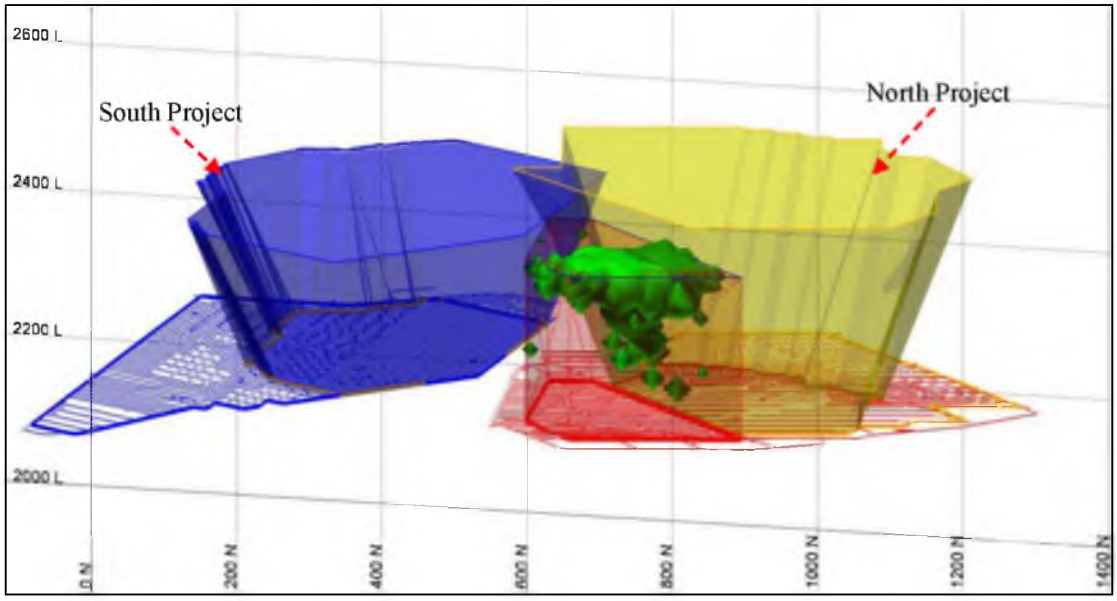

FIGURE 6.4 Seismicity associated with mining activities from the North Project from year 1992 to 1996

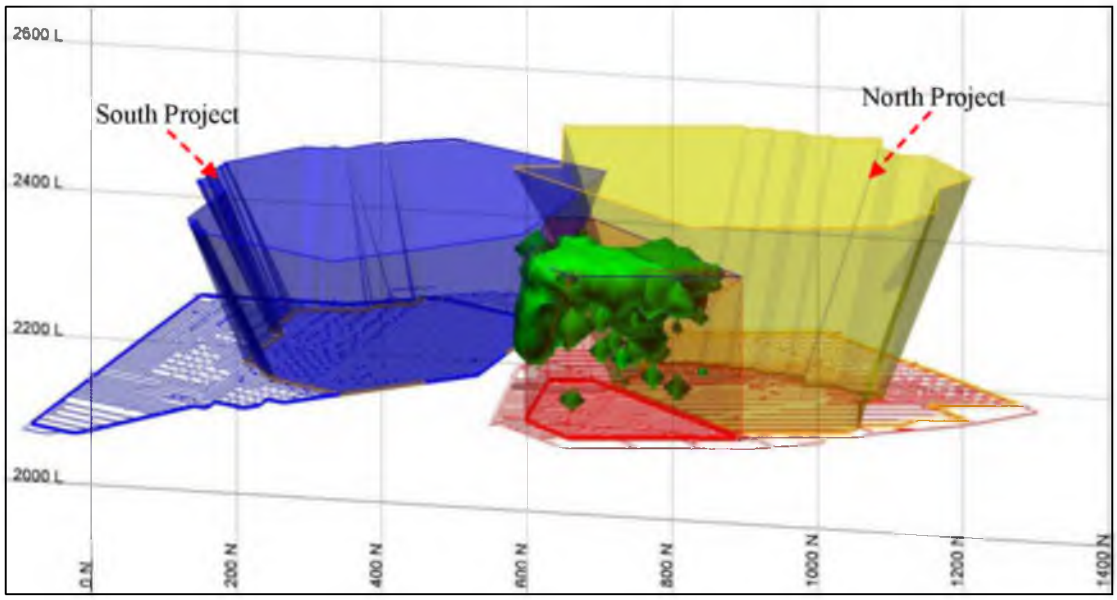

FIGURE 6.5 Seismicity associated with mining activities from the South Project from year 1992 to 1999

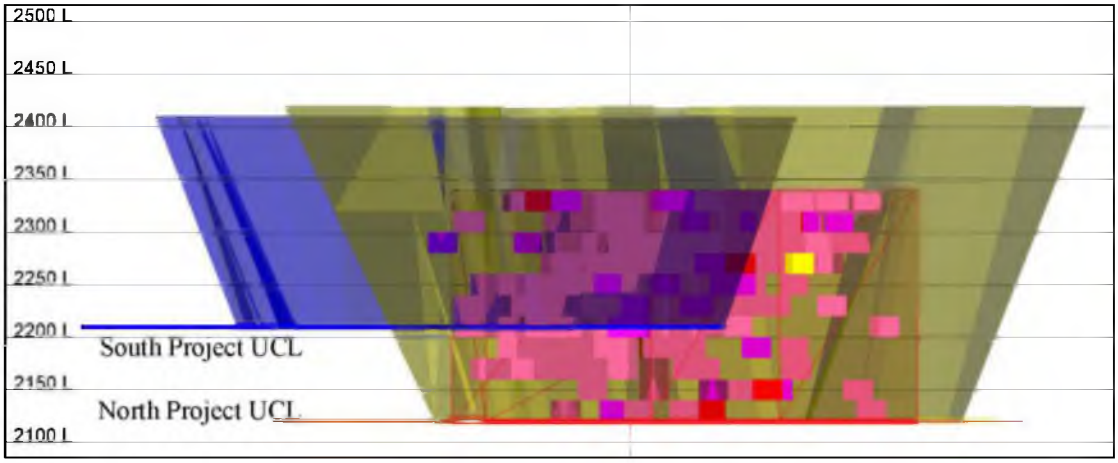

FIGURE 6.6 W-E view of blocks with accumulated seismic activity inside of the volume to cave up to year 2009

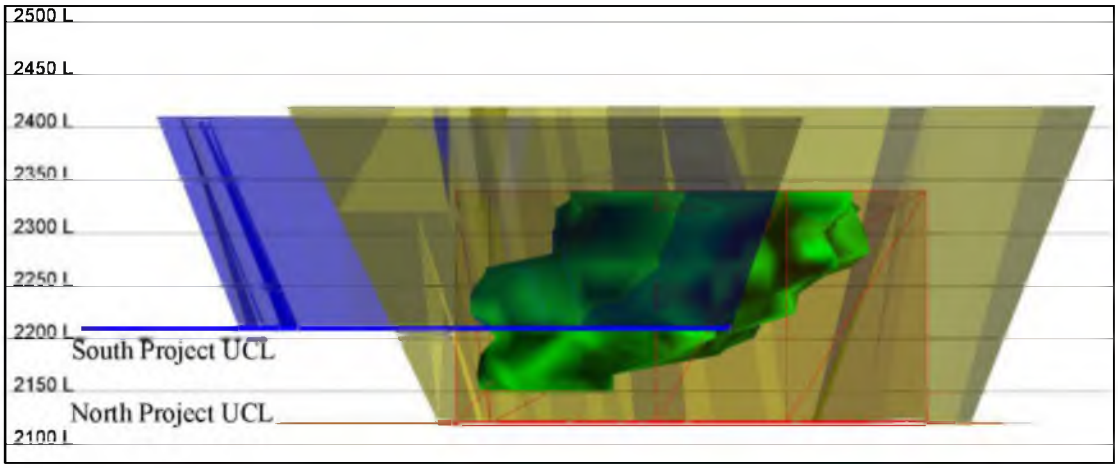

FIGURE 6.7 W-E view of interpreted solid covering the most important accumulated seismic activity (up to year 2009) inside the area to cave

The seismicity associated with the new project in the central area (in red) showed that there was no relevant seismic activity on the east side, and the evolution of the seismicity that was generated from top to bottom from 1992 to 2009.

The effect of the accumulated seismicity was analyzed up to 2009, when the new, central project was scheduled to start, and continued to July 2012 to examine the evolution of the seismicity afterwards.

Figures 6.8 to 6.28 show how seismicity evolved from 1999 to 2012. The new project area is shown from different angles for each year.

On the upper left side of the figures is a view looking to the east; on the top right is a plan view of the area; on the lower left is a west-east view; and on the lower right is a view looking to the west.

The energy, shown in green in the figures, represents the accumulated radiated energy from 1992 to 2012, with a cut-off value of 90,000 Joules.

6.1.2 Progressive Evolution of Seismic Magnitude

The evolution of the accumulated seismic magnitude was analyzed to define how the area of the new project had been affected by the induced seismicity from the two adjacent projects to the north and the south. The accumulated magnitude was analyzed for the period from 1992 to 2009, before the project was planned to start. Figure 6.29 shows the arrangement of the volumes studied. The new project is shown in red, between the North and South Projects, shown in yellow and blue respectively.

A new set of data was developed to display the accumulation of the seismic magnitude in the blocks inside the volume of the new project.

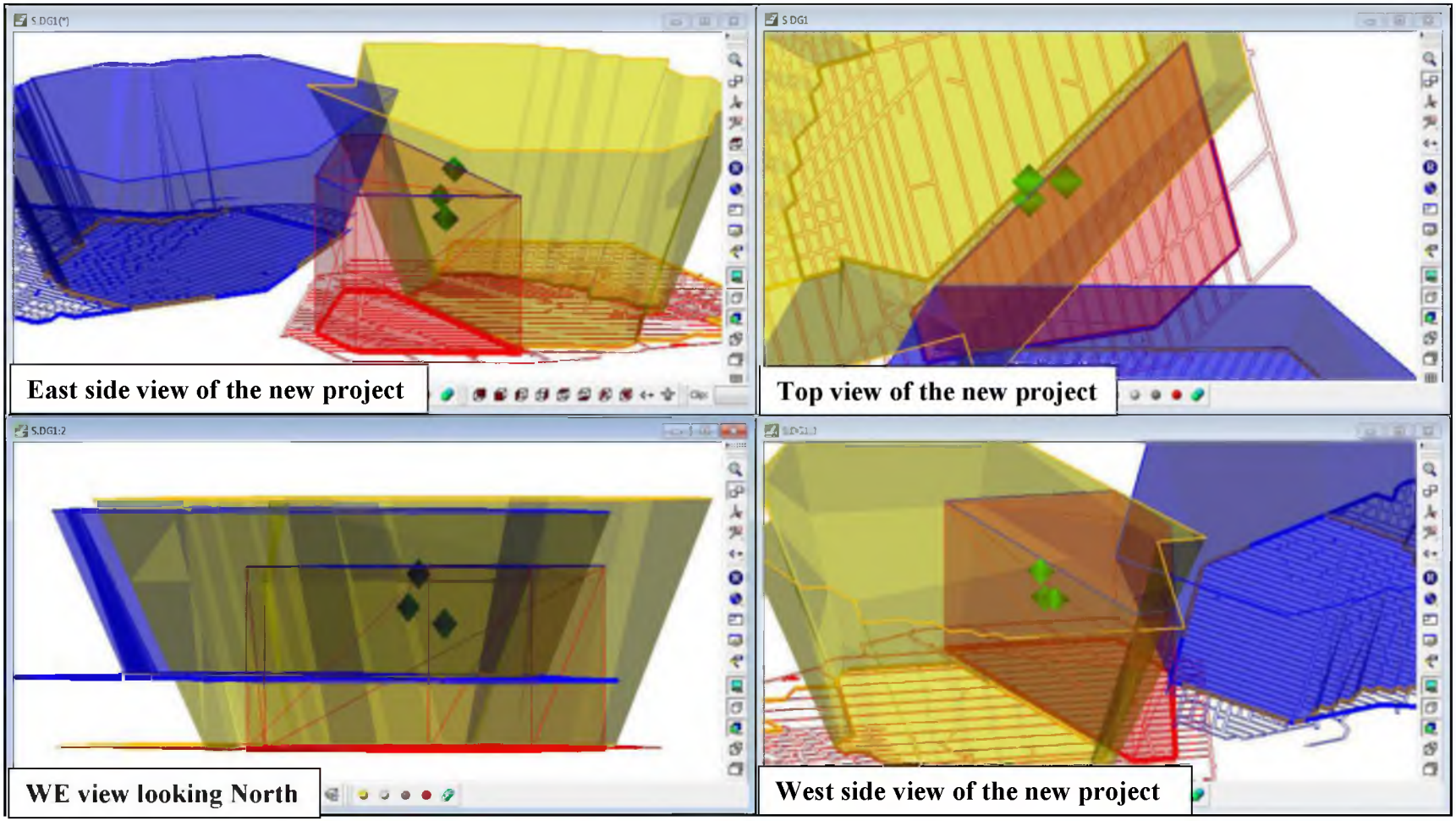

FIGURE 6.8 Different views of accumulated seismic energy inside new project area for year 1992

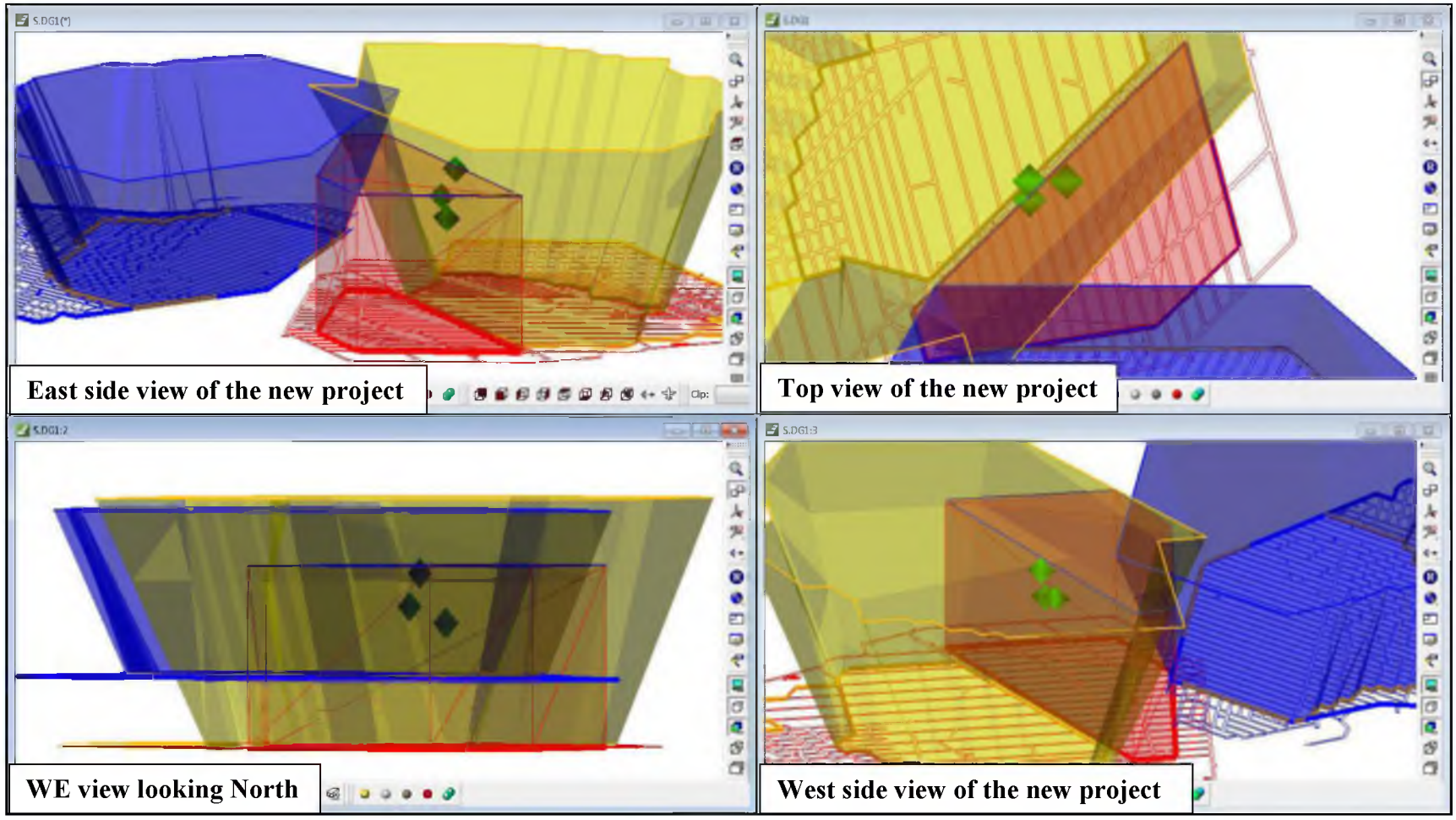

FIGURE 6.9 Different views of accumulated seismic energy inside new project area for year 1993

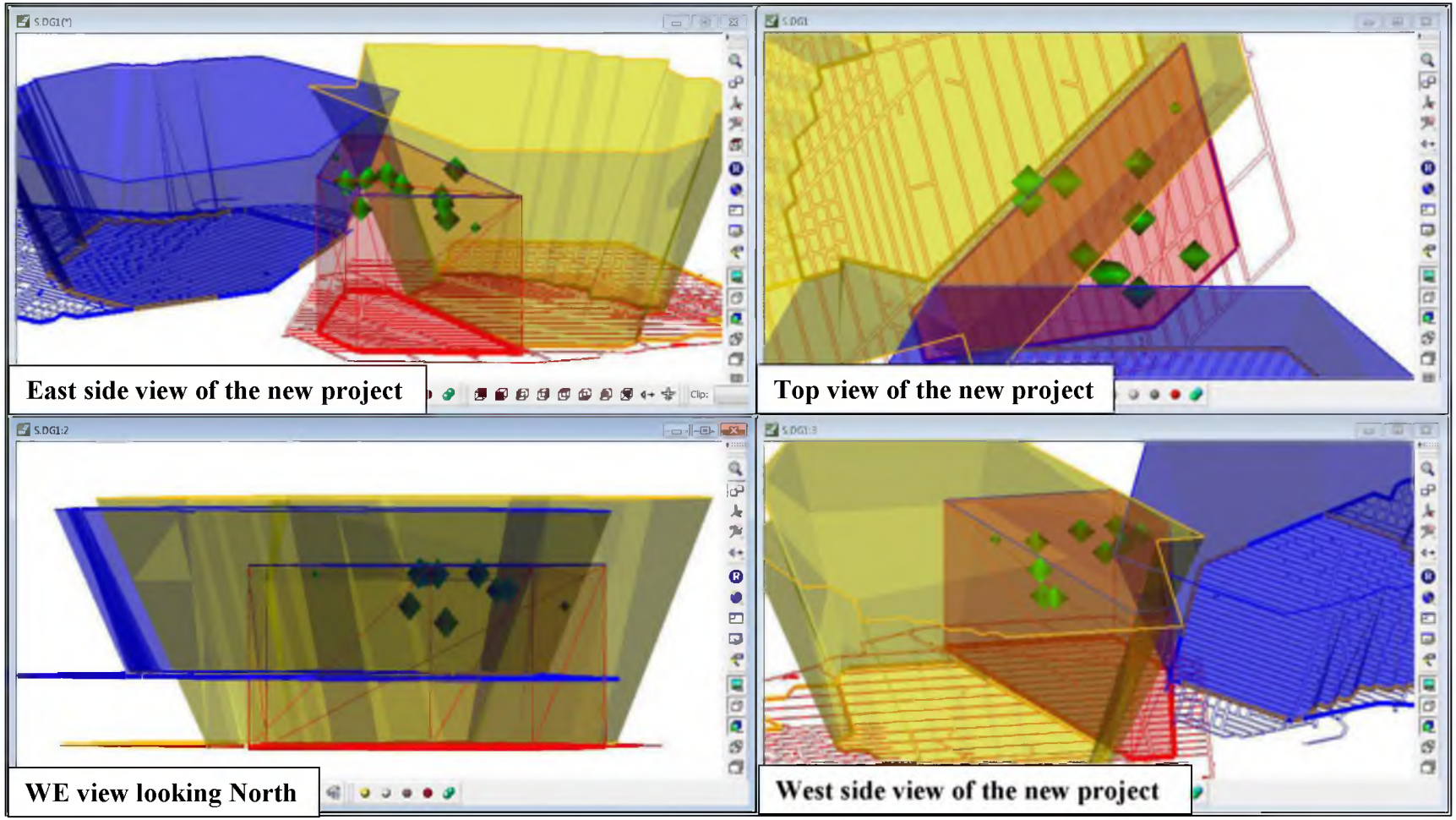

FIGURE 6.10 Different views of accumulated seismic energy inside new project area for year 1994

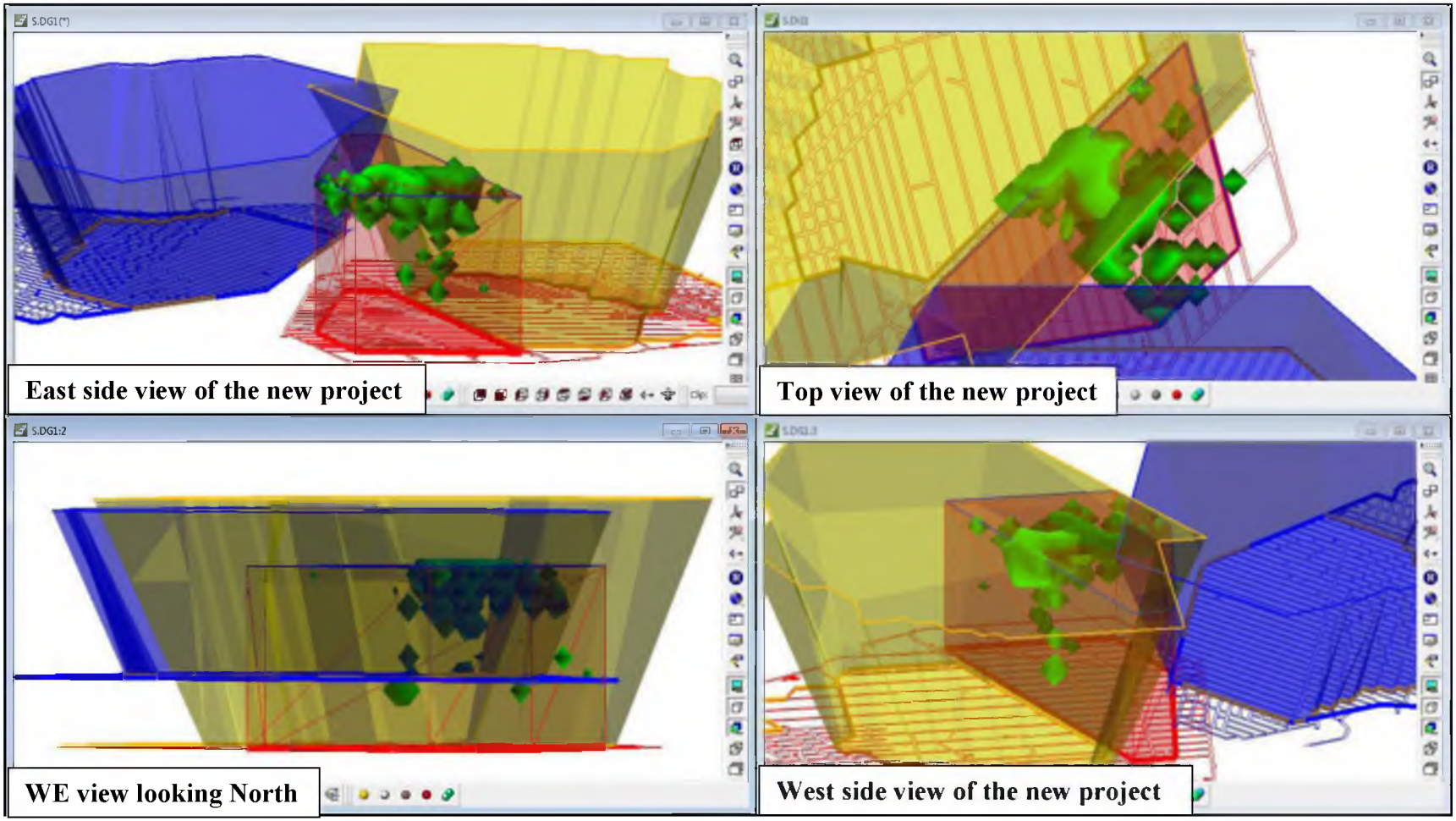

FIGURE 6.11 Different views of accumulated seismic energy inside new project area for year 1995

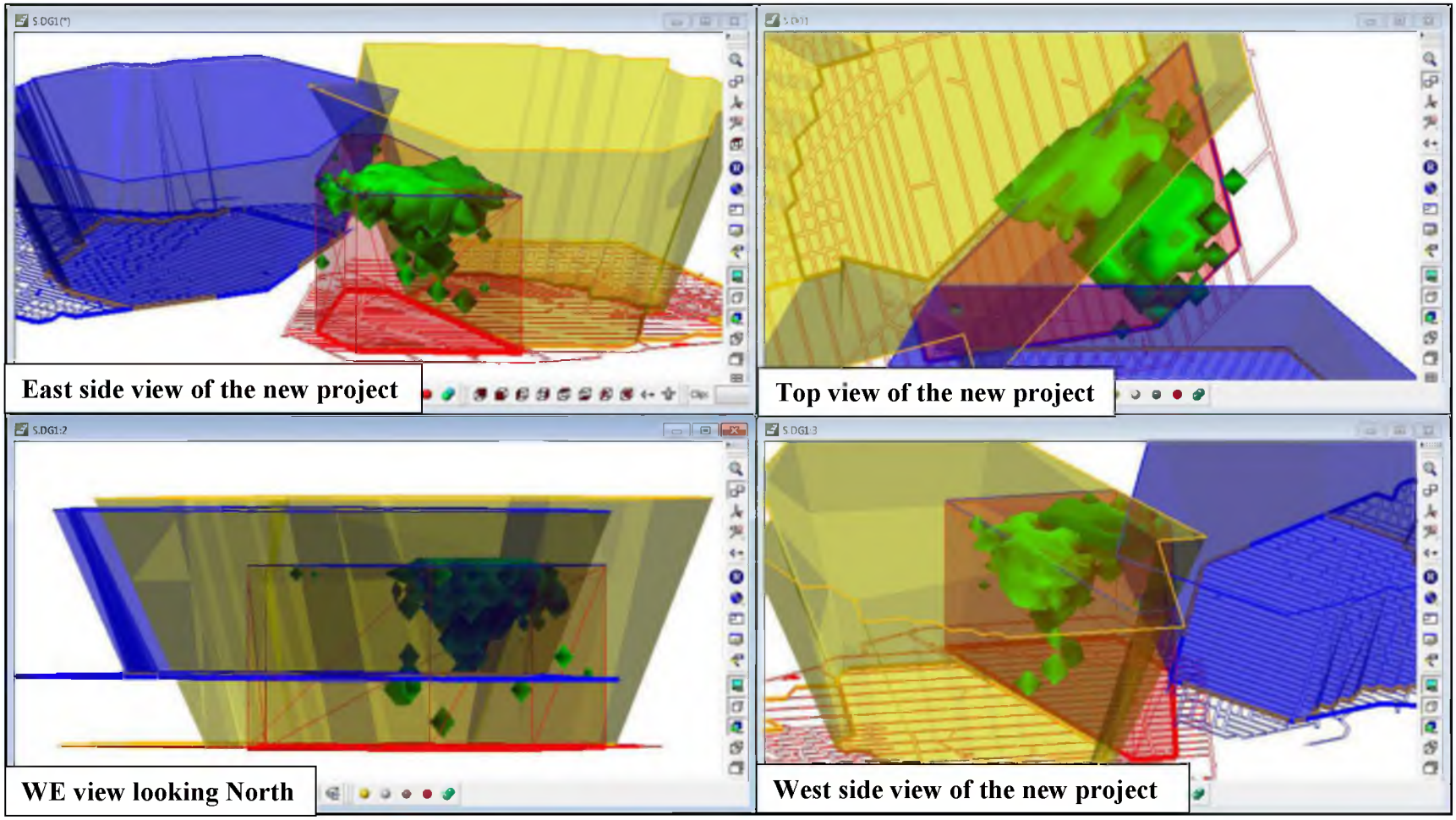

FIGURE 6.12 Different views of accumulated seismic energy inside new project area for year 1996

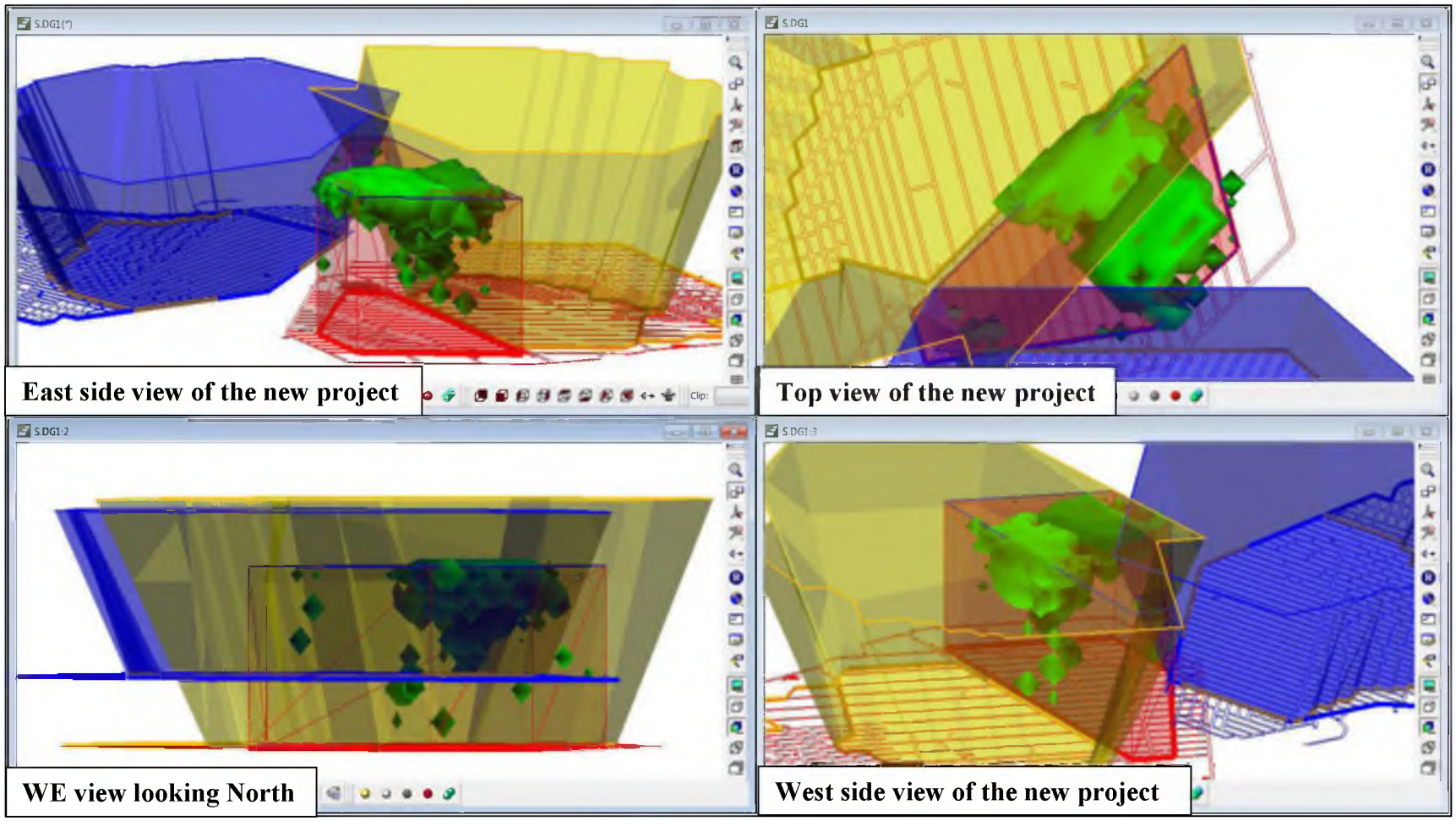

FIGURE 6.13 Different views of accumulated seismic energy inside new project area for year 1997

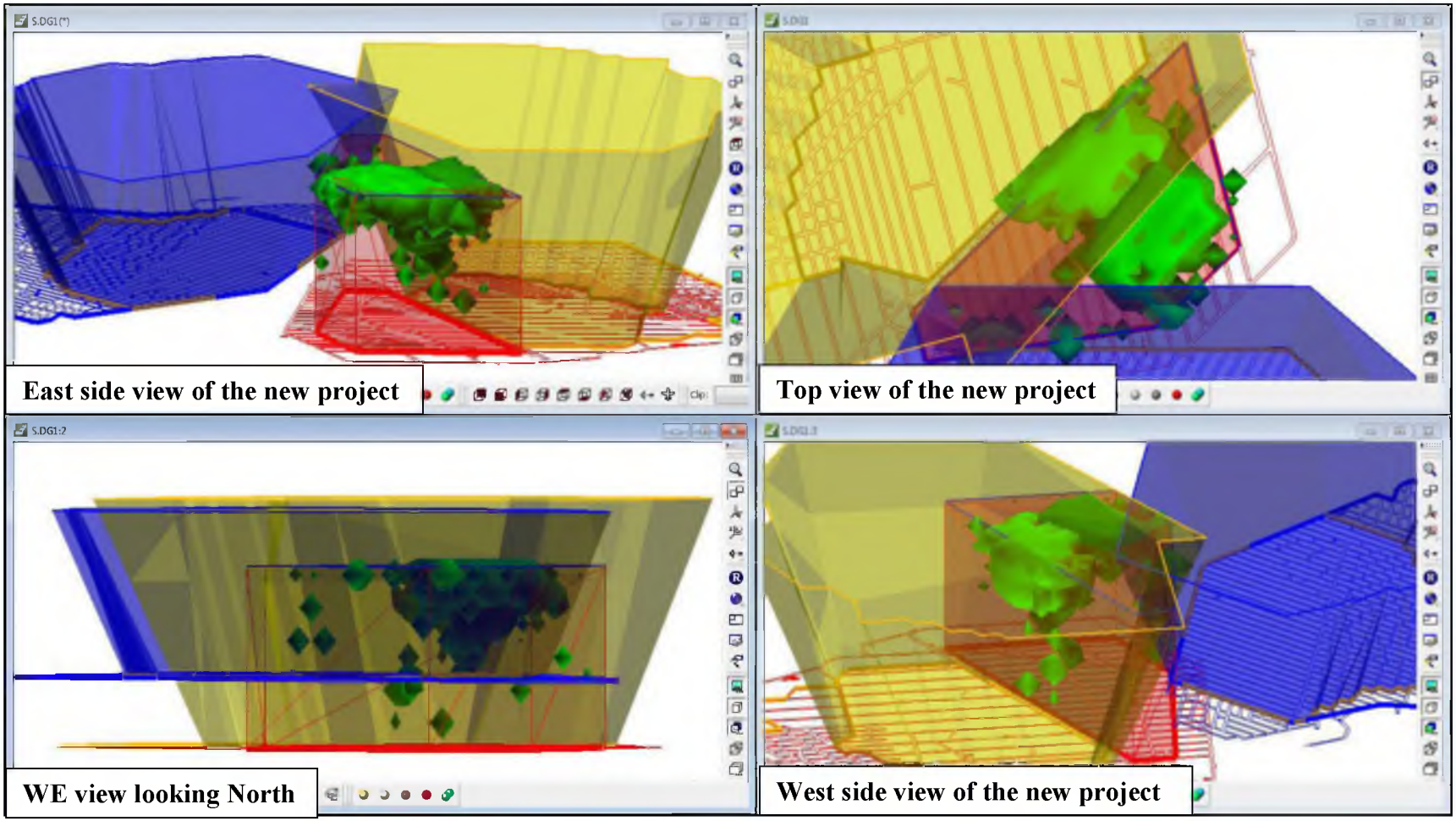

FIGURE 6.14 Different views of accumulated seismic energy inside new project area for year 1998

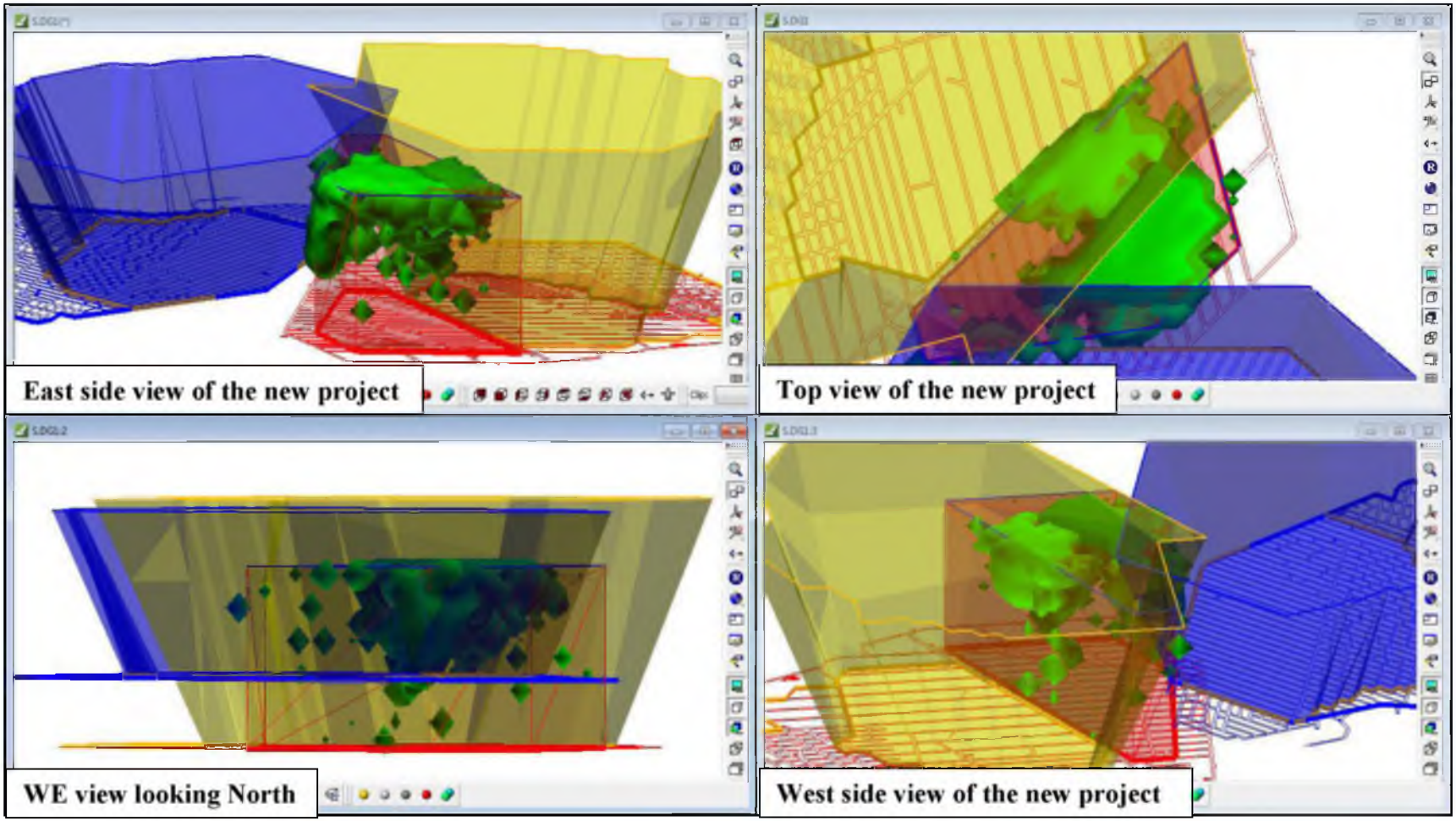

FIGURE 6.15 Different views of accumulated seismic energy inside new project area for year 1999

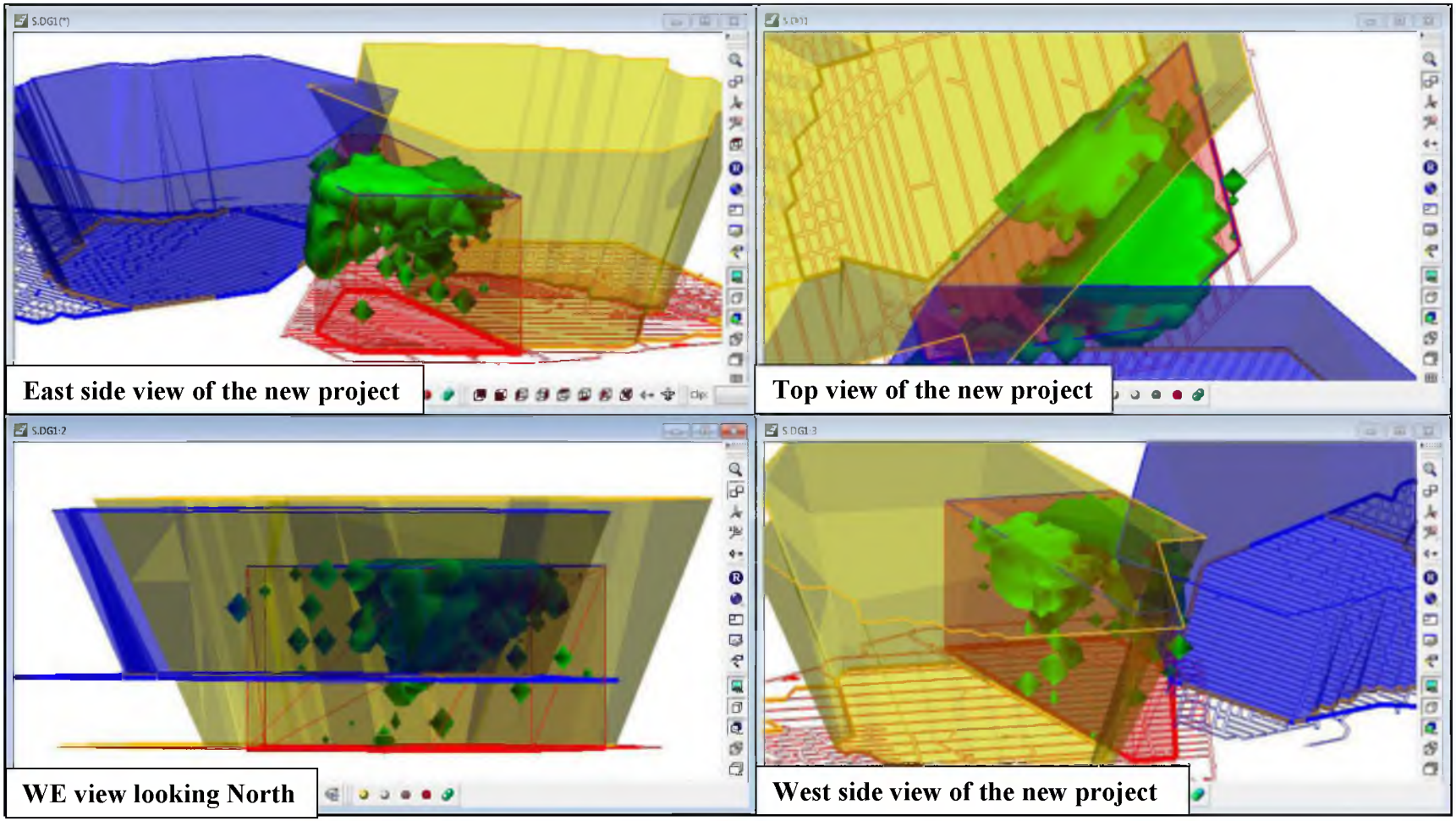

FIGURE 6.16 Different views of accumulated seismic energy inside new project area for year 2000

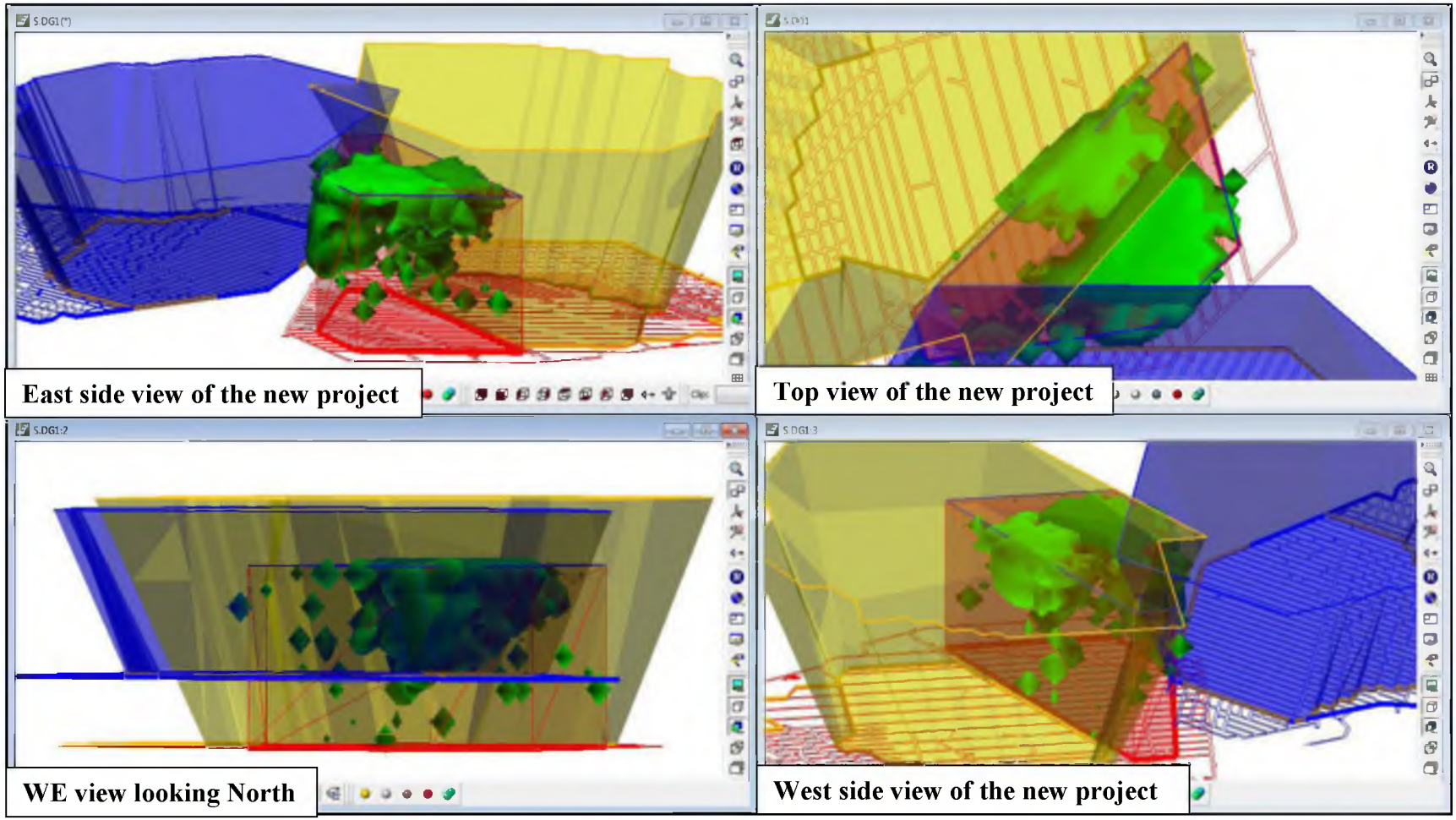

FIGURE 6.17 Different views of accumulated seismic energy inside new project area for year 2001

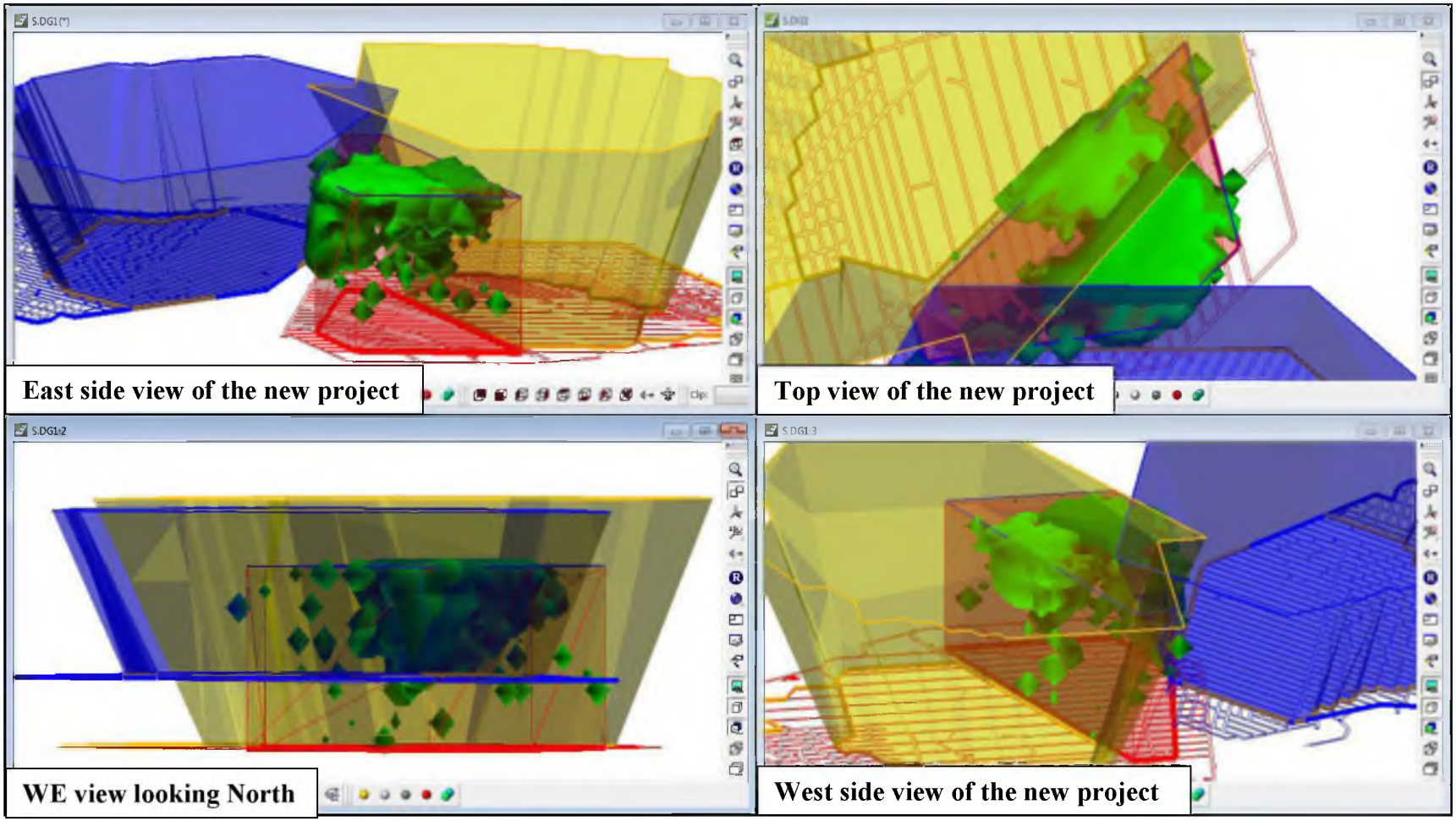

FIGURE 6.18 Different views of accumulated seismic energy inside new project area for year 2002

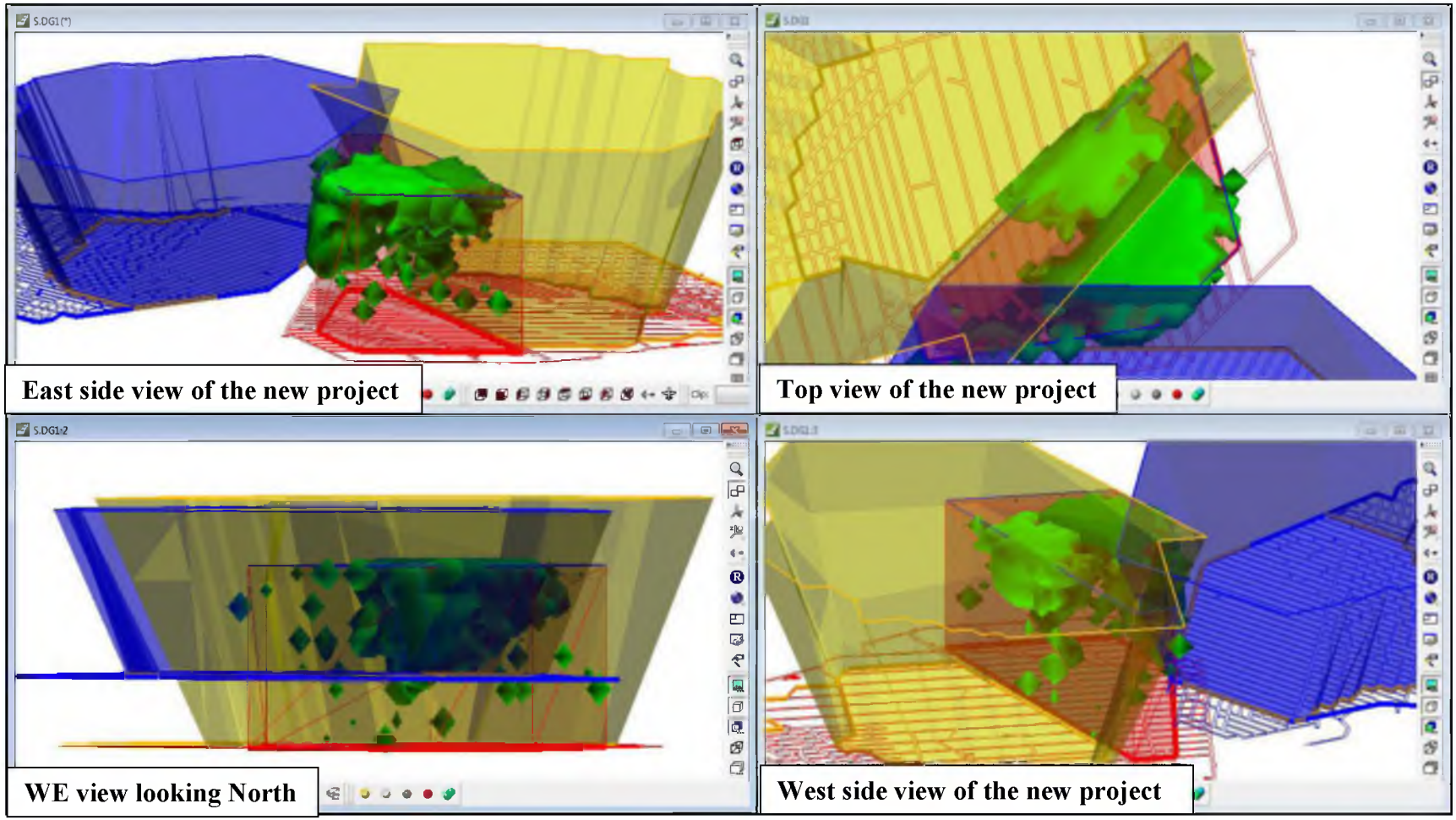

FIGURE 6.19 Different views of accumulated seismic energy inside new project area for year 2003

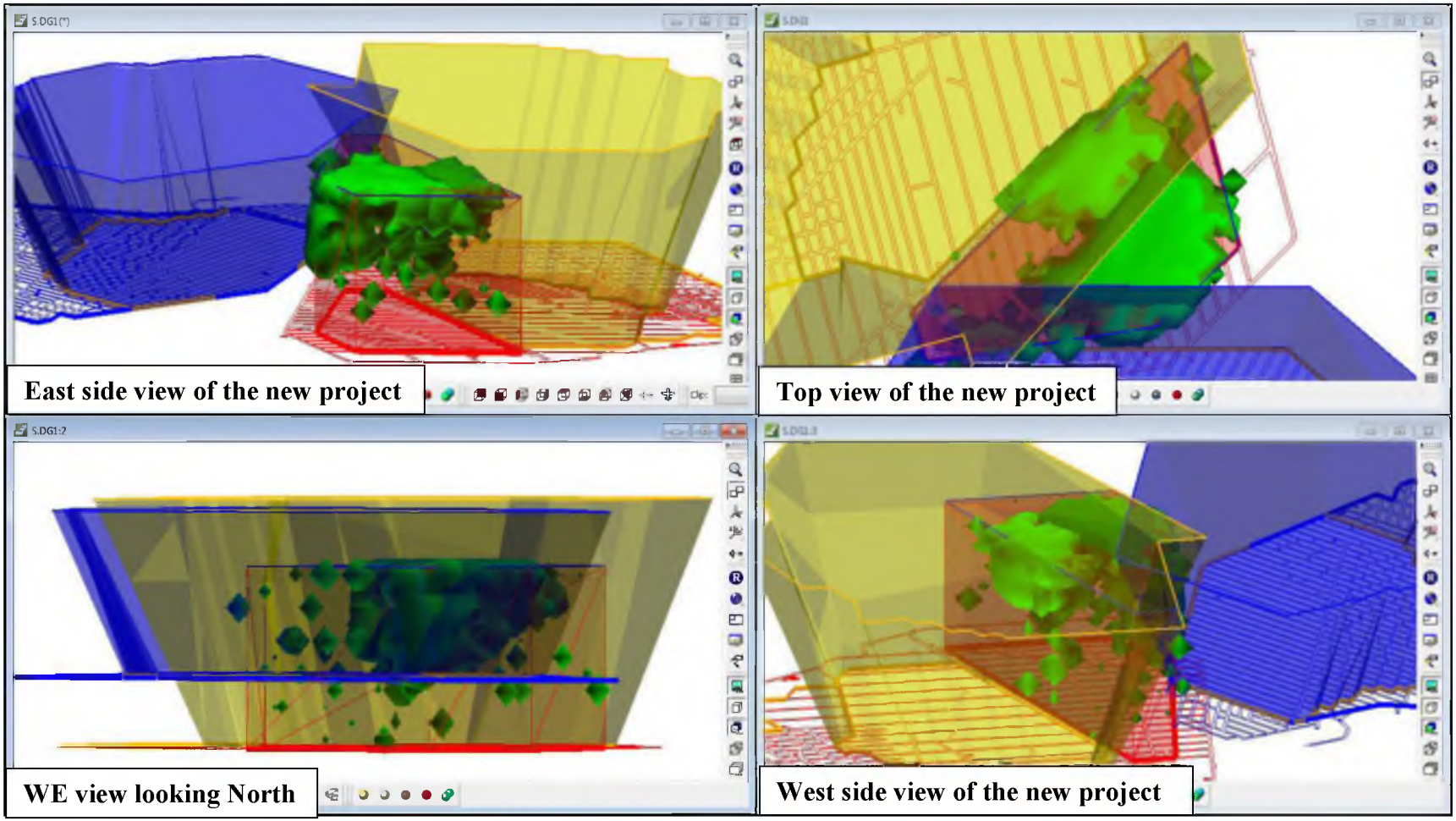

FIGURE 6.20 Different views of accumulated seismic energy inside new project area for year 2004

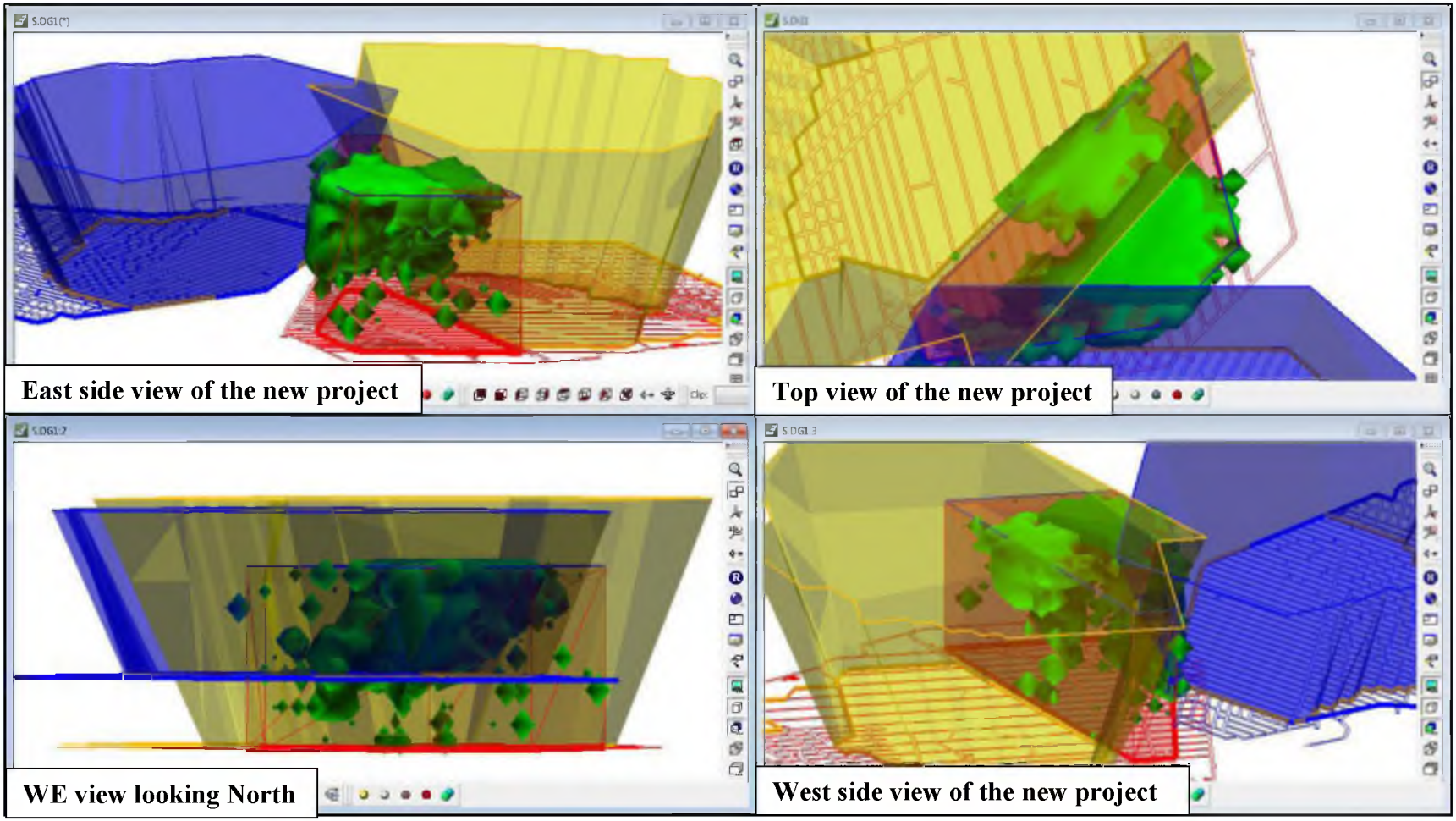

FIGURE 6.21 Different views of accumulated seismic energy inside new project area for year 2005

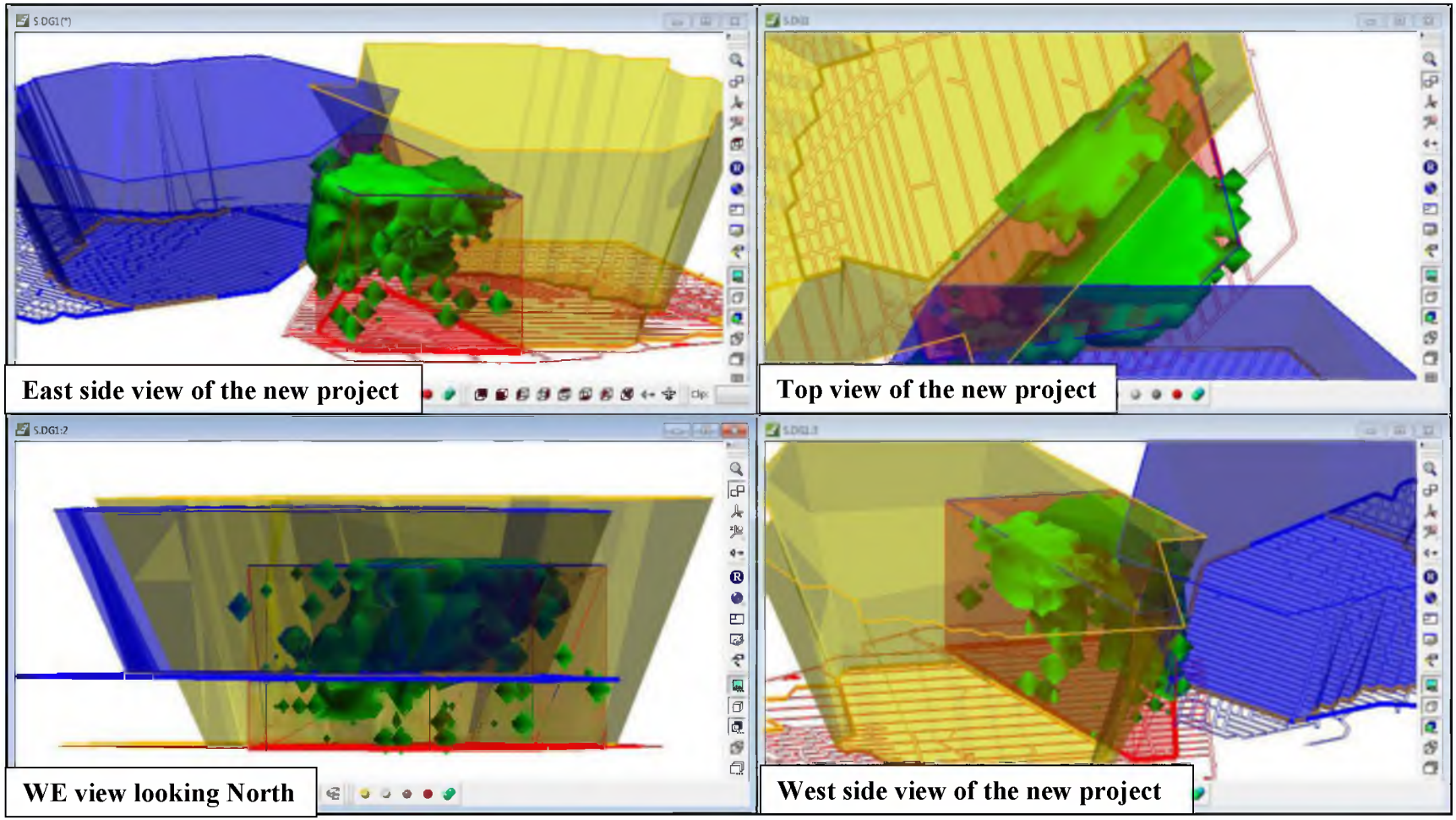

FIGURE 6.22 Different views of accumulated seismic energy inside new project area for year 2006

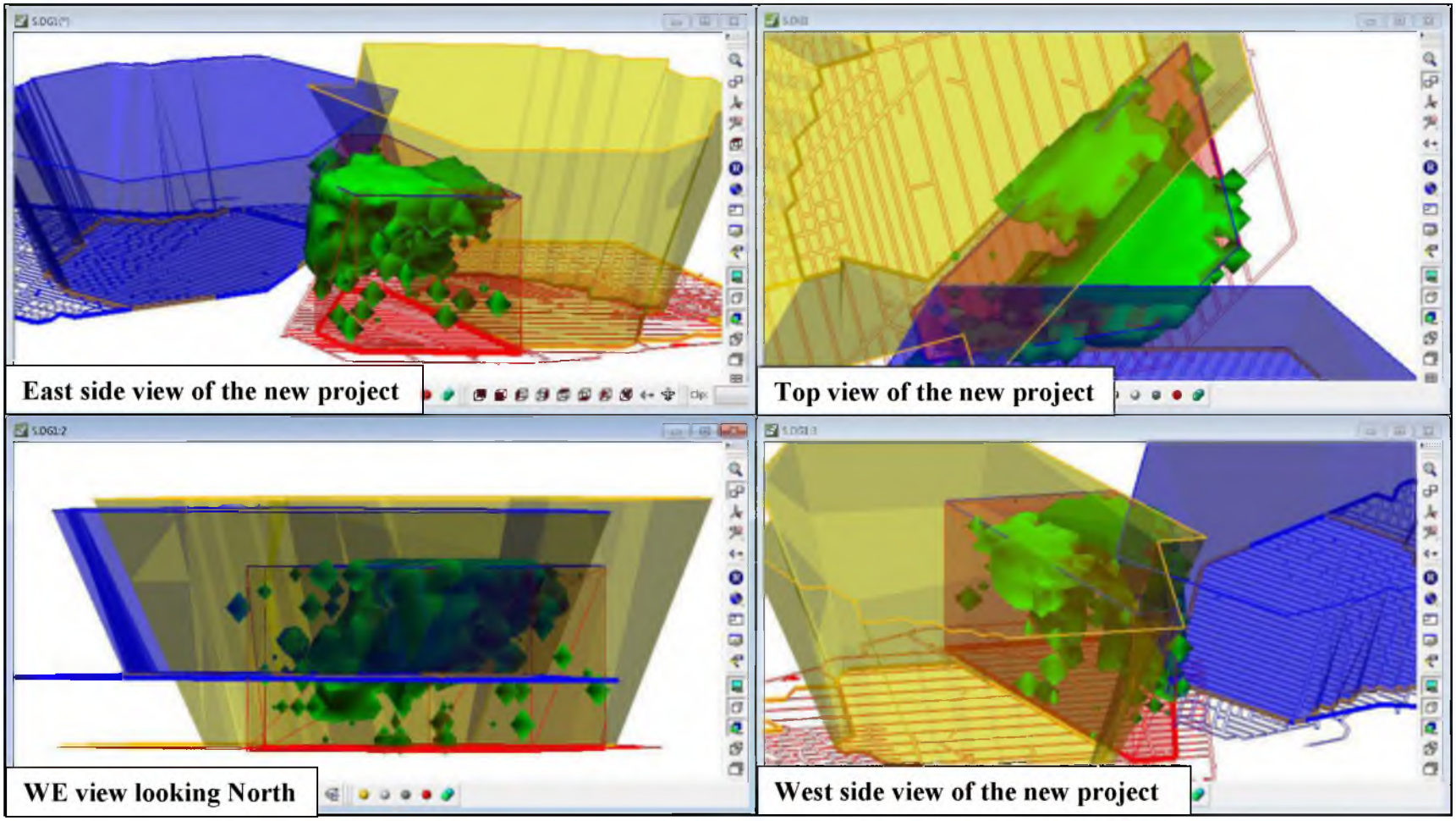

FIGURE 6.23 Different views of accumulated seismic energy inside new project area for year 2007

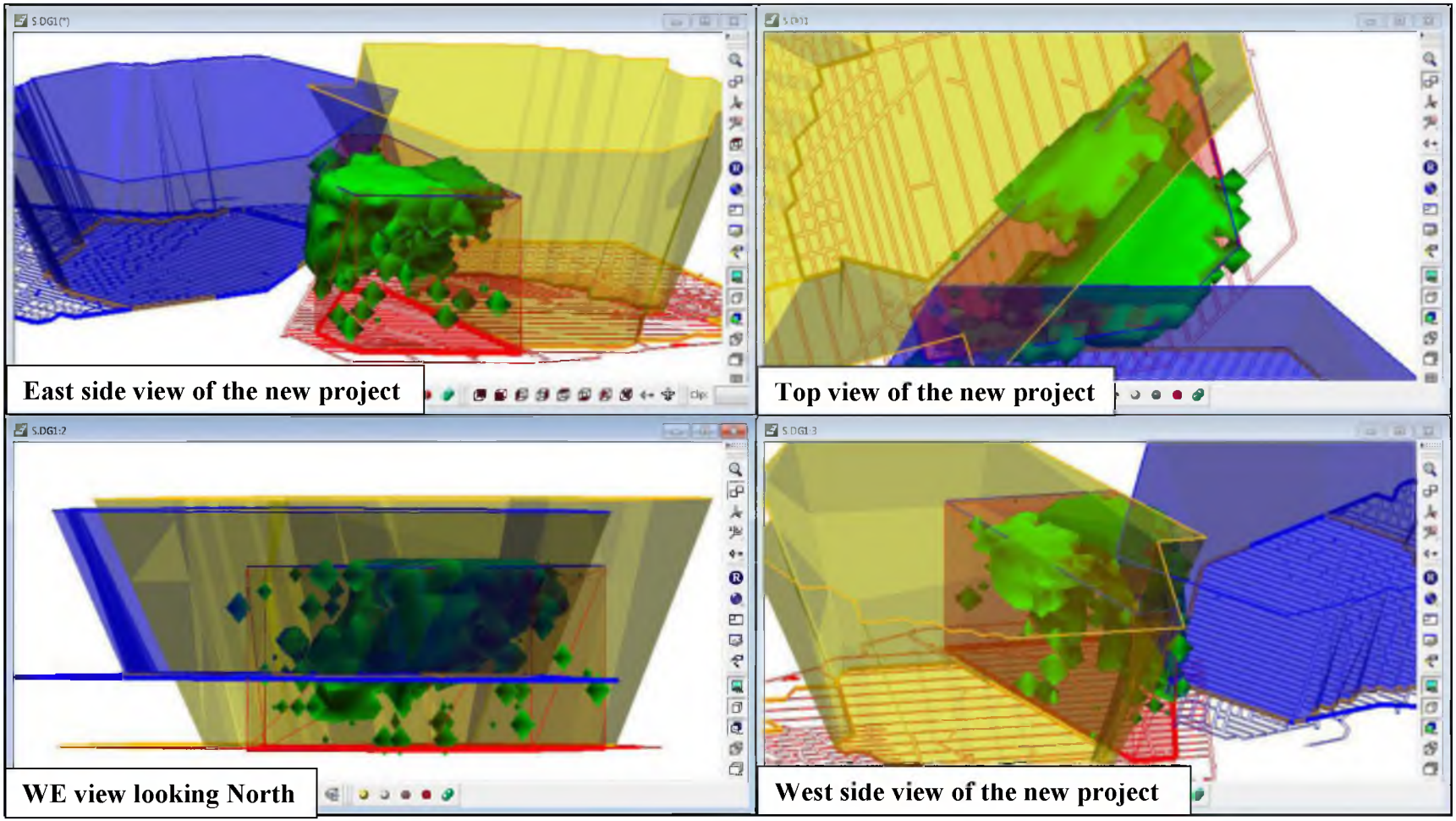

FIGURE 6.24 Different views of accumulated seismic energy inside new project area for year 2008

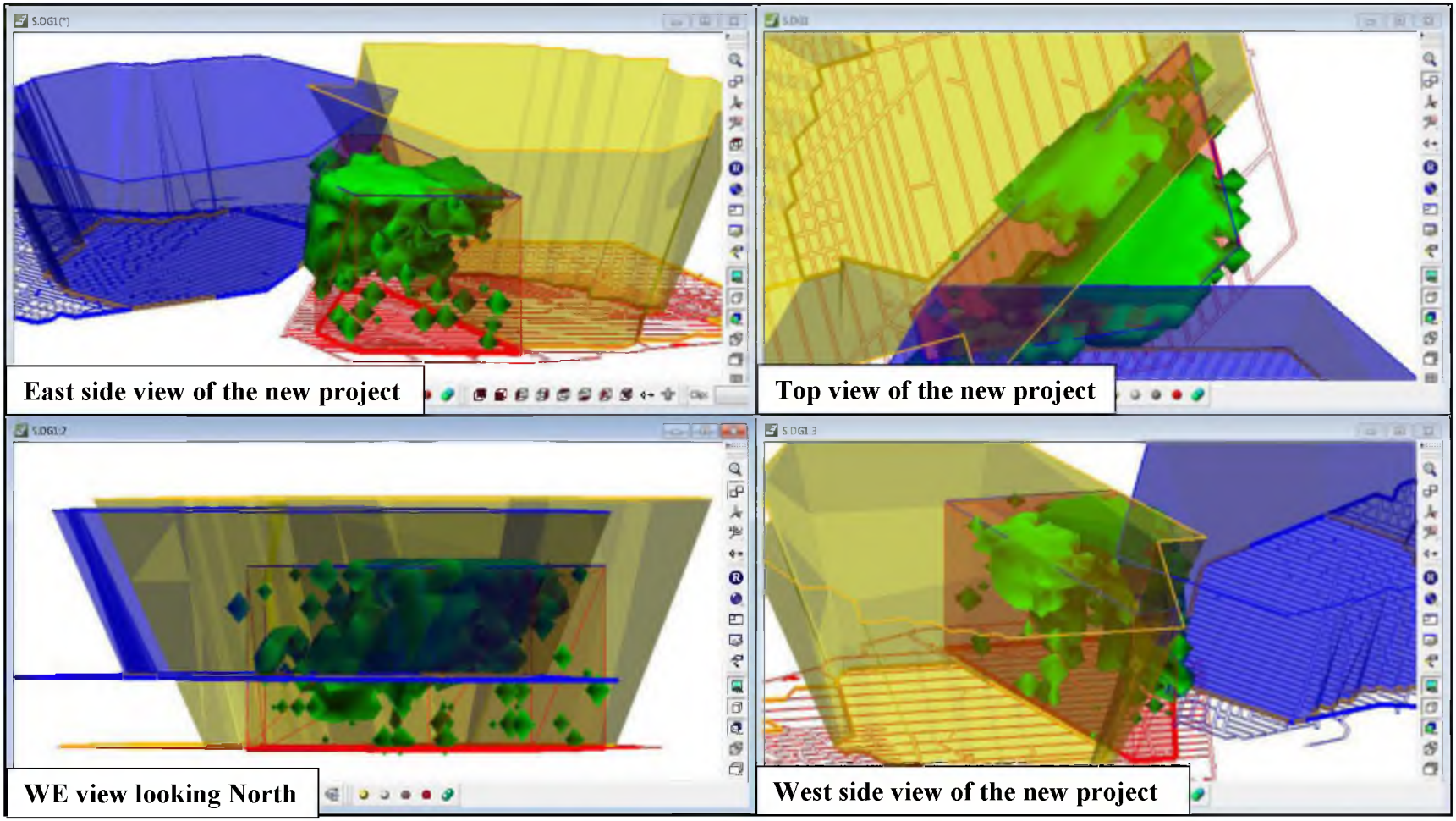

FIGURE 6.25 Different views of accumulated seismic energy inside new project area for year 2009

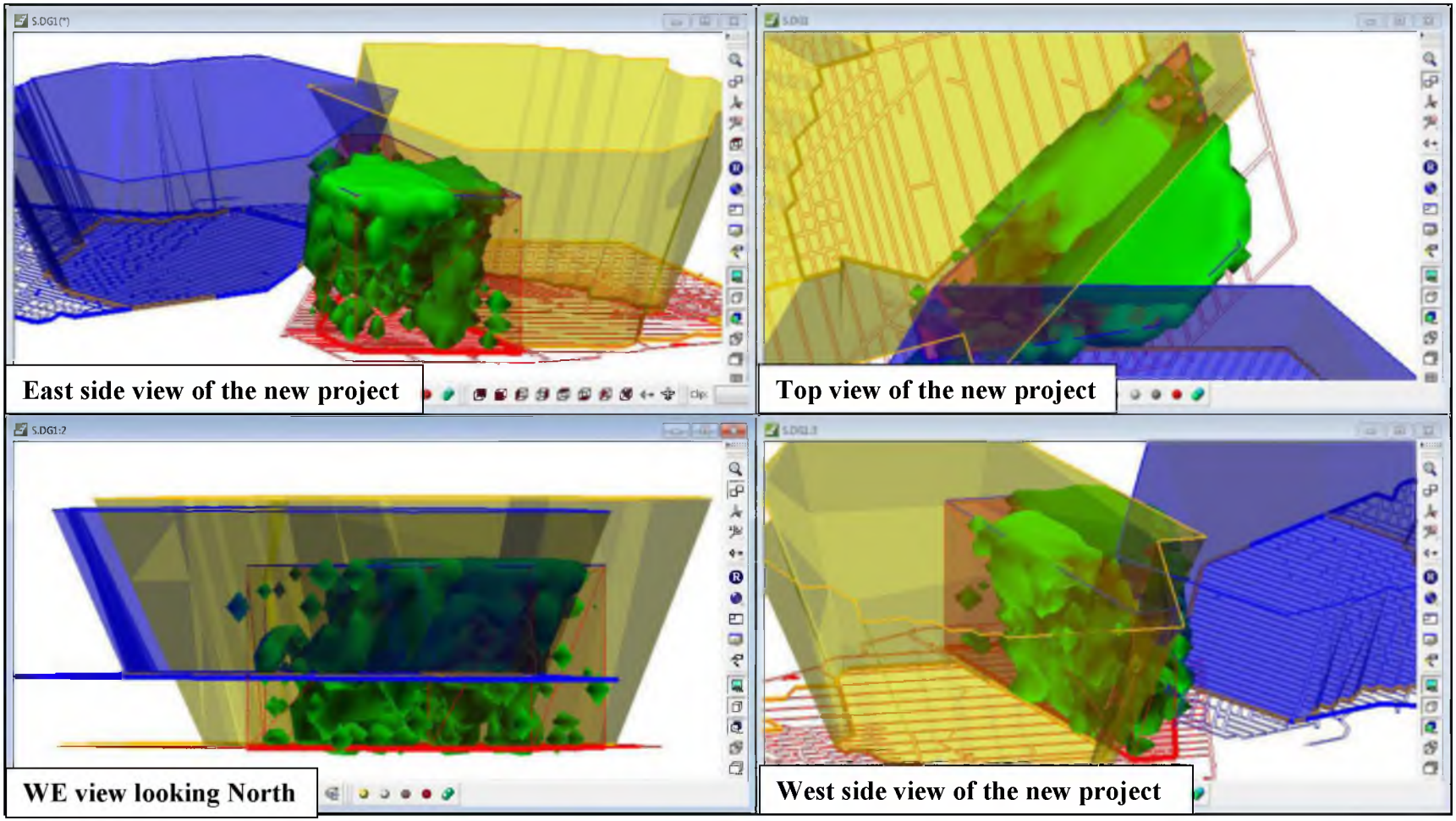

FIGURE 6.26 Different views of accumulated seismic energy inside new project area for year 2010

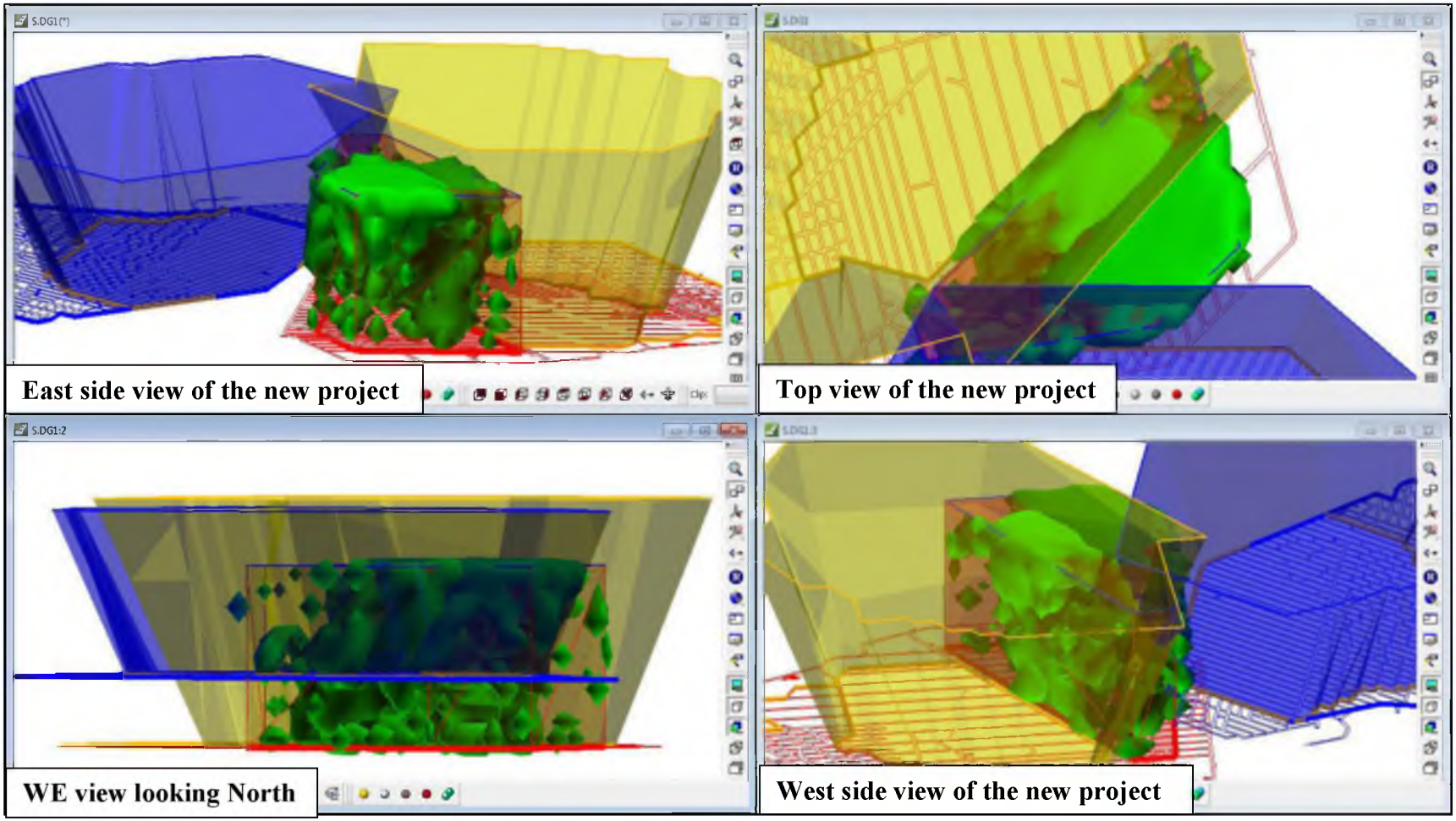

FIGURE 6.27 Different views of accumulated seismic energy inside new project area for year 2011

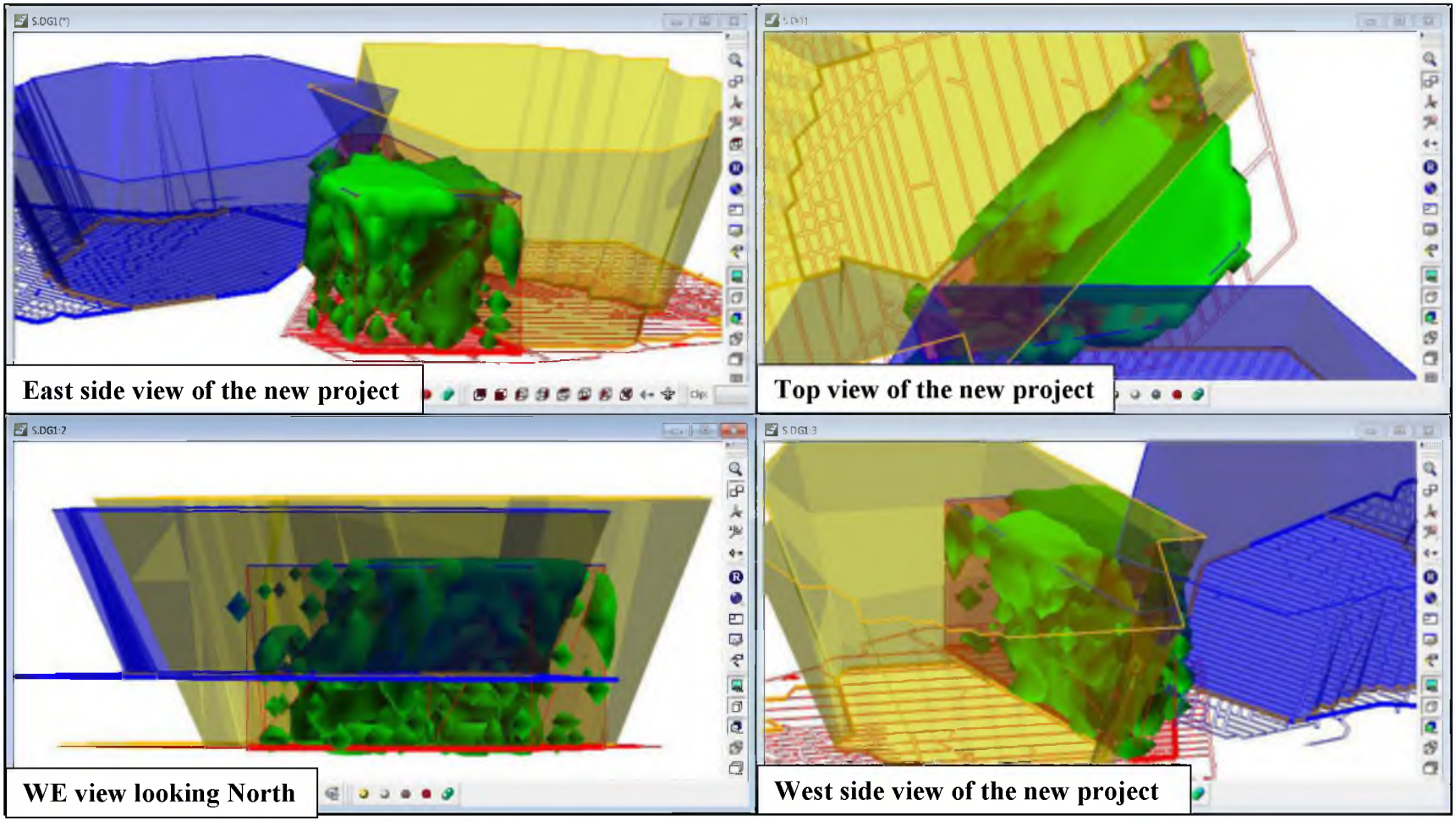

FIGURE 6.28 Different views of accumulated seismic energy inside new project area for year 2012

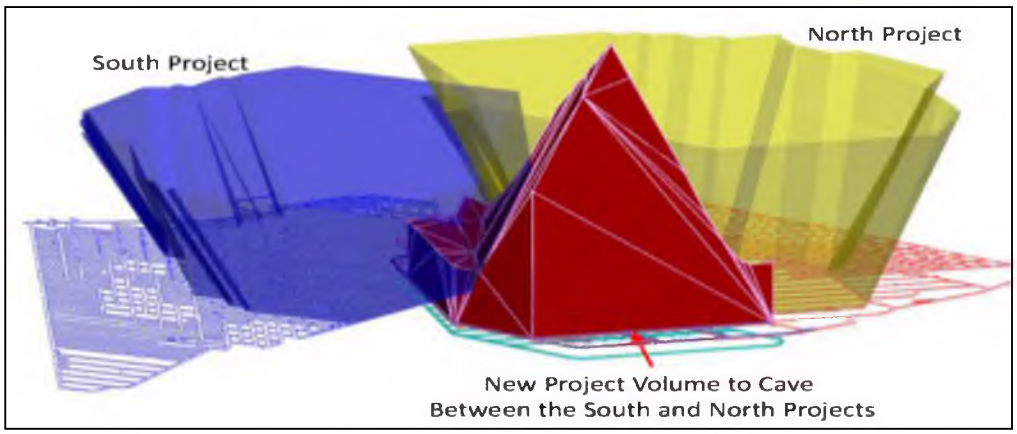

FIGURE 6.29 Real expected project volume between the caving shapes of the North and South Projects

The seismic magnitude for an event inside a given block was added to the accumulated value when that event had an associated magnitude greater than one.

The volume to be caved, as shown in Figure 6.29, is different than the volume to be caved that was studied in Section 6.1.1. In this case, the volume has been cut to the expected, actual shape resulting from its interaction with the North and South Projects, to limit the study to the effects inside that volume. In Section 6.1.1, the projected caving volume for the new project extended up vertically, to allow visualization of the seismic effect of the adjacent projects.

The volume of the future project is shown in a west-east view in Figure 6.30. Here it is seen that the accumulation of seismic magnitude throughout the area has been mostly on the west side of the block. The dashed lines in Figure 6.30 indicate boundaries for the magnitudes of the events, with red being greater or equal to 10, yellow greater than or equal to five and less than 10, blue greater or equal than one and less than five. The magnitudes displayed show the areas that had more seismic activity from year 1992 to 2009.

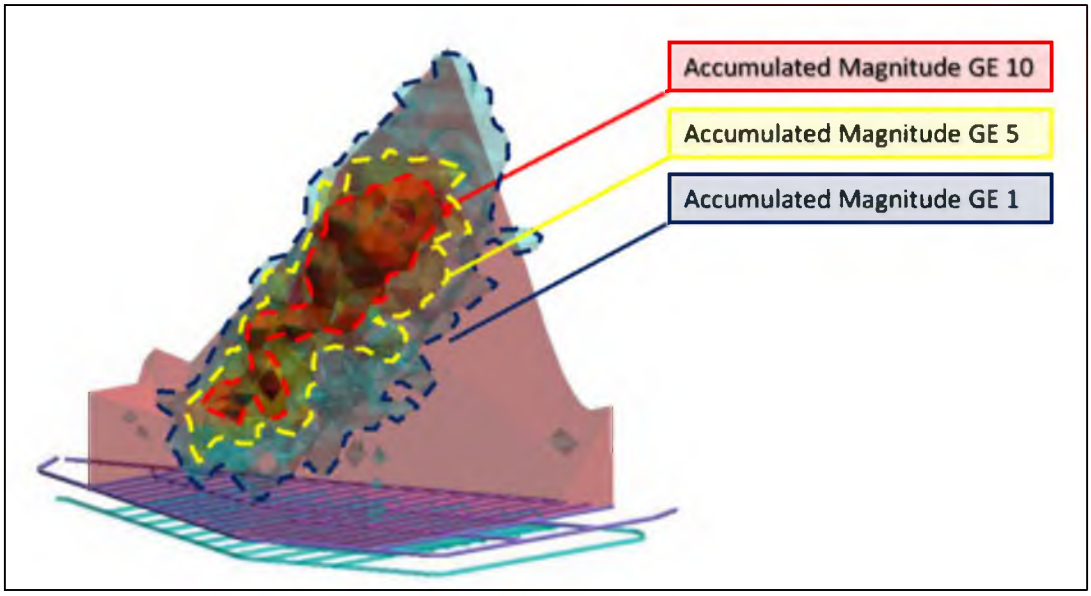

FIGURE 6.30 Project volume between the caving shapes of the North and South Projects showing values greater than or equal (GE) to the defined magnitude index

The analysis then examined how the seismicity moved through the new project volume from 1995 to 2009. As shown in by the green triangulations in Figures 6.31 to 6.35, the seismic activity related to the modeled magnitude moved from the top to the bottom of the light blue volume.

6.2 Areas with Potential Seismic Activity

In another application of this method, modeling of the progressive evolution of seismicity could be used as an initial guide to locate and define possible areas where seismicity might be increased by nearby mining activities.

The model was used to review the progressive, seismic deterioration in blocks close to a seismic event of magnitude 2.2 that occurred in August 2012, and to check if some of the areas closer to the event could have been flagged with the use of the model.

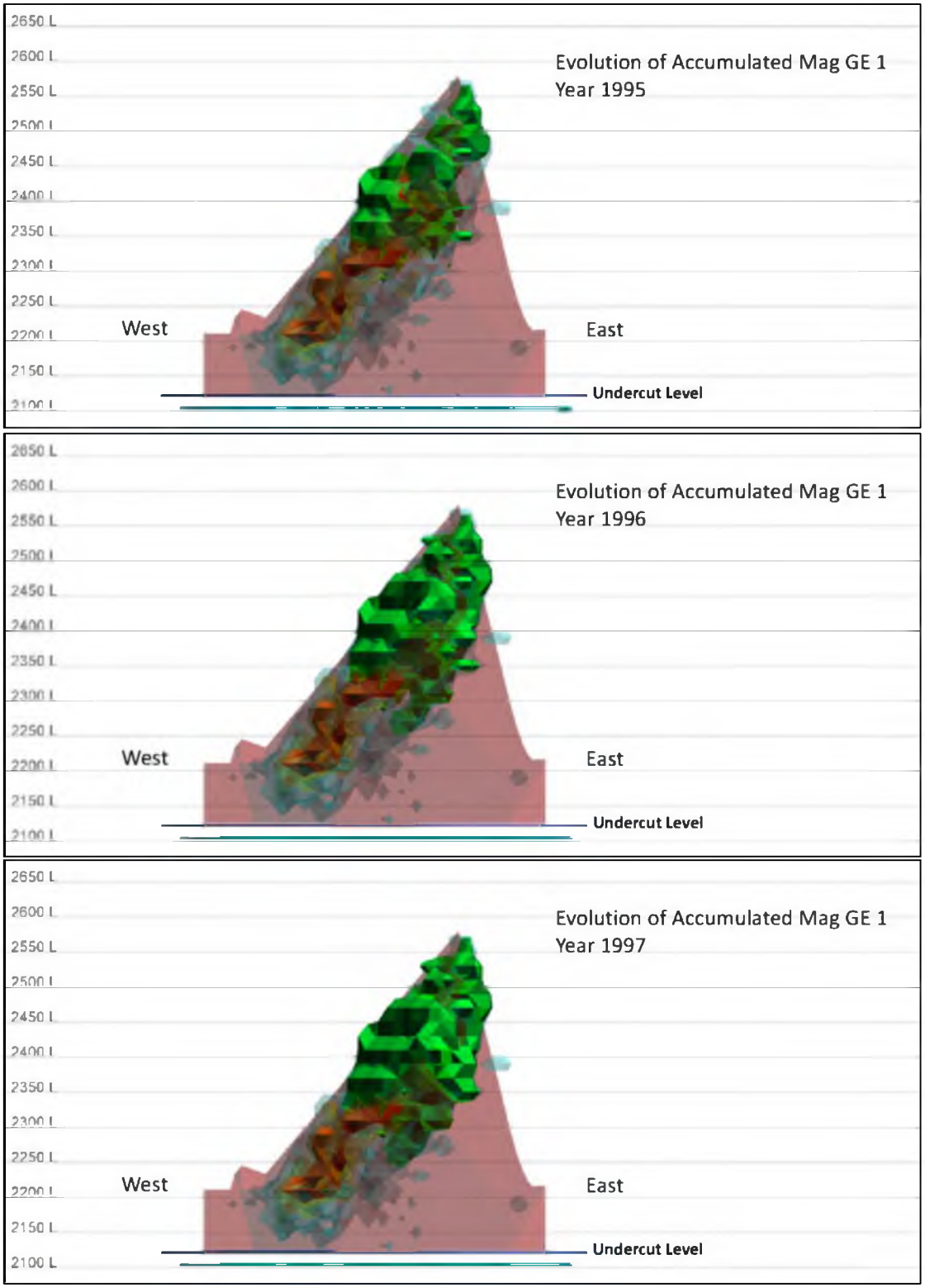

FIGURE 6.31 Accumulated magnitude greater than or equal to one in the project volume for year 1995 to 1997

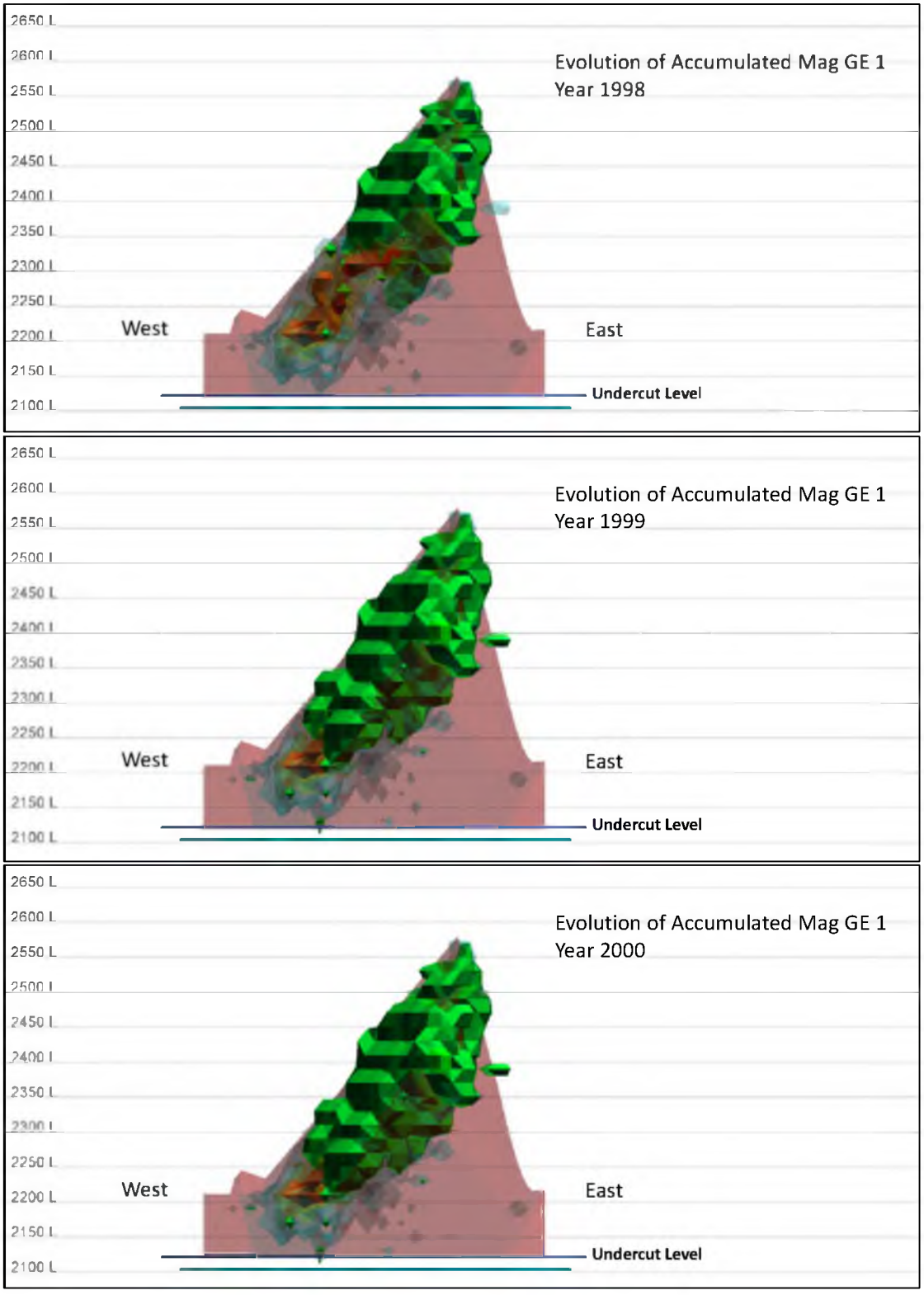

FIGURE 6.32 Accumulated magnitude greater than or equal to one in the project volume for year 1998 to 2000

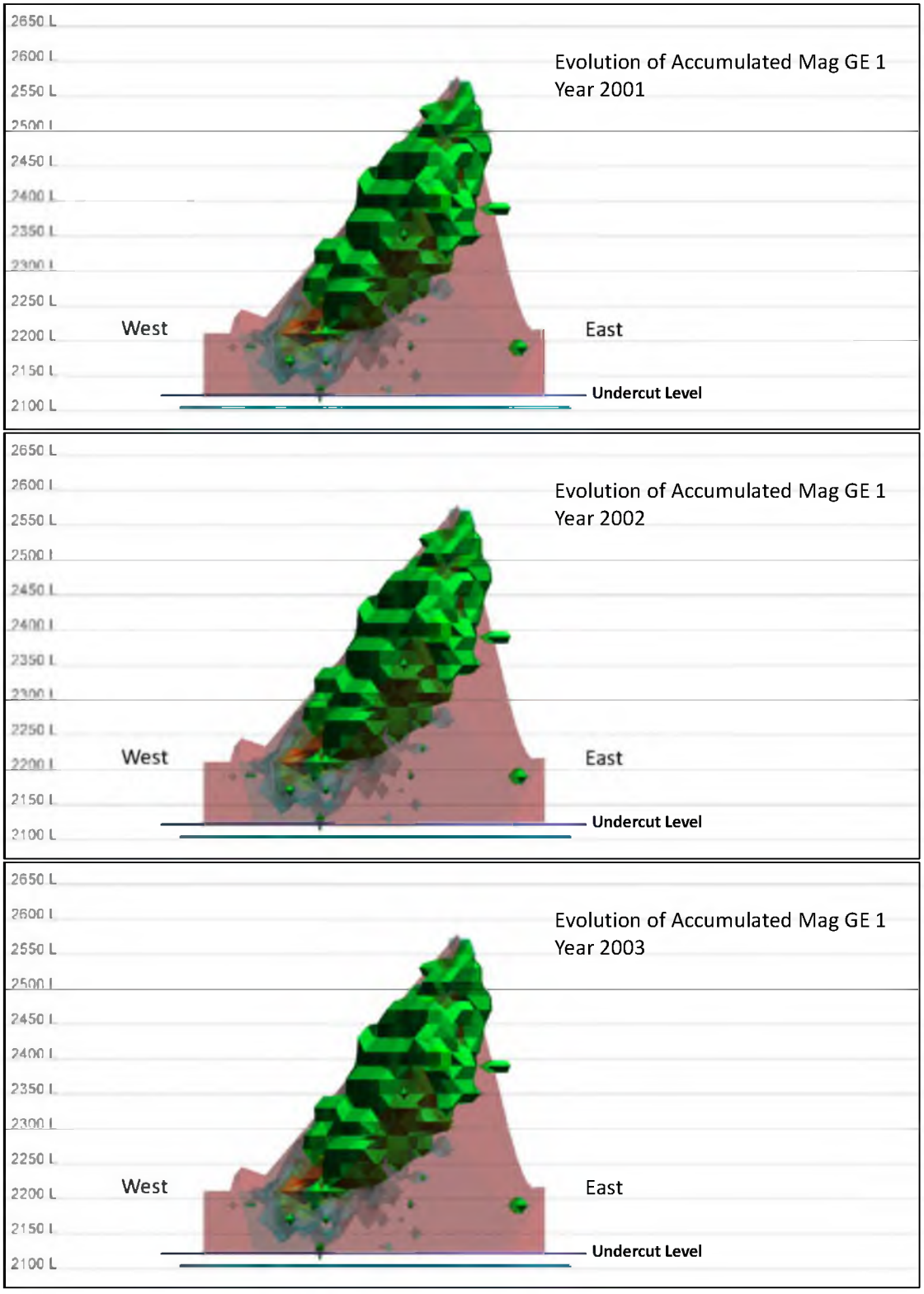

FIGURE 6.33 Accumulated magnitude greater than or equal to one in the project volume for year 2001 to 2003

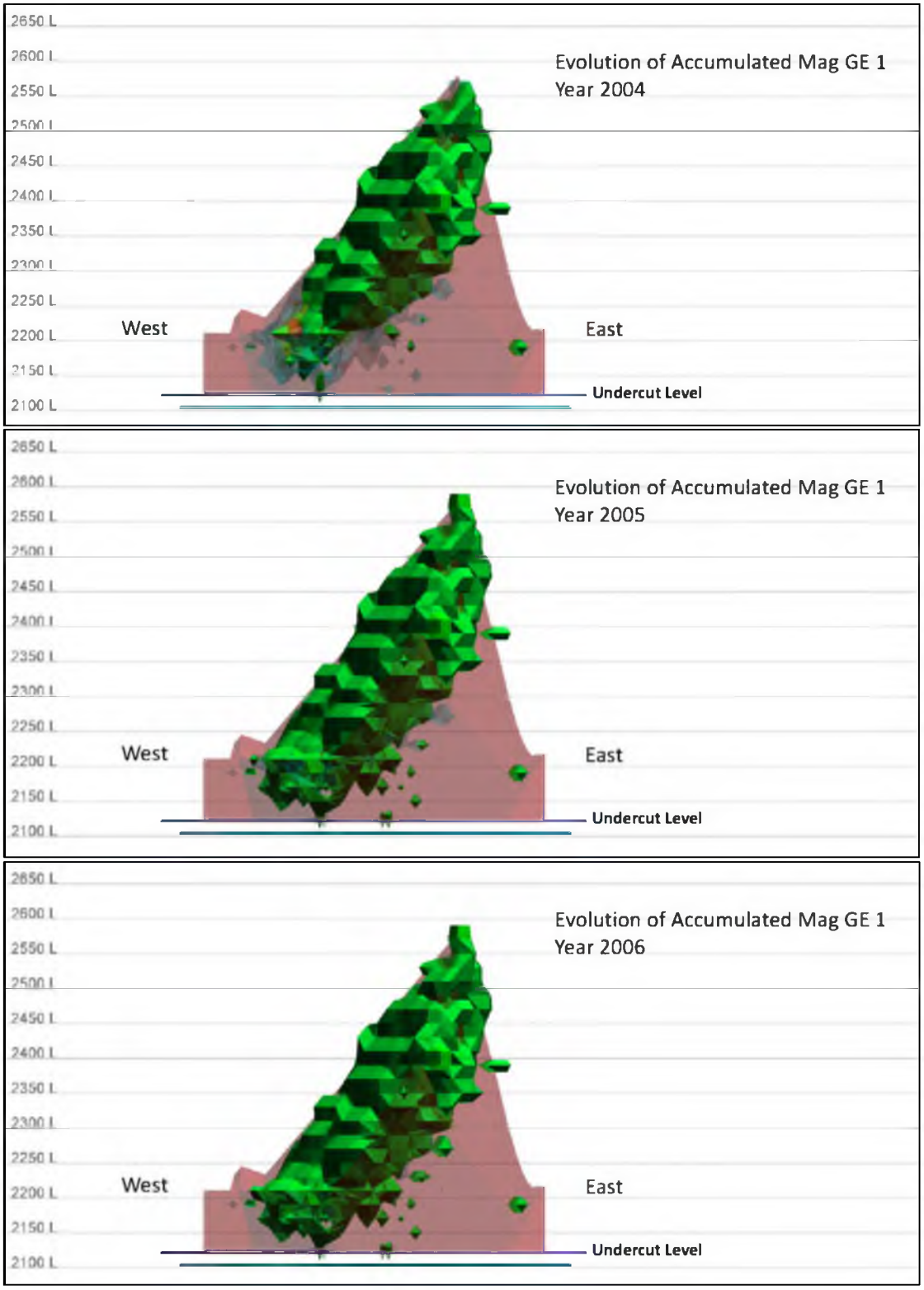

FIGURE 6.34 Accumulated magnitude greater than or equal to one in the project volume for year 2004 to 2006

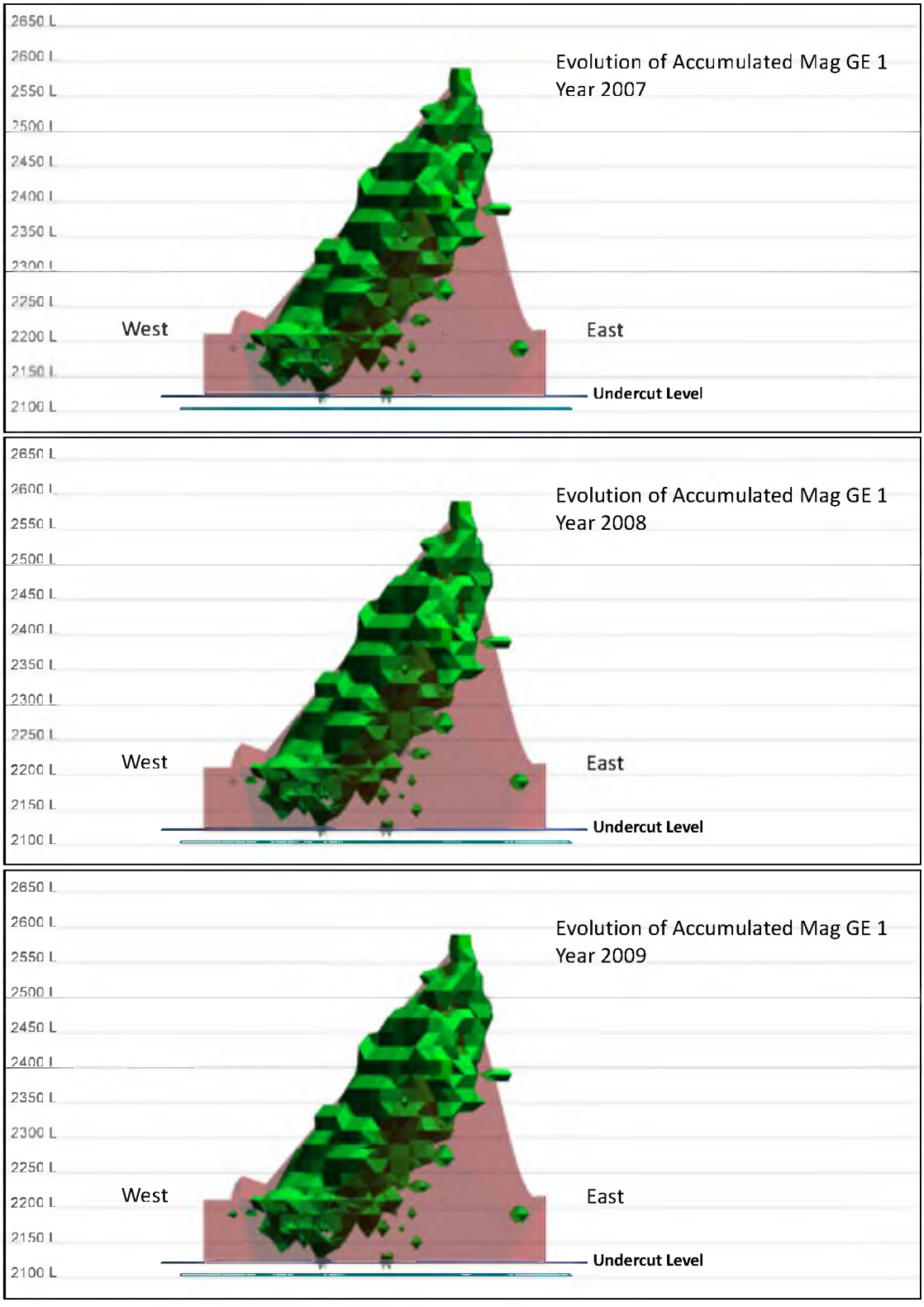

FIGURE 6.35 Accumulated magnitude greater than or equal to one in the project volume for year 2007 to 2009

The event occurred at the coordinates 678 East, 786 North and Elevation 2,084 at 8:05 P.M., with a magnitude of 2.2.

The block above the block where the event occurred showed values much higher than the rest of the surrounding blocks (Figure 6.36). It had a peak value of 103,000 J. This block sustained a series of energy releases that started with one event in 2009, then 18 events in 2010, followed by 51 events in 2011, and 35 events from January to May 2012. The highest event on the block occurred in April 2010, with an energy associated of 102,000 J.

The energy associated with the block that sustained the event was 853 J, and the blocks at the same elevation showed most of the associated values between 1,000 J to 3,000 J, with two blocks to the west showing higher values, around 16,000 J and 38,000 J, as shown in Figure 6.37.

The model can be used to establish the location of areas with high energy values at a selected elevation. For example, Figure 6.38 shows the areas at level 2,300 that have values higher than 90,000 J.

The seismic event can be localized at a selected level, as shown in Figure 6.36, where with the block to the left has an accumulated energy of 15,863.64 J. This particular event shows a nearby block with an unusual accumulation of energy for the area of 103,158 J where the block is on top of the event localization, as shown in Figure 6.36. In addition, all of the blocks surrounding the event at the same level can be viewed, as shown in Figure 6.37.

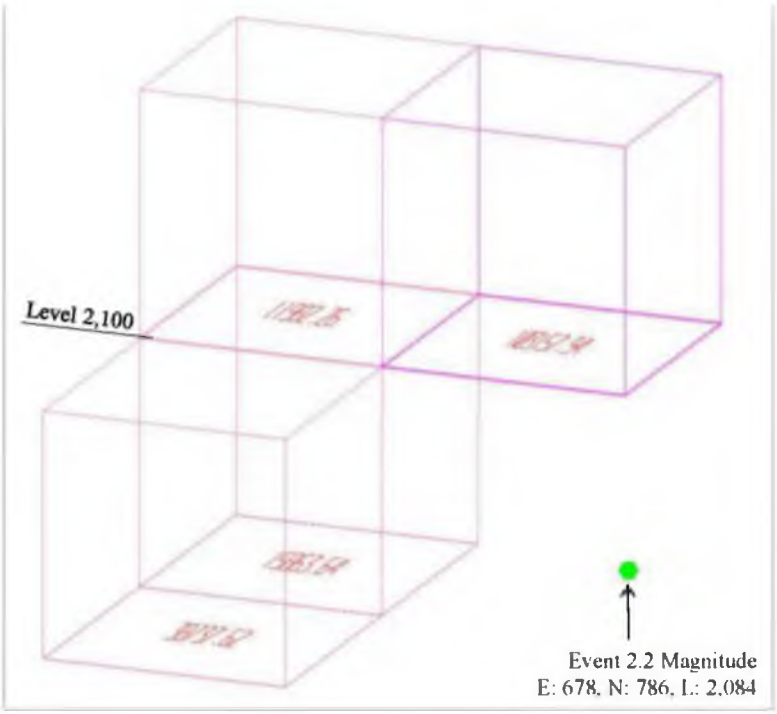

FIGURE 6.36 Seismic event location with high energy block on top (103,158 J)

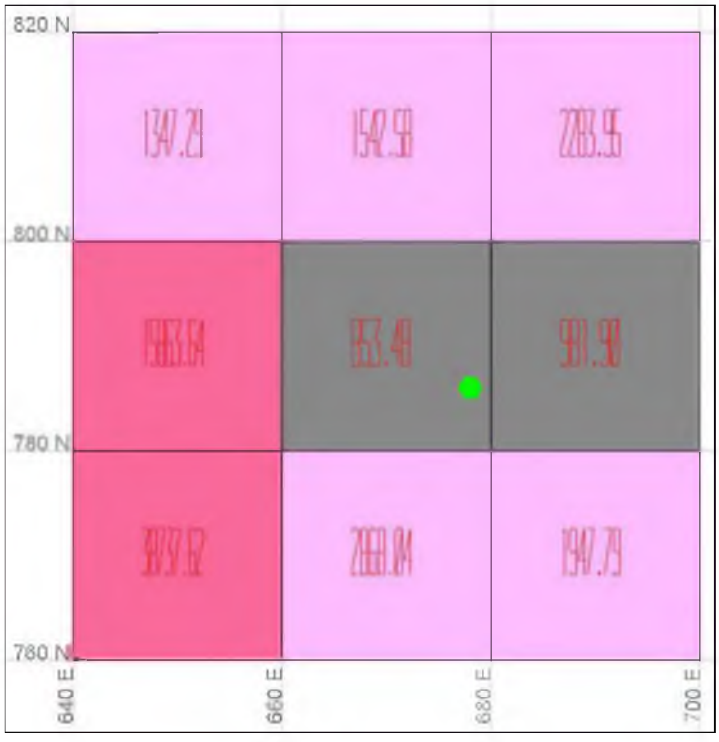

FIGURE 6.37 Seismic accumulated energy on surrounding blocks of the seismic event

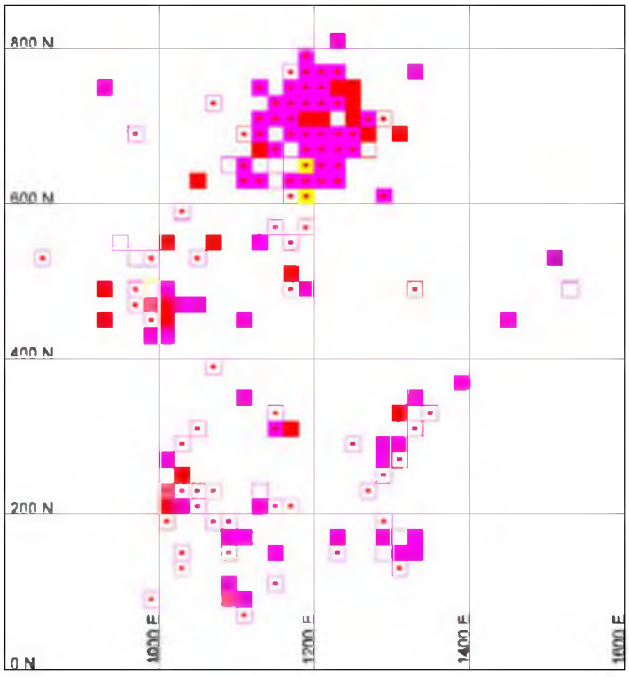

FIGURE 6.38 Sample 20 m x 20 m areas with seismic accumulated energy over 90,000 J

6.3 Relationship between Relevant Events and Model Information

The technique that was developed for modeling progressive seismic activity was used to examine areas where significant geomechanical events had taken place, and determine whether nearby blocks showed unusual increases in energy prior to the event in question. In this study, significant geomechanical events were those that resulted in a disruption of mine production or other operations.

Thirty-four geomechanical events in one area were located within the developed block model. The relevant events were analyzed with the modeled data and the locations of the events were used to look for blocks that showed unusual seismic activity prior to the occurrence of each event. A monthly resolution model was used to find the blocks that had sudden increased seismic activity up to one month before the relevant event occurred.

The events that showed a correlation with the modeled seismic data are shown in Table 6.1. The table shows the location of the block closest to the event that showed the highest accumulated seismic energy. It also shows the associated energy value, the difference in months between the seismic event and the time the seismic accumulation occurred, the distance between the event and the center of this block, and the date that this sudden accumulation of energy occurred.

The study of the events and their correlations showed the following results:

- There were 34 relevant geomechanical events in the mine area studied, which had a footprint of 160,000 m^2. Those events were used to compare the locations of these relevant events and the accumulated energy distributions in the blocks surrounding the event one month before the occurrence of the event.
- Out of 34 major studied for the same level of the mine, 16 events (47%) took place near blocks that showed increased seismic activity prior to the relevant event taking place.
- The 16 relevant geomechanical events took place from March 1997 to December 2012, with two events in 1997, three in 1998, three in 1999, two in 2001, one in 2002, and five in 2003.
- Out of the 16 events, there were four events that showed seismic activity in the 10 months preceding the event, in a block close to the relevant seismic event.
- Out of the 16 events, 12 (called main events) showed an increase of energy in a nearby blocks in a period 4.1 months or less before the event.
- Of these 12 main events, 75% showed an increase in energy from 1 to 6 months before the event took place.

TABLE 6.1: Relevant geomechanical events and correlation with model blocks and accumulated energy

Relevant Events					Block with Increased Seismic Energy						
Number	Date	East (m)	North (m)	Level (m)	East (m)	North (m)	Level (m)	Acc.Energy (J)	Acc.Date	Diff.Months	Distance (m)
1	Mar-97	1,117	537	2,205	1,130	530	2,210	164,000	Jan-97	2	16
2	Apr-97	1,095	514	2,200	1,110	530	2,210	14,317,752	Mar-97	1	24
3	Jul-98	969	486	2,288	990	490	2,290	16,722,190	Sep-97	10	21
4	Nov-98	1,120	559	2,337	1,130	570	2,350	18,600,000	Jul-98	4	20
5	Dec-98	956	462	2,165	990	450	2,170	328,500	Jun-98	6	36
6	Mar-99	1,000	433	2,313	1,010	430	2,310	660,000	Feb-92	86	11
7	May-99	992	441	2,177	970	450	2,170	4,800,009	Mar-99	2	25
8	Aug-99	1,372	464	2,158	1,370	490	2,150	288,000	Jul-99	1	27
9	Jun-01	1,024	354	2,216	1,030	370	2,210	656,320	Nov-00	7	18
10	Dec-01	1,440	322	2,322	1,430	290	2,330	235,000	May-01	7	34
11	Feb-02	1,155	288	2,230	1,170	310	2,210	364,101	Sep-00	17	33
12	Mar-03	1,006	272	2,277	1,030	290	2,290	391,201	Feb-03	1	33
13	Jun-03	1,027	259	2,310	1,030	290	2,290	391,293	Feb-03	4	37
14	Aug-03	1,010	275	2,275	1,030	290	2,290	391,366	Feb-03	6	29
15	Oct-03	1,274	275	2,258	1,250	290	2,230	94,977	Jul-01	27	40
16	Dec-03	1,306	314	2,203	1,330	330	2,210	538,293	Apr-03	8	30

- The average accumulated energy on the blocks that are closer to the events is 3.6 MJ.
- All of the blocks with increased seismic energy close to one of the main events showed an accumulated energy value of more than 90,000 J.
- For the blocks close to the 12 main events that showed increased seismic energy, four blocks showed increases in energy of 4 MJ or more, eight showed increases between 300,000 and 1,000,000 J, and the rest showed increases between 90,000 and 300,000 J.
- In most of the blocks that showed an energy increase, the increase resulted from a single seismic event that represented a sudden accumulation of energy, and not from a series of smaller energy releases.
- The average distance between the blocks that showed increased seismic energy and the location of the relevant event was 27 m. The minimum and maximum distances four such blocks were 11 m and 39 m, respectively.
- The average distance of the relevant event and the blocks that presented increased energy activity was 16 m in the North and East directions and 11 m in the Z axis.

These results show that the developed model has potential to provide a useful tool to establish certain areas of the mine where relevant geomechanical events might occur, by defining an energy cutoff value and establishing surrounding areas that show sudden energy increases.

6.4 Areas with Higher Damage Potential

In another application, a seismicity model using the radiated energy can be used to define areas where the seismicity induced by mining operations may include rock that has a higher potential for structural activation.

A block model can be constructed with different energy cut-off levels to show areas that have had increased dissipations of seismic energy (Figures 6.39 and 6.40).

Figures 6.39 and 6.40 show two options for viewing this information. Figure 6.39 shows 2-D representations of triangulated solids, while Figure 6.40 shows a section through the same solids.

6.5 Seismicity Related to the Advance of the Undercut Front

The model developed in this study can also be used to visualize how the seismic activity relates to the advance of the undercut front in panel caving. In the following example, the model is use to show how seismicity evolves with the movement of the undercut front in two nearby projects, from 1996 to 2010 (Figures 6.41 to 6.55).

The model shows the difference between the seismicity associated with the undercut front advancing to the north-west in the North Project, in red, and to the south in the South Project, in blue. In the North Project, there is less seismicity associated with the undercut front. The South Project shows higher activity behind the undercut front up to 2002. Then, from 2003 to 2006, the seismicity is almost in line with the undercut front, and from 2006 to 2010, it is concentrated ahead of the undercut front.

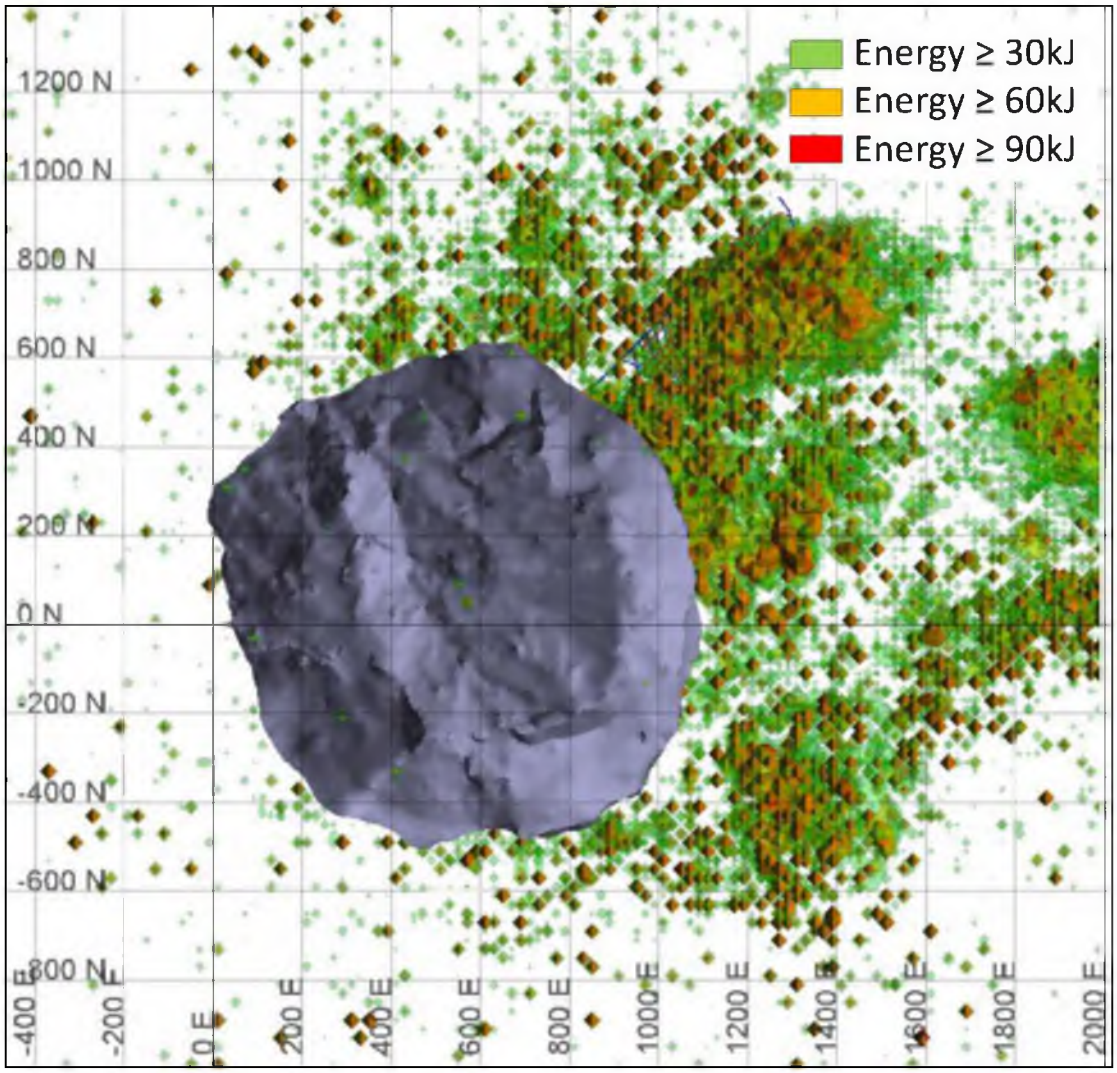

FIGURE 6.39 Plan view of three levels of seismic energy from the model with areas in red showing a higher potential of damage from seismic activity

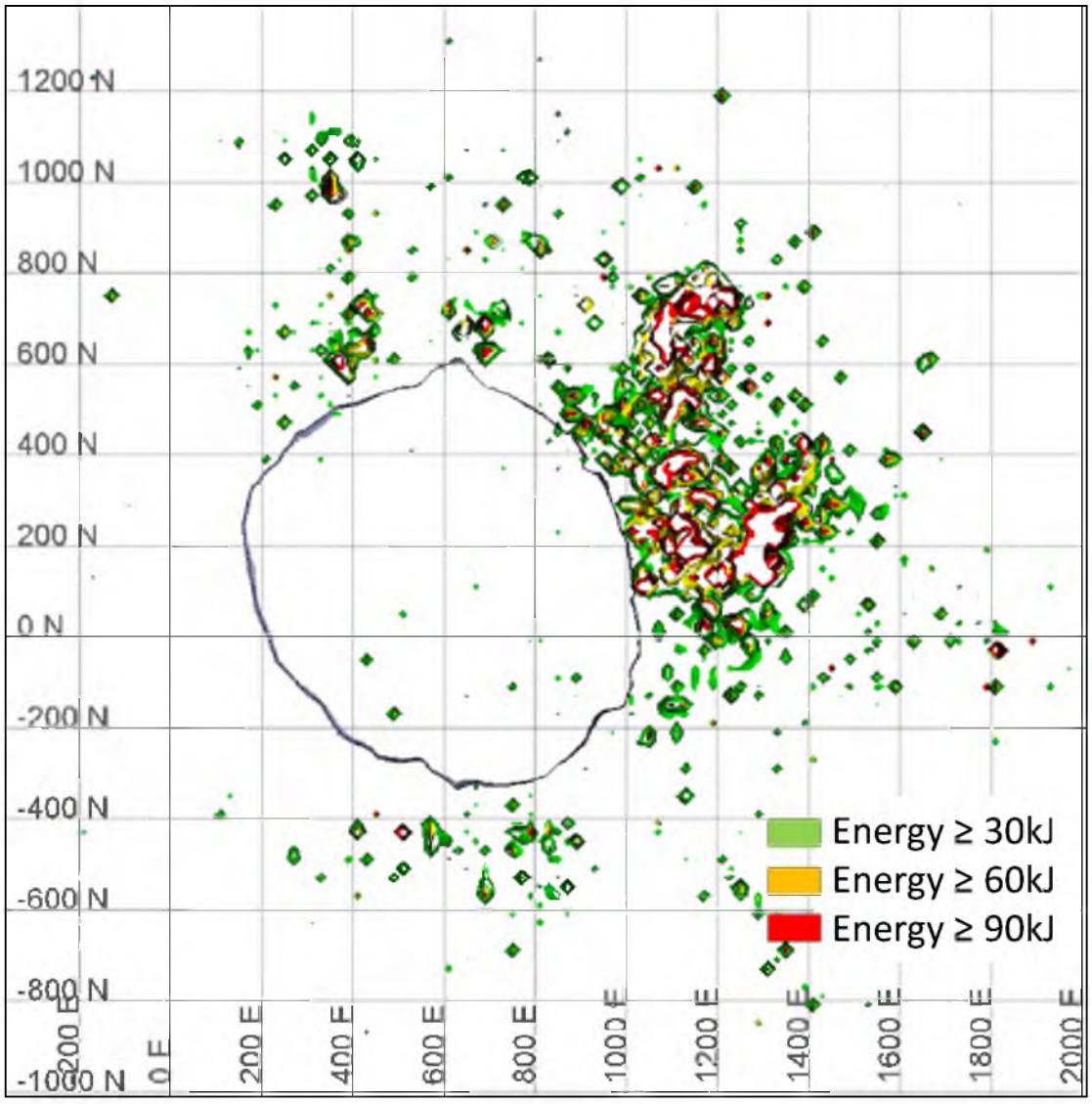

FIGURE 6.40 Plan section of three levels of seismic energy from the model with areas in red showing a higher potential of damage from seismic activity (elevation: 2210 m, section width: 20 m)

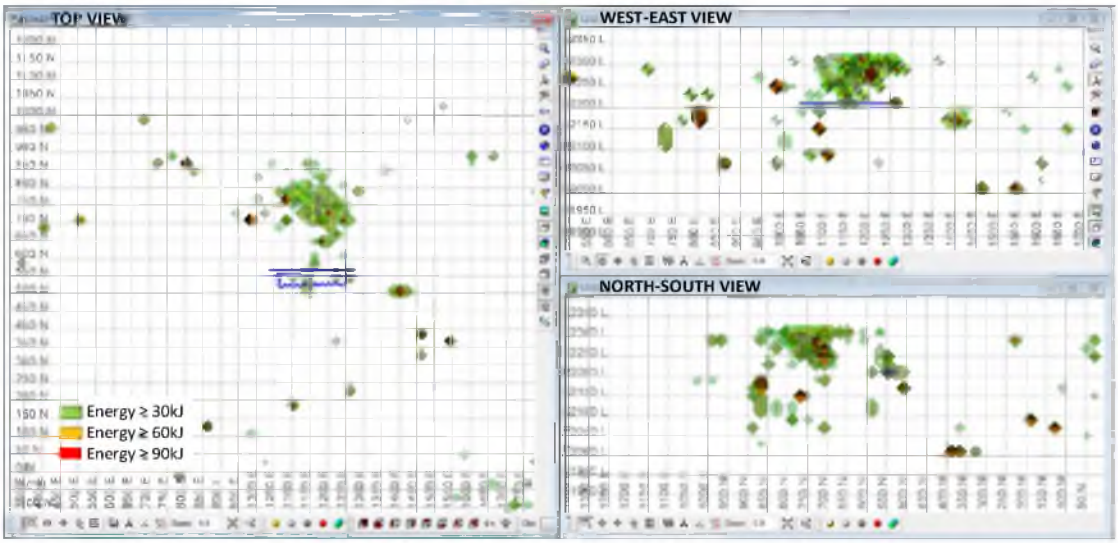

FIGURE 6.41 Seismic energy model (for year 1996) with undercut advance from two projects south (blue) and north (red), showing three energy cut-offs in different views (Top, Front, and Left side views)

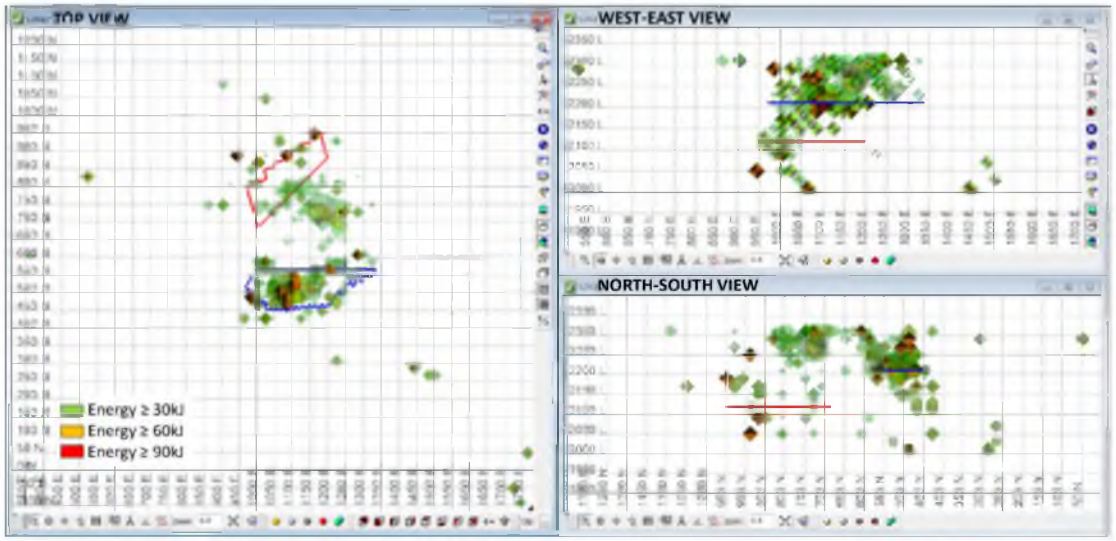

FIGURE 6.42 Seismic energy model (for year 1997) with undercut advance from two projects south (blue) and north (red), showing three energy cut-offs in different views (Top, Front, and Left side views)

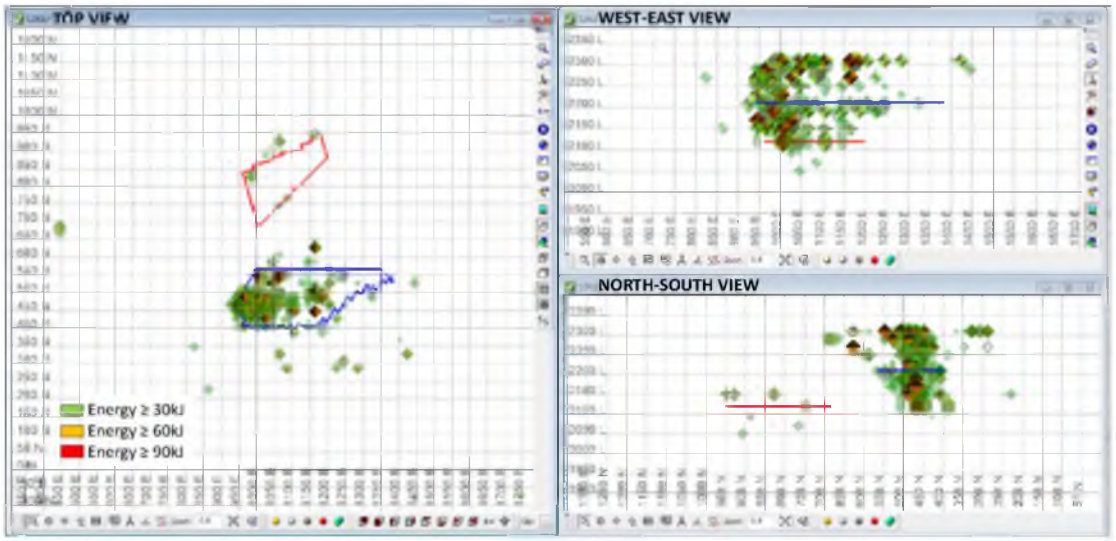

FIGURE 6.43 Seismic energy model (for year 1998) with undercut advance from two projects south (blue) and north (red), showing three energy cut-offs in different views (Top, Front, and Left side views)

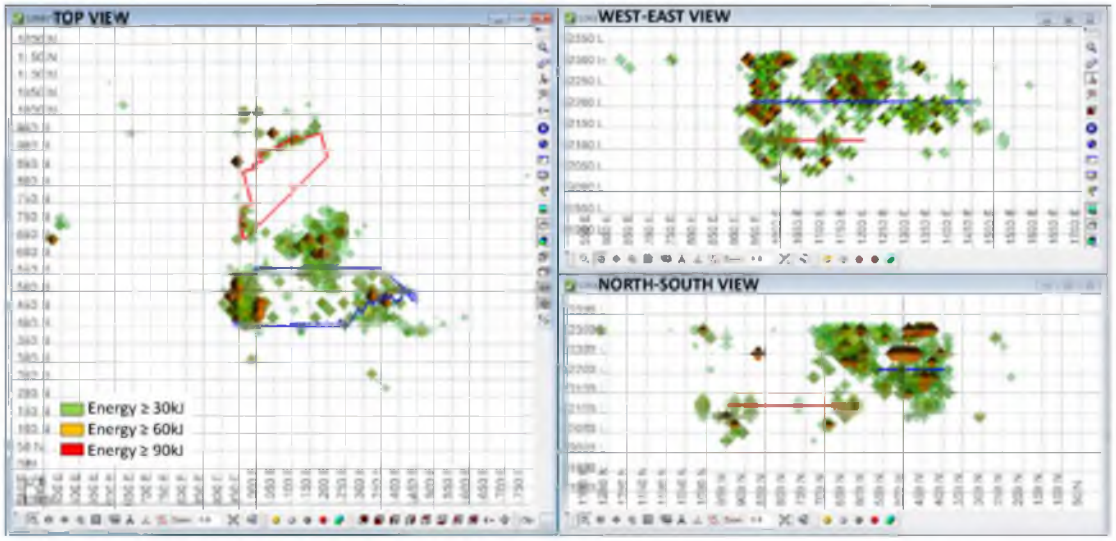

FIGURE 6.44 Seismic energy model (for year 1999) with undercut advance from two projects south (blue) and north (red), showing three energy cut-offs in different views (Top, Front, and Left side views)

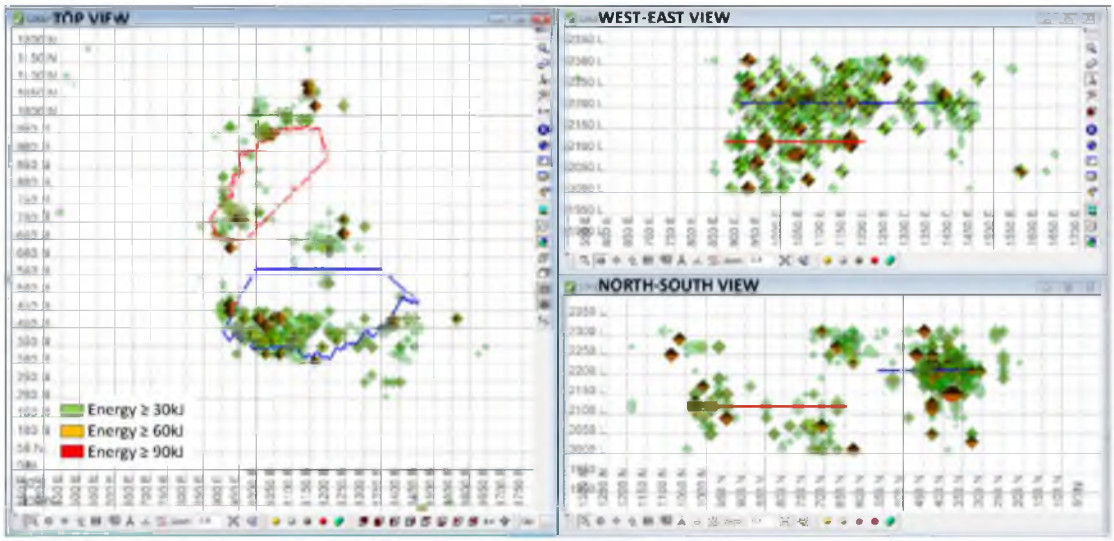

FIGURE 6.45 Seismic energy model (for year 2000) with undercut advance from two projects south (blue) and north (red), showing three energy cut-offs in different views (Top, Front, and Left side views)

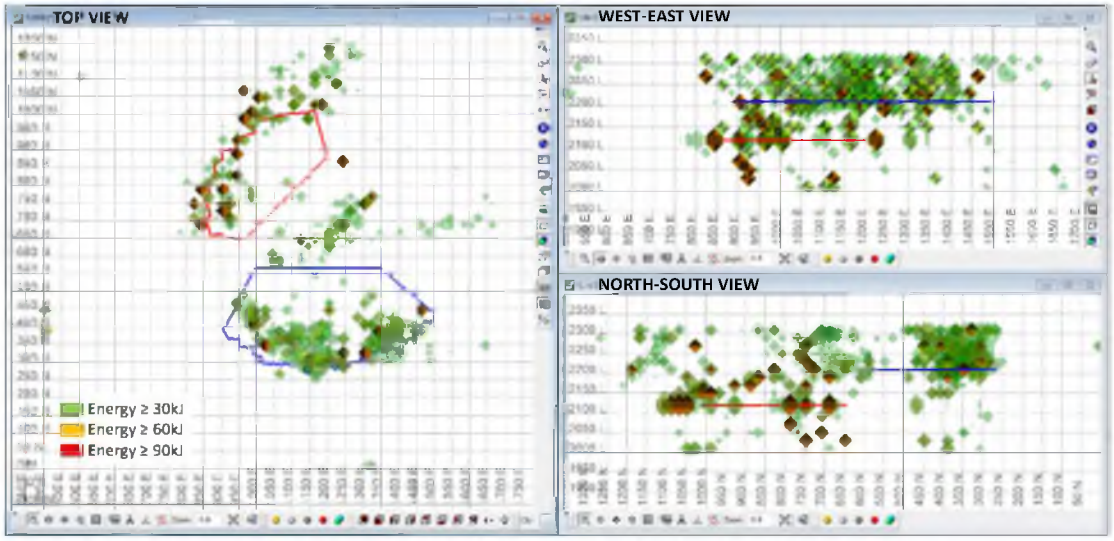

FIGURE 6.46 Seismic energy model (for year 2001) with undercut advance from two projects south (blue) and north (red), showing three energy cut-offs in different views (Top, Front, and Left side views)

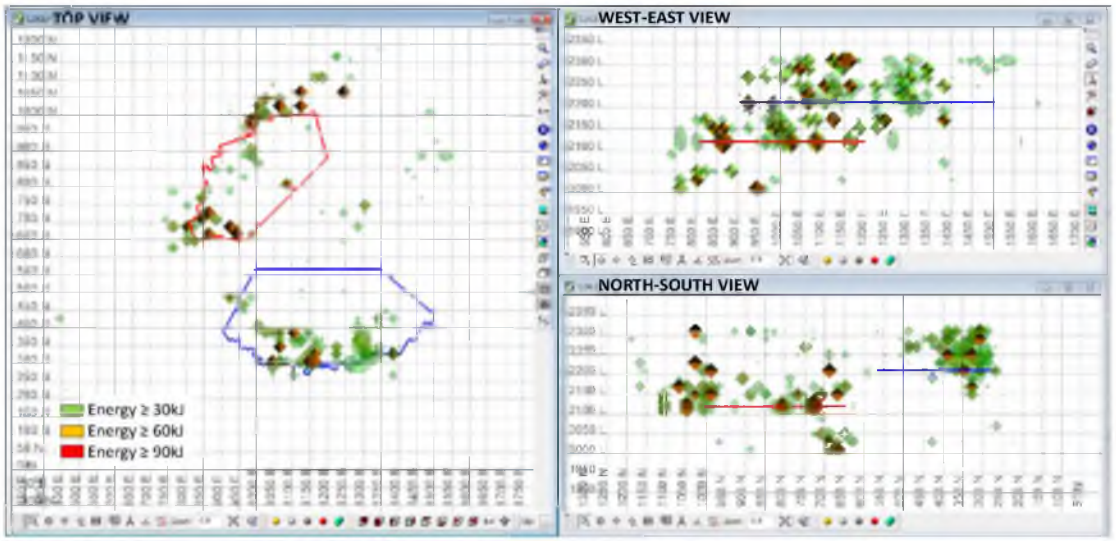

FIGURE 6.47 Seismic energy model (for year 2002) with undercut advance from two projects south (blue) and north (red), showing three energy cut-offs in different views (Top, Front, and Left side views)

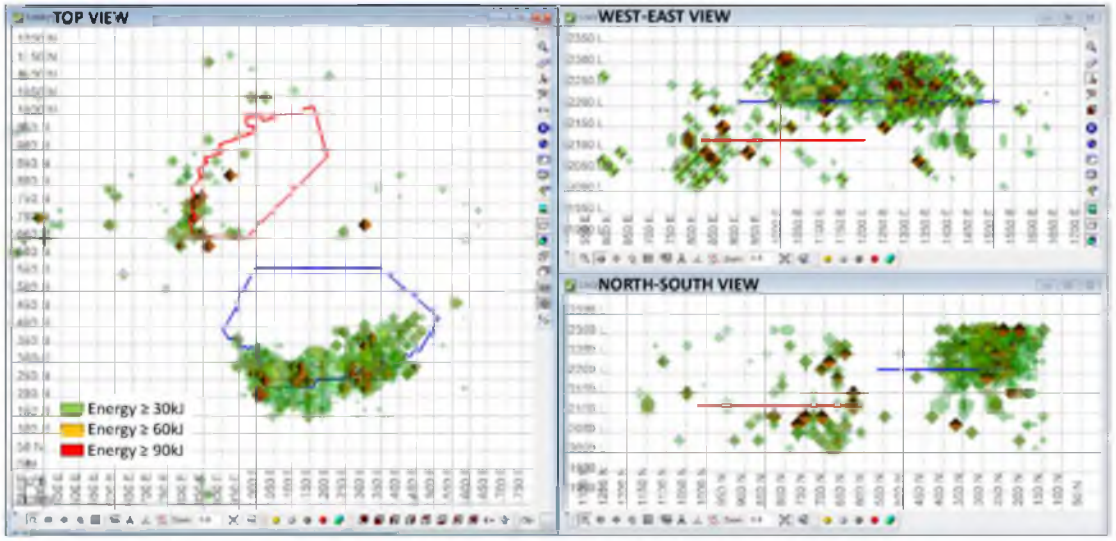

FIGURE 6.48 Seismic energy model (for year 2003) with undercut advance from two projects south (blue) and north (red), showing three energy cut-offs in different views (Top, Front, and Left side views)

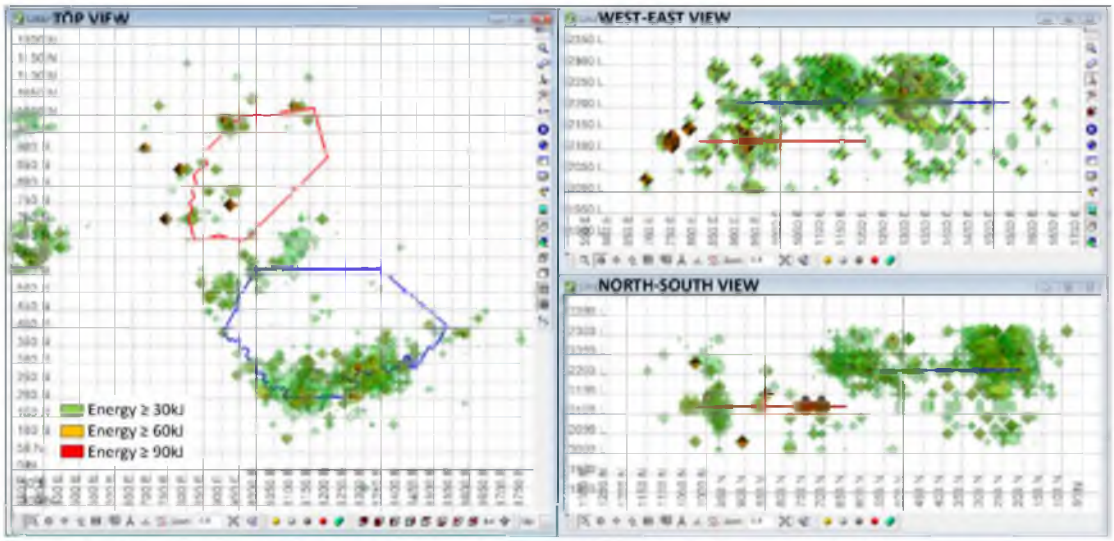

FIGURE 6.49 Seismic energy model (for year 2004) with undercut advance from two projects south (blue) and north (red), showing three energy cut-offs in different views (Top, Front, and Left side views)

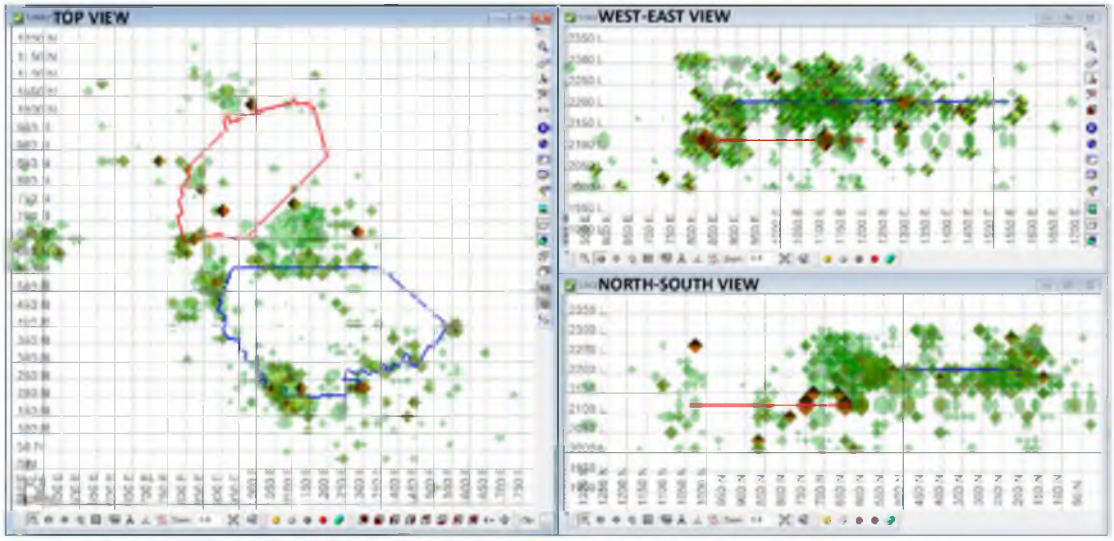

FIGURE 6.50 Seismic energy model (for year 2005) with undercut advance from two projects south (blue) and north (red), showing three energy cut-offs in different views (Top, Front, and Left side views)

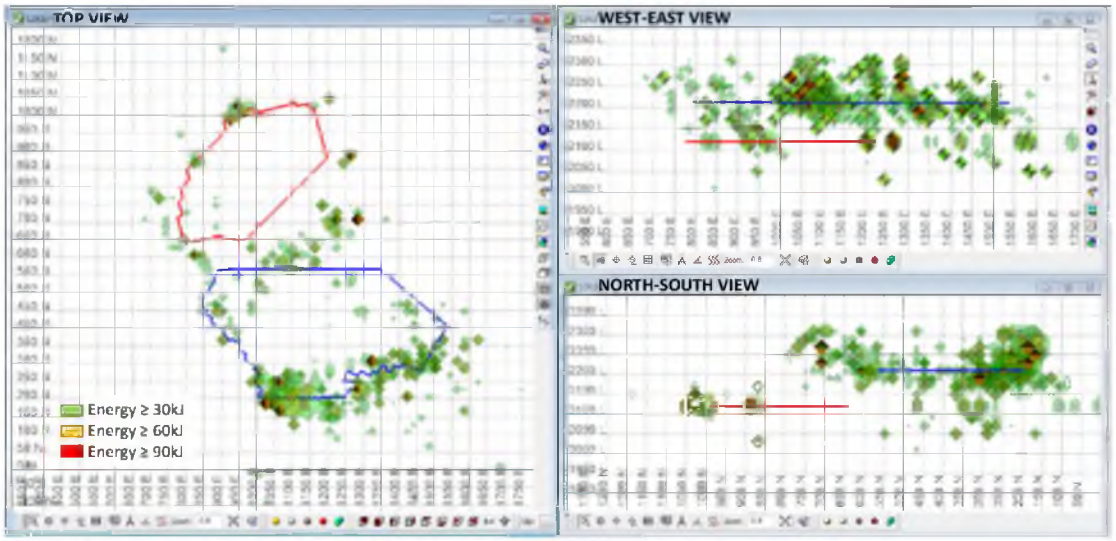

FIGURE 6.51 Seismic energy model (for year 2006) with undercut advance from two projects south (blue) and north (red), showing three energy cut-offs in different views (Top, Front, and Left side views)

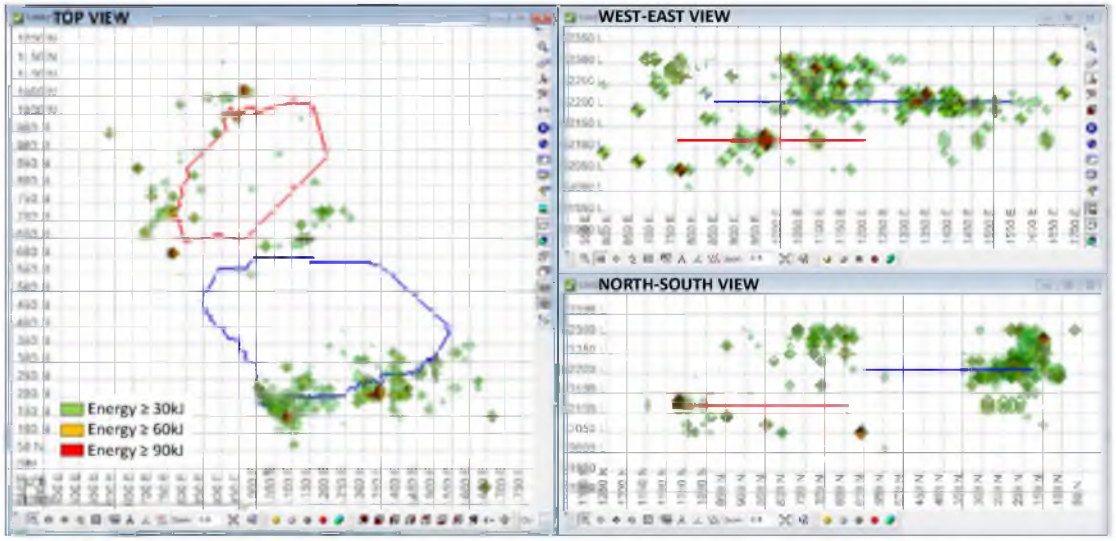

FIGURE 6.52 Seismic energy model (for year 2007) with undercut advance from two projects south (blue) and north (red), showing three energy cut-offs in different views (Top, Front, and Left side views)

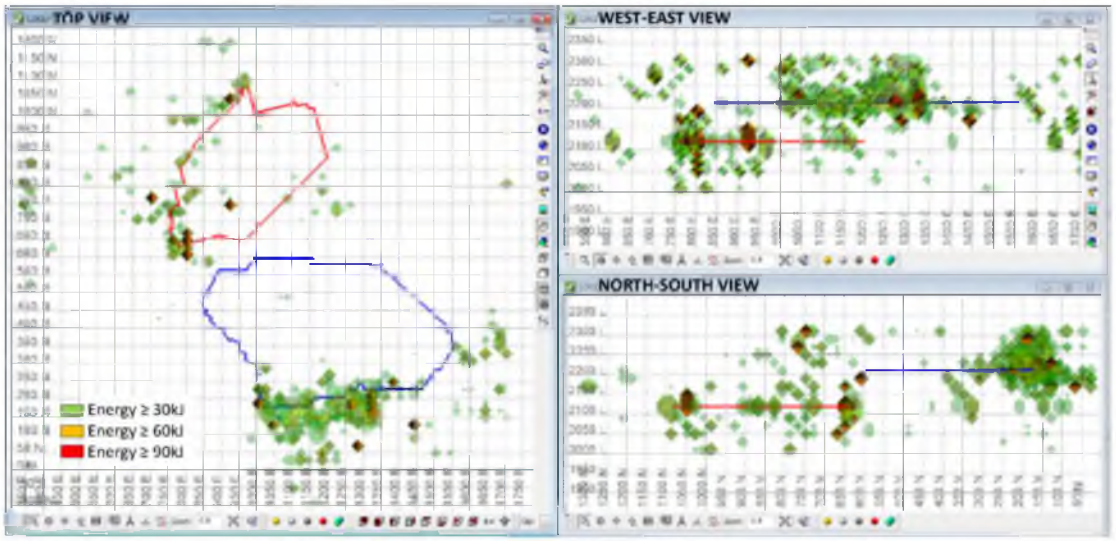

FIGURE 6.53 Seismic energy model (for year 2008) with undercut advance from two projects south (blue) and north (red), showing three energy cut-offs in different views (Top, Front, and Left side views)

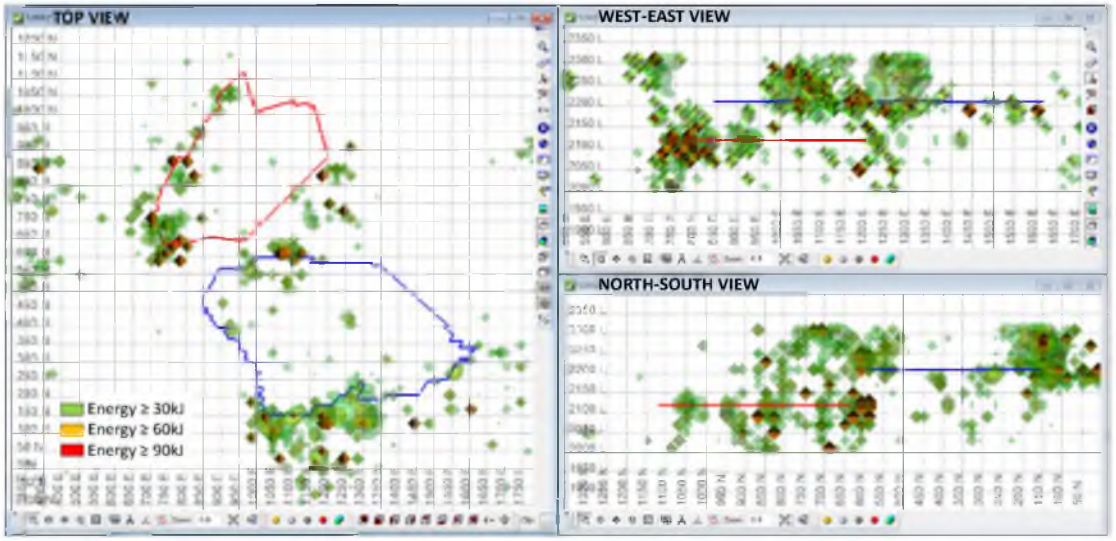

FIGURE 6.54 Seismic energy model (for year 2009) with undercut advance from two projects south (blue) and north (red), showing three energy cut-offs in different views (Top, Front, and Left side views)

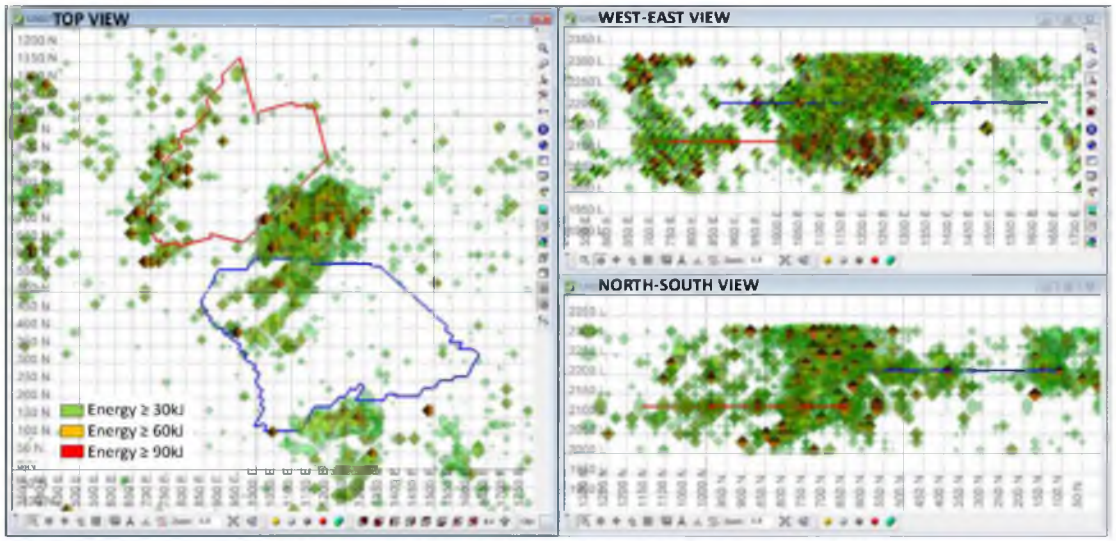

FIGURE 6.55 Seismic energy model (for year 2010) with undercut advance from two projects south (blue) and north (red), showing three energy cut-offs in different views (Top, Front, and Left side views)

7 COMMENTS AND RECOMMENDATIONS

The approach of storing the seismic history of a mine in a standard block model creates an effective tool for analyzing and understanding how various seismic events have migrated and affected different areas of the mine over time. The progression of seismicity can be used to establish the seismic history of areas that might have been affected by previous mining activities.

Analyzing how the seismicity has affected the surroundings of new areas to be mined by caving techniques can be useful in establishing the most suitable for the start of the undercutting of the block.

When the seismicity data are embedded in the blocks, seismic activity can be related in space and time to activities in the mine, and the block viewing filters can be manipulated to display the information contained in certain areas to show the seismic effects in desired areas and times. The behavior of a given area and the energy associated with other caving areas nearby can be tracked to show the effects from the caving process over time.

The analyses can be filtered for the individual blocks to achieve a higher confidence in the data. The two filters studied here, location error and the number of triggers activated by a given event, can also be used alone or together to increase the consistency of the data being used in a particular analysis.

8 CONCLUSIONS

The modeling approach used in this study has shown that the energies and magnitudes associated with seismic events, along with the numbers of triggers and the location errors, can be effectively interpolated into a block model, and that the resultant data can be used to determine areas with historic seismicity that may have resulted in accumulated deterioration of the rock mass.

The ability to model the seismic energy associated with the blocks over time allows analysis of the evolution of the seismicity in different areas of the mine. The resulting information can be displayed as two-dimensional sections in any direction required, or as triangulated solids to better understand how the seismic events evolve through the mine.

The new method presented here for interpolation of the seismic data facilitates the accumulation of the seismic history within a block model, and the modeling of potential deterioration solids. These can be used to study how previous mining activities have influenced areas where new projects are being planned for the future.

The seismic data can be displayed and located at different levels of the mine where seismicity has been recorded through time, for example in the undercut, production, haulage, and ventilation levels of a panel or block caving mine. These visualizations can be used to define areas where significant seismicity has occurred in the past, indicating where potential problems may occur in the future.

The interpolated data provide a powerful tool that facilitates analysis of how the seismicity has evolved in an area where mining with a caving technique is planned. This will allow the identification of preferred locations for the initiation of the undercutting of the block, leading to optimized caving performance and minimizing hangups.

The progressive analysis of seismic activity as presented shows a new way of looking at the evolution of seismic data by combining the data with inverse-distance interpolations and block modeling techniques. Induced seismicity occurs mainly as a consequence of caving and undercutting, both of which are dynamic processes. Undercutting events can vary depending on the undercut method used and when undercutting takes place in relation to other development activities. These variations in undercutting procedures will affect the "cavability" of the rock mass, and the accumulation of seismic area in particular is one good indicator of how the rock mass will behave during caving.

The methods presented here constitute a new approach to the study of seismic information, by allowing the association of several variables related to seismicity with the blocks in a block model. This is convenient and useful because mine operators, planners, and engineers use block models regularly, and are familiar with the organization and presentation of data in this manner. The association of seismic variables with the blocks in a model allows the seismic information to be filtered based on one or more parameters. Such filtering can eliminate minor or unimportant seismic events, allowing a much clearer visualization of the accumulation of seismic energy in a particular area of interest.

There is great potential in applying this modeling method to studying the correlation between relevant, geo-mechanical events that have caused problems at the

mine and the blocks that have shown unusual increases in seismicity prior to the occurrence of the relevant event taking place. The example presented in Section 6.3 considered 34 relevant geomechanical events, and the model showed that in 16 of them, there was a nearby block that experienced a sudden accumulation of energy prior to the occurrence of the relevant event.

Though examples are not shown here, it is clear that this modeling approach can be readily used in conjunction with numerical modeling packages, such as Flac, Map3d, or Abaqus, to define zones where rock mass properties have changed, and damage potential might be increased by mining resulting in geomechanical events leading to problems in production and operation.

The volumes derived with this approach, showing progressive seismic activity, can be used in finite element modeling analyses to define areas where the rock mass has been changed over time, providing an important tool for enhancing numerical analyses in the future.

APPENDIX A

SEISMIC ENERGY MODELED BY YEAR

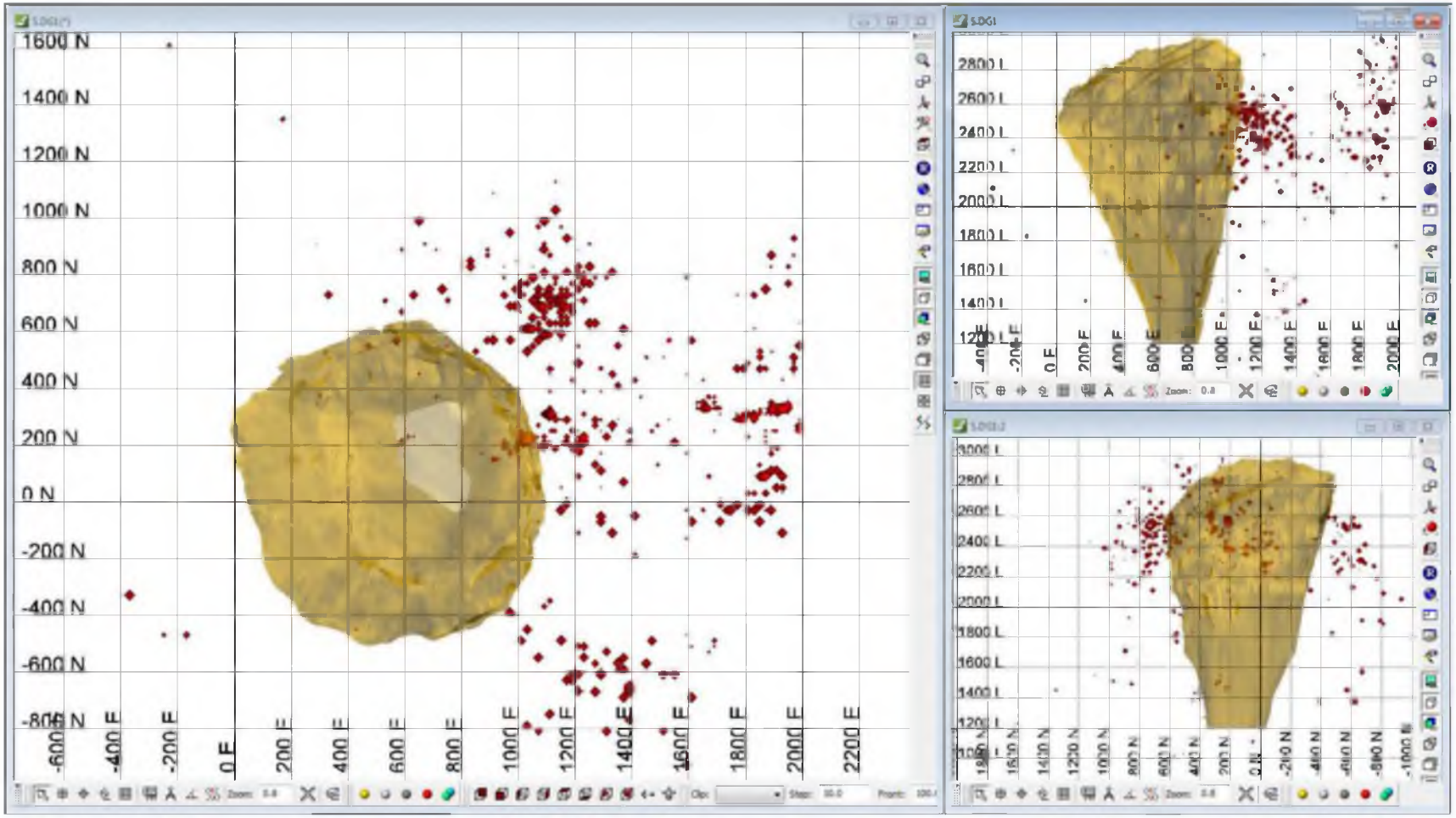

FIGURE A.1 Seismic energy for year 1992

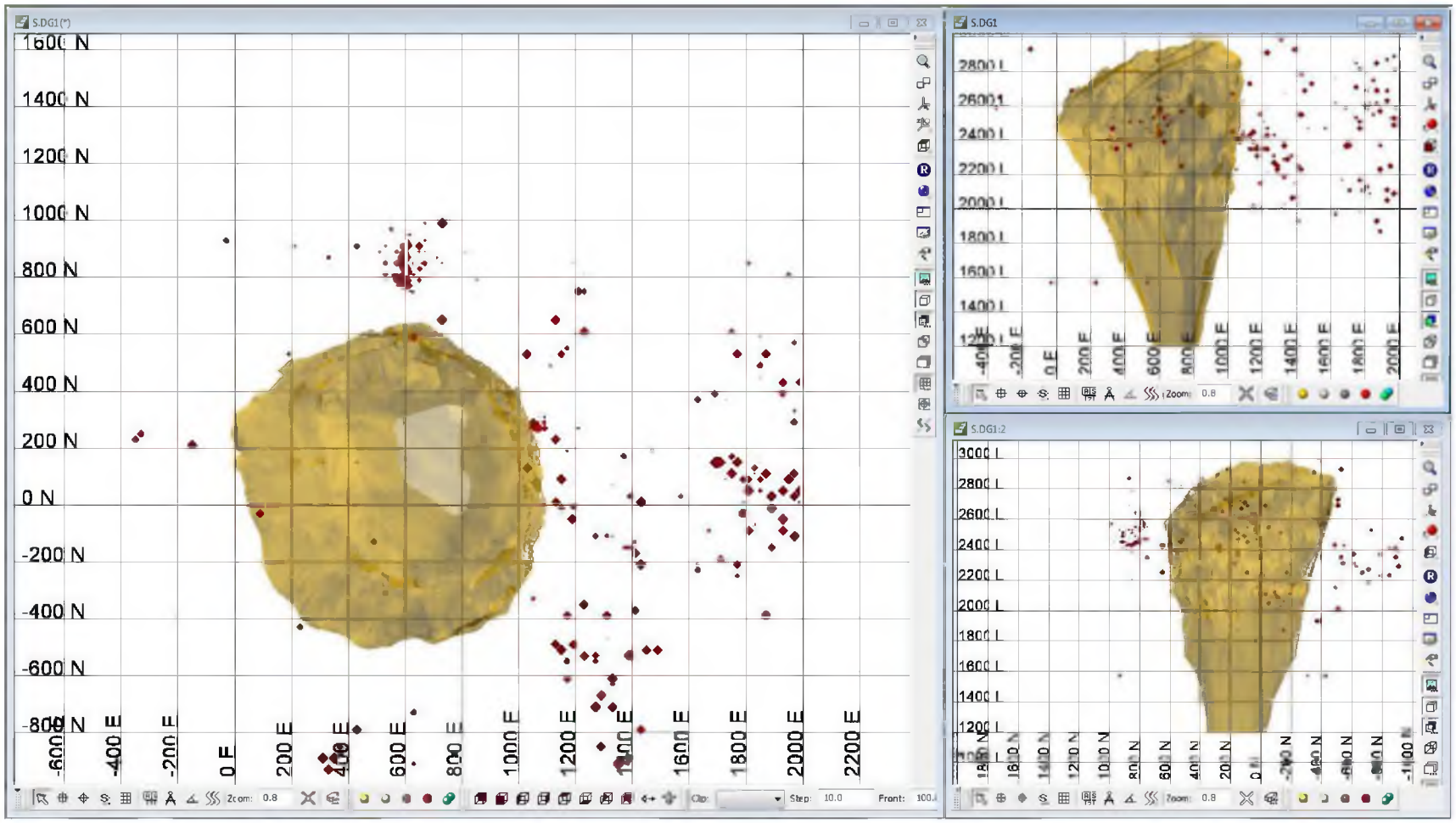

FIGURE A.2 Seismic energy for year 1993

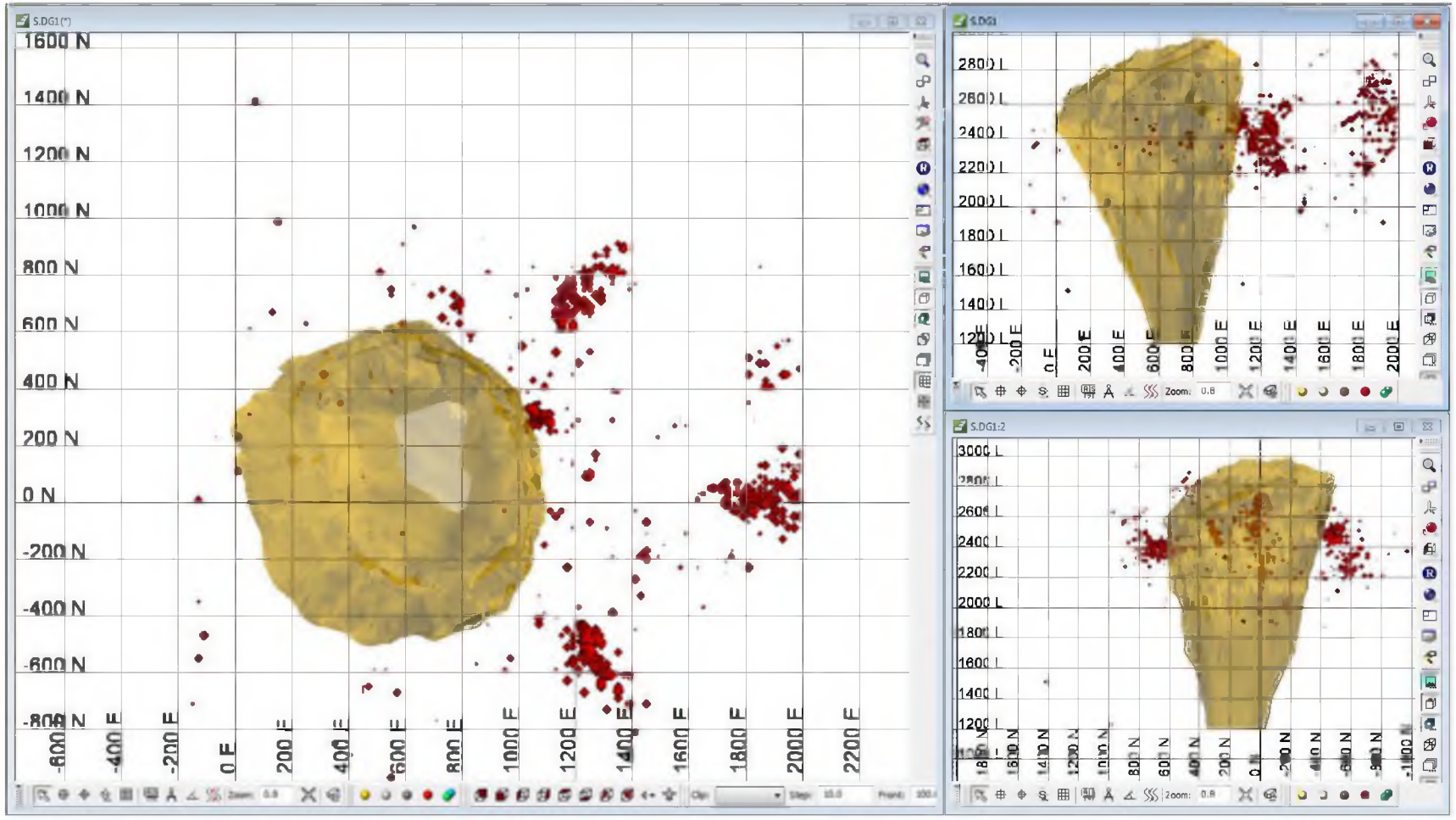

FIGURE A.3 Seismic energy for year 1994

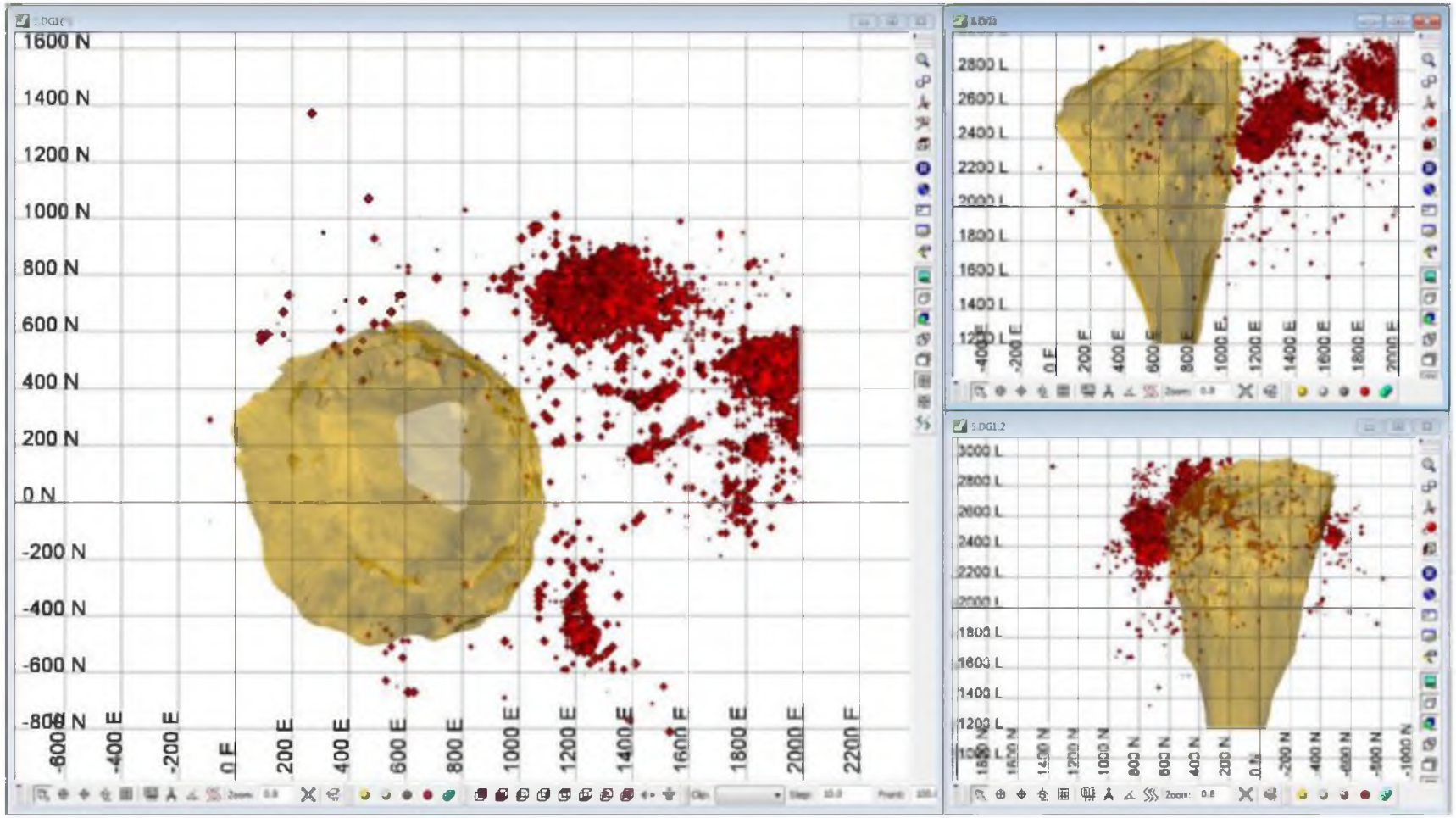

FIGURE A.4 Seismic energy for year 1995

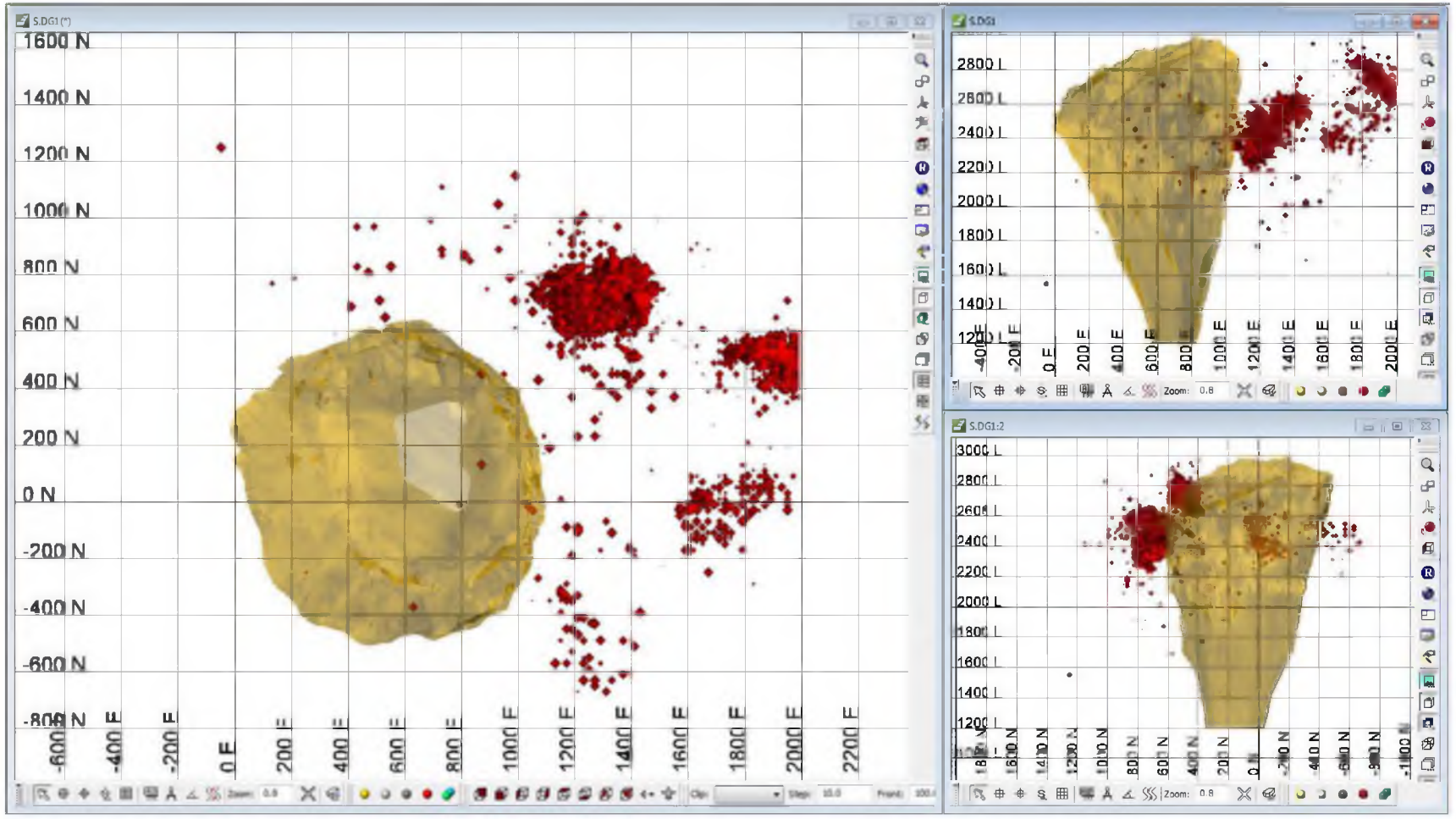

FIGURE A.5 Seismic energy for year 1996

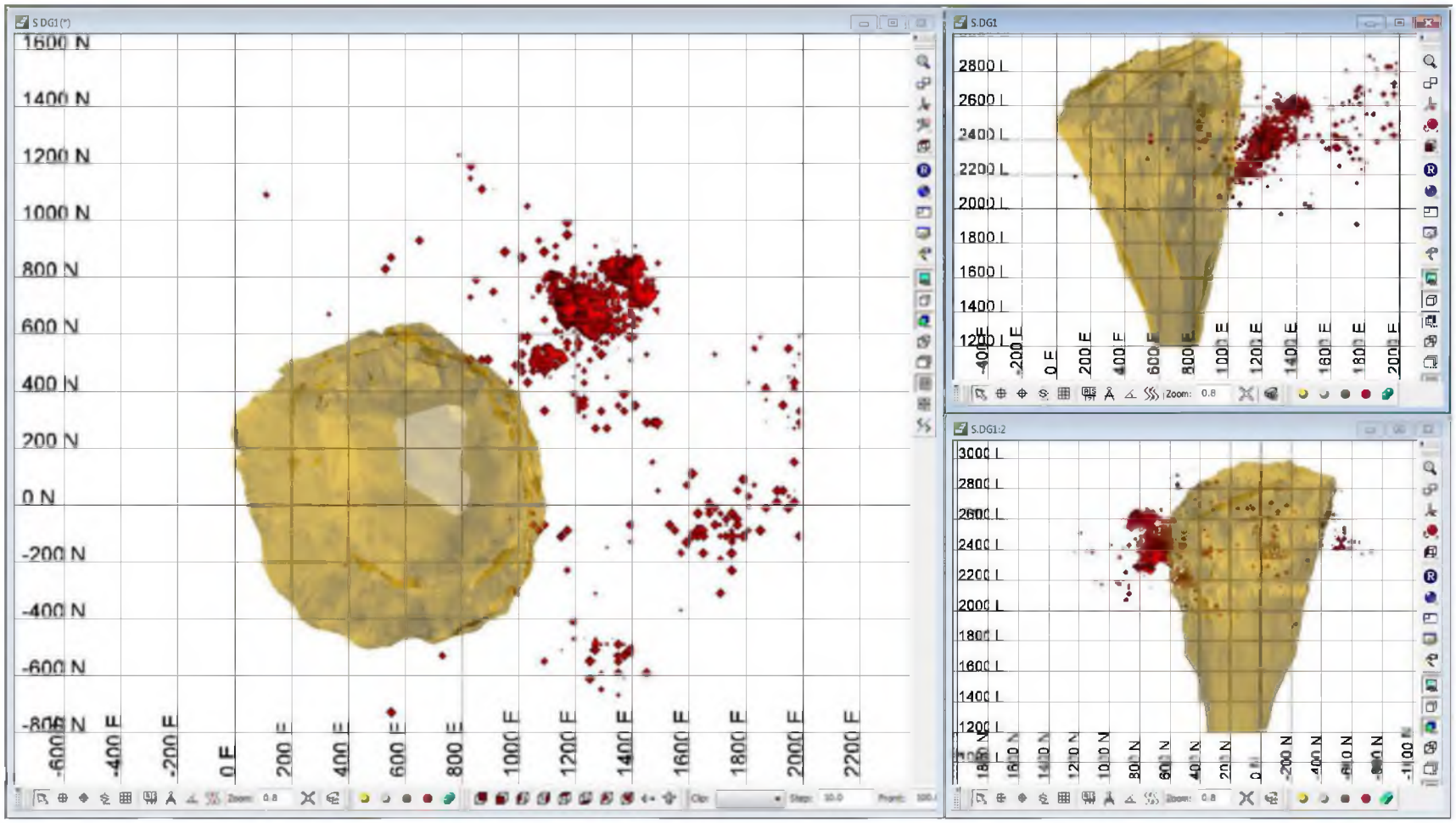

FIGURE A.6 Seismic energy for year 1997

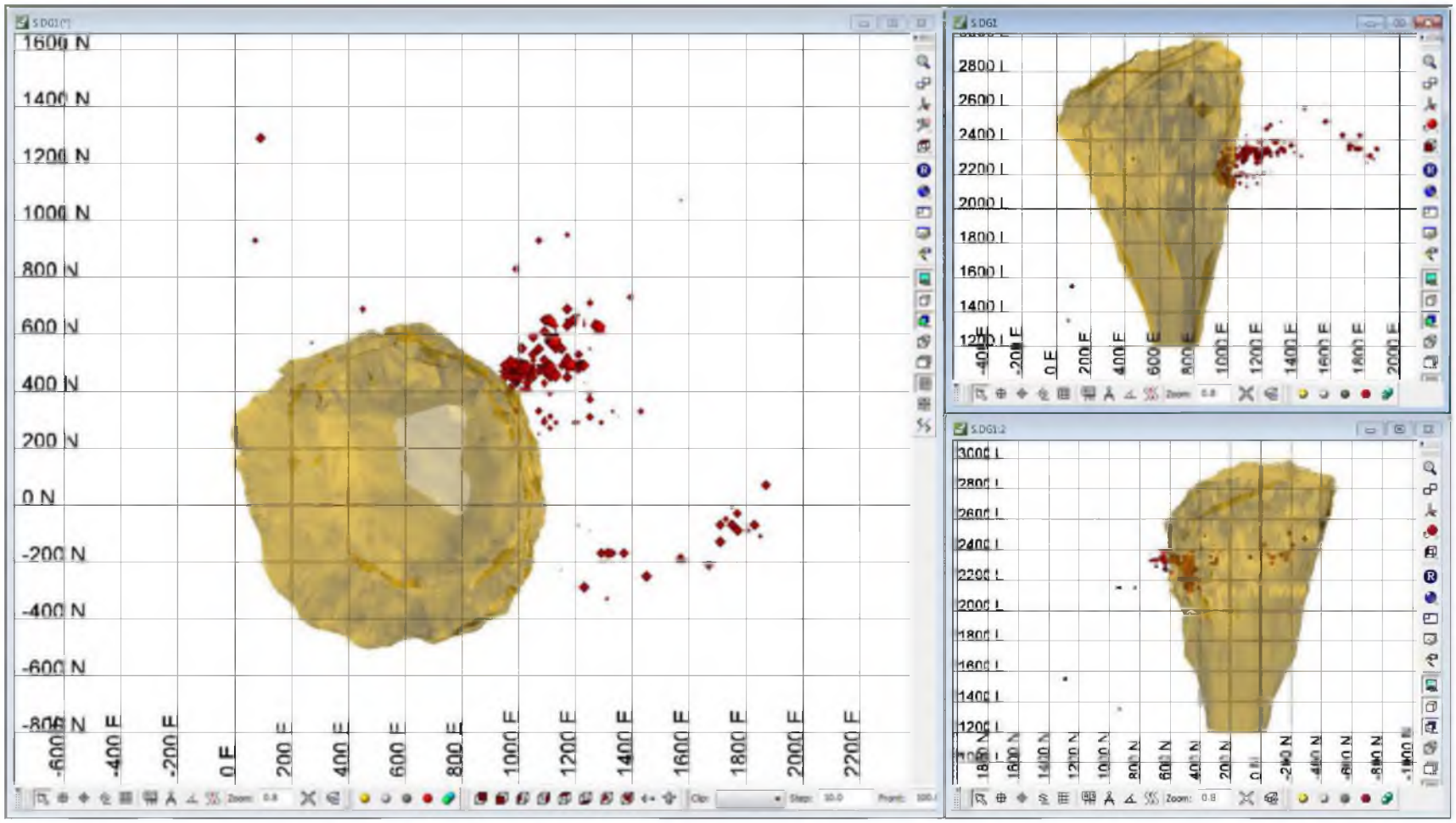

FIGURE A.7 Seismic energy for year 1998

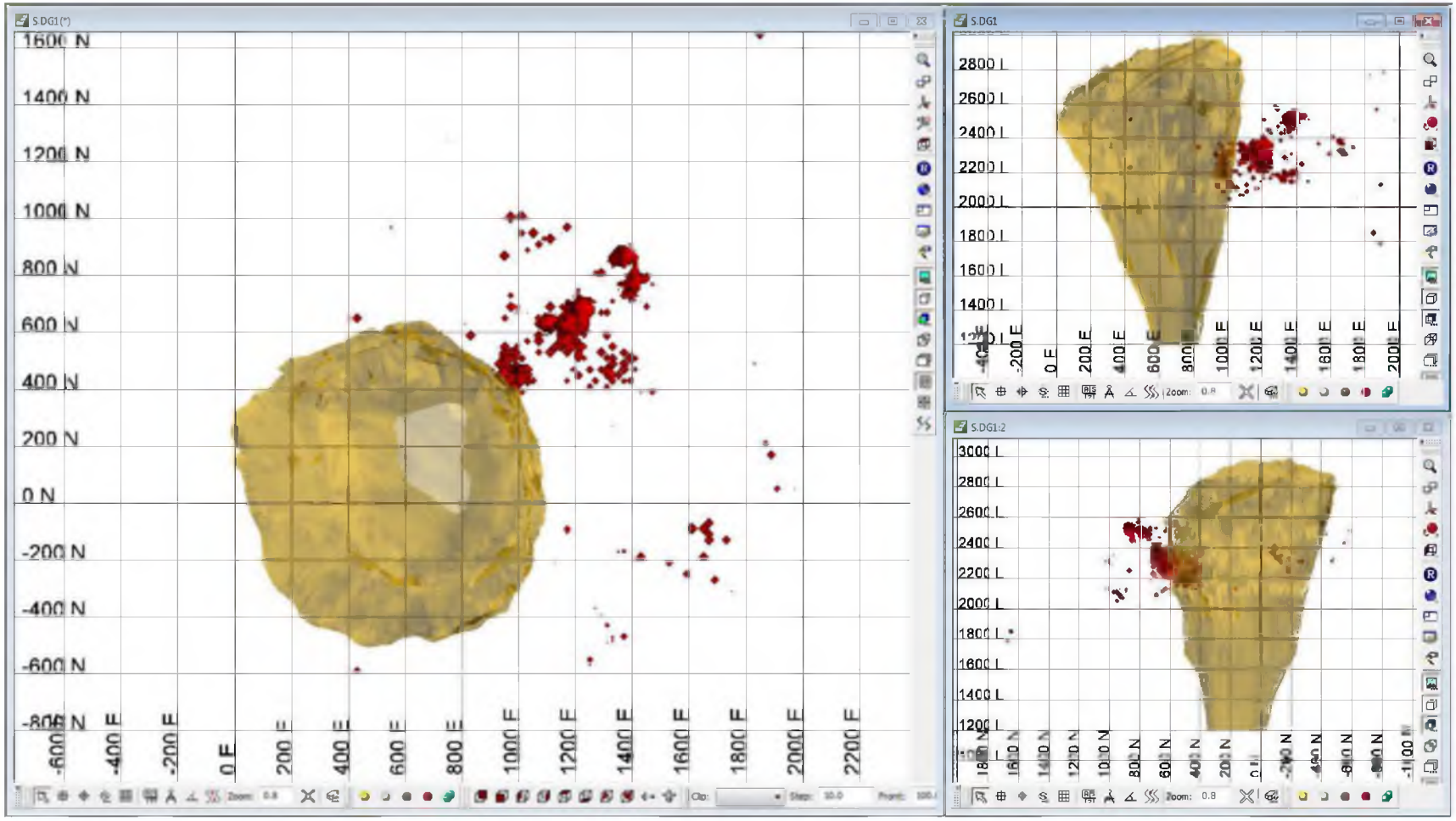

FIGURE A.8 Seismic energy for year 1999

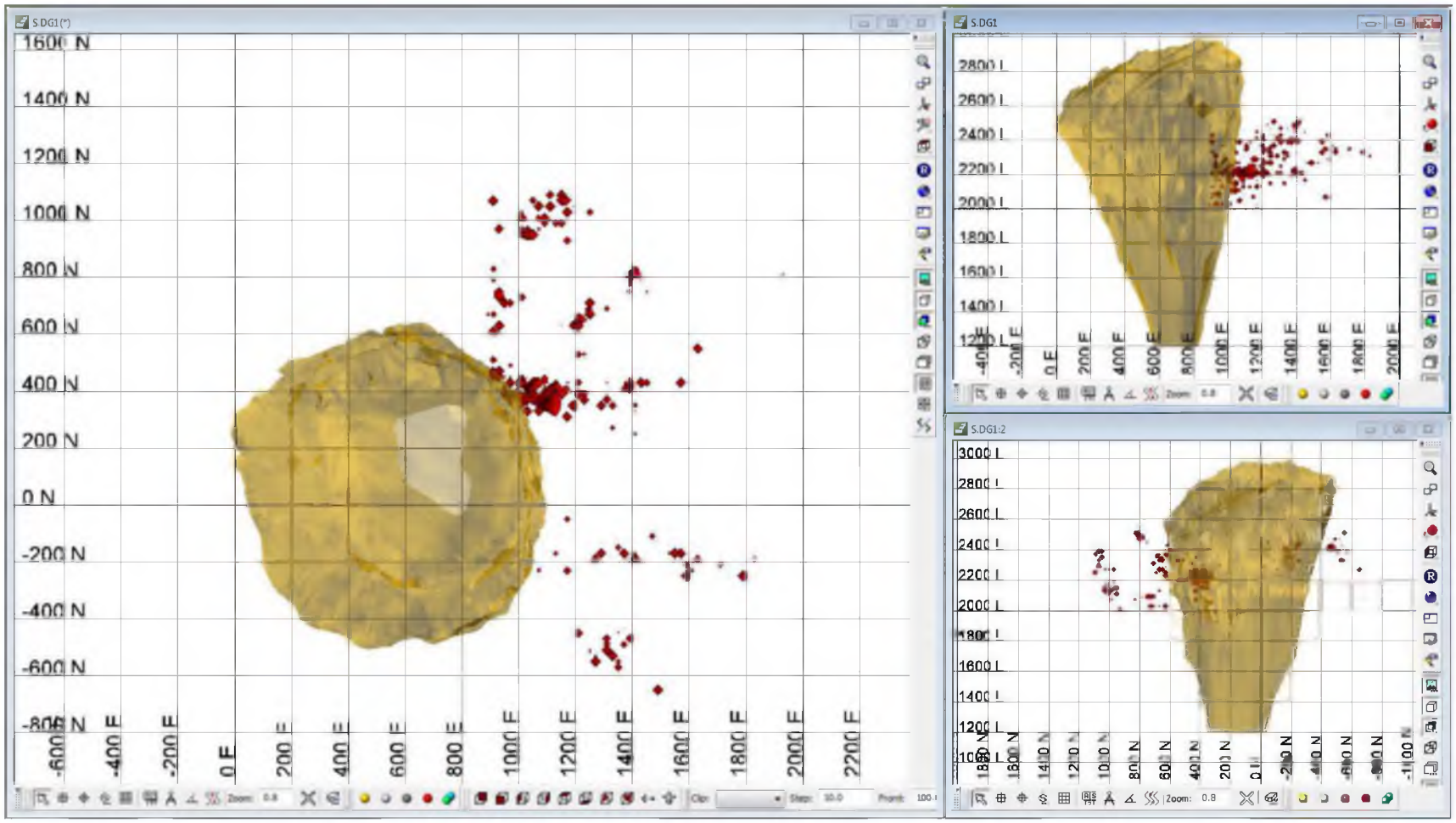

FIGURE A.9 Seismic energy for year 2000

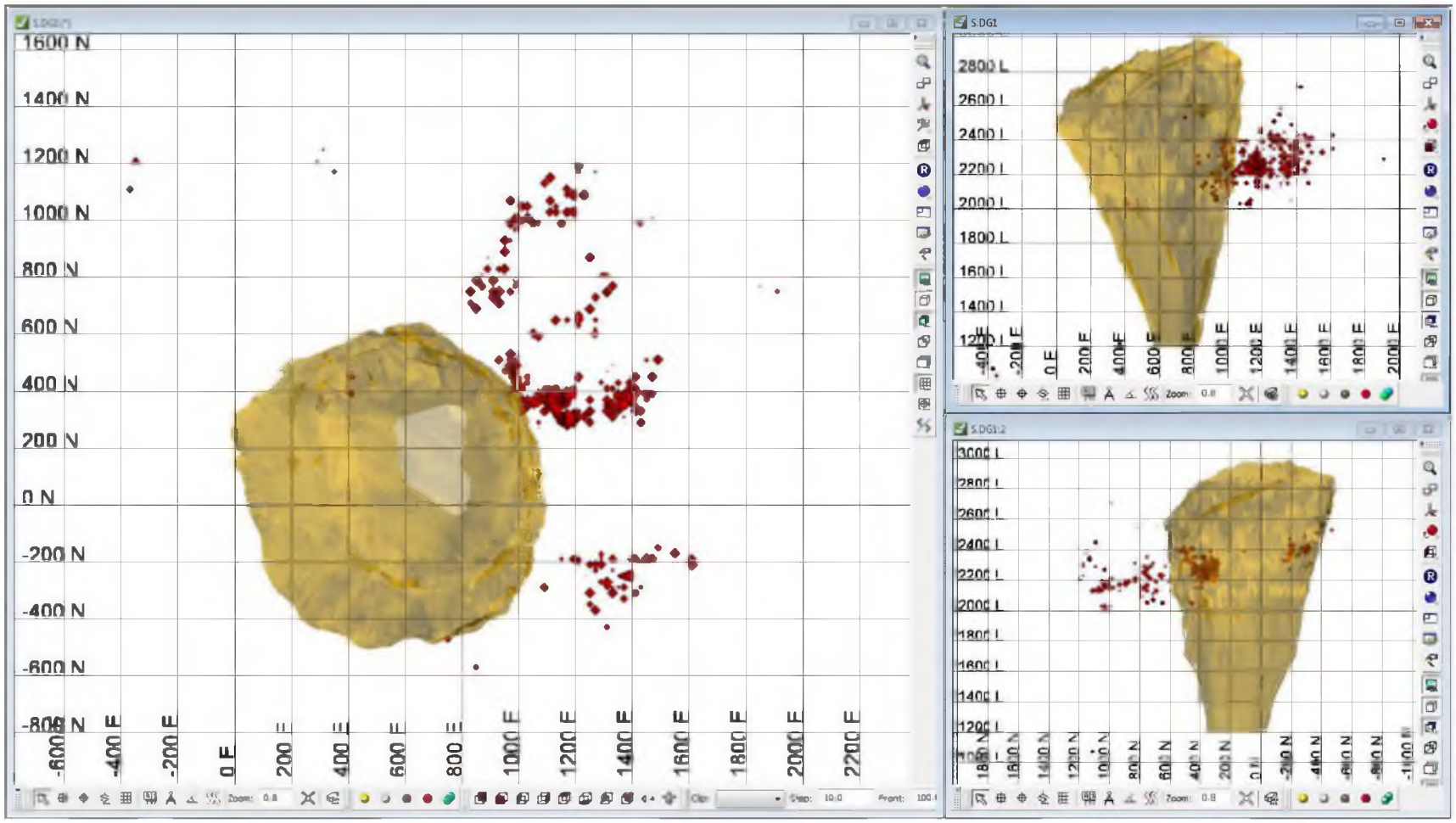

FIGURE A.10 Seismic energy for year 2001

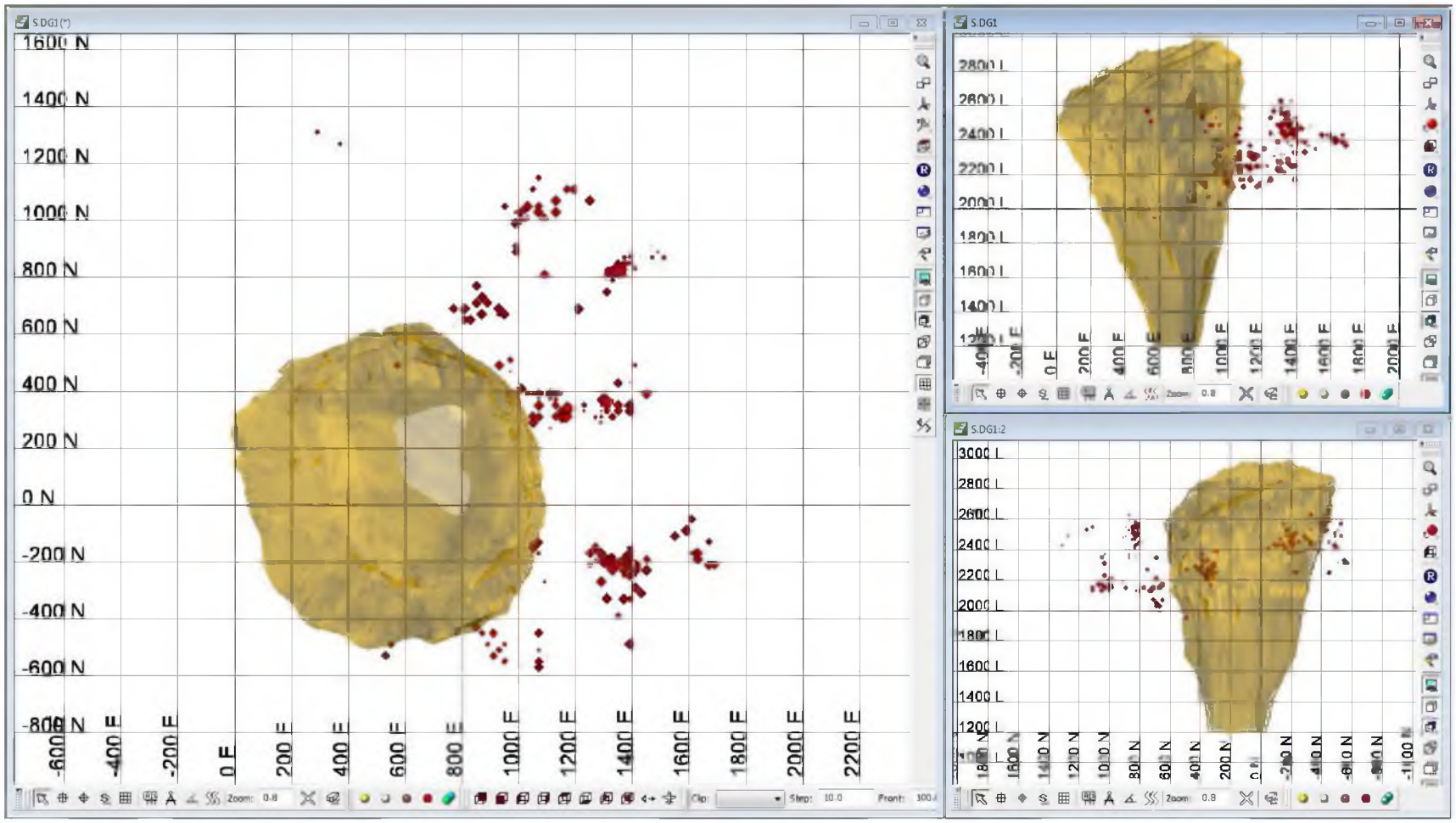

FIGURE A.11 Seismic energy for year 2002

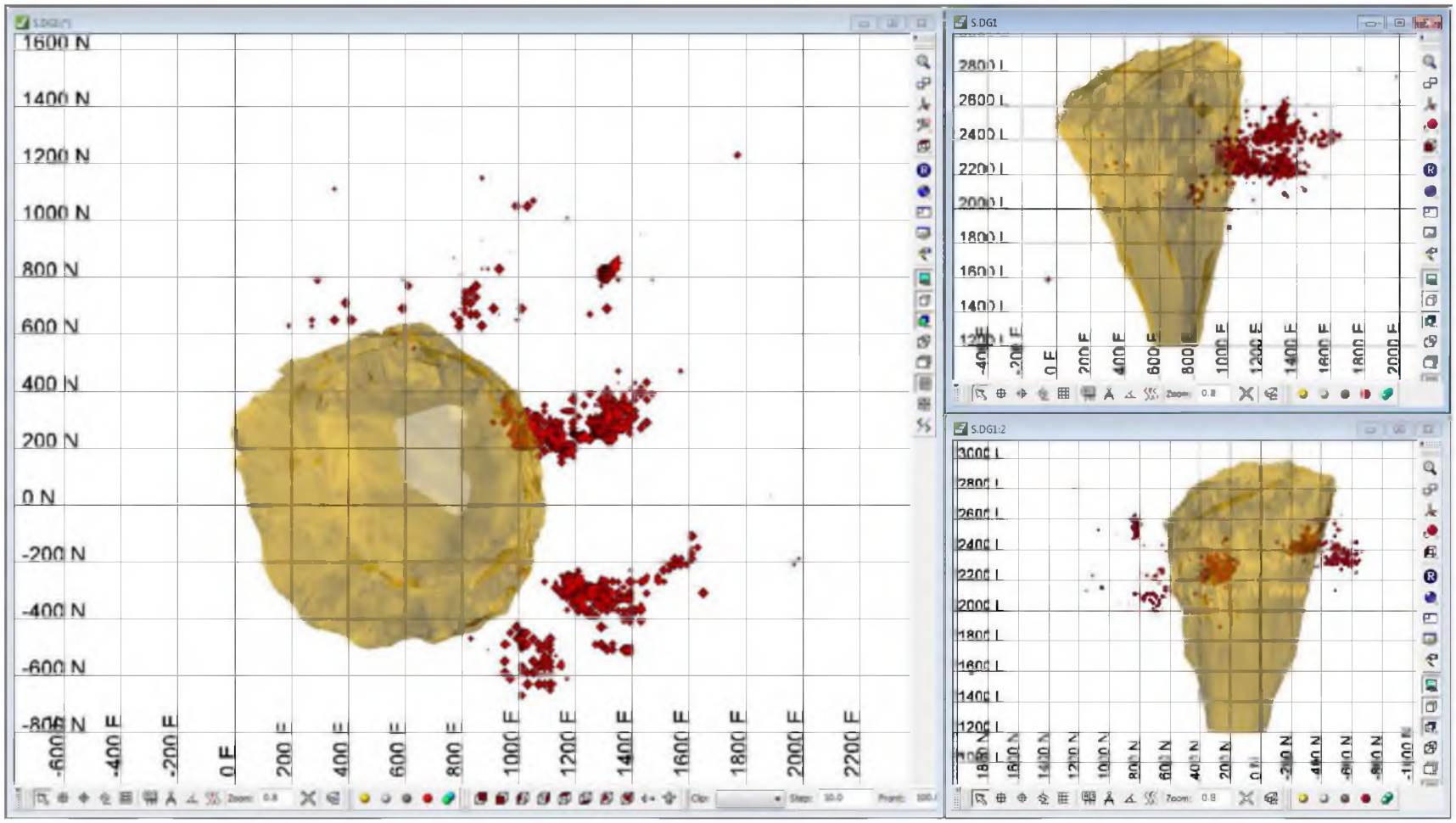

FIGURE A.12 Seismic energy for year 2003

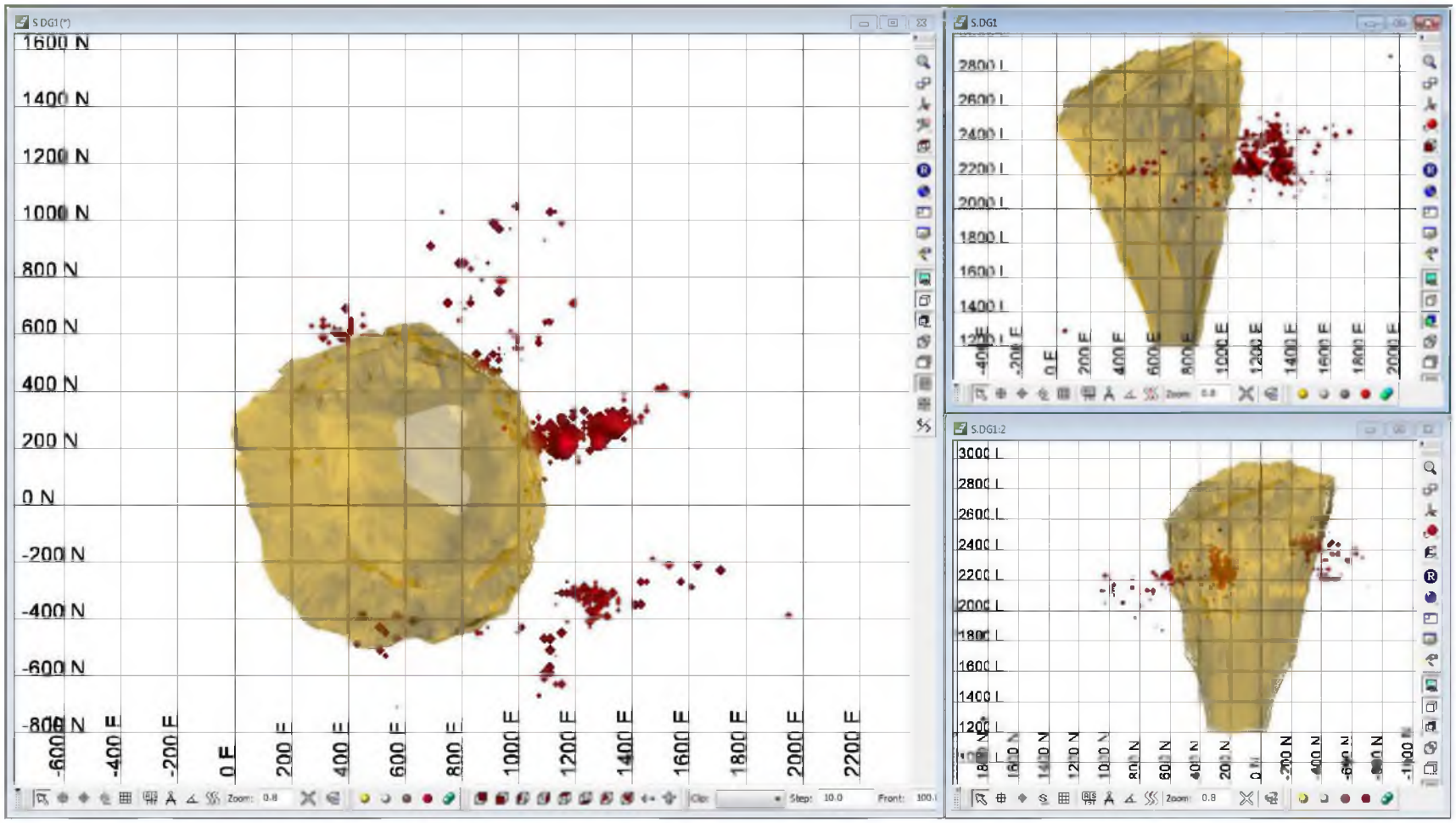

FIGURE A.13 Seismic energy for year 2004

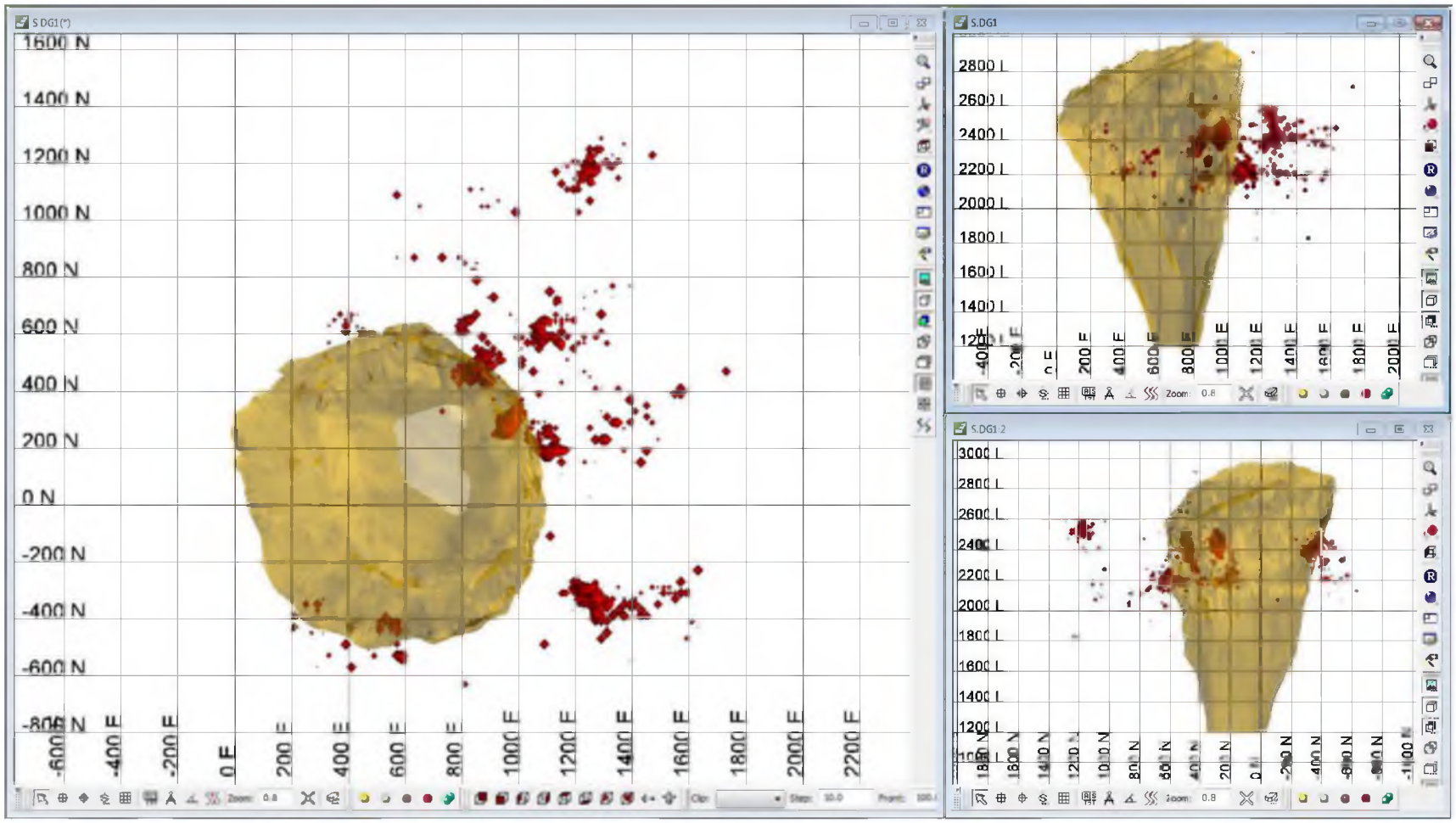

FIGURE A.14 Seismic energy for year 2005

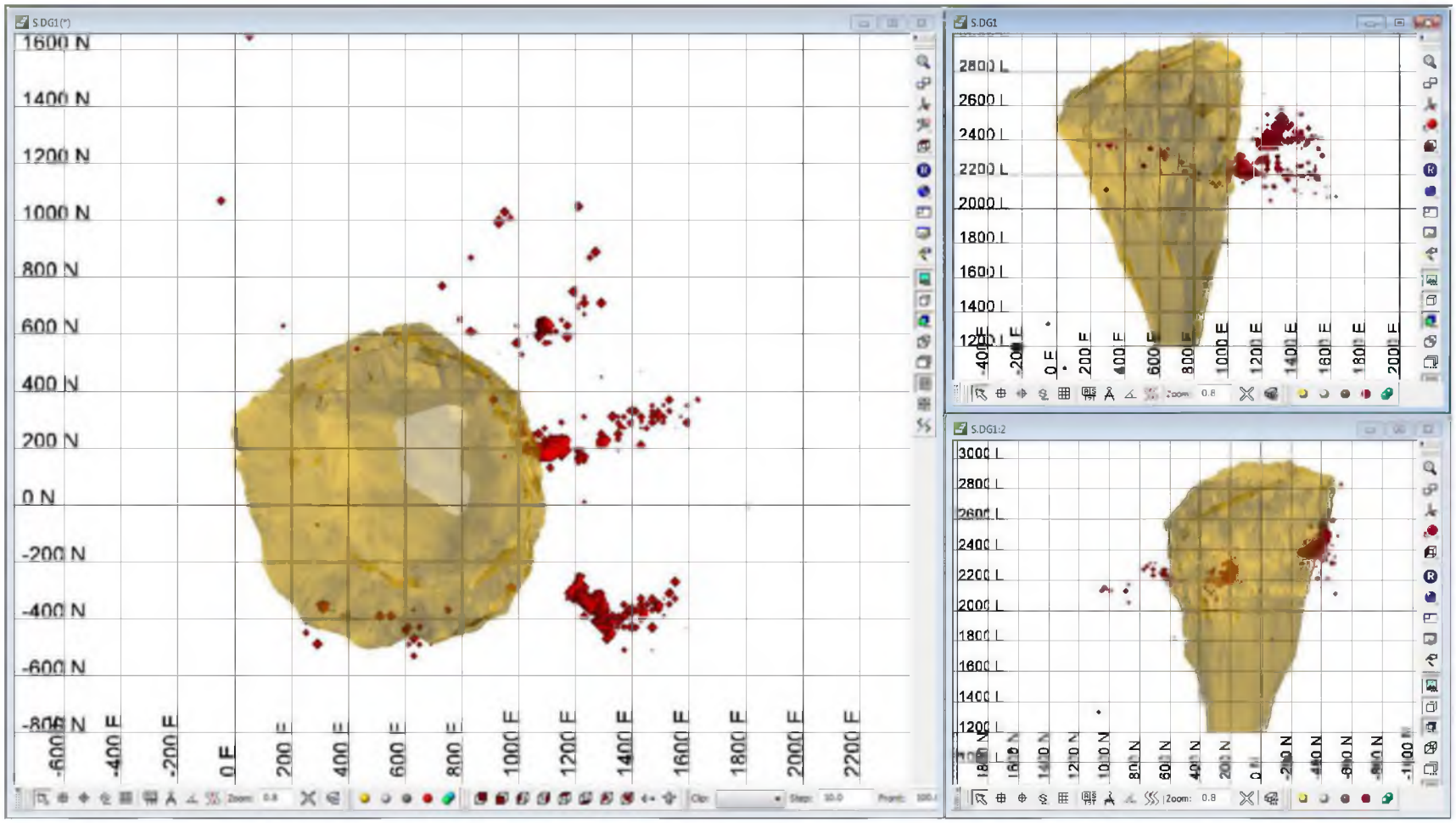

FIGURE A.15 Seismic energy for year 2006

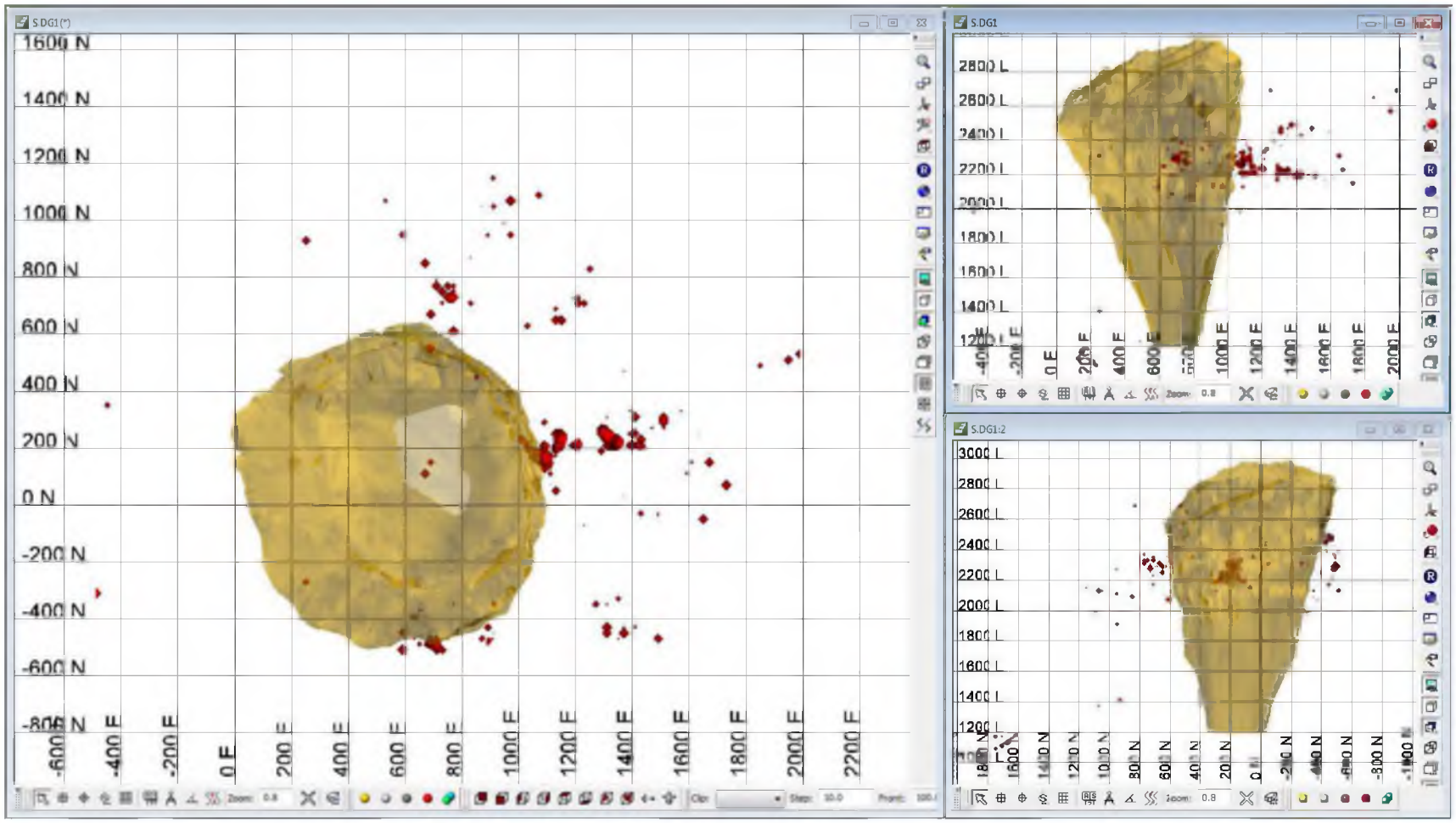

FIGURE A.16 Seismic energy for year 2007

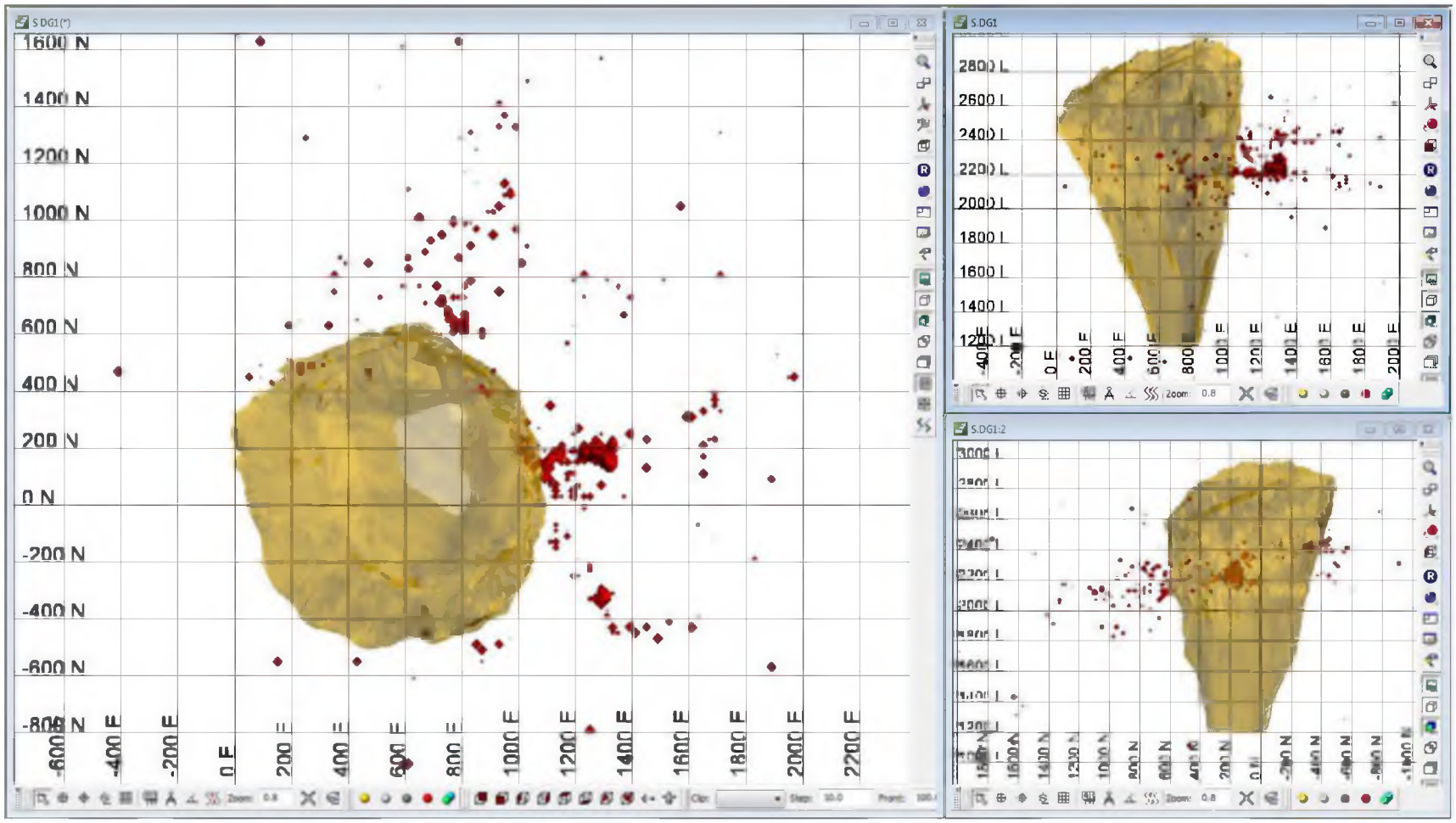

FIGURE A.17 Seismic energy for year 2008

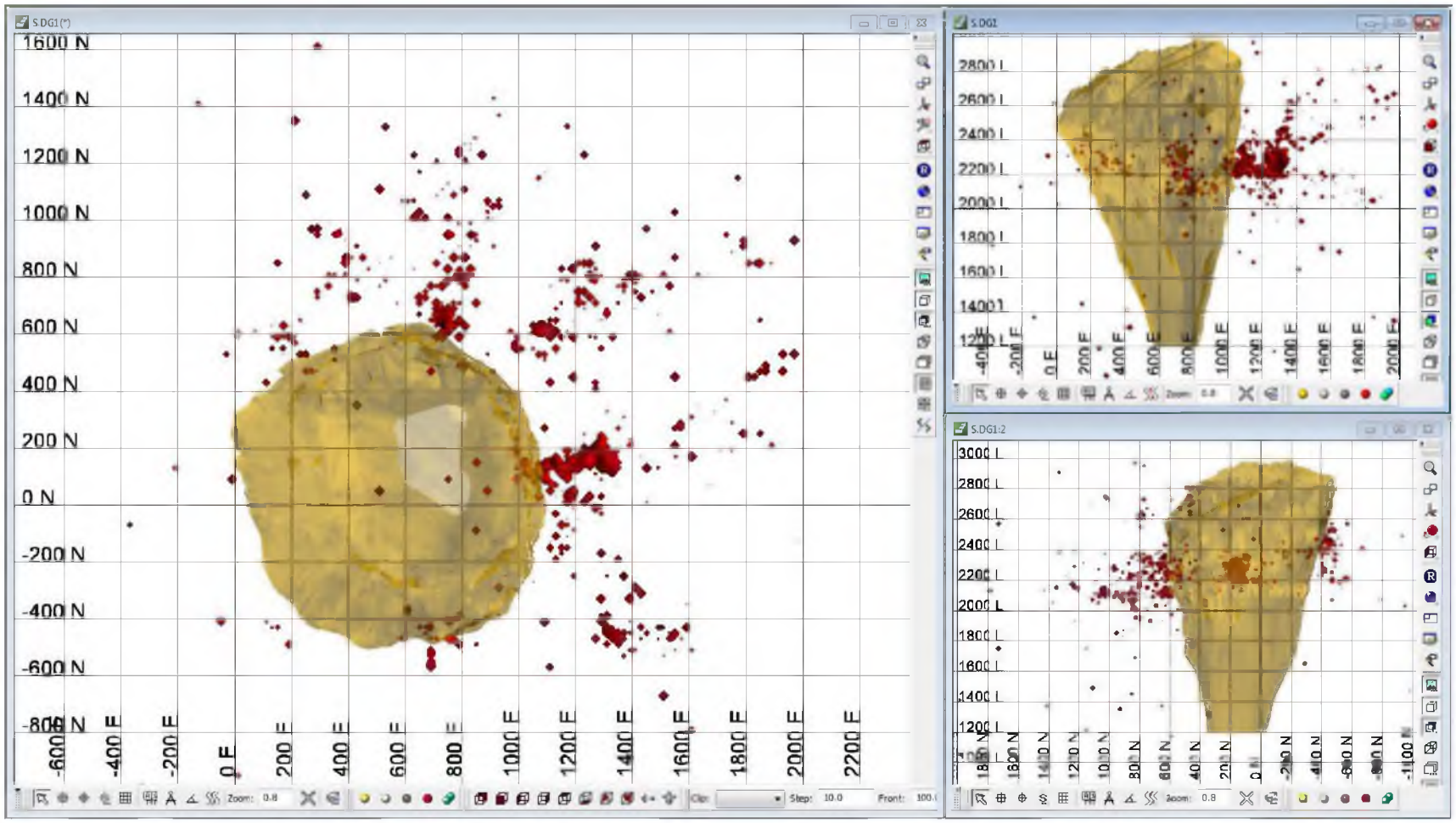

FIGURE A.18 Seismic energy for year 2009

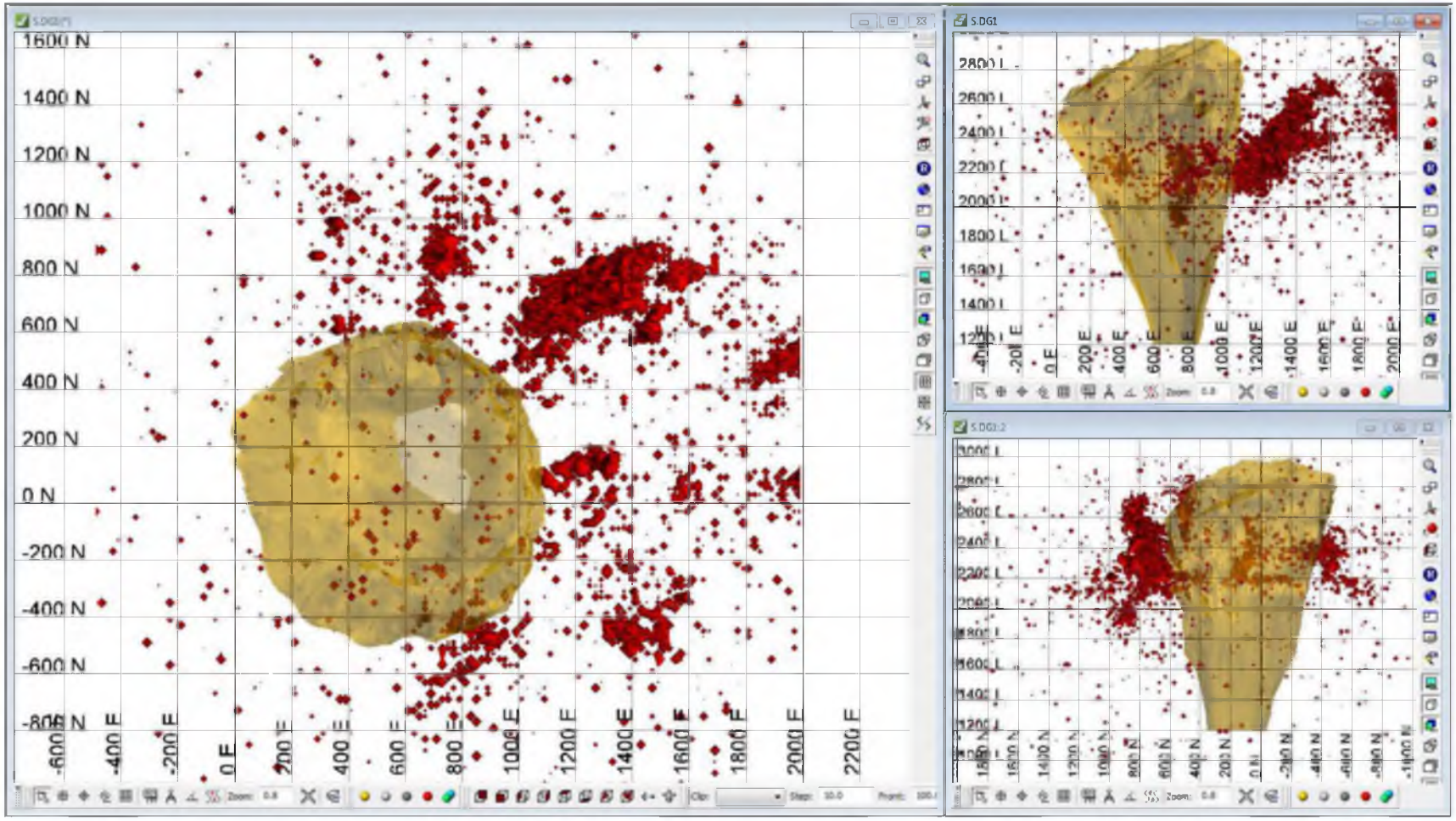

FIGURE A.19 Seismic energy for year 2010

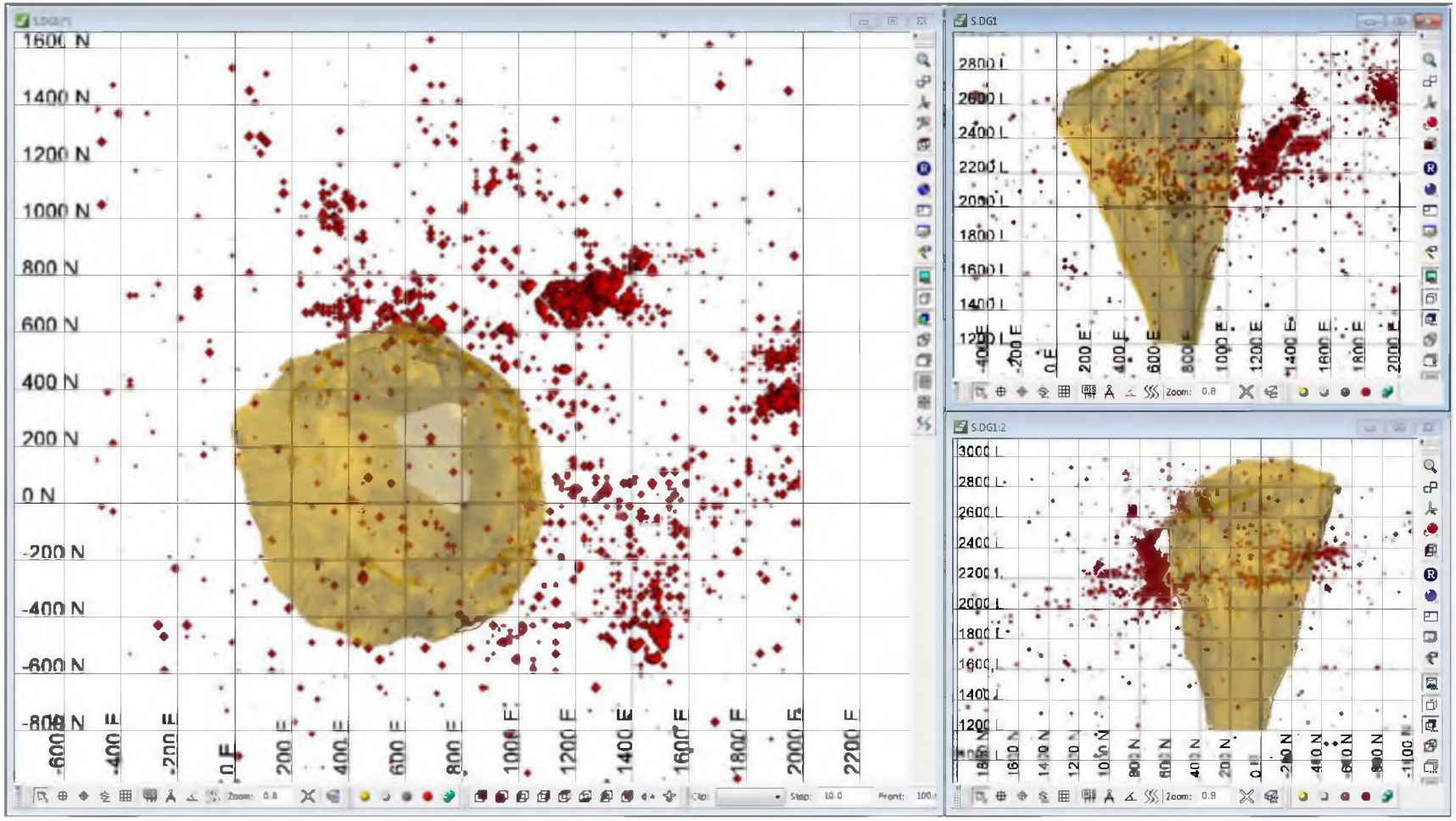

FIGURE A.20 Seismic energy for year 2011

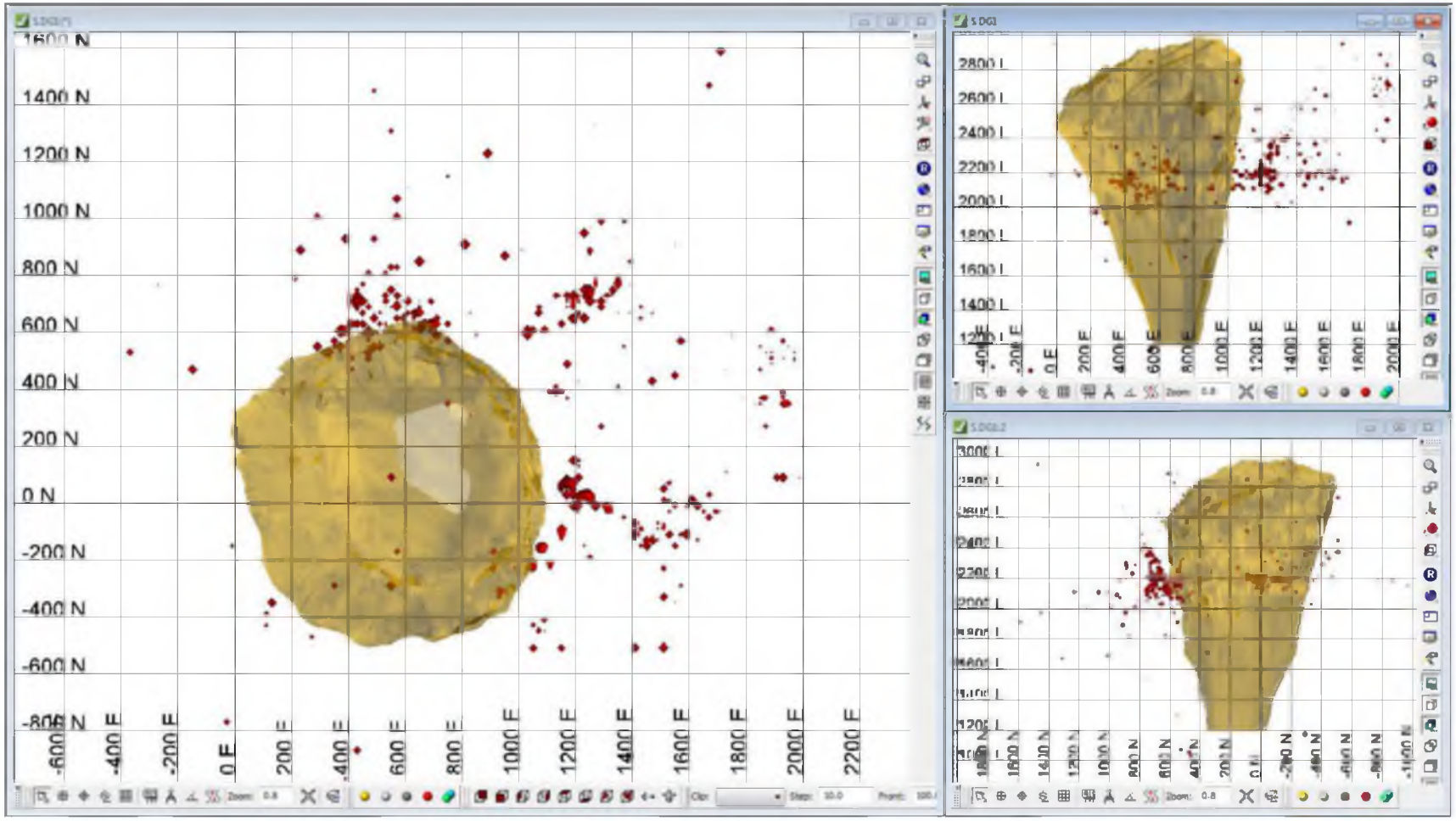

FIGURE A.21 Seismic energy for year 2012

APPENDIX B

SEISMIC ENERGY MODELED BY MONTH

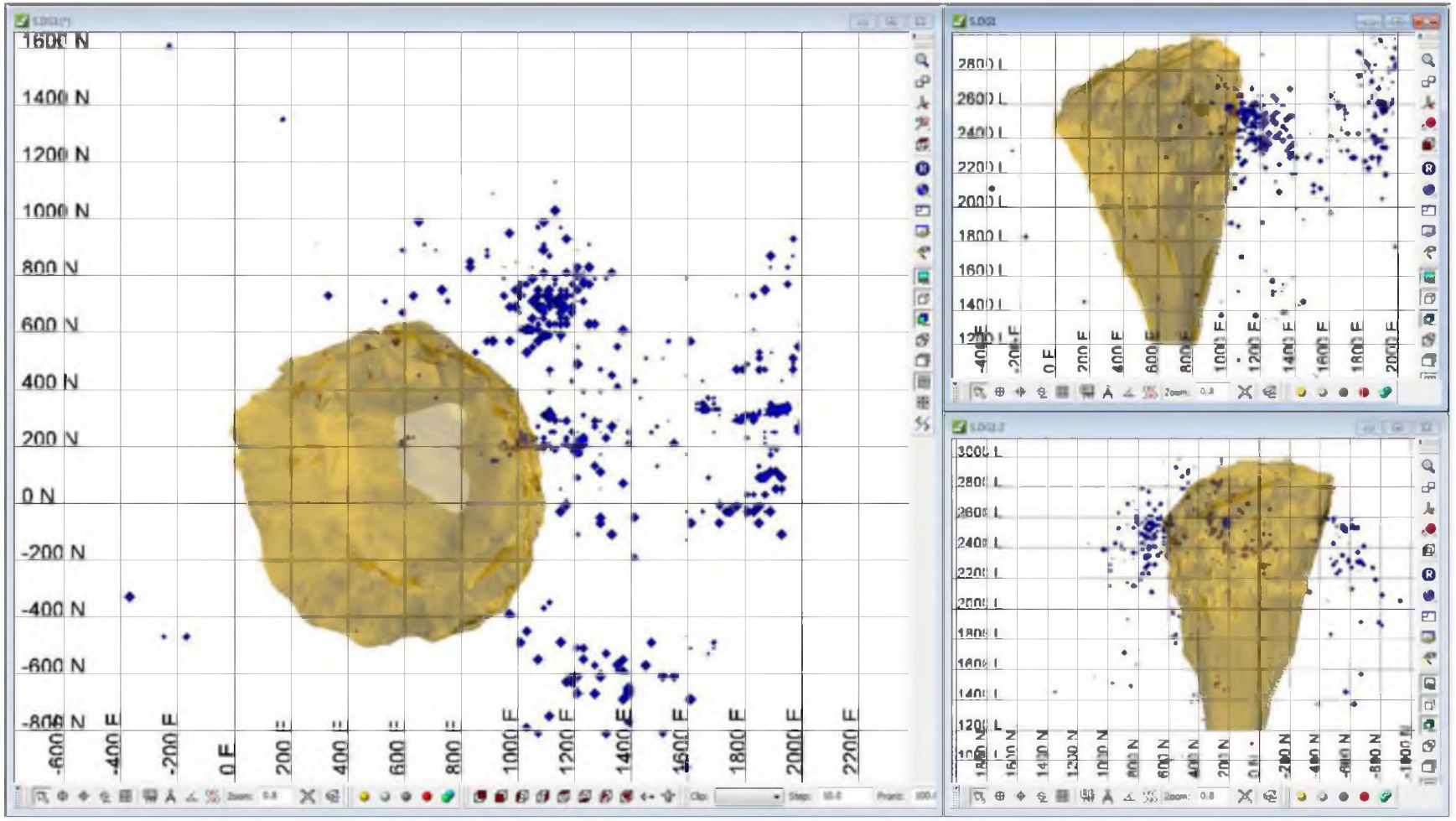

FIGURE B.1 Accumulated seismic energy up to the year 1992

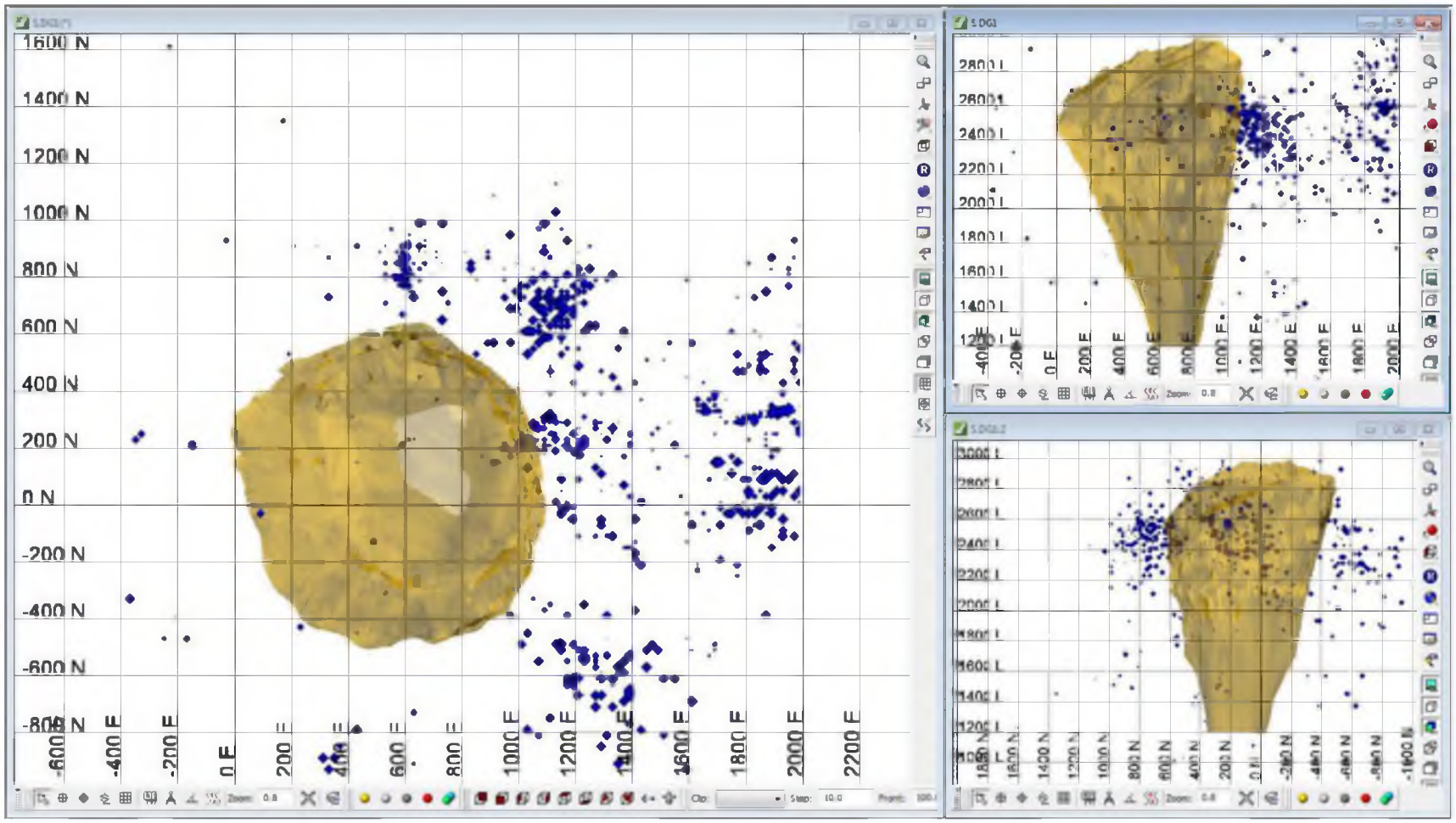

FIGURE B.2 Accumulated seismic energy up to the year 1993

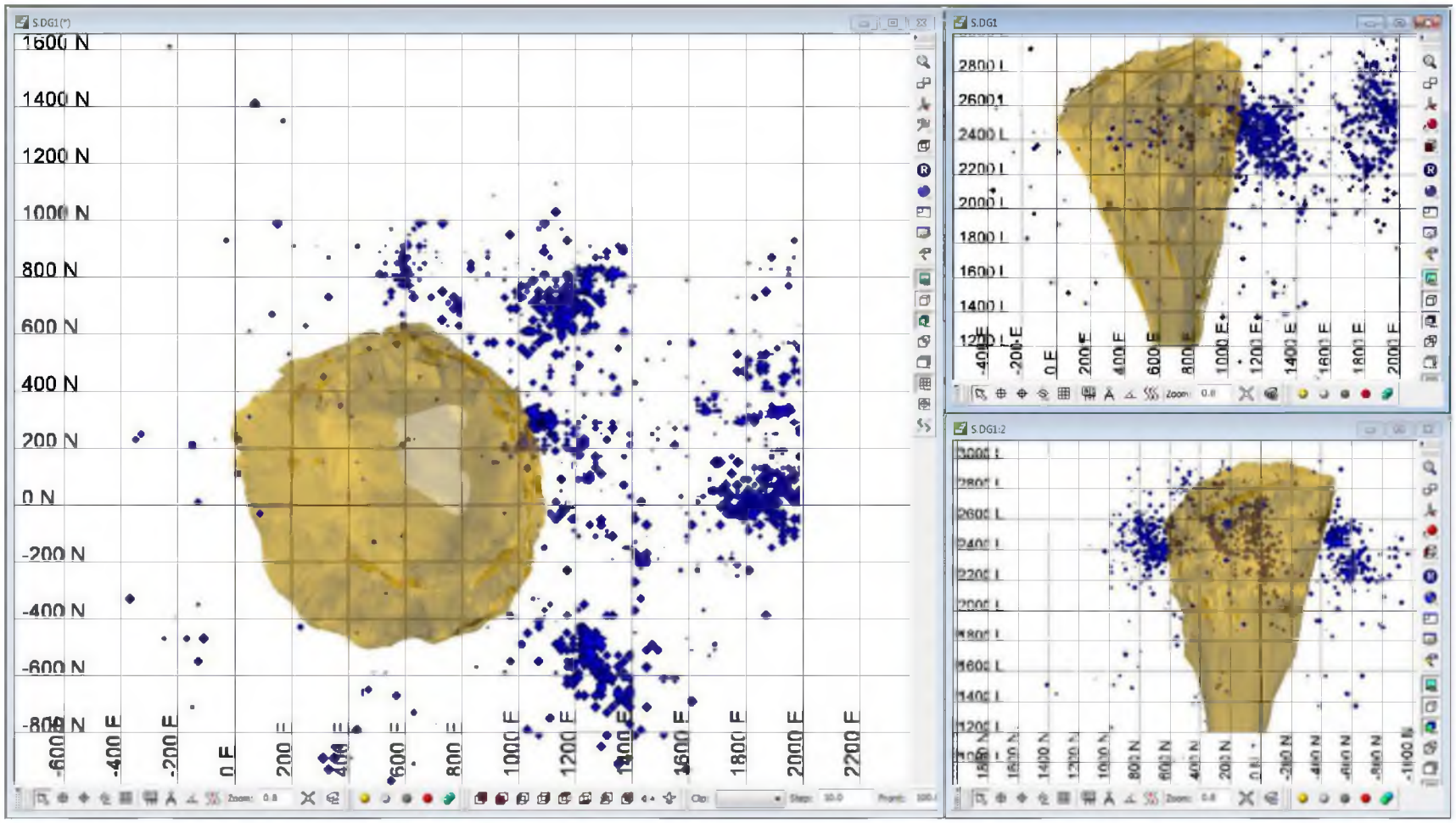

FIGURE B.3 Accumulated seismic energy up to the year 1994

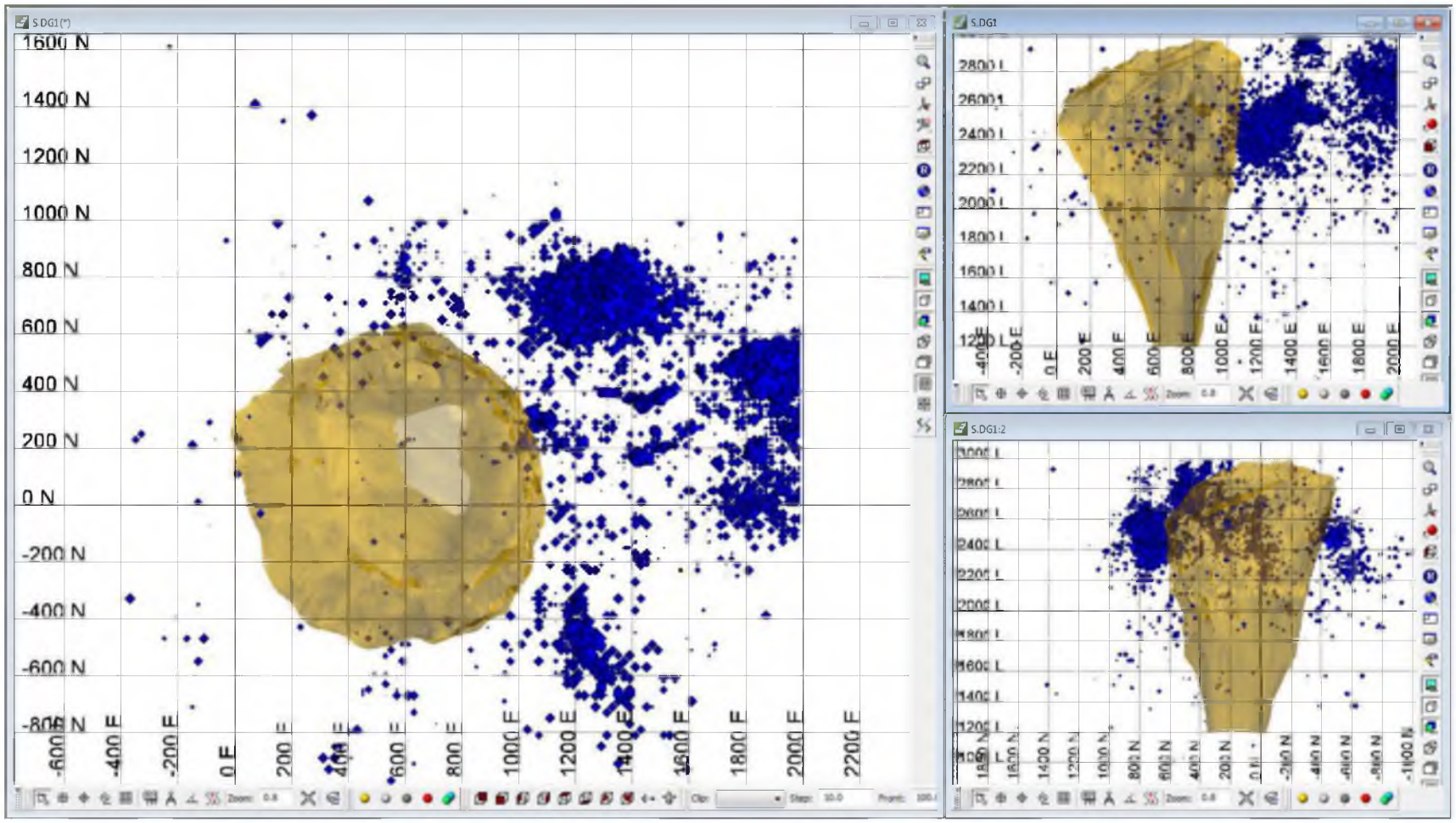

FIGURE B.4 Accumulated seismic energy up to the year 1995

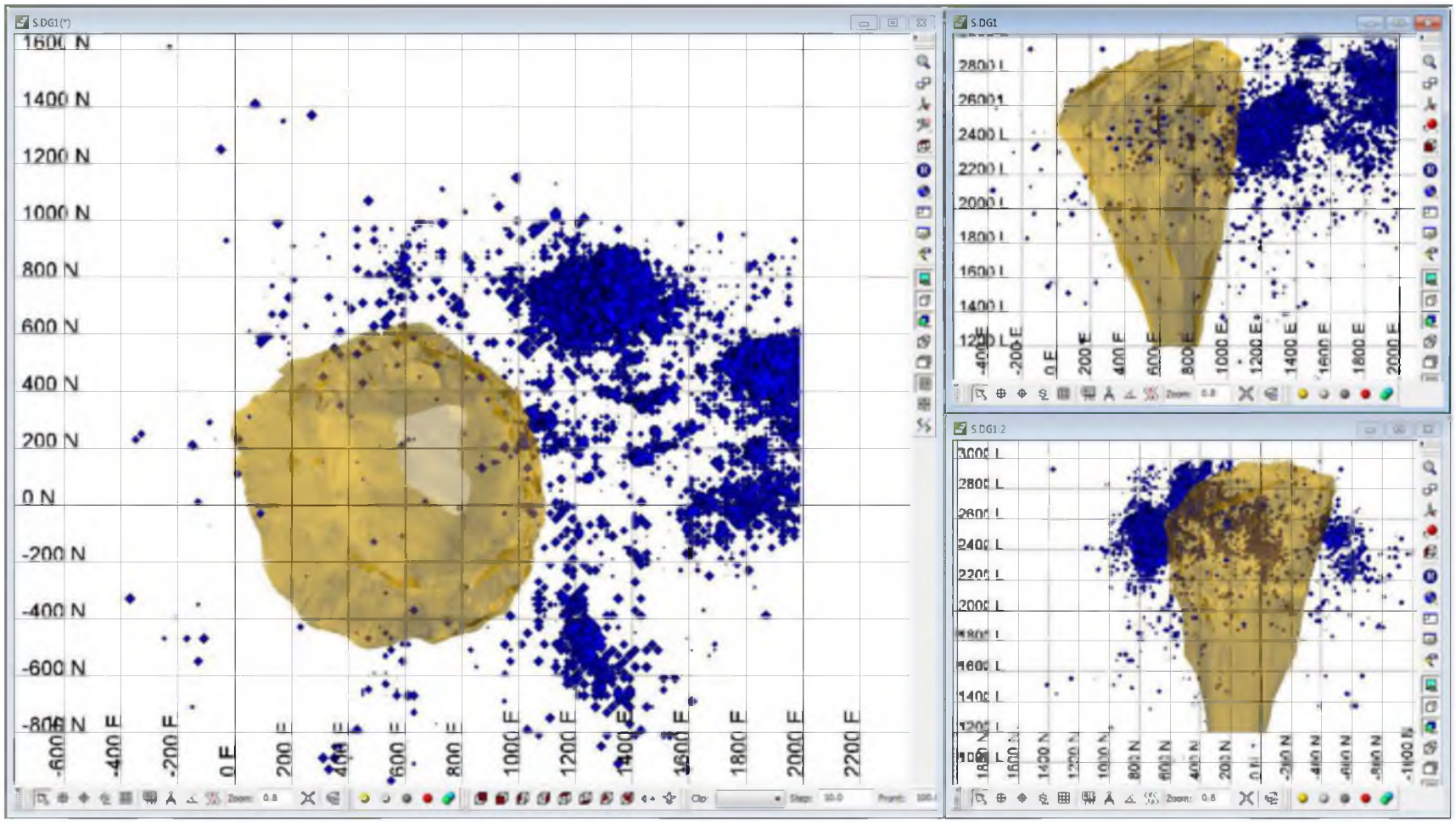

FIGURE B.5 Accumulated seismic energy up to the year 1996

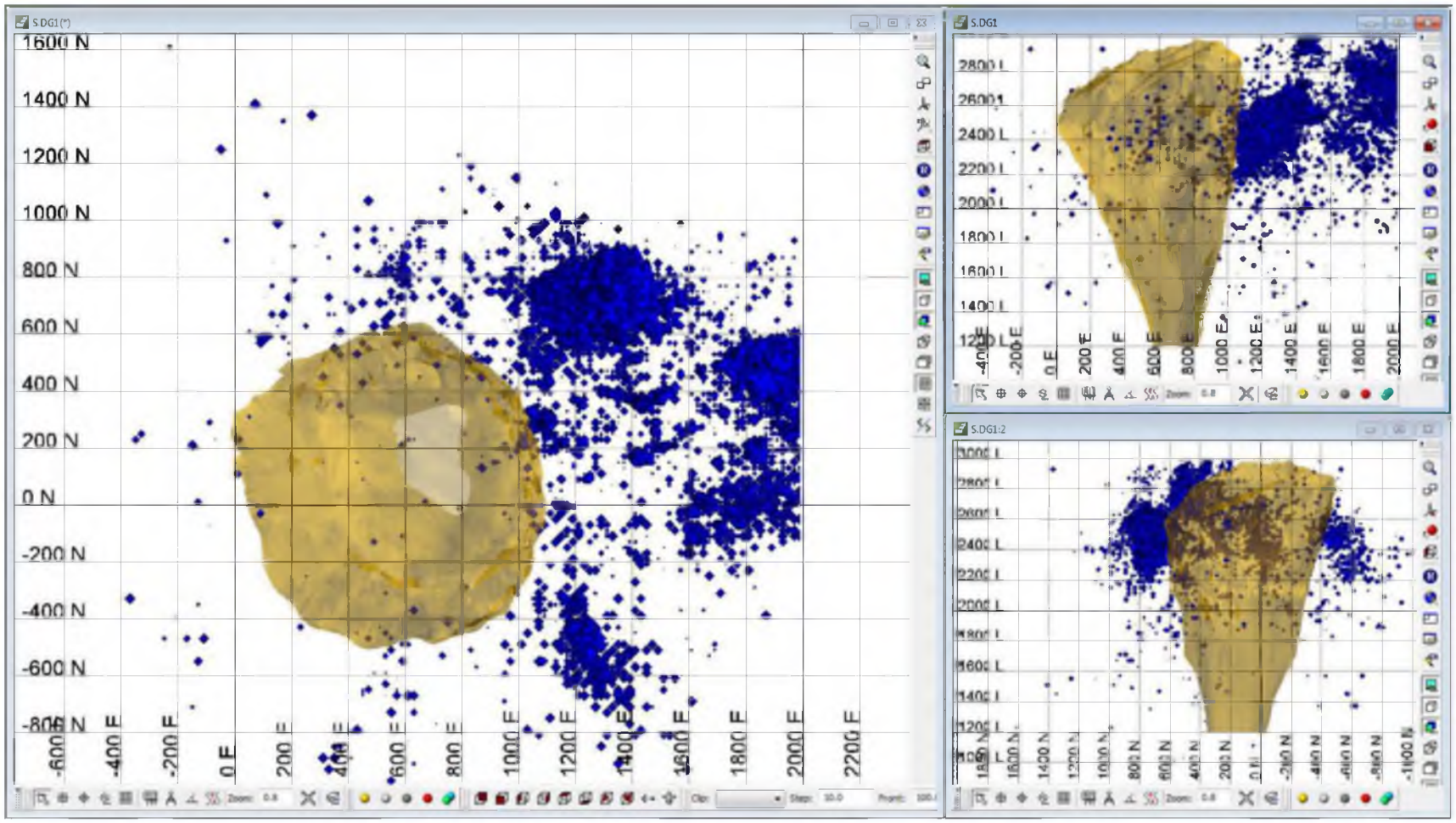

FIGURE B.6 Accumulated seismic energy up to the year 1997

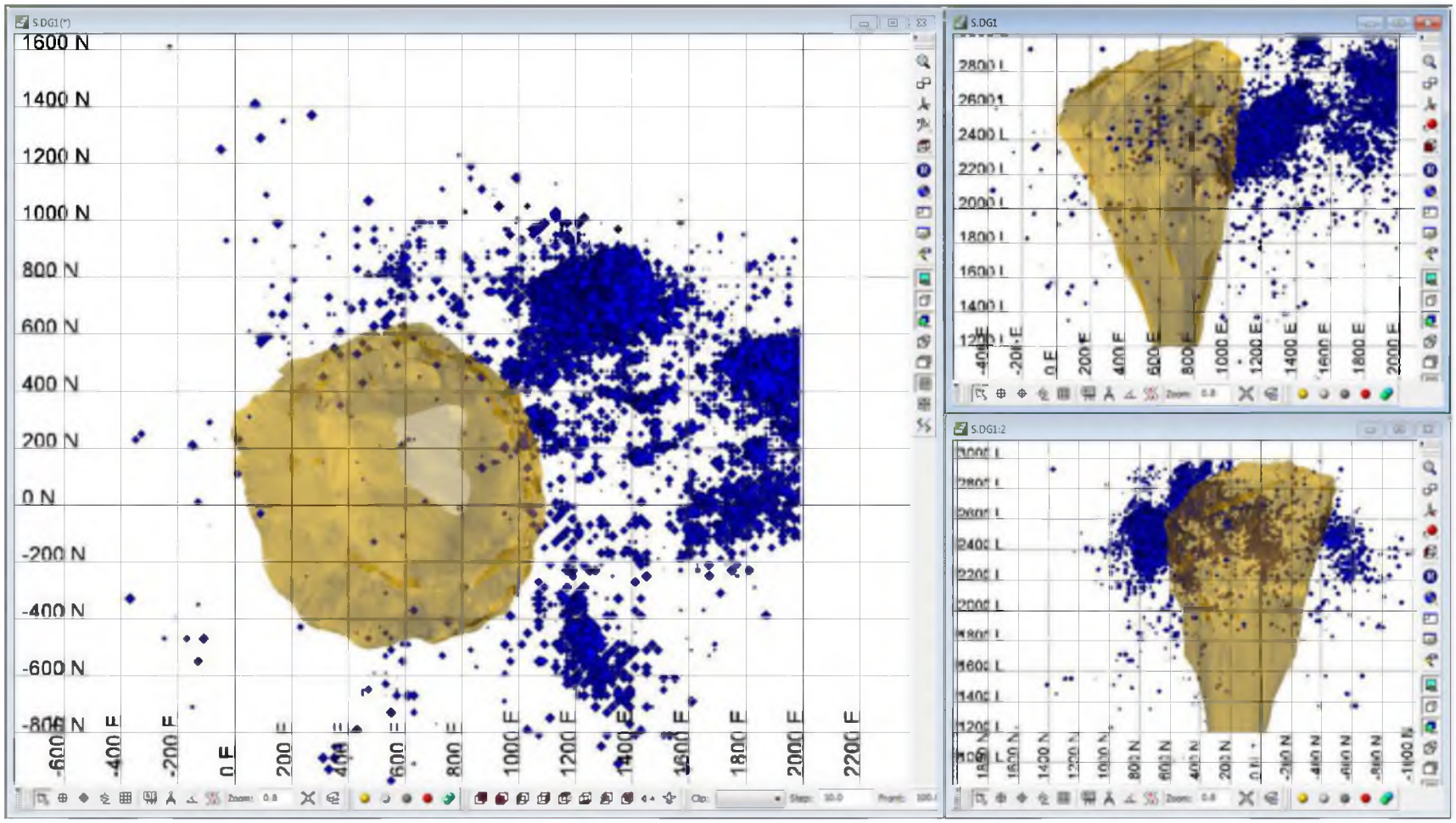

FIGURE B.7 Accumulated seismic energy up to the year 1998

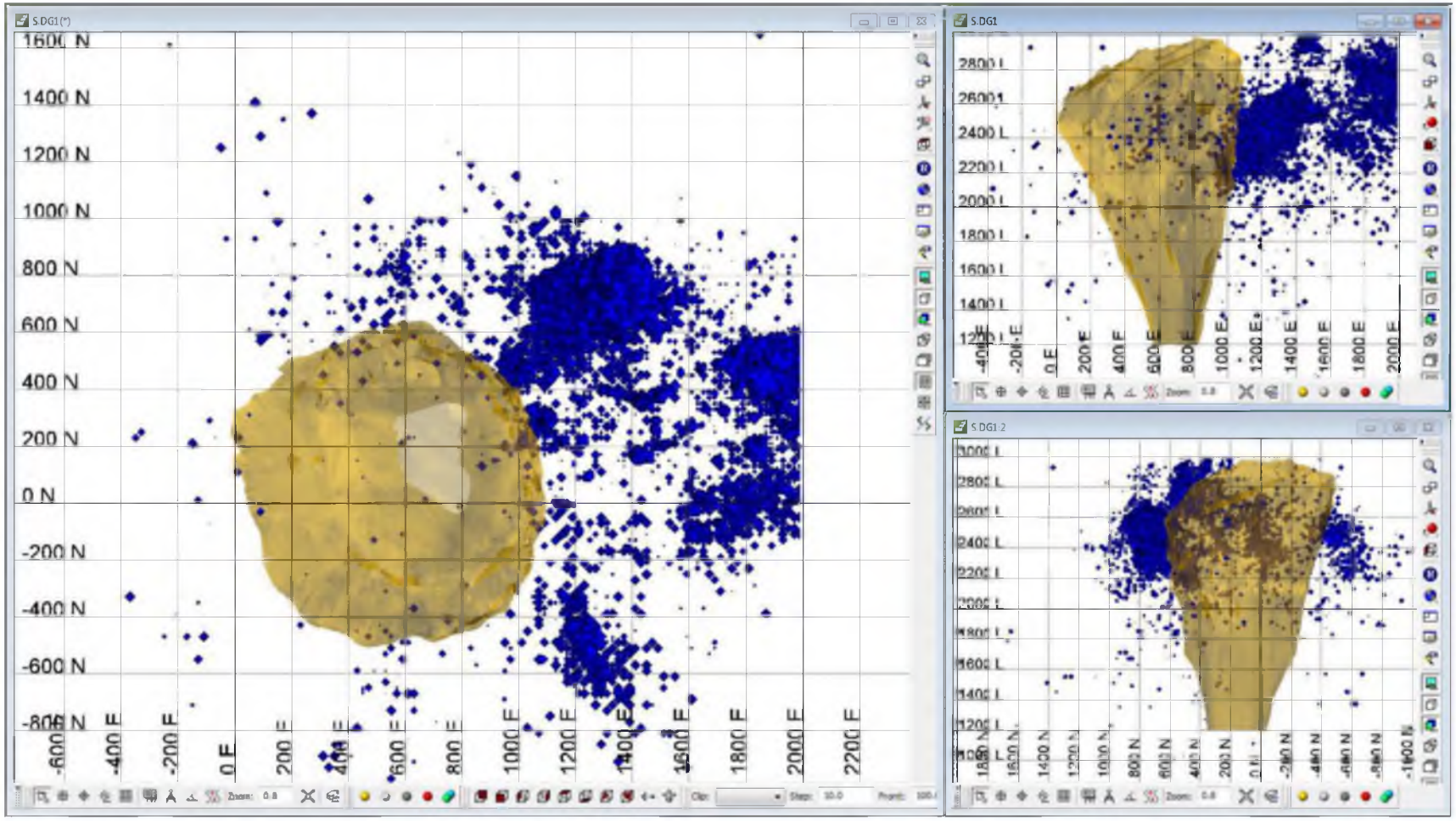

FIGURE B.8 Accumulated seismic energy up to the year 1999

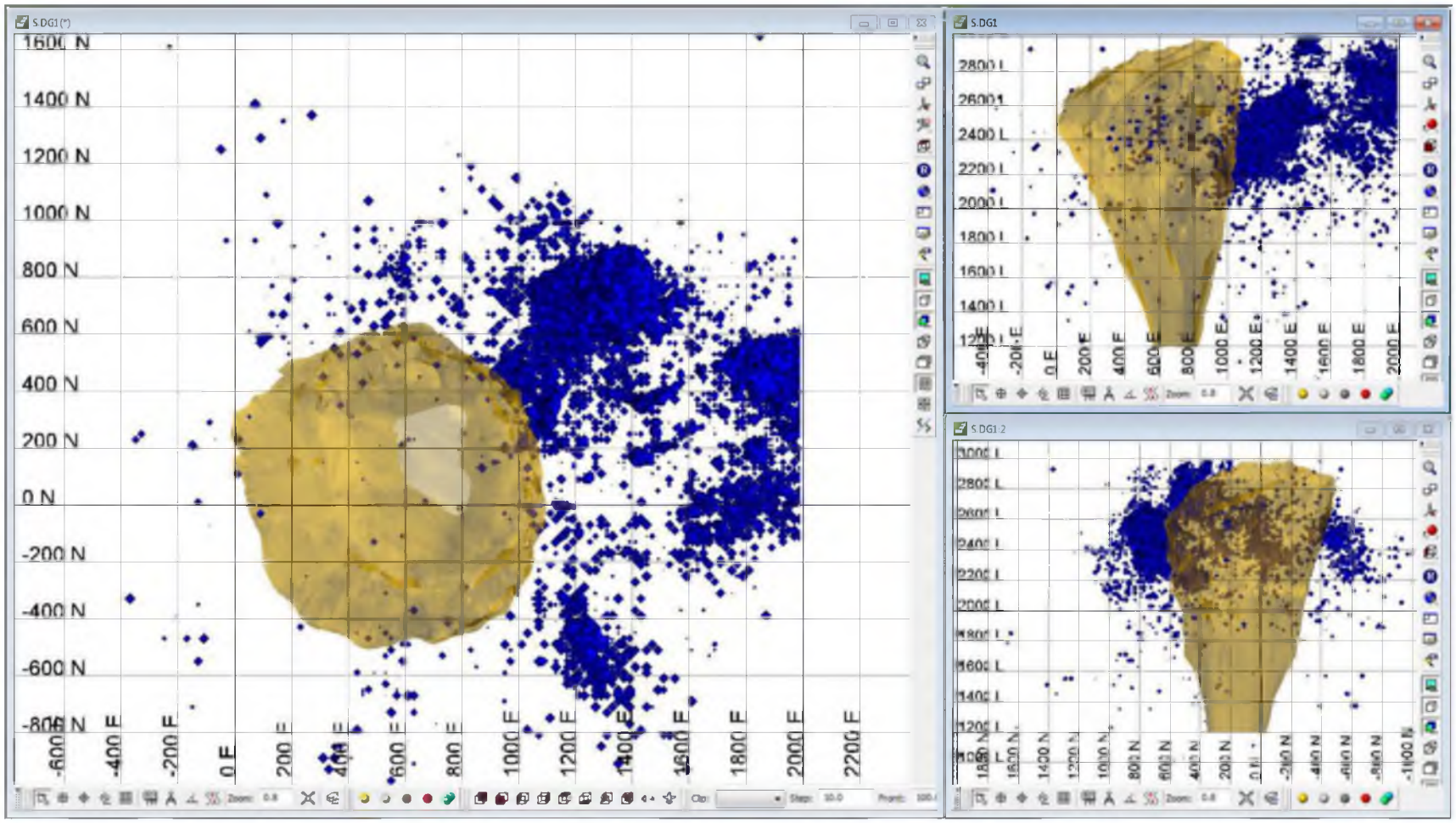

FIGURE B.9 Accumulated seismic energy up to the year 2000

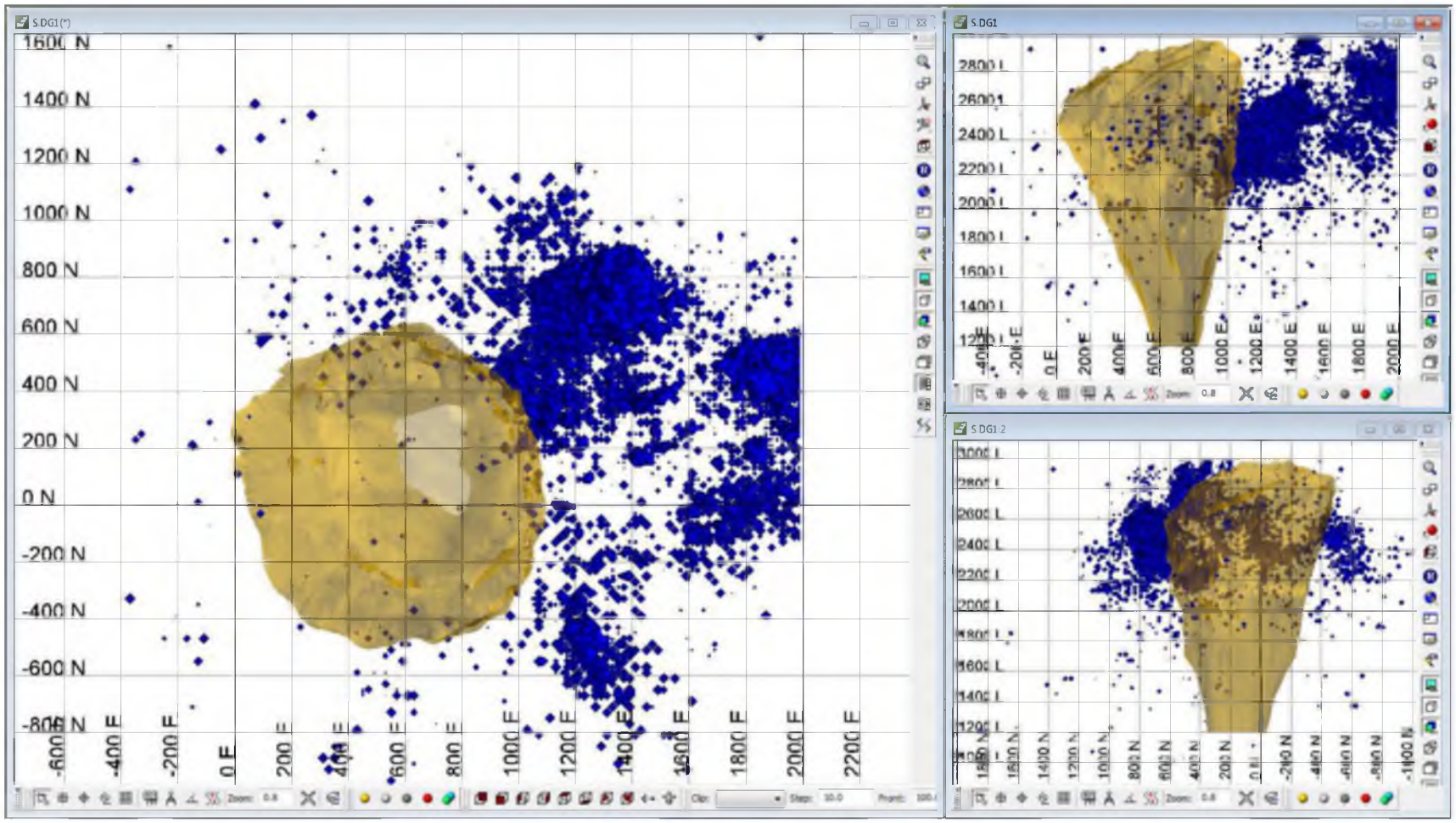

FIGURE B.10 Accumulated seismic energy up to the year 2001

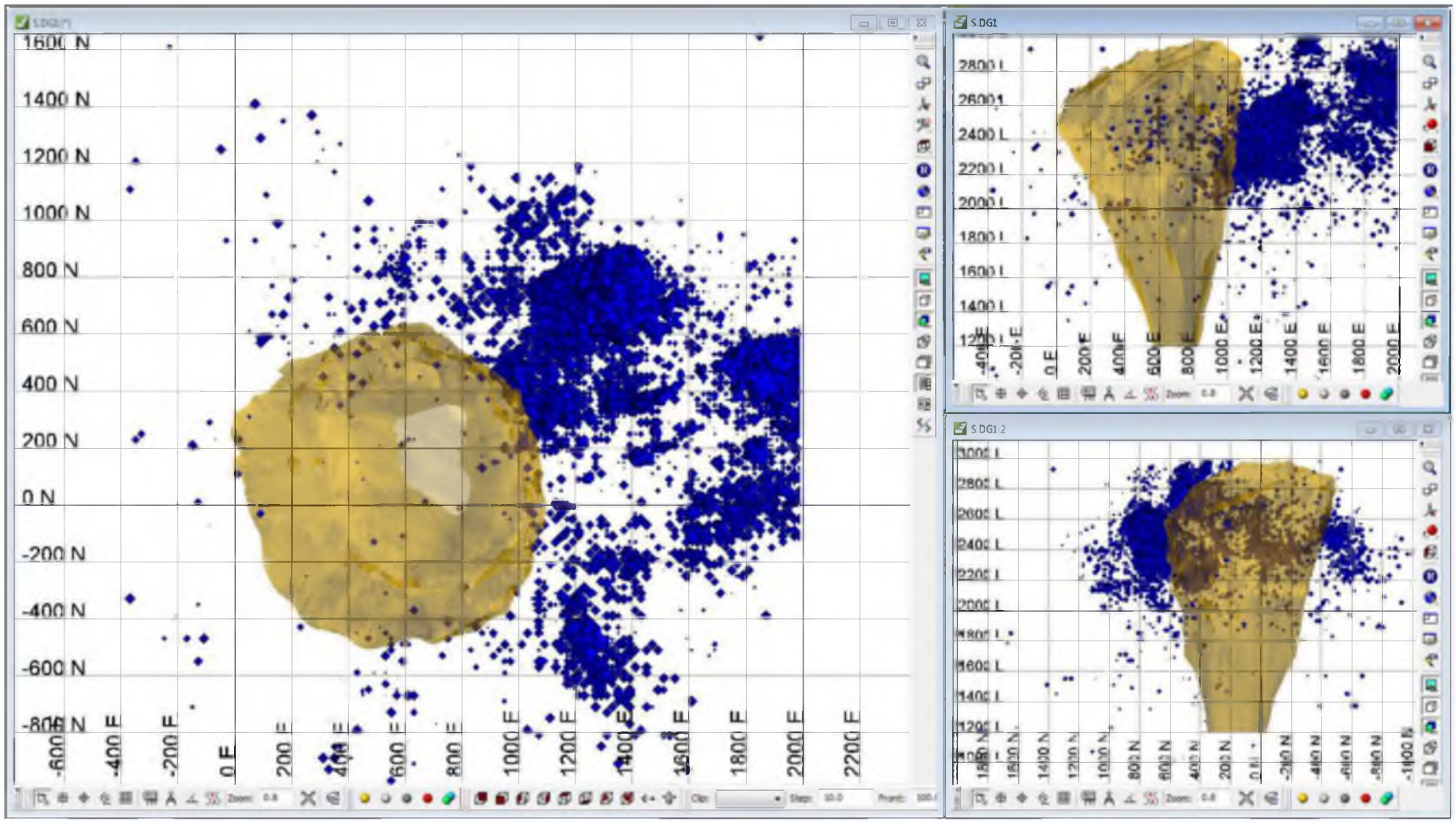

FIGURE B.11 Accumulated seismic energy up to the year 2002

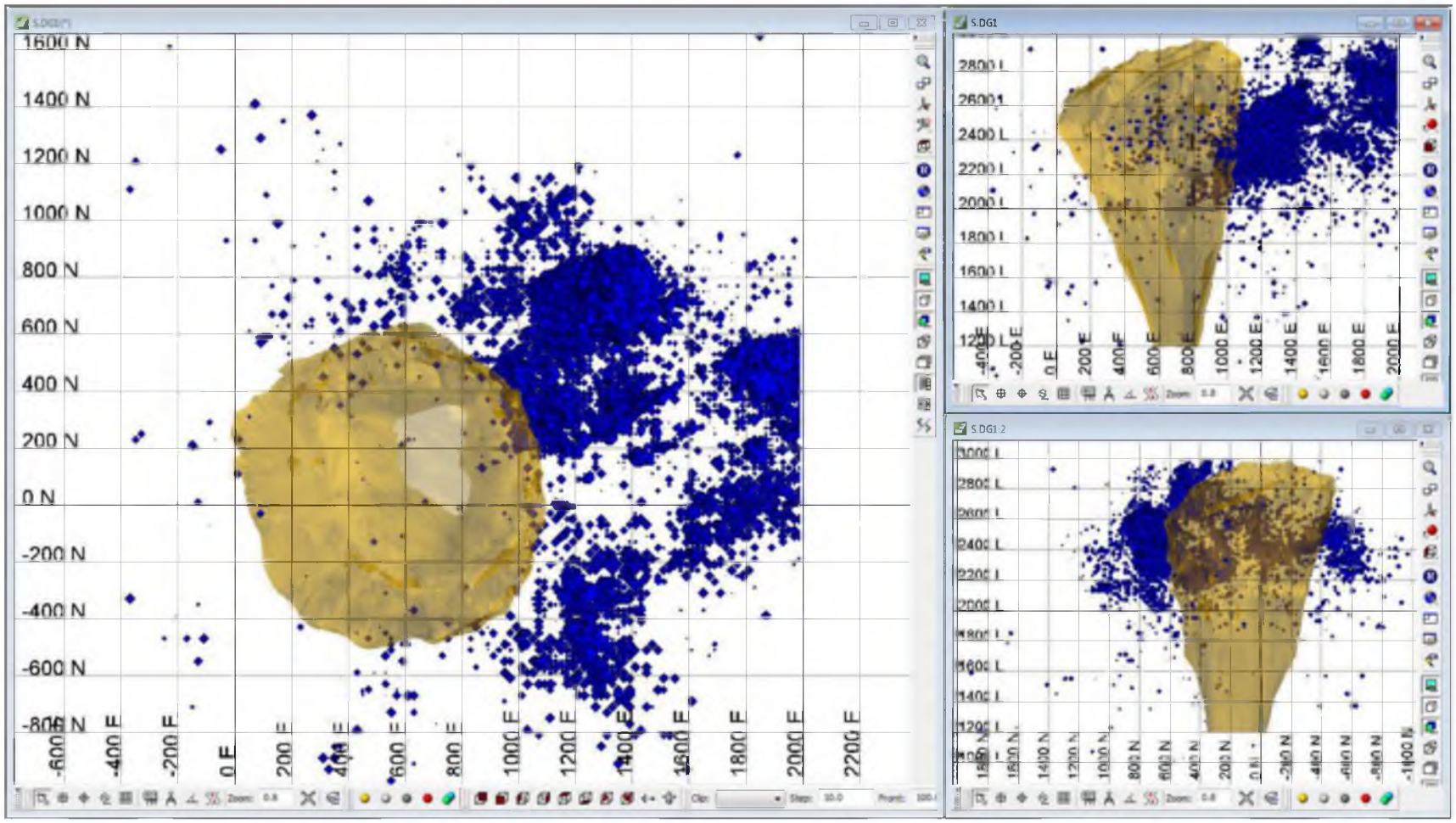

FIGURE B.12 Accumulated seismic energy up to the year 2003

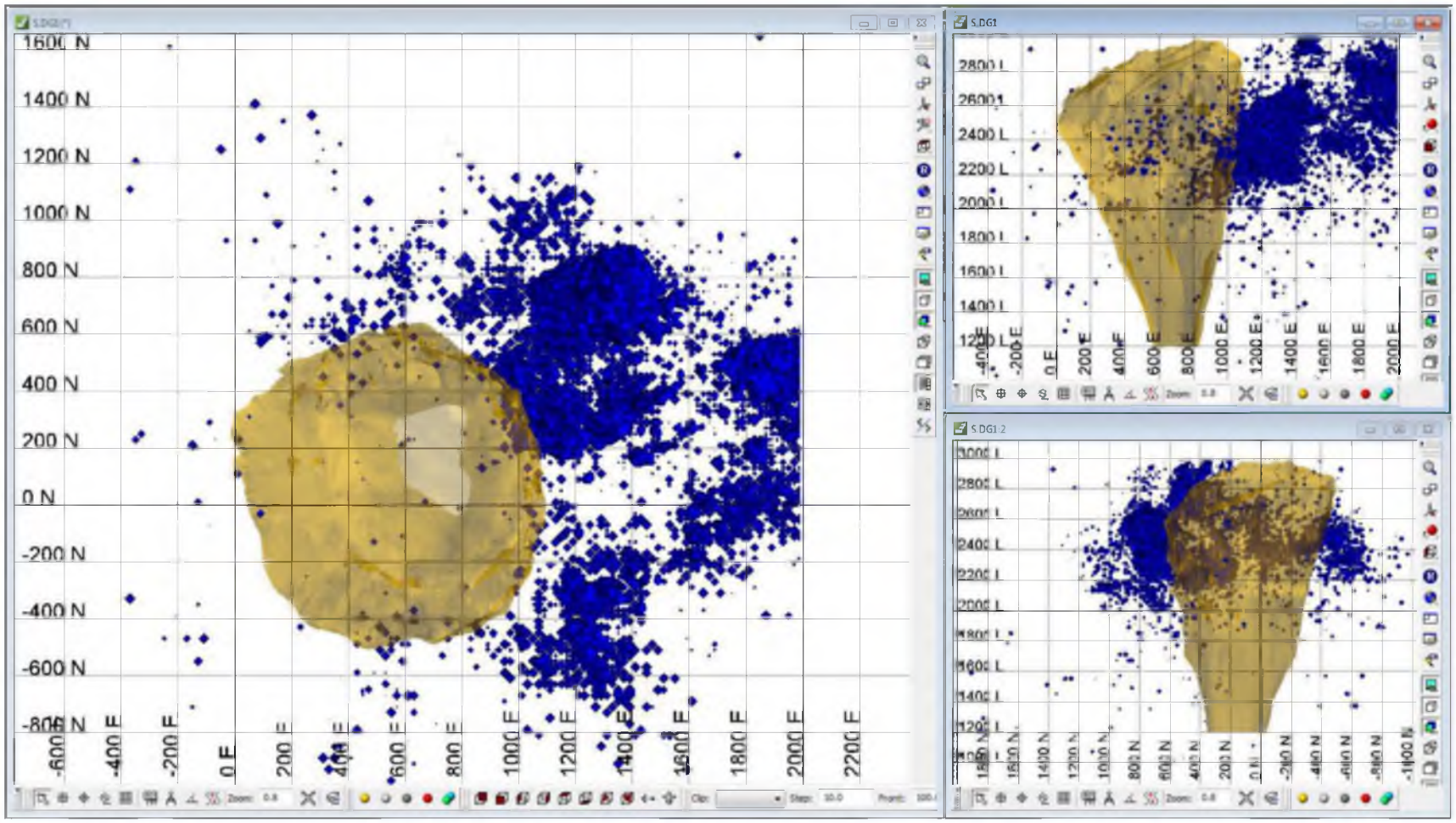

FIGURE B.13 Accumulated seismic energy up to the year 2004

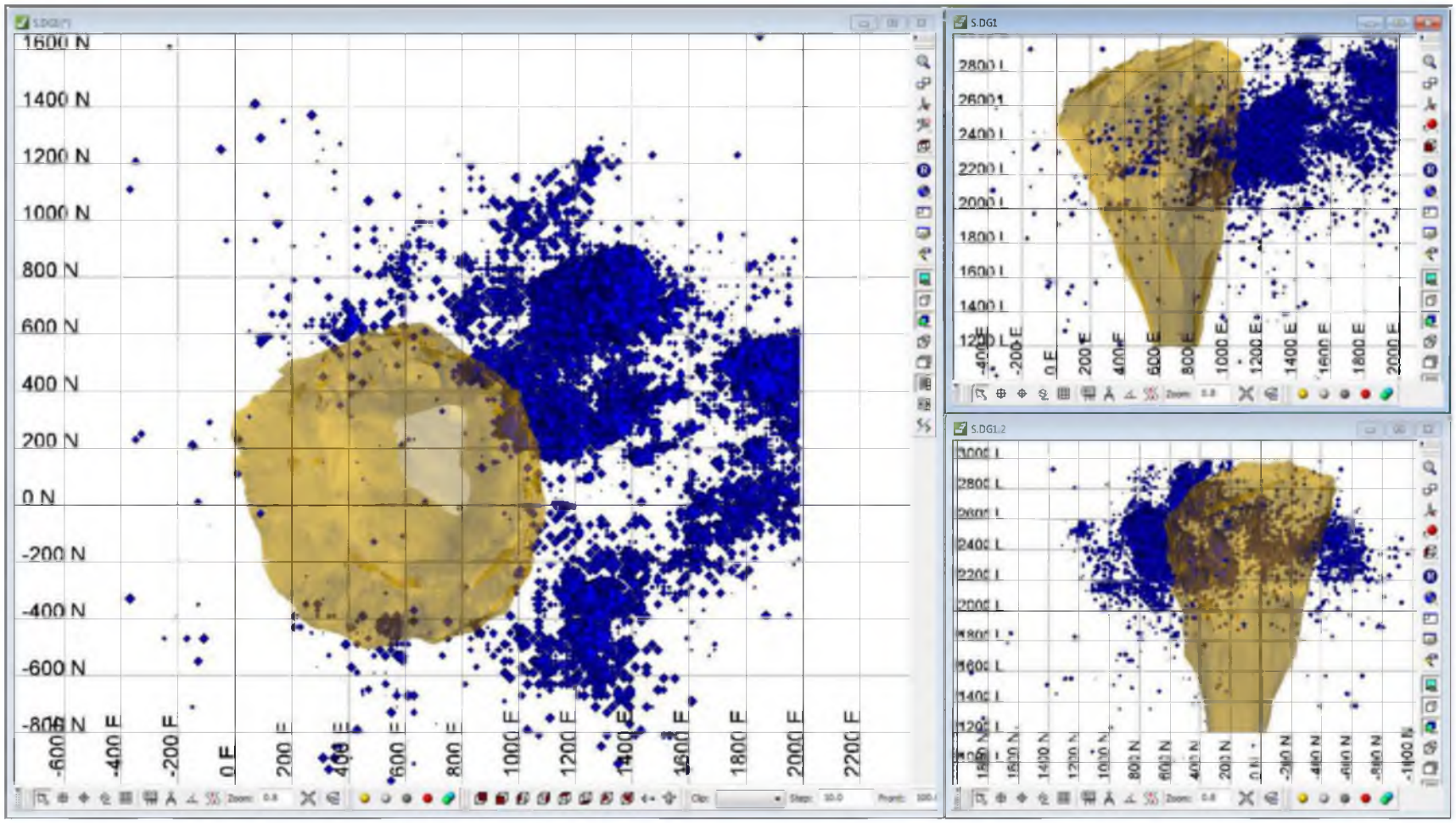

FIGURE B.14 Accumulated seismic energy up to the year 2005

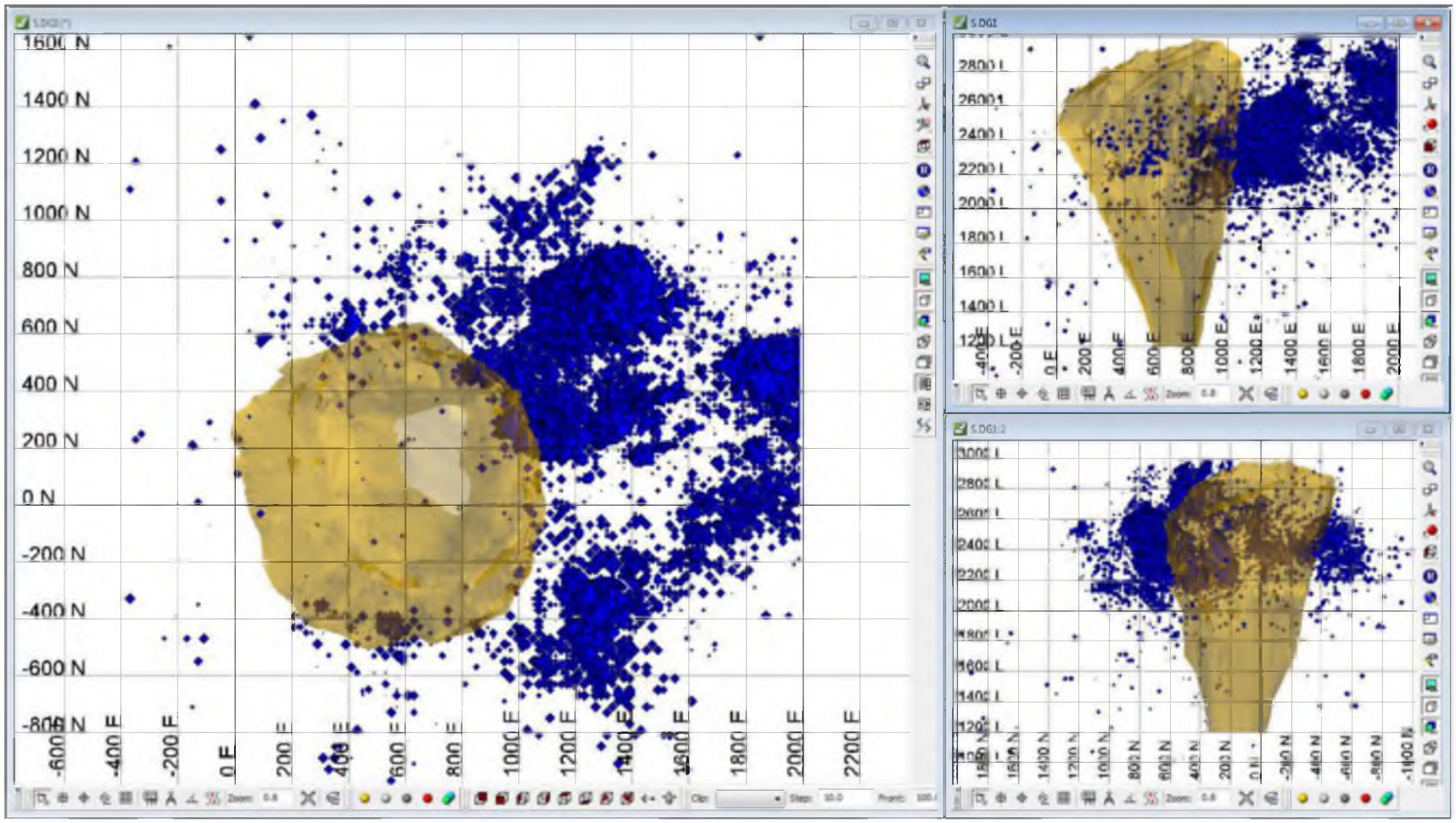

FIGURE B.15 Accumulated seismic energy up to the year 2006

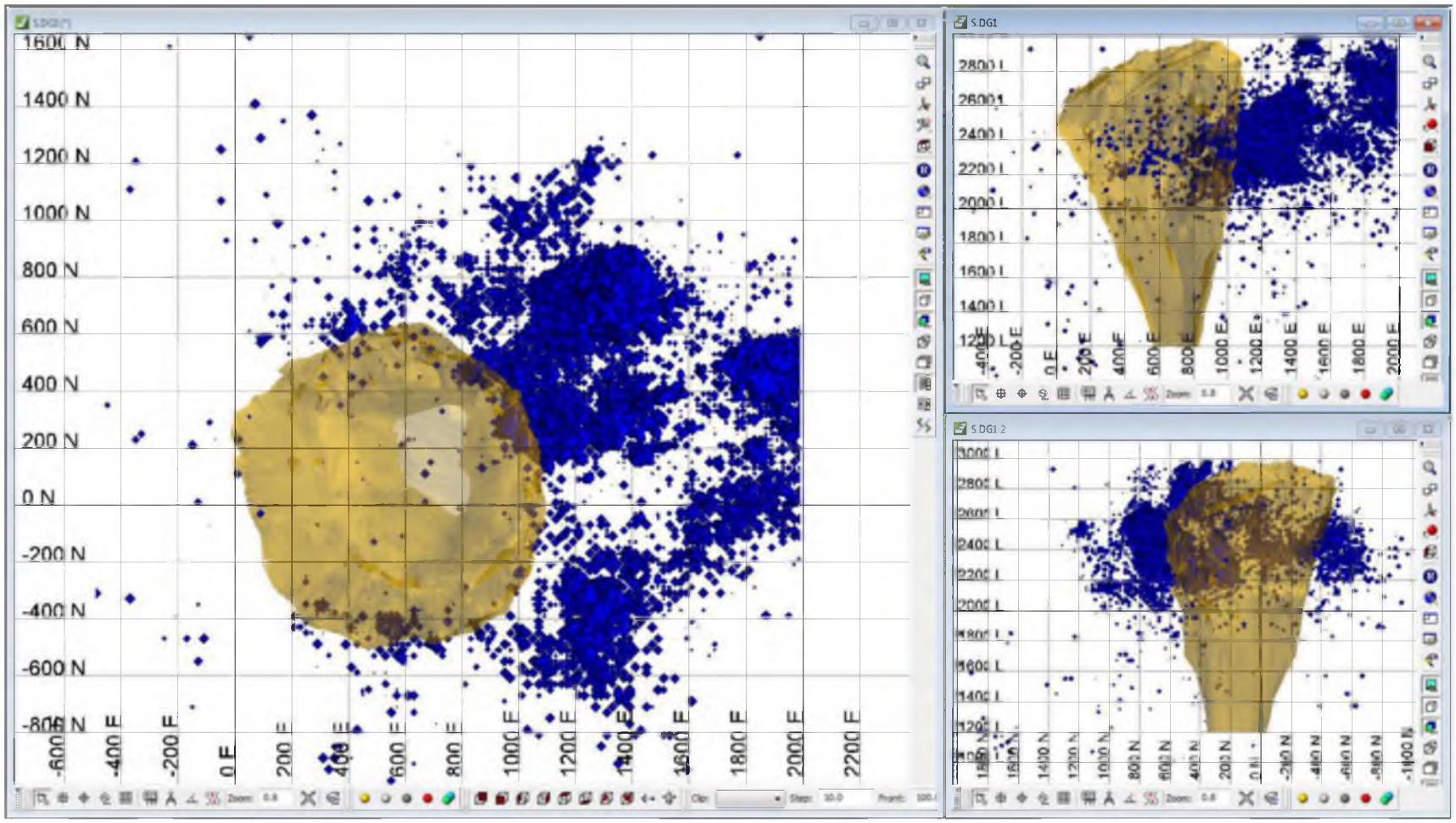

FIGURE B.16 Accumulated seismic energy up to the year 2007

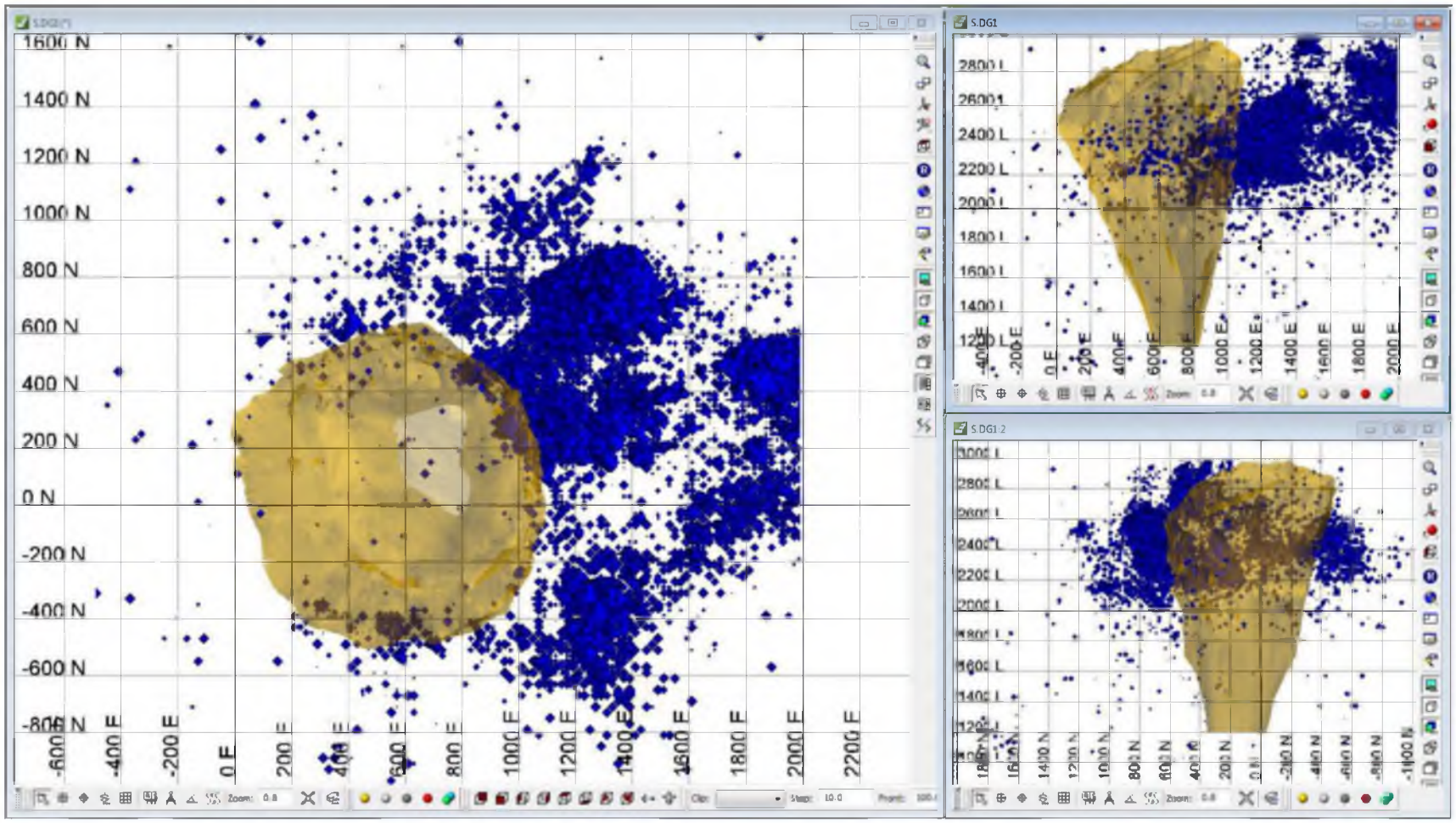

FIGURE B.17 Accumulated seismic energy up to the year 2008

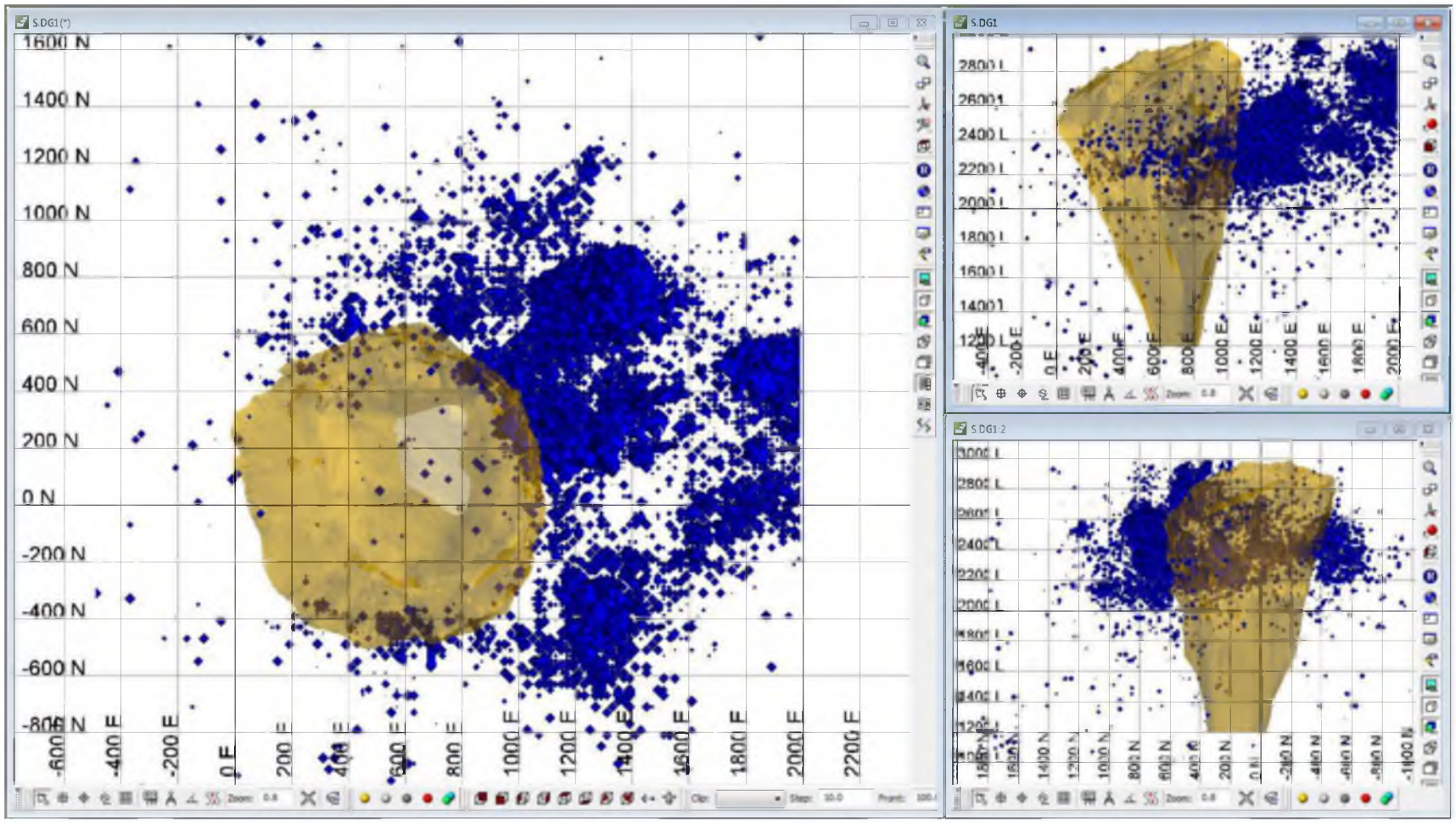

FIGURE B.18 Accumulated seismic energy up to the year 2009

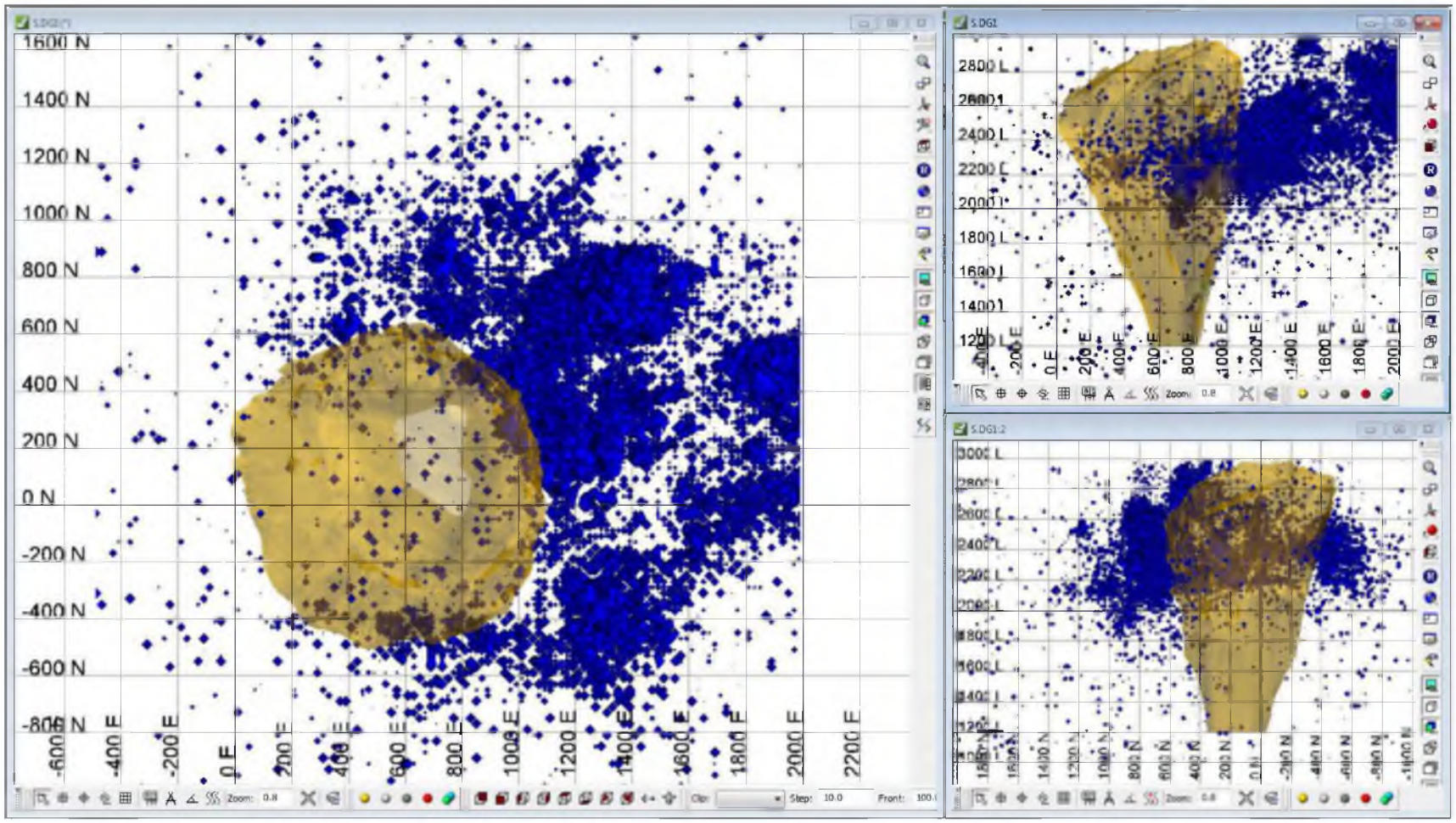

FIGURE B.19 Accumulated seismic energy up to the year 2010

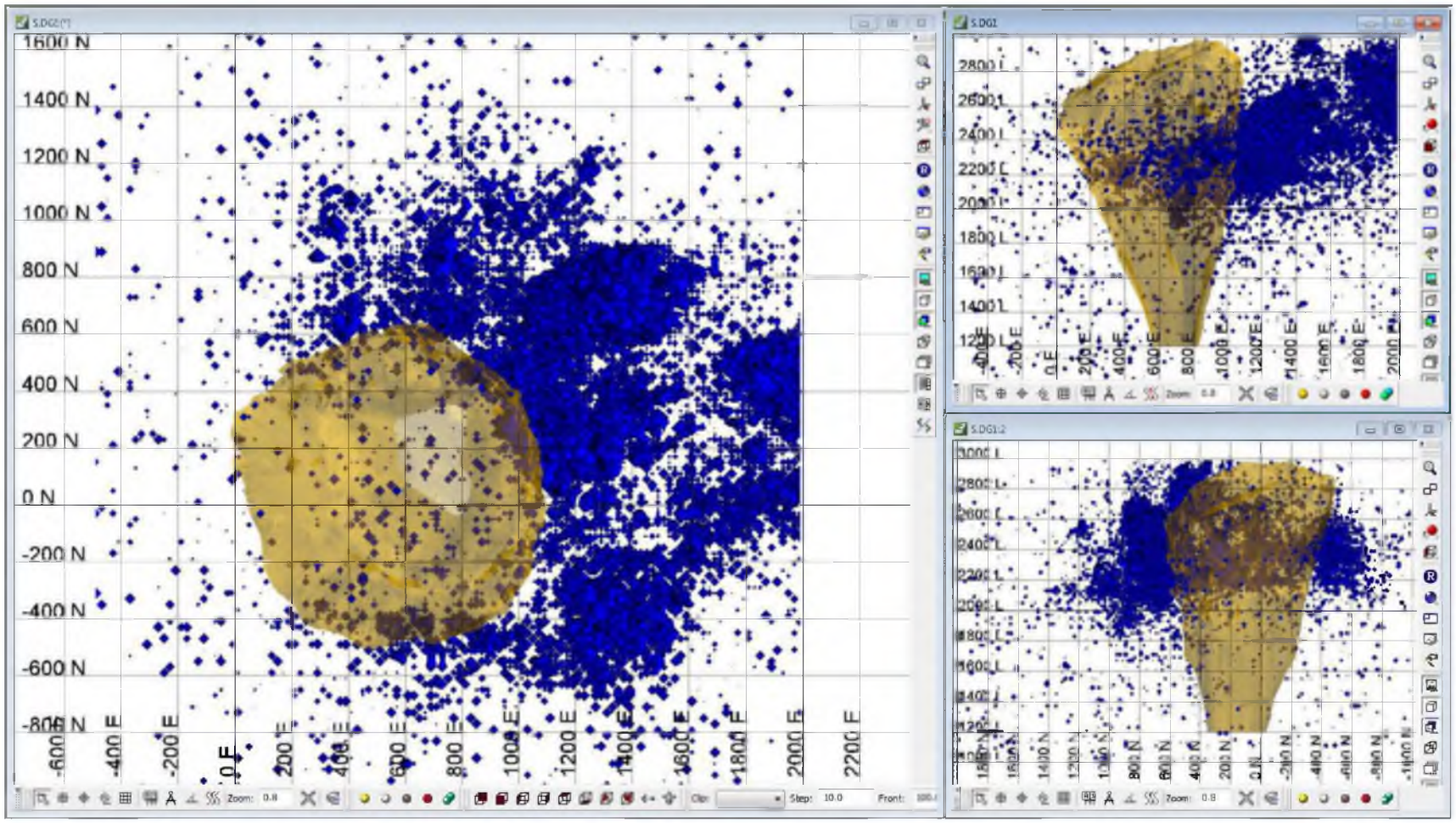

FIGURE B.20 Accumulated seismic energy up to the year 2011

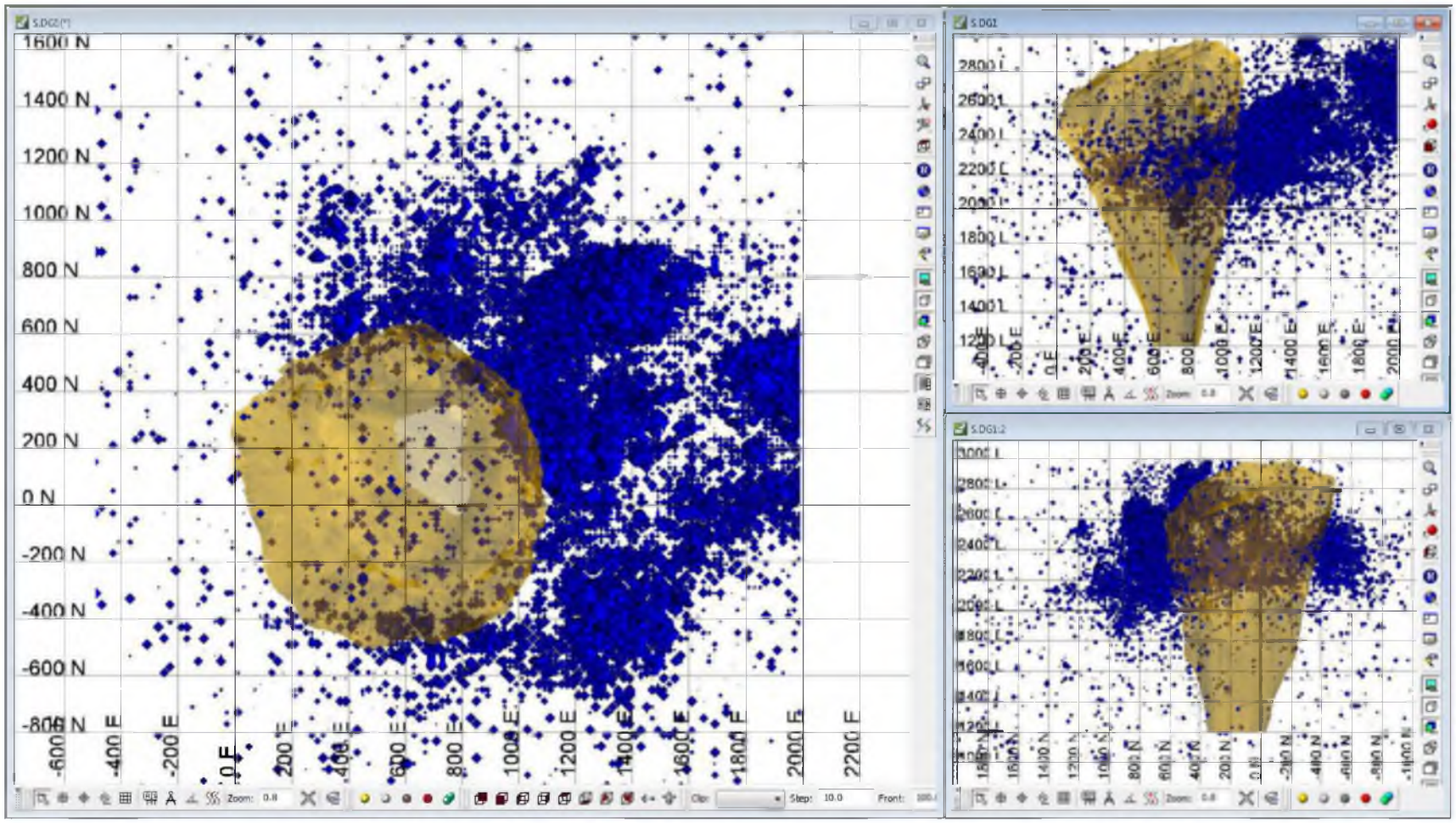

FIGURE B.21 Accumulated seismic energy up to the year 2012

REFERENCES

Barnes, M.P. 1979. Drill Hole Interpolation: Estimating Mineral Inventory. *Open Pit Mine Planning and Design.* New York: SME of AIME.

Brown, A.R., 2004. *Interpretation of Three-Dimensional Seismic Data,* 6th ed. AAPG Memoir 42. Investigations in Geophysics, No.9. American Association of Petroleum Geologists and the Society of Exploration Geophysicists.

Codelco, 2001. Fundamentals to the Seismicity Conduction Response in a Caving Method. Internal Mine Report. Codelco – División El Teniente. Rancagua, Chile.

Durheim, R.J., Spottiswoode, S.M., Roberts, M.K.C., and Brink, A.van Z. 2006. Comparative Seismology of the Witwatersand Basin and Bushveld Complex and Emerging Technologies to Manage the Risk of Rockbursting. *Journal - South African Institute of Mining and Metallurgy.* 105.6 (409-416).

Essrich, F. 2005. Mine Seismology for Rock Engineers – An Outline of Required Competencies. In *Controlling Seismic Risk, Proceedings of the Sixth International Symposium on Rockburst and Seismicity in Mines,* March 9–11, Perth, Western Australia: Australian Centre for Geomechanics.

Gibowicz, S.J., and Kijko, A. 1994. *An Introduction to Mining Seismology*, 1st ed. International Geophysics Series, Vol. 55. San Diego. Academic Press.

Glazer, S., and Hepworth, N. 2004. Seismic Monitoring of Block Cave Crown Pillar – Palabora Mining Company, RSA. In *Proceedings of Massmin 2004.* Santiago Chile, 22-25 August 2004, pp. 565-569. Santiago: Instituto de Ingenieros de Chile.

Gutenberg, B., and C.F. Richter. 1954. *Seismicity of the Earth and Associated Phenomena*, 2nd ed. Princeton, N.J.: Princeton University Press.

Hudyma, M.R., Frenette, P., and Leslie, I. 2010. Monitoring Open Stope Caving at Goldex Mine. *Proceedings of Caving 2010 – Second International Symposium on Block and Sublevel Caving,* April 20–22, Perth, Western Australia. Australian Centre for Geomechanics.

Hughes, W.E., and Davey, R.K. 1979. Drill Hole Interpolation: Mineralized Interpolation Techniques. In *Open Pit Mine Planning and Design.* New York: SME of AIME.

K-UTEC Sondershausen. 2003. *Seismic Monitoring*. K-UTEC GmbH: Sondershausen, Germany.

Mendecki, A.J. 1997. Seismic Monitoring in Mines. 1st ed. Chapman & Hall. 2-6 Boundary Row, London SE1 8HN, UK.

Moss, A., Diachenko, and Townsend, P. (2006) Interaction between the block cave and the pit slopes at Palabora Mine. In Symposium Series S44, *Stability of Rock Slopes in Open Pit Mining and Civil Engineering Situations.* Johannesburg: SAIMM.

Spottiswoode, S. 2009. Mine Seismicity: Prediction or Forecasting? HARD ROCK SAFE *Safety Conference, A sense of safety urgency. Proceedings of the 1st Hardrock Safe Safety Conference*, held on 28-30 September 2009 at Sun City-Mine. Journal of the South African Institute of Mining and Metallurgy. 110.1 (81-98).

Stanley, B.T., 1979. Mineral Model Construction: Principles of Ore-Body Modeling. In *Open Pit Mine Planning and Design.* New York: SME of AIME.

Swanson, P.L., and Sines, C.D. 1991. Characteristics of Mining-Induced Seismicity and Rock Bursting in a Deep Hard-Rock Mine. Report of Investigations, RI-9393. Washington, DC: U.S. Bureau of Mines.

Turner, M.H., and Player, J.R. 2000. Seismicity at Big Bell Mine. In *Proceedings of Massmin 2000*. Melbourne, Victoria: AusIMM.

White, H., Van As, A., Allison, D. 2004. Design and Implementation of Seismic Monitoring Systems in a Block-Cave Environment. In *Proceedings of Massmin 2004.* Santiago Chile, 22-25 August 2004. Santiago: Instituto de Ingenieros de Chile.

Whyat, J.K., White, B.G., and Blake, W. 1996. Structural Stress and Concentration of Mining-Induced Seismicity. *Trans. SME* 300:74-82.